Eesti Maaülikool
Estonian University of Life Sciences

ROLE OF LEAF ANATOMY IN PHOTOSYNTHETIC MODIFICATIONS DURING PLANT ONTOGENY AND UPON ENVIRONMENTAL ACCLIMATION

LEHTEDE ANATOOMILISTE MUUTUSTE ROLL TAIMEDE FOTOSÜNTEESIVÕIME MÄÄRAMISEL

VIVIAN KUUSK

A Thesis
for applying for the degree of Doctor of Philosophy
in Applied Biology

Väitekiri
filosoofiadoktori kraadi taotlemiseks
rakendusbioloogia erialal

Tartu 2024

Eesti Maaülikooli doktoritööd

Doctoral Theses of the Estonian University of Life Sciences

Eesti Maaülikool
Estonian University of Life Sciences

ROLE OF LEAF ANATOMY IN PHOTOSYNTHETIC MODIFICATIONS DURING PLANT ONTOGENY AND UPON ENVIRONMENTAL ACCLIMATION

LEHTEDE ANATOOMILISTE MUUTUSTE ROLL TAIMEDE FOTOSÜNTEESIVÕIME MÄÄRAMISEL

VIVIAN KUUSK

A Thesis
for applying for the degree of Doctor of Philosophy
in Applied Biology

Väitekiri
filosoofiadoktori kraadi taotlemiseks
rakendusbioloogia erialal

Tartu 2024

Institute of Agricultural and Environmental Sciences
Estonian University of Life Sciences

According to the verdict No 6-14/20-2 of November 11, 2024, the Doctoral Committee of Environmental Sciences and Applied Biology of the Estonian University of Life Sciences has accepted the thesis for the defence of the degree of Doctor of Philosophy in Applied Biology.

Opponent: **Professor Dr. Beatriz Fernández-Marín**
Universidad de La Laguna - San Cristóbal de La Laguna / Spain

Supervisor: **Professor Ülo Niinemets**
Institute of Agricultural and Environmental Sciences
Estonian University of Life Sciences

Defence of the thesis: Estonian University of Life Sciences, room D239, Kreutzwaldi 5, Tartu, on Dec 20, 2024

Publication of this thesis is supported by the Estonian University of Life Science and by the Doctoral School of Earth Science and Ecology created under the auspices of European Social Fund.

This study was supported by the European Commission through the European Research Council advanced grant 322603, SIPVOL+, the European Regional Development Fund (Centre of Excellence EcolChange), the Estonian Research Council team grant PRG537, the Estonian Ministry of Science and Education grant IUT-8-3, the Estonian Science Foundation grant 9253, the European Commission through the European Regional Fund (the Center of Excellence in Environmental Adaptation) and the Estonian Research Council grant ETAG PRG 2207.

© Vivian Kuusk, 2024
ISSN 2382-7076
ISBN 978-9916-91-010-8
ISBN 978-9916-91-011-5 (pdf)

CONTENTS

LIST OF ORIGINAL PUBLICATIONS 7
CONTRIBUTIONS 8
LIST OF TERMS AND ABBREVIATIONS 9
1. INTRODUCTION 13
2. REVIEW OF THE LITERATURE 18
2.1 The importance of *Pinus* species 18
2.2 Heteroblasty, heterophylly and juvenility 18
2.3 Age-dependent changes in conifer needles 20
2.3.1 Biochemical differences 21
2.3.2 Photosynthetic properties 21
2.4 Elevated temperature influence on leaf anatomy, photosynthesis and isoprene emission 22
3. AIM OF THE STUDY AND HYPOTHESES 24
4. MATERIAL AND METHODS 25
4.1 Description of studied species 25
4.2 Measurement sites and plant growth conditions 27
4.3 Foliage sampling and measurements of morphological and anatomical characteristics 29
4.4 Gas exchange measurements 33
4.6 Data analysis 37
5. RESULTS 39
5.1 Needle structure and age 39
5.2 Photosynthesis and needle age (Article II) 50
5.3 Changes in leaf structure, photosynthesis and isoprene emission due to growth at elevated temperature (Article III) 53
6. DISCUSSION 56
6.1 Age-dependent modifications in needle morphology and needle photosynthetic properties in Mediterranean pines (Articles I and II) 56
6.2 Age-dependent modifications in needle photosynthetic properties in Mediterranean pines (Article II) 57

6.3 Temperature-dependent modifications in leaf anatomy and physiological performance (Article III) 58
7. CONCLUSIONS 60
REFERENCES 62
SUMMARY IN ESTONIAN.....81
ACKNOWLEDGEMENTS 83
ORIGINAL PUBLICATIONS.....85
CURRICULUM VITAE.....137
CURRICULUM VITAE.....138
LIST OF 1.1 PUBLICATIONS.....140

LIST OF ORIGINAL PUBLICATIONS

This thesis is based on the following research papers, which are referred to in the text by their Roman numerals:

I. **Vivian Kuusk**, Ülo Niinemets, Fernando Valladares (2018a) A major trade-off between structural and photosynthetic investments operative across plant and needle ages in three Mediterranean pines. *Tree Physiology* 38: 543–557.

II. **Vivian Kuusk**, Ülo Niinemets, and Fernando Valladares (2018b) Structural controls on photosynthetic capacity through juvenile-to-adult transition and needle aging in Mediterranean pines. *Functional Ecology* 32:1479–1491.

III. Bahtijor Rasulov, Irina Bichele, Katja Hüve, **Vivian Vislap**, Ülo Niinemets (2015) Acclimation of isoprene emission and photosynthesis to growth temperature in hybrid aspen: resolving structural and physiological controls. *Plant, Cell and Environment* 38: 751–766.

CONTRIBUTIONS

	I	II	III
Idea	ÜN, FV, **VK**	ÜN, **VK**, FV	BR, ÜN
Data collection	**VK**, FV	**VK**, FV	BR, IB, KH, **VV**
Data analyses	**VK**, ÜN	**VK**, ÜN	BR, ÜN, **VV**
Manuscript preparation	**VK**, ÜN, FV	**VK**, ÜN, FV	BR, **VV**, ÜN

VK – Vivian Kuusk, FV – Fernando Valladares, ÜN – Ülo Niinemets, BR – Bahtijor Rasulov, IB – Irina Bichele, KH – Katja Hüve, **VV** – Vivian Vislap (Vivian Kuusk)

LIST OF TERMS AND ABBREVIATIONS

Article I and II

A	net assimilation rate per area (μmol m^{-2} s^{-1})
A_m	net assimilation rate per unit needle dry mass (μmol g^{-1} s^{-1})
A_P	net assimilation rate per unit needle projected area (μmol m^{-2} s^{-1})
C_c	chloroplastic CO_2 concentration (μmol mol^{-1})
C_i	intercellular CO_2 concentration (μmol mol^{-1})
C_i- C_c	CO_2 drawdown from substomatal cavities to chloroplasts (μmol mol^{-1})
C_m	carbon content per dry mass (%)
D	needle density (needle volume per dry mass) (g cm^{-3})
E_N	photosynthetic nitrogen use efficiency (μmol g^{-1} s^{-1})
f_{chl}	fraction of chloroplasts in needle cross-section
f_{ma}	fraction of mesophyll in needle cross-section without intercellular air space
$g_{m,m}$	mesophyll diffusion conductance per unit needle dry mass (mmol g^{-1} s^{-1})
$g_{m,P}$	mesophyll diffusion conductance per unit needle projected area (mmol m^{-2} s^{-1})
J_{max}	capacity for photosynthetic electron transport: mass basis (μmol g^{-1} s^{-1}), area basis (μmol m^{-2} s^{-1})
juv	current year juvenile needles
L	total needle length (mm)
L_E	the length of enclosed needle section in gas-exchange cuvette (mm)
m0	current year needles in mature trees
m1	1-year old needles in mature trees
m2	2-year-old needles in mature trees
$M_{A,P}$	needle dry mass per unit projected area (g m^{-2})

$M_{A,T}$	needle dry mass per unit total needle area (g m^{-2})
$N_{A,P}$	needle nitrogen content per unit projected area (g m^{-2})
$N_{A,T}$	needle nitrogen content per unit total area (g m^{-2})
N_m	nitrogen content per unit dry mass (%)
$R_{D/F}$	needle dry to fresh mass ratio
S_c	chloroplast surface area exposed to intercellular air space (μm^2)
S_c/S_m	chloroplast surface area exposed to intercellular air space/ mesophyll surface area exposed to intercellular air space
$S_{c/}S_P$	chloroplast surface area exposed to intercellular air space per unit of projected leaf area (m^2 m^{-2})
S_m	mesophyll surface area exposed to intercellular air space (μm^2)
$S_{m/SP}$	mesophyll surface area exposed to intercellular air space per unit of projected leaf area (m^2 m^{-2})
S_P	needle projected area (mm^2)
S_S	needle cross-sectional area (mm^2)
S_S/W	needle volume to projected area ratio
S_T	needle total area (mm^2)
S_T/S_P	needle total to projected area ratio
T	needle thickness (mm)
TEM	transmission electron microscope
U	needle circumference (mm)
V	needle volume (mm^3)
V/A_T	needle volume to total area ratio
V/S_P	needle volume to projected area ratio
V/S_T	needle volume to total area ratio
V_c	volume of chloroplasts (mm^3)
$V_{c/SP}$	volume of chloroplasts per projected area (mm)
V_m	volume of mesophyll (mm^3)
$V_m/_{SP}$	volume of mesophyll per needle projected area (mm)

V_{cmax}	maximum carboxylase activity of ribulose 1,5-bisphosphate carboxylase (Rubisco): mass basis (μmol g^{-1} s^{-1}), area basis (μmol m^{-2} s^{-1})
W	needle width (mm)

Article III

A_p	net assimilation rate per unit projected leaf area (μmol m^{-2} s^{-1}),
A_m	net assimilation rate per unit dry mass (μmol g^{-1} s^{-1})
α_{CO2}	quantum yield for CO_2 exchange (mol mol^{-1})
α_I	quantum yield for isoprene emission (mol mol^{-1})
BVOC	biogenic volatile organic compounds
C_{DMADP}	dimethylallyl diphosphate pool size: per area (nmol m^{-2} s^{-1}), per dry mass (nmol g^{-1} s^{-1})
DMADP	dimethylallyl diphosphate
F	steady-state light-adapted fluorescence yield
F_m	dark-adapted maximum fluorescence yield
F_m'	light-adapted maximum fluorescence yield
F_0	dark-adapted minimum fluorescence yield
Φ_{PSII}	quantum yield of illuminated leaves
I	isoprene emission rate per area (nmol m^{-2} s^{-1}) and per dry mass (nmol g^{-1} s^{-1})
IDP	isopentenyl diphosphate
J_{ETR}	photosynthetic electron transport from chlorophyll fluorescence
J_{max}	capacity for photosynthetic electron transport per area (μmol m^{-2} s^{-1}) and per dry mass (μmol g^{-1} s^{-1})
k	rate constant of isoprene synthase (s^{-1})
K_m	Michaelis-Menten constant for isoprene synthase per area (nmol m^{-2}) and per dry mass (nmol g^{-1})

M_A	leaf dry mass per unit area
n_{chl}	chloroplast number pear leaf area (m^{-2})
$n_{c.p}$	number of cells in the palisade tissue per unit leaf area (m^{-2})
$n_{c.s}$	number of cells in the spongy parenchyma tissue per unit leaf area (m^{-2})
$n_{chl.p.p}$	chloroplast number per cell in the palisade parenchyma estimated from the paradermal section
$n_{chl.p.c}$	chloroplast number per cell in the palisade parenchyma estimated from the cross-section
$n_{chl.s.p}$	chloroplast number in the spongy parenchyma estimated from the paradermal section
$n_{chl.s.c}$	chloroplast number in the spongy parenchyma estimated from the cross-section
PSII	photosystem II
PTR-MS	proton transfer reaction mass spectrometer
V_D	water pressure deficit (kPa)
V_{cmax}	maximum carboxylase activity of Rubisco per area (μmol m^{-2} s^{-1}) and per dry mass (μmol g^{-1} s^{-1})
V_{max}	Maximum activity of isoprene synthase per area (nmol m^{-2} s^{-1}) and per dry mass (nmol g^{-1} s^{-1})
Q	incident quantum flux density (μmol m^{-2} s^{-1})
ξ	leaf absorptance
β	fraction of absorbed light used to drive PSII electron transport
t	time (s)
TEM	transmission electron microscope

1. INTRODUCTION

There is a huge variation in leaf anatomy among plants species and within any plant species, and the anatomical variations have important implications for the efficiency of operation of photosynthetic machinery in chloroplasts (Niinemets et al. 2005, 2009, Carriquí et al. 2021, Jahan et al. 2023). Thus, there is an increasing interest in how leaf morphological and anatomical traits affect leaf physiological function (Flexas et al. 2021, Knauer, et al. 2022, Cao et al. 2024, Joffe et al. 2024, Sáez et al. 2024, Viveros et al. 2024).

Plants have undergone anatomical modifications during their evolution, leading to vast differences in structural differentiation among plant lineages, including differences in the share of mesophyll and structural tissues, amount and architecture of vasculature, presence and structure of specialized tissues for secondary defensive metabolites (Scarpella et al. 2004, Lange, 2015). Furthermore, almost all plants show a certain degree of variation in their leaf structural and physiological traits during ontogeny, a type of phenotypic variation that is also called heteroblasty (Zotz *et al.* 2011, Barton, 2024, Percival *et al.* 2024). Heteroblastic modifications are especially large in long-living species, and in some cases these changes are very abrupt (Zotz *et al.* 2011). However, the functional significance, adaptive and evolutionary role of this type of heteroblastic change is still unresolved, especially in woody plants (Winn, 1999, Zotz *et al.* 2011, Climent *et al.* 2006a).

Miller *et al.* (1995) investigated *Juniperus occidentalis* Hook., a plant species with distinct heterophylly between young and adult needles. They stated that juvenile foliage is less costly to produce and has a higher CO_2 assimilation rate than adult foliage, and consequently, it should enhance establishment and early growth. On the other hand, greater photosynthetic activity requires a higher stomatal conductance, and therefore, juvenile foliage might have excessive water loss (Miller *et al.* 1995). As the plants increase in size and reach the canopy, they become exposed to greater environmental stress including higher solar radiation, vapor pressure deficit and temperature. Thus, the transition to more stress-tolerant mature scale-like foliage is advantageous as it allows the plants to use resources more conservatively.

To gain an insight into the ecological significance of juvenile needles, Climent *et al*. 2009 tested the hypothesis that juvenile needles are more cold-hardy than adult needles in Mediterranean pines that have a particularly pronounced juvenile phase. He proved the assumption wrong and concluded that ontogenetic delay has other, yet unclear, causes.

In a review by Steppe *et al*. (2011) the effects of plant age and size on photosynthesis were analyzed in different plant functional types, whereas the greatest variation in foliage photosynthetic rates during plant ontogeny was observed in needle-leaved conifers. It was emphasized that there is a variety of factors responsible for tree height- and age-related decline in net photosynthetic rates and more integrated studies are needed that consider the simultaneous roles of leaf structure, chemistry, stomatal and mesophyll factors are needed to disentangle the importance of various factors responsible for decreases in carbon gain with tree age and size.

Significant changes in cell structural features during leaf growth and development, such as cell wall thickness, chloroplast size, and their distance from cell walls, primarily affect photosynthetic efficiency by altering CO_2 diffusion resistance (Carriquí et al. 2021, Alonso-Forn *et al*. 2022, Jahan *et al*. 2023, Barton et al. 2024). Understanding these processes is made even more complex by the influence of environmental conditions and possible stress (Tosens *et al*. 2012, Carriquí et al. 2021, Barton 2023, Jahan *et al*. 2023).

Apart from plant age-dependent modifications in leaf structure and function, there are major modifications in leaf functional traits during leaf development and aging. Aasamaa *et al*. (2005) showed that the continuous increase in leaf dry mass during leaf ontogeny (continuous deposition of cell wall material) significantly affects leaf hydraulic conductivity. Tosens *et al*. (2012) have further demonstrated that important modifications in foliage architecture, photosynthetic activity and CO_2 diffusion occur in developing leaves. Leaf age-dependent changes include modifications in dry mass per unit area, leaf thickness and density, mesophyll diffusion conductance, net assimilation rate, exposed mesophyll and chloroplast to leaf area ratio, leaf internal air space, cell wall thickness and chloroplast dimensions (Wright *et al*. 2001, 2004, Jahan *et al*. 2023).

There is still limited information of needle morphological, anatomical, chemical and physiological traits upon juvenile-to-adult transition, and especially limited is the information of the interaction of plant ontogeny with needle ontogeny in woody species with long-living needles. The current research (Kuusk *et al.* 2018a, 2018b) was designed to address these gaps of knowledge. For investigating morphological and physiological properties of juvenile and adult needles, three phylogenetically close Mediterranean *Pinus* species - *Pinus halepensis* Mill., *P. nigra* J. F. Arnold subsp. *salzmannii* (Dunal) Franco and *P. pinea* L. needles of different age classes were chosen. According to Klaus (1989) they show more significant ontogenetic delay compared to other Eurasian pines, and as such constitute an ideal system to analyze the interactive effects of plant and leaf developmental stages on leaf functional activity.

Apart from whole plant and leaf age, there is also a large phenotypic variability in leaf functional traits caused by environmental conditions (Poorter *et al*. 2006a, Wright *et al*. 2004). Palacio-Lopez *et al*. (2015) propose that in heterogeneous environments, plants capable of plastic modifications of leaf size and shape are expected to have better fitness compared to other plants. There is a wealth of information on how leaf structure and photosynthetic activity change upon acclimation to variation in light availability (Poorter *et al*. 2006b, 2005, Poorter 1999). In general, increases in light availability result in greater leaf thickness and stacking of mesophyll per unit leaf area, resulting in light-dependent increases in leaf photosynthetic capacity per unit leaf area (Niinemets *et al*. 2015, Poorter *et al*. 2006b, 1999.). For conifers, this has been confirmed for multiple species, including Mexican weeping pine (*Pinus patula* Schiede ex Schltdl. et Cham.) and Monterey pine (*Pinus radiata* D. Don) (Niinemets *et al*. 2007), and such environmental plasticity further adds to the large variability of foliage photosynthetic activity as driven by plant and leaf ontogeny.

However, there is much less information of how foliage structural and physiological traits respond to long-term modifications in temperature. At temperatures higher than optimal, the ability of plants to fix CO_2 is lower, damage to PSII can occur, enzyme and proteine activity, electron transport rate, stomatal conductance and cloroplasts functioning are affected (Hussain *et al*. 2021). Leaves can acclimatize to hot temperatures to achieve the maximum photosynthetic rates, but the limits of the acclimatization process and all its mechanisms, especially anatomical ones,

are still uclear (Hussain *et al*. 2021). Only a few studies have described anatomical changes in leaves during growth at elevated temperatures; typically, leaves grown at higher temperatures are thinner and wider (Higuchi *et al*. 1999, Hartikainen et al. 2009, Muller et al. 2014, Cohu et al. 2014, Benomar et al. 2019). Thus, differently from growth light effect, higher temperatures are expected to reduce leaf photosynthetic capacity, but the information of the scaling of leaf photosynthetic activity across leaves grown at different temperatures has not been studied. In addition to alterations in thickness, leaf photosynthetic activity at the given thickness will also depend on leaf ultrastructural characteristics such as cell wall thickness and number of chloroplasts per cell.

Another aim of the thesis was to clarify the importance of foliage structural traits on leaf physiological acclimation to growth temperature. Apart from photosynthesis that is typically considered as the measure of leaf physiological activity, we also studied foliage isoprene emissions.

Isoprene is the most abundant plant emitted volatile organic compound (Guenther et al., 2006), which protects plants from excessive heat and oxidative damage (Sharkey *et al*. 2001, Vickers *et al*. 2009) (Sharkey *et al*. 2008) and plays an important role in atmospheric chemistry (Li *et al*. 2011). Given that global change is associated with an overall increase in temperature and increased frequency and severity of heatwaves (Barriopedro *et al*. 2023), to improve global models of isoprene emission, it is especially important to know how isoprene emissions acclimate to elevated temperature (Arneth *et al*. 2008).

As isoprene is synthesized in chloroplasts and mainly relies on photosynthetic intermediates, isoprene emission is strongly related to leaf photosynthetic activity (Niienemets *et al.* 2010). However, there is evidence that isoprene emissions can respond more plastically to environmental variation than photosynthesis (Niinemets *et al.* 2015) for the hue variation in isoprene emission rates in response to long-term variations in light availability, but structural and biochemical factors responsible for the differences in the magnitude of environmental responses of these two key processes have not been analyzed.

To describe and understand structural and biochemical controls on temperature-dependent changes in foliage photosynthetic and isoprene emission rates, hybrid poplar (*Populus tremula x P. tremuloides*) - a fast-

growing isoprene emitting species - plants were grown under elevated temperature. Their photosynthesis, isoprene emission, biochemical and anatomical properties were measured and the corresponding differences characterized. The data shown in this thesis emphasize the importance of leaf anatomy in determining phenotypic variation in leaf physiological activity through variations in plant and leaf ontogeny and upon acclimation to growth temperature.

2. REVIEW OF THE LITERATURE

2.1 The importance of *Pinus* species

Genus *Pinus* is without a doubt the most ecologically and economically significant tree genus in the world. Pines are source of timber, pulp, nuts, resin and other products. They influence ecosystems by affecting biogeochemical processes, hydrological and fire regimes, provide food and create habitats for animals (Rundel, *et al*. 1998). Pines are suitable for reforestation of very many different types of land. They can grow everywhere from tropical to boreal and arctic climate, in lowlands and in high altitudes, in boggy soils an in sandy soils and they cope with very low amount of nutrients in the soil. The growth is fast and timber easily processed. (Le Maitre, 1998) Mediterranean pines are known for stress tolerance as they live in harsh environment where shortage of water is very common. All pines possess juvenile needles in young plants; such a juvenile phase takes from six months up to five years, and is especially long in Mediterranean pines (usually more than two years) Farjon, 2010. The change from juvenile to adult needles is called ontogenetic change or heteroblasty (Jones, 2001). There is a further a gradual change in needle traits with plant age beyond the juvenile phase, often called ontogenetic shift (Zotz *et al.*). Young pine juvenile needles are relatively soft, contain more photosynthetic tissue and have much less support tissue than adult needles (Climent *et al.* 2011). Only after proper establishment of root system and couple of shoots, more durable adult type needles are grown (Miller *et al.* 1995). Therefore Mediterranean pines like *Pinus halepensis*, *Pinus pinea* and *Pinus nigra* are excellent study species for better understanding of the juvenility phenomena and its role in ecological adaptation.

2.2 Heteroblasty, heterophylly and juvenility

There is a continuous age- and size-dependent change in leaf traits through plant life called ontogenetic drift, which has been studied in the majority of investigations looking at tree age and size effects on foliage structure and function (Kuusk *et al.* 2018a). Changes in leaf traits are characteristically the largest during development from juvenile to adult

leaves and many species exhibit an almost abrupt developmental change called heteroblasty (Zotz *et al.* 2011).

In many species, the adult leaf shape is attained in the seedling leaves or within the first year of growth. In other species, the adult leaf shape is associated with a clear transition to reproduction. And in some cases (e.g., *Pinus sylvestris*), the transition from juvenile to adult leaves occurs in association with the onset of the first dormant period, whereas in others (e.g., *Pinus pinea*), these events are not coupled (Goebel 1900).

Currently, the term heteroblasty is most often used to describe changes in the vegetative body, such as in the shape, size, and anatomical properties of leaves, phyllotaxy, potential and fate of axillary buds, shoot transectional symmetry, rooting ability, and so forth (Jones, 1990). In the current work it does not refer to reproductive competency, but to the change from the first soft needles to durable thick ones which we are used to see on pine trees.

In this study the term "heteroblastic" is used in the same sense that it was originally introduced by Karl Goebel (1898, 1913) to describe a form of plant development, in which substantial differences between earlier ("Jugendform" = juvenile form) and later stages ("Folgeform" = subsequent form) are observed as opposed to the "homoblastic" type of development with small and gradual changes.

Heterophylly describes differences in plant habit and morphology which has been associated with adaptation to light, nutrient and water availability, frost or protection against herbivory attack (Greenwood *et al.* 1977, Givnish *et al.* 1994, Zotz *et al.* 2011). Heteroblastic species include both relatively short-lived and long-lived taxa and ecological context of those plants is also diverse. It should verify that there is hardly a single cause behind this phenomenon, which justifies the diverse and partly contradictory hypotheses found in the literature regarding its possible function, but if the juvenile phase lasts longer, it is more likely the consequence of giving some advantages to the plant under current ecological conditions (Zotz *et al.* 2011). Mediavilla *et al.* (2013) stated that greater plasticity and more intense strategy shifts along ontogeny are necessarily associated with long leaf life span at maturity. It is suggested that heteroblastic species offer fascinating research opportunities for the study of general ecological and evolutionary questions concerning

developmental regulations, plant adaptation and speciation (Zotz *et al.* 2011).

2.3 Age-dependent changes in conifer needles

Heteroblastic change of pines has been described by Doak (1935) and Lester (1968): „After the cotyledonary stage, seedlings have only solitary needles, euphylls. Later, axillary shoots start developing; first, fascicles of juvenile needles appear in many species, followed by the distinctive dwarf shoots with clustered secondary needles.“ In most pine species, secondary needles are produced from the second vegetative period onward or even during the first growing season (Climent *et al.* 2006b). Juvenile needles are bluish, short, and elliptical in shape, while adult secondary needles are dark green and significantly longer and thicker (Climent *et al.* 2006b). In many Mediterranean species, such as *P. halepensis*, *P. pinea* and *P. canariensis* primary needles remain on the seedlings for a period of several years (Lester, 1968). Species investigated in current study - *P. pinea*, *P. halepensis* and *P. nigra* bear single juvenile needles in fascicles and paired needles as adults and keep juvenile needles for more than two years.

According to Niinemets (2002) young trees of *Picea abies* and *Pinus sylvestris* have lower needle dry mass and needle dry mass per unit area (LMA). Mediavilla *et al.* (2013) also reported of *Pinus pinea* and *Pinus pinaster* seedlings having lower leaf thickness and LMA. Apple *et al.* (2002) found that the needles of saplings of *Pseudotsuga menziesii* (Mirb.) were longer than the mature needles and had proportionally smaller vascular cylinders, larger resin canals, few hypodermal cells and few astrosclereids, which are lignified structures that are abundant in old trees needles and occupy space inside mesophyll and reduce an average of 11% of photosynthetic tissue. Boddi *et al.* (2002) stated that the juvenile needles of North Eubean (Greece) *P. halepensis* population didn`t have the morpho-anatomic characteristics of the mature pine needles, which are generally correlated with resistance to aridity. Boddi *et al.* (2002) suggest that the juvenile type needles may enable high photosynthesis. The conclusion of the study of Apple *et al.* (2002) was that the influence of tree age on needle anatomy is greater than that of canopy position or site differences and the differences in needle anatomy reflect the need for different ecological strategies during different periods in ontogeny.

2.3.1 Biochemical differences

Mediavilla *et al.* (2013) studies of *Pinus pinea* and Miller *et al.* (1995) research of *Juniperus occidentalis* revealed that juvenile plants have lower investments into needle biomass. The same study of Mediavilla *et al.* found that *Pinus pinea* adult needles contained more cellulose and hemicellulose, but juvenile needles supportive tissue had higher lignin content. *Juniperus occidentalis* juvenile needles had lower content of nitrogen per unit of foliar area (Miller *et al.* 1995). Research of Oleksyn *et al.* (1997) found that total phenols and glucose concentrations increased linearly with needle age in *Pinus heldreichii* and there were significant declines in water and nitrogen content with needle age. Niinemets (2002) concluded in a study based on 114 publications about photosynthetic and morphological data of *Picea abies* and *Pinus sylvestris* that needle nitrogen concentration was not correlated with tree age or height in either species and varied more than threefold among current year needles which was probably due to soil nutrient availability. Apple *et al.* (2002) explained plants investment into lignified hypodermal cells and astrosclereids with the need of defense against damage by abiotic and biotic factors. In the same study high structural investments were positively correlated with needle longevity. Niklas (1989, 1991) and Niinemets (2001) pointed out that higher fiber content may increase tolerance of low water potentials, but according to Parkhurst (1994), Syvertsen *et al.* (1995) and Hanba *et al.* (1999) this may also decrease the CO_2 diffusion conductance from intercellular air space to carboxylation sites in the chloroplasts.

2.3.2 Photosynthetic properties

Compared with small adults, juvenile *Juniperus occidentalis* plants have higher rates of CO_2 assimilation, leaf stomatal conductance, and transpiration (Miller *et al.* 1995). Nitrogen-use efficiency, light saturated net assimilation rates, foliar stomatal conductance to water vapor and biochemical foliage photosynthesis potentials (*V*cmax) decline with increasing tree age in *Picea abies* and *Pinus sylvestris* (Niinemets 2002). Juvenile foliage of *Juniperus occidentalis* has higher rates of CO_2 assimilation than adult ones and therefore also higher rates of water loss (Miller *et al.* 1995).

The study of Oleksyn *et al.* (1997) reveals that mass-based photosynthetic capacity (light saturated net photosynthesis rate, A_{sat}) decreased with needle age in *Pinus heldreichii* Christ and the variation in A_{sat} was linearly related to needle N concentration. Net assimilation rate per unit needle dry mass decreased with increasing tree age and net assimilation rate per unit projected area scaled positively with tree age in *Picea abies* and *Pinus sylvestris* (Niinemets 2002).

Niinemets (2002) hypothesized that the decline in V_{cmax} of old-tree needles result from increasing diffusive resistances between the needle intercellular air space and carboxylation sites in chloroplasts. Increased diffusive limitations may be the inevitable consequence of morphological adaptation (changes in needle dry mass per unit projected area and needle density) to greater water stress in needles of larger trees (Niinemets 2002).

2.4 Elevated temperature influence on leaf anatomy, photosynthesis and isoprene emission

There is quite good information on the factors controlling isoprene (2-methyl-1,3-butadiene, C_5H_8) emission (Niinemets *et al.* 2010, , 2015b, 2021, Sharkey *et al.* 2008, 2017, Sun *et al.* 2013), but little is known about its adaptation to temperature rise (Niinemets *et al.*, 2015a Sharkey, 2005, Hartikainen et al. 2009, Rasulov *et al.* 2010, Fares *et al.* 2011). Acclimation of foliage to growth temperature involves both structural and physiological modifications, but the relative importance of these two mechanisms of acclimation is poorly known, especially for isoprene emission responses (Rasulov *et al* 2015).

Several widespread tree species emit volatile organic compounds (VOCs) continuously throughout their life (Taipale *et al.* 2021) from which the most abundant one is isoprene (Guenther et al. 2006). Isoprene emission of ~ 600 Tg per year from plants is one of the largest hydrocarbon fluxes from the biosphere into the atmosphere (12). According to Loreto *et al.* (2015) isoprene is emitted by c. 20% of the perennial vegetation of tropical and temperate regions of the world. They also conclude that emission is nearly absent in C4, CAM and annual plants, but common in temperate perennials and deciduous plants. Isoprene emission from broadleaf trees is highly temperature dependent and has a profound effect on atmospheric chemistry (Li *et al.* 2011) as its reactions with hydroxyl radicals contribute to the formation of tropospheric ozone and

affect aerosol formation (Went, 1960, Trainer et al. 1987, Chameides et al. 1988, Fehsenfeld et al. 1992, Kindler-Scharr et al. 2009). Isoprene can also potentially affect current global climate change by lengthening the lifetime of greenhouse gases, such as methane (Li *et al.* 2011).

The role of isoprene in plants is to improve their thermotolerance (Sharkey *et al*. 1995, Singsaas *et al.* 1997) and it may also act as an antioxidant (Loreto *et al.* 2001a, 2001b) by reducing ozone damage and membrane peroxidation (Niinemets 2004). Peñuelas and Llusià (2002, 2003) have suggested that isoprene and monoterpenes can protect plants from heat stress by scavenging reactive oxygen species that are produced during heat stress. Loreto *et al*. (2015) suggested that isoprene emission may not have evolved to help plants face heavy or prolonged stresses, but rather assists C3 plants to run efficient photosynthesis and to overcome transient and mild stresses, especially during periods of active plant growth in warm seasons.

The response of plants to temperature rise and isoprene emission depends on the species, light, CO_2 and water availability (Sharkey *et al.* 1996) and in order to refine global models of isoprene emission it is necessary to find out the details of its release under different conditions in different plant groups. As one of predictions for climate change is the rising temperature on Earth it is important to understand its effect on vegetation.

3. AIM OF THE STUDY AND HYPOTHESES

The main goal of the doctoral thesis was to separate the roles of leaf anatomical, biochemical and physiological changes in determining the phenotypic variability in leaf photosynthetic activity during aging, in different aged leaves and upon acclimation to elevated temperature.

Hypotheses:

Article I

Needle anatomical modifications upon juvenile-to-adult transition lead to a trade-off between investments in support and photosynthetic tissues. Analogous changes occur with needle aging but to a lower degree.

Article II

Differences in juvenile, adult and different-age adult needles photosynthetic potentials, nitrogen use efficiency and mesophyll conductance are driven by structural, diffusional and chemical controls. Some of these differences contribute to juvenile plants early growth and establishment.

Article III

Acclimation to high growth temperature leads to improved heat resistance of foliage photosynthetic apparatus, and the temperature-dependent modifications are associated with improved leaf photosynthetic activity per unit dry mass as the result of ultrastructural changes. High growth leaf temperature also enhance leaf isoprene emissions and isoprene concentrations in leaf intercellular airspace.

4. MATERIAL AND METHODS

4.1 Description of studied species

The study included three evergreen conifer species - *Pinus halepensis* Mill., *Pinus nigra* J.F. Arnold, *Pinus pinea* L. - and a broad-leaved deciduous poplar hybrid *Populus tremula x tremuloides* Michx. These conifers stand out for keeping juvenile needles longer than average and the structure of the needles varies greatly with the age of the tree, which makes it possible to study the phenomena of heteroblasty. Selected Poplar hybrid is a promising biomass production culture and a strong isoprene emitter.

Pinus halepensis

Pinus halepensis Mill., the Aleppo pine, is growing in marls, limestone, dolomites, acid sands and sandstone, mostly in subhumid and semiarid climates from lowlands (up to 700 m) to submontane (from 700 to 1300 m) areas, and is the most drought tolerant of the three investigated species (Barbéro *et al.* 1998, Atzmon *et al.* 2004). Trees are up to 20 m tall and 80-100 cm diameter at breast height (dbh) (Mauri *et al.* 2016). Primary needles are formed three to four years before being replaced by secondary needles (Boddi *et al.* 2002). Juvenile pine needles are very different from adult ones. They are shorter and thinner than adult needles, solitary and have different cross-sectional shape, ellipsoidal or rhomboidal, compared to adult needles that have semi-elliptical (two-needled species) or sectorial (species with three or more needles in fascicles) shape (Climent *et al.* 2006). They are bluish in color while mature needles are dark green. Mature needles are in fascicles of 2(–3), 5–12 cm × 1 mm, twisted, edges minutely serrate, with stomata on all surfaces and arrayed along the branchlets rather sparsely. (Dallimore et al. 1967, Farjon, 1984) Needle life span in mature plants is 2.7 years (Niinemets, 2010). In the eastern Mediterranean area, *Pinus halepensis* forests are important for resin, fuelwood and forest honey production and also for livestock grazing (Moussouris et al. 1999).

Pinus nigra

Pinus nigra J. F. Arnold *subsp. salzmannii* (Dunal) Franco, the Austrian pine or black pine, prefers limestone, dolomites, acid sands and

volcanic (ultrabasic) rocks and mostly humid areas in mid-montane to mountainous (from 900–1000 m up to 1600–1800 m) areas (Kienast *et al*. 1987, Barbéro *et al*. 1998). It is Native to Algeria, Andorra, France, Morocco and Spain, at elevations of 400-1500 m (Farjon *et al*. 2013). It is widespread in Spain, both as natural stands and in plantation forestry (Farjon, 2010). Its value as a street tree is largely due to its resistance to salt spray (from road de-icing salt) and various industrial pollutants (including ozone), and its intermediate drought tolerance (Farjon, 2010). Trees of *Pinus nigra* are up to 50 m tall and 190 cm dbh, usually with a single round trunk and ascending branches forming a broad-conical to domed crown that flattens with age. Needles are in fascicles of 2 with a persistent 10-12 mm long sheath, straight to curved, stiff to flexible, (4-)8-16(-18) cm long and 1-2 mm thick, light to dark green, edges minutely serrate, apex acute, stomata in lines on both faces. (Farjon, 2010). Juvenile needles are shorter and thinner than adults, bluish in color and different in shape, with a cross-section of intermediate between sectorial and rhomboid shape (Kuusk *et al*. 2018a). Needle life span in mature plants is 3.8 years (Withington *et al.* 2006). Juvenile needles are kept at least 2 years and gradually replaced by adult needles.

Pinus pinea

Pinus pinea L., the stone pine, grows on dolomites and sandstone in subhumid climates, mostly at lowland to submontane areas, and its environmental requirements are in between *P. halepensis and P. nigra*. (Cabanettes *et al.* 1978, Barbéro *et al.* 1998). It is found throughout all the Mediterranean area and tends to naturalize in regions with Mediterranean climates (Viñas, *et al*. 2016). Stone pine is a source for a large variety of products such as nuts, wood, firewood, resins, bark, pastures/livestock, hunting and honey (Moussouris *et al.* 1999). Maximum mature tree height is reported to be 30 m (Climent *et al.* 2004) and over 200 cm dbh (Viñas, *et al*. 2016). Adult needles are mid-green, retained for 2-4 years (according to Mediavilla *et al.* 2014 - 4.1 years) with a persistent 1-1.5 cm sheath, in fascicles of two, 10-18(28) cm long, about 1.5 mm thick, with serrulate margins and fine lines of stomata on both faces (Frankis, 1999). The juvenile needles are glaucous, 1.5-4 cm long, and continue to be grown for 3-10 years, mixed with the first adult leaves from the third year. (https://www.conifers.org/pi/Pinus_pinea.php by Frankis, 1999)

Populus tremula x P. tremuloides

Hybrid aspen (*Populus tremula* L. × *P. tremuloides* Michx.) (syn. *Populus* × *wettsteinii* Hämet-Ahti) is a fast-growing hybrid species between European (*Populus tremula* L.) and North American (*Populus tremuloides* Michx.) aspen. It belongs to family *Salicaceae* and genus *Populus* (Tullus 2008). In the current study, the micropropagated clone H200 was used. Hybrid aspen is a strong isoprene emitter.

In Northern Europe hybrid aspen is one of the most promising species for short-rotation forestry and may meet the increasing demand for energy based on renewable resources. Hybrid aspen regenerates vegetatively, and it can be managed in several consecutive rotations without new establishment between rotations. No major negative environmental impacts have been found with the cultivation of hybrid aspen what is especially important when plantations are established on abandoned agricultural land or otherwise degraded land (Tullus *et al.* 2013). It has been planted extensively for almost 70 years in southern Sweden and it is suitable for both biomass production and traditional production of roundwood. Biomass is an important renewable resource as a substitute for less climate-friendly products, and forest species have the potential to sequester large amounts of carbon in northern latitudes. An increased use of woody biomass is probably a prerequisite to meeting future climate goals in the Nordic countries (Fahlvik 2021). According to Vares *et al*. 2003, since 2004, it has been allowed to grow hybrid aspen as forest wood in Estonia. The authors suggest that the species could be suitable for reforestation of abandoned agricultural land and depleted quarries. By 2005, nearly 700 ha of hybrid aspen plantations have been established and to date, a network of 51 permanent test sites covering Estonia has been established, where the suitability of the hybrid aspen for our conditions is being studied (Vares *et al.* 2003).

4.2 Measurement sites and plant growth conditions

The mature cone-bearing plants of *Pinus* species - *halepensis, nigra and pinea* were studied at Alto Tajo Natural Park which is situated in central Spain. The exact location is Los Cerrillos sampling site, Guadalajara, Castilla-La Mancha (40.8480°N, 2.1812°W). The climate in Alto Tajo is continental Mediterranean with hot and dry summers and cold and dry winters. The mean annual rainfall is 490 mm and mean annual

temperature is 10.2 °C. The site has a mean elevation of 950 m. Steep slopes and cliffs are covered with Mediterranean-type vegetation where *Quercus ilex*, L. subsp. *ballota* (Desf.) Samp. dominates on south-facing slopes and *P. nigra* subsp. *salzmannii* on north-facing slopes. The soil is basic, rocky and poorly developed over the limestone bedrock. (Kuusk *et al.* 2018a)

Five trees were randomly chosen for each species for sampling of needles of different age classes. Mean tree diameter at breast height for *P. halepensis* was 40 cm, mean tree height 15 m and estimated tree age 95 years. The corresponding values for *P. pinea* were 44 cm, 17 m and 90 years and for *P. nigra* 60 cm, 21 m and 100 years. Representative terminal branchlets which were carrying only needles and not cones were sampled from mid-height and from the southern aspect of upper canopy. They were exposed to a daily integrated quantum flux density of ~40 mol m^{-2} day^{-1}. (Kuusk *et al.* 2018a)

Studying juvenile plants and adults in the same environmental setting was challenging because juvenile plants were scarce and often shaded by other vegetation. Shade significantly alters foliage structure, which could confound comparisons (Poorter *et al.* 2009, Niinemets *et al.* 2015c, Keenan *et al.* 2016). Therefore, to avoid these shade effects and ensure experimental replicability, two year old juvenile plants were bought from a local nursery at El Seranillo Forestry Center, Guadalajara. They were transplanted to 5 L pots which were filled with a mixture (4:4:1:1, v/v) of compost, vermiculite, perlite and sand, with slow release N:P:K (14:13:13) fertilizer with micronutrients (Osmocote, Scotts Miracle-Gro Company, Marysville, OH, USA, Baquedano *et al.* 2007, Baquedano *et al.* 2008 for details). Juvenile saplings were grown at the greenhouses of Museo Nacional de Ciencias Naturales, CSIC, Madrid, Spain (40.440°N, 3.690°W, elevation 682 m). The pots had big holes in the bottom and were buried into soil. There were nine pots per m^2 and the soil temperature was ambient. The plants were grown under full sunlight with the mean daily integrated photosynthetic quantum flux density during spring of 41 mol m^{-2} day^{-1}. Current-year juvenile needles that had formed under the new growth conditions were used for the measurements. (Kuusk *et al.* 2018a)

Seedlings of hybrid aspen (*P. tremula* L. x *P. tremuloides* Michx.) clone H200 (more information about clone properties: Rasulov *et al.* 2009a,b

and 2011) were grown in 4 L plastic pots which were filled with a mixture of peat and sand (1:1). Plants were kept in growth chambers Percival AR-95 HIL (CLF PlantClimatics, GmbH, Wertingen, Germany) with contrasting temperature regimes (day/night) of 25/20 °C (lower temperature, control) and 35/27 °C (higher temperature). The ambient CO_2 concentration was between 380 and 420 μmol mol^{-1}. The relative humidity was maintained between 60 and 65% and the quantum flux density of 500 μmol m^{-2} s^{-1} was provided for 14 h. The plants were watered daily to field capacity. Hoagland nutrient solution was used for watering to ensure optimal supply of water and nutrients to the plants. All measurements were conducted with 20–24 days old leaves that were fully expanded and exhibiting peak physiological activity.

4.3 Foliage sampling and measurements of morphological and anatomical characteristics

Articles I and II

In October 2005 and in August 2006 samples from mature plants were collected. At the field site one branch from each individual was taken. The trees were randomly chosen mature plants growing in full sunlight. Samples were collected from the mid-height of the canopy to reduce the influence of light on needle characteristics (Gebauer *et al*. 2011, Niinemets *et al*. 2015c). In adult trees, secondary needles of different age classes with at least 50% needles present were studied. Three different age classes (current-year, 1-year-old and 2-year-old needles) were investigated in *P. nigra* and *P. pinea*. In *P. halepensis*, which has a shorter leaf life span than the other two species, current-year and 1-year-old needles were studied. The canopy of juvenile plants consisted of more than 90% of juvenile (primary) current-year needles and only this needle age class was studied. A minimum of 10 needles from each age class were randomly sampled from each branch. Altogether 190 (juvenile current year and mature different age classes) needles were measured for *P. halep*ensis, 290 for *P. pinea* and 310 for *P. nigra*. Needles for preparation of approximately 20-60 μm thick free-hand cross-sections for anatomical measurements were randomly selected from the set of harvested needles (a subsample of three needles) for each species, branch and age class. The sections taken from the central parts of the needles were stained with phloroglucinol and HCl to specifically discern the lignified tissues by red color (Weisner test) as described in Niinemets *et al*. 2007. The images were viewed under

light microscope Nikon Eclipse E600 at 20–100× magnification and digital pictures were taken with a Nikon digital DS-Fi1 camera (Nikon Corporation, Tokyo, Japan).

List of needle traits measured from light microscopy images, measured by digital calipers and calculated from the measured traits:

1. L total needle length (mm)
2. W needle width (mm)
3. T needle thickness (mm)
4. S_T needle total area (mm^2)
5. S_P needle projected area (mm^2)
6. needle cross-section width (mm)
7. needle cross-section thickness (mm)
8. U needle circumference (mm)
9. S_S needle cross-sectional area (mm^2)
10. area of the lignified tissues (mm^2)
11. S_T/S_P=U/W needle total to projected area ratio
12. V/S_T needle volume to total area ratio
13. S_S/W needle volume to projected area ratio

Measurement methods are described in Niinemets *et al.* 1995b and 2007.

Leaf samples for anatomical measurements under transmission electron microscope (TEM) were taken with a razor blade from the central part of the needles after gas-exchange measurements. Approximately 1 mm long pieces were fixed by infiltrating with buffered (0.2 M phosphate buffer, pH = 7.2) 2% glutaric aldehyde in a syringe under negative pressure, dehydrated in ethanol series and embedded in Epoxy Embedding Medium (Sigma-Aldrich Chemie, Steinheim, Germany) as described in Copolovici *et al*. 2011 and Bozzola *et al*. 1992. Semi-thin sections for light microscopy were cut with an OM U2 Ultra Microtome (American Optical Corporation, Reichert Products, Buffalo, NY, USA) using a 45° diamond knife (Diatome, Hatfield, PA, USA) and stained with Toluidine Blue as described in Burns, 1978 and Mercer, 1963 for 30 sec on a hotplate. Photos were taken with a Zeiss Axioplan 2 (Carl Zeiss Microscopy, Jena, Germany) at 40× magnification with 0.63 × lens and a digital camera AxioCam HRc (Carl Zeiss Microscopy, Jena, Germany).

Images were analyzed with UTHSCSA Image Tool for Windows Version 3.00 (UTHSCSA, Texas, USA 1995–2002).

Ultra-thin sections with a thickness of 70-100 nm were cut with the aforementioned Ultra Microtome and contrasted with 2% uranyl acetate in 50% ethanol solution for 2 minutes and in 0.2% lead citrate in 0.1 M sodium hydroxide solution for 2 minutes as described in Bozzola *et al.* 1992. Samples were viewed with a Philips Tecnai 10 TEM (FEI, Eindhoven, Netherlands) with an accelerating voltage of 80 kV. Images of ultra-thin sections were also analyzed with UTHSCSA Image Tool for Windows Version 3.00 (UTHSCSA, Texas, USA 1995–2002).

From the TEM images the following parameters were measured:

1. cell wall thickness (μm),
2. chloroplast length (μm),
3. chloroplast thickness (μm),
4. chloroplast circumference (μm),
5. epidermis area (μm^2),
6. endodermis area (μm^2),
7. hypodermis area (μm^2),
8. mesophyll area (μm^2),
9. mesophyll air spaces area (μm^2),
10. central cylinder area (μm^2),
11. resin ducts area (μm^2).

Measurements were made as described in Niinemets *et al.* 2007.

Mesophyll (Sm/S_p) and chloroplast (Sc/S_p) surface area exposed to intercellular air space per unit of projected leaf area were measured from the TEM micrographs and calculated according to Evans *et al.* (1994) using a curvature correction factor of 1.27 (Thain 1983).

The volume of mesophyll per needle projected area (Vm/S_p) and the volume of chloroplasts per projected area (Vc/S_p) were calculated, and the fraction of chloroplasts in needle cross-section ($f$chl), was calculated as $V_c/V_m f_{ma}$, where f_{ma} is the fraction of mesophyll in needle cross-section without intercellular air space. Needle fresh mass, dry mass, nitrogen (N_m) and carbon (C_m) contents per dry mass were also measured as described in Kuusk *et al.* 2018a.

Following characteristics were further calculated:

$M_{A,T}$ needle dry mass per unit area,
D needle density (g cm^3),
needle dry to fresh mass ratio,
$M_{A,P}$ needle dry mass (per projected area),
$N_{A,P}$ needle nitrogen content (per projected area),
V/S_T needle volume to total area ratio.

Carbon and nitrogen contents were measured using pulverized oven-dried (48 h at 70 °C) needles with a Perkin Elmer series II CHNS/O Analyzer 2400 (Perkin Elmer Life and Analytical Sciences, Inc., Boston, MA; USA). (Kuusk *et al.* 2018a)

Article III

Immediately after the gas-exchange measurements, leaf discs of 4 cm^2 were taken between the major leaf veins for estimation of leaf fresh and dry mass. The fresh mass of the leaf discs was estimated immediately and the dry mass after drying in an air-ventilated oven at 70 °C for at least 48 h. For anatomical measurements, leaf samples were taken with a razor blade between the major veins from the central part of the leaves and cut into approximately 1 × 1 mm pieces for fixation. The samples were fixed by infiltrating with buffered (0.2 M phosphate buffer, pH = 7.2) 2% glutaric aldehyde, dehydrated in ethanol series and embedded in Epoxy Embedding Medium (Sigma-Aldrich Chemie, Steinheim, Germany). Semi-thin (1.5–2 μm) cross- and paradermal sections and ultrathin (70–90 nm) cross-sections were cut with a Leica EM UC7 ultramicrotome (Leica Mikrosysteme GmbH, Vienna, Austria) equipped with a 45° diamond knife (Diatome, Hatfield, PA, USA). Exact protocol is to be found in Copolovici *et al*. 2011. The semi-thin sections were stained for 30 s with Toluidine Blue as described in Burns, 1978 and Mercer, 1963, viewed at 400–1000× magnification with a Zeiss Axioplan 2 microscope and the digital images were taken with an AxioCam HRc (Carl Zeiss Microscopy, Jena, Germany).

Five cross-sections per leaf sample were measured in three locations for:

1. total leaf thickness (μm),
2. palisade mesophyll thickness (μm),

3. spongy mesophyll thickness (μm),
4. chloroplast count (for article III),
5. cell count (for article III).

Chloroplast and cell numbers were estimated from 10 paradermal sections per sample. Five sections were cut through the palisade and five through the spongy mesophyll. From these measurements, the chloroplast number per leaf area (*n*chl) was calculated as:

$$n_{chl}=n_{c,p}n_{chl,p,p}n_{chl,p,c}+n_{c,s}n_{chl,s,p}n_{chl,s,c},$$

where $n_{c,p}$ is the number of cells in the palisade and $n_{c,s}$ is the number of cells in the spongy parenchyma per unit leaf area. $n_{chl,p,p}$ is the chloroplast number per cell in the palisade parenchyma estimated from the paradermal section and $n_{chl,p,c}$ is the chloroplast number per cell estimated from the cross-section. $n_{chl,s,p}$ is the chloroplast number in the spongy parenchyma estimated from the paradermal section and $n_{chl,s,c}$ is the chloroplast number in the spongy parenchyma estimated from the cross-section.

Ultrathin sections for TEM were contrasted with uranyl acetate and lead citrate (Copolovici *et al.* 2011 for details) and samples were viewed with a Philips Tecnai 10 TEM (FEI, Eindhoven, the Netherlands) with an accelerating voltage of 80 kV. Digital images were taken with Olympus Veleta 2K × 2K sidemounted TEM CCD camera (Olympus Soft Imaging Solutions GmbH, Germany, Münster, Germany). Magnifications of 7000–10000× were used to take pictures from where to measure: chloroplast length, chloroplast thickness and chloroplast area (ca. 40 chloroplasts were measured in each case) along with cell wall thickness and chloroplast distance from cell wall. All anatomical characteristics were separately measured for palisade and spongy mesophyll. Digital image analysis was carried out with UTHSCSA Image Tool for Windows ver. 3.00 (UTHSCSA, San Antonio, TX, USA).

4.4 Gas exchange measurements

Article II

Gas-exchange measurements were carried out with a Li-Cor 6400 portable gas-exchange system equipped with leaf chamber fluorimeter

with a window area of 2 cm^2 (Li-Cor, Inc., Lincoln, NE, USA). Needles were enclosed side by side to avoid overlap between the needles. Standard environmental conditions of chamber were: block temperature of 25 °C, ambient CO_2 concentration of 400 μmol mol^{-1}, quantum flux density of 2000 μmol m^{-2} s^{-1} (10% blue light). Needles were conditioned in the chamber until stomata opened and steady-state gas-exchange rates were established, which usually it took 30 minutes. After reaching the steady state, the CO_2 response curve was measured first, followed by the light response curve. For the CO_2 response curve, CO_2 concentrations were prepared in sequence of 400, 600, 900, 1200, 1600, 200, 300, 200 and 50 μmol mol^{-1} and steady-state rates of net assimilation were recorded at each CO_2 concentration. For measuing the light response curve, light intensity was changed in the sequence of 1200, 1800, 800, 500, 250, 125, 80, 30 and 0 μmol m^{-2} s^{-1} and steady-state rates at each light level were recorded. At the end of the measurements, light was switched off and the rate of dark respiration was measured when the cuvette temperature stabilized and leaf gas-exchange reached a steady state, typically in 4-5 min after switching off the light. At each CO_2 and light level a saturating light flash of 6800 μmol m^{-2} s^{-1} was given to estimate the effective quantum yield of photosystem II. (Kuusk *et al.* 2018b)

Article III

An ultra-fast gas-exchange system (system half-time of approximately 0.15 s) was used for the photosynthesis measurements (Laisk *et al*. 2002; Rasulov *et al*. 2010). In this system the leaf is enclosed in a clip-on type leaf chamber with a volume of 2.4 cm^3 and a cross-sectional area of 8.04 cm^2 by glueing upper leaf surface to the chamber glass window by starch paste. The leaf chamber has a thermostatic water jacket and the temperature of the chamber is constantly measured to prevent overheating. Fast measurement of transient physiological responses is achieved by two identical gas lines where different gas concentrations can be prepared and almost instantaneously switched (in less than 1 s) between the sample and the reference line. Delays in the detection of leaf gas-exchange response signals are avoided because stabilization of gas concentrations is not required. The enclosed leaf area was illuminated with a Schott KL 1500 light source equipped with a heat-reflecting filter (Optical Coating Laboratory, CA, Santa Rosa, USA). The air was mixed from pure nitrogen, oxygen and CO_2 using calibrated dynamic mixers,

and the air flow rate through the system was kept at 0.5 mmol s^{-1} (Laisk *et al*. 2002). A LI-6251 infrared gas analyser (LI-Cor, Inc., Lincoln, NE, USA) was used to measure the CO_2 concentration. A custom-made micropsychrometer

was used for the water vapour concentration and a proton transfer reaction mass spectrometer (PTR-MS, highsensitivity version; Ionicon Analytik GmbH, Innsbruck, Austria) for the isoprene concentration. The response time of the PTR-MS was approximately 0.1 s and the isoprene detection limit about 10 pmol mol^{-1}. The instrument was calibrated with an isoprene standard mixture of 5.74 μmol mol^{-1} isoprene in N2 (Hills Scientific, Boulder, CO, USA).

The standard conditions used in these experiments were the leaf chamber CO_2 concentration of 360 μmol mol^{-1}, O_2 concentration of 21%, leaf temperature of 30 °C, light intensity (photosynthetic quantum flux density) of 650 μmol m^{-2} s^{-1} and water vapour pressure deficit between the leaf and the atmosphere (V_D) of 1.7 kPa.

The measurements were conducted with attached leaves. All measurements began with leaf enclosure, leaf stabilization under the standard conditions until the steady-state rates of CO_2 and H_2O vapour exchange, and isoprene emission were established. After that either CO_2 (360 versus 1200 μmol mol^{-1}), O_2 (21 versus 2%), light (quantum yield measurements) or temperature (temperature response curves) were changed to measure different environmental responses.

Temperature response curves were measured as described in Rasulov *et al*. (2010) by changing leaf temperature in steps of 5 °C and each temperature change was followed by returning to the standard temperature and leaf stabilization. Chamber air water vapour concentration was adjusted at each temperature to maintain the constant V_D and avoid changes in stomatal conductance because of altered V_D.

The quantum yields for CO_2 exchange (α_{CO2}) and isoprene emission (α_I) were measured over the incident light range of 20–75 μmol m^{-2} s^{-1} where the influence of the Kok effect is negligible. In addition, the initial slopes of the net assimilation versus CO_2 response curves over an ambient CO_2 range of 0–100 μmol mol^{-1} at both O_2 concentrations of 21 and 2% were also measured at the standard light intensity of 650 μmol m^{-2} s^{-1}.

All leaf gas-exchange characteristics were calculated according to von Caemmerer and Farquhar (1981). The maximum carboxylase activity or Rubisco (V_{cmax}) was estimated from the initial slopes of the CO_2 response curve at both O_2 concentrations and the capacity for photosynthetic electron transport (J_{max}) from the high-CO_2 concentration (1200 μmol mol^{-1}) measurements according to Niinemets *et al.* (1999b).

Measurements of chlorophyll fluorescence

A PAM 101 fluorimeter (Walz GmbH, Effeltrich, Germany) was used to simultaneously measure chlorophyll fluorescence characteristics alongside CO_2 and water vapor exchange.

A Schott KL 1500 light source was used to emit saturated pulses of white light at 14 000 μmol m^{-2} s^{-1} for 2 seconds, allowing for the measurement of either the dark-adapted (*F*m) or light-adapted ($F_{m'}$) maximum fluorescence yields. Additionally, another Schott KL 1500 lamp, equipped with a 720-nm narrow-pass interference filter (Andover Corp., Salem, NH, USA), provided far-red light to estimate the dark-adapted minimum fluorescence yield (F_0). The fluorimeter operated at a frequency of 1.6 kHz for darkened leaves and 100 kHz for illuminated leaves during saturated pulses. F_m and F_0 were typically recorded 20 minutes after the leaves were darkened. The dark-adapted PSII quantum yield was calculated as $(F_m - F_0)/F_m$, while the quantum yield of illuminated leaves, ΦPSII, was determined as $(F_{m'} - F)/F_{m'}$, where F represents the steady-state fluorescence yield. The rate of photosynthetic electron transport from chlorophyll fluorescence (J_{ETR}) was further calculated using the formula from Schreiber et al. (1994):

$$J_{ETR} = \Phi_{PSII} \xi \beta Q,$$

where Q = incident quantum flux density,
ξ = leaf absorptance (0.86 for the control and 0.81 for the high temperature-grown plants),
β = fraction of absorbed light used to drive PSII electron transport (taken as 0.5 in this study). Rasulov *et al.* 2015

4.6 Data analysis

Articles I and II

Differences in average trait values among study years, needle ages and among adult and juvenile trees were tested by ANOVA followed by Tukey's post-hoc tests with Statistica 6 (StatSoft Inc., Tulsa, USA) and R 3.1.1 with default packages (R Development Core Team, 2012) as in Kuusk *et al.* (2018). As the year of study was not significant in any of the analyses, it was removed from the final analyses. Two-way ANOVAs were used to test for effects of species and heteroblasty among current-year needles, and effects of species and needle age among adult needles. Relationships among leaf traits were explored by linear (Pearson) correlation and non-linear regression analyses. All statistical effects were considered significant at $P < 0.05$. The data accompanying this article are available from the Dryad Digital Repository. (Kuusk *et al.* 2018b)

Article III

Carbon fraction that was used for isoprene emission was calculated like in Niinemets *et al.* 1999a:

$$6I/A,$$

where I = the isoprene emission rate and A = the net assimilation rate. It is considered that for the formation of one molecule of isoprene fixation of six molecules of CO_2 is needed. The temperature responses of net assimilation rate, photosynthetic electron transport rate and isoprene emission characteristics (trait pi) were fitted by an Arrhenius-type temperature response function with an optimum:

$$p_{\mathrm{i}} = \frac{e^{c_{\mathrm{i}} - \Delta H_{\mathrm{a,i}}/RT}}{1 + e^{(\Delta S_{\mathrm{i}} T - \Delta H_{\mathrm{d,i}})/RT}}$$

where c_{i} is the scaling constant for the trait i, ΔHa,i (J mol^{-1}) is the activation energy, ΔHd,i (J mol^{-1}) is the deactivation energy, ΔS_{i} (J mol^{-1} K^{-1}) is the entropy term, T (K) is the leaf temperature and R (8.314 J mol^{-1} K^{-1}) is the gas constant. The temperature optimum for the trait i, $T_{\mathrm{opt,i}}$, (Niinemets *et al* 1999b) was further calculated as:

$$T_{\mathrm{op,i}} = \frac{\Delta H_{\mathrm{d,i}}}{\Delta S_{\mathrm{i}} + R\ln\left(\frac{\Delta H_{\mathrm{d,i}}}{\Delta H_{\mathrm{a,i}}} - 1\right)}$$

Treatment means for all traits (n = 4–32) were compared by analyses of variance (ANOVA) using Statistica 6.0 (StatSoft, Inc., Tulsa, OK, USA) and the growth temperature effects were considered significant at P < 0.05. (Rasulov *et al* 2015)

5. RESULTS

5.1 Needle structure and age

Cross-sections of adult needles showed a clear visual difference between each other and juvenile needles in both shape and size (Figure 1, Table 1). The cross-sections of the juvenile needles of *P. halepensis* were rhomboidal, those of P. pinea sectorial and those of *P. nigra* intermediate between sectorial and rhomboidal shape while the adult needles had a hemi-elliptical cross-section shape (Figure 1).

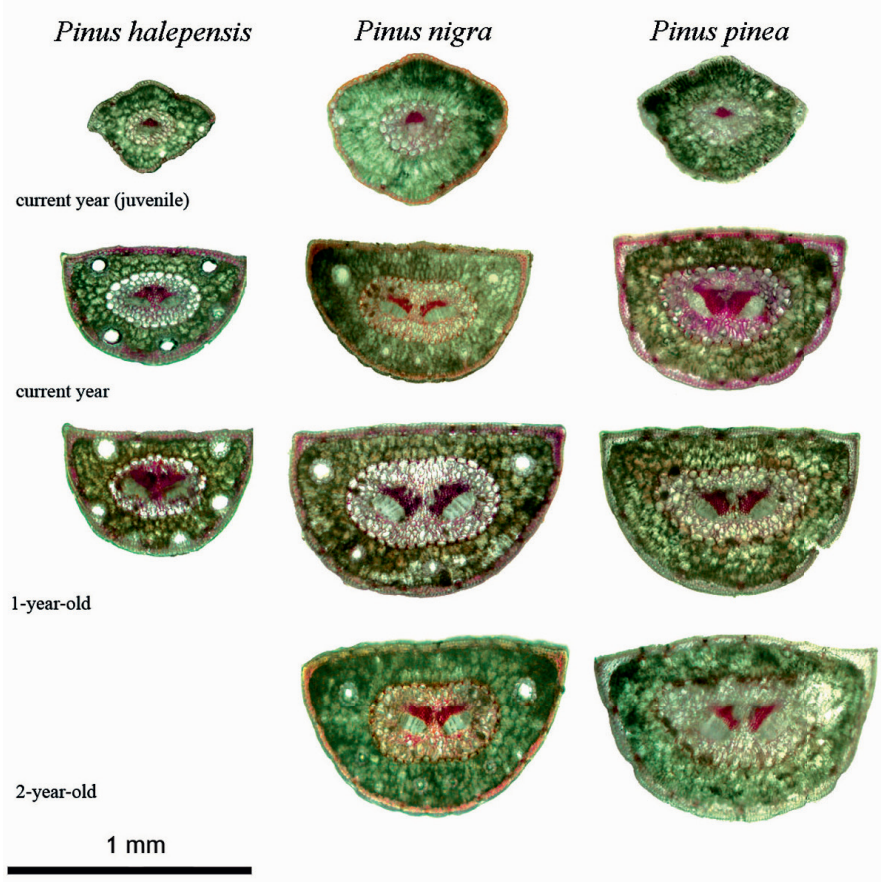

Figure 1
Free-hand needle cross-sections of juvenile (primary) current-year and different-aged adult (secondary) needles in three Mediterranean pine species under light microscope. Needle cross-sections were stained with phloroglucinol to reveal lignified tissues.
(Figure reproduced from Kuusk *et al.* 2018a)

Table 1. Effects of tree and needle age on average (±SE) needle linear dimensions (thickness (T), width (W), circumference (U)), needle total area (ST) and total to projected area ratio (ST/SP) in the three Mediterranean *Pinus* species. Table reproduced from Kuusk *et al.* 2018a.

Species	Tree age class	Need-le age	*T* (mm)	*W* (mm)	*U* (mm)	S_T (mm2)	S_T/S_p
P. halepensis	Seedling	(juv)	0.431 ± 0.014^{a}	0.541 ± 0.015^{a}	1.412 ± 0.042^{a}	19.1 ± 0.8^{a}	2.608 ± 0.015^{a}
P. halepensis	Mature	(m0)	0.478 ± 0.016^{a}	0.738 ± 0.017^{a}	2.065 ± 0.043^{ab}	26.1 ± 1.0^{a}	2.798 ± 0.017^{bc}
P. halepensis	Mature	(m1)	0.479 ± 0.014^{a}	0.773 ± 0.018^{a}	2.21 ± 0.06^{bc}	28.7 ± 0.5^{ab}	2.862 ± 0.043^{c}
P. nigra	Seedling	(juv)	0.615 ± 0.012^{b}	0.727 ± 0.036^{a}	1.95 ± 0.10^{ab}	24.4 ± 1.7^{a}	2.69 ± 0.07^{ab}
P. nigra	Mature	(m0)	0.579 ± 0.010^{b}	1.008 ± 0.020^{b}	2.85 ± 0.08^{cd}	37.7 ± 1.2^{bc}	2.826 ± 0.026^{bc}
P. nigra	Mature	(m1)	0.637 ± 0.024^{b}	1.126 ± 0.036^{ab}	3.14 ± 0.09^{de}	44.3 ± 1.4^{c}	2.789 ± 0.034^{bc}
P. nigra	Mature	(m2)	0.660 ± 0.028^{b}	1.179 ± 0.042^{ab}	3.29 ± 0.10^{de}	43.0 ± 1.6^{c}	2.792 ± 0.032^{bc}
P. pinea	Seedling	(juv)	0.644 ± 0.019^{b}	0.74 ± 0.09^{a}	2.02 ± 0.26^{ab}	28.3 ± 1.5^{ab}	2.722 ± 0.036^{abc}
P. pinea	Mature	(m0)	0.612 ± 0.027^{b}	1.134 ± 0.032^{ab}	3.15 ± 0.08^{de}	42.4 ± 1.7^{c}	2.778 ± 0.021^{abc}
P. pinea	Mature	(m1)	0.674 ± 0.025^{b}	1.33 ± 0.12^{b}	3.68 ± 0.36^{e}	46.8 ± 5.6^{c}	2.760 ± 0.023^{abc}
P. pinea	Mature	(m2)	0.651 ± 0.019^{b}	1.250 ± 0.017^{b}	3.41 ± 0.06^{de}	44.1 ± 1.5^{c}	2.726 ± 0.017^{abc}
F-values for two-way ANOVA (juvenile vs adult current-year needles)							
Tree age (*F*1,32)			0.22 ns	134.9***	155.0***	83.2***	18.7***
Species (*F*2,32)			38.3***	59.0***	57.0***	39.8***	1.02 ns
Tree age × Species (*F*2,32)			2.64 ns	4.91*	3.55*	3.04 ns	1.79 ns
F-values for two-way ANOVA (adult needles of different age)							
Needle age (*F*2,51)			3.72*	4.85*	4.09*	2.77 ns	0.63 ns
Species (*F*2,51)			29.7***	42.7***	36.6***	28.7***	3.17 ns
Needle age × Species (*F*3,51)			1.16 ns	1.13 ns	0.96 ns	0.36	1.11 ns

n = 5–8 (on average 6.7) for all average values. Seedlings were two years old and 0.2–0.3 m tall at the time of sampling, while the mean height of mature trees was 15 m for *P. halepensis*, 17 m for *P. pinea* and 21 m for *P. nigra* at the time of sampling. Needle ages as: juv, juvenile current year; m0, mature current year; m1, mature one-year-old; m2, mature two-year-old needles. Different letters denote statistical significance of average values for different species and needle age class combinations at $P < 0.05$ (one-way ANOVA followed by a Tukey post-hoc test based on *F*10,63). In the case of two-way ANOVA, significance levels as: *$P < 0.05$, **$P < 0.01$, ***$P < 0.001$, ns, not significant.

Measuring the needles revealed that thickness of juvenile and adult current-year needles was similar, but juvenile needles were narrower and had smaller circumference and cross-sectional area than adult needles (Table 1).

Needle shape determined lower total to projected area ratio (S_T/S_p) of juvenile needles compared to adults, but *P. nigra* was an exception. The S_T/S_p of juvenile and current-year adult needles of this species was similar (Table 1).

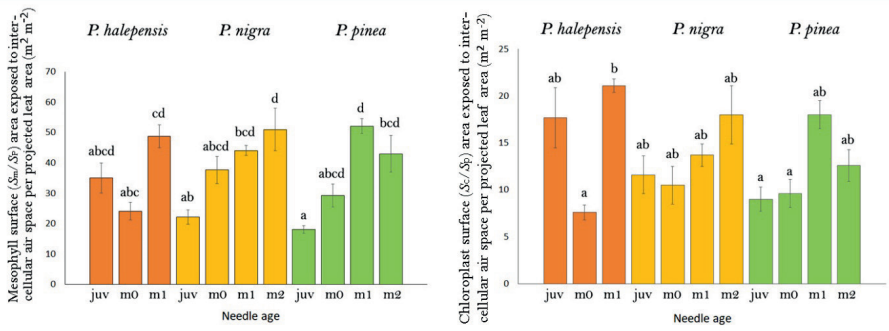

Figure 2
Mesophyll surface area (S_m/S_p) and chloroplast surface area (S_c/S_p) exposed to intercellular air space per projected leaf area (m^2 m^{-2}).

Needle dry mass per unit total ($M_{A,T}$) and projected area ($M_{A,P}$, Table 2.) was lower in juvenile than in adult needles in all species. Analysis of the variation showed that $M_{A,T}$ components – needle volume to total area ratio (V/S_T) were lower than current-year adults in juvenile needles of all species, and needle density (D) was lower in juvenile needles of *P. nigra*.

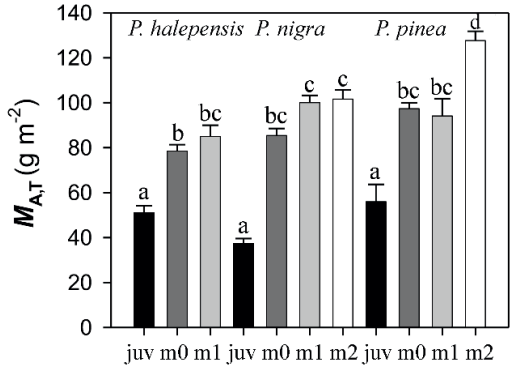

Figure 3
Differences in leaf dry mass per unit total needle area ($M_{A,T}$) in dependence of needle and plant age in *Pinus halepensis*, *P. nigra* and *P. pinea*. Needle ages are: juv = juvenile current year, m = mature current year, m1 = mature 1-year-old, m2 = mature 2-year-old. Data correspond to average ±SE values of 5-8 replicates. Different letters show statistical significance among needle age classes and species at $P < 0.05$ (ANOVA followed by a Tukey post-hoc test). Figure reproduced from Kuusk *et al*. 2018a.

Needle dry to fresh mass ratio was lower for juvenile than for adult current-year needles in *P. halepensis*. Among adult needles in mature trees, needle linear dimensions (needle thickness, width and circumference) increased a bit with needle age (Table 1). Lignified cell walls (stained red with phloroglucinol) occurred in the area of epidermis, hypodermis, endodermis, xylem and also partly the cells of the transfusion tissue that surrounds the vascular bundles in the central cylinder and were visibly greater in adult than in juvenile needles (Figure 1). The volume fraction of epidermal tissues was lower in juvenile than in adult current-year needles of *P. halepensis* and current-year needles of *P. nigra*, and the fraction of central cylinder was lower in juvenile than in adult needles in all species. The total fraction of mechanical tissues (epidermal tissues together with the central cylinder) was in all cases lower in juvenile than in adult current-year needles (Table 2). The volume fraction of resin ducts was smaller, and the fractions of total mesophyll, mesophyll without air spaces, mesophyll air spaces and chloroplasts were greater in juvenile than in adult current-year needles (Table 2).

Table 2. Variations in needle dry mass pear unit area ($M_{A,P}$) dry to fresh mass ratio ($R_{D/F}$), Density (D) and carbon content (C_m) in relation to tree and needle age in three Mediterranean *Pinus* species. Table reproduced from Kuusk *et al*. 2018a.

Species	Tree age class	Needle age	$M_{A,P}$ (g m^{-2})	$R_{D/F}$ (g g^{-1})	D (g cm^{-3})	C_m (%)
P. halepensis	Seedling	(juv)	133 ± 9^{a}	0.393 ± 0.007^{a}	0.555 ± 0.026^{bc}	48.12 ± 0.15^{a}
P. halepensis	Mature	(m0)	219 ± 8^{b}	0.4687 ± 0.0035^{cd}	0.611 ± 0.027^{c}	50.62 ± 0.61^{cde}
P. halepensis	Mature	(m1)	244 ± 16^{bc}	0.514 ± 0.010^{e}	0.586 ± 0.034^{c}	51.3 ± 0.6de
P. nigra	Seedling	(juv)	99.9 ± 4.8^{a}	0.357 ± 0.007^{a}	0.308 ± 0.021^{a}	49.71 ± 0.31^{abc}
P. nigra	Mature	(m0)	241 ± 7^{bc}	0.3798 ± 0.0021^{a}	0.498 ± 0.023^{bc}	49.50 ± 0.11^{abc}
P. nigra	Mature	(m1)	279 ± 8^{bc}	0.472 ± 0.019^{cde}	0.518 ± 0.038^{bc}	51.54 ± 0.20^{de}
P. nigra	Mature	(m2)	284 ± 12^{c}	0.511 ± 0.010^{de}	0.501 ± 0.032^{bc}	52.24 ± 0.33^{e}
P. pinea	Seedling	(juv)	153 ± 23^{a}	0.4009 ± 0.005^{ab}	0.44 ± 0.06^{ab}	50.15 ± 0.11^{bcd}
P. pinea	Mature	(m0)	270 ± 8^{bc}	0.382 ± 0.007^{a}	0.495 ± 0.019^{bc}	48.78 ± 0.26^{ab}
P. pinea	Mature	(m1)	260 ± 21^{bc}	0.4442 ± 0.0006^{bc}	0.464 ± 0.041^{bc}	49.28 ± 0.08^{abc}
P. pinea	Mature	(m2)	347 ± 9^{c}	0.484 ± 0.008^{cde}	0.611 ± 0.023^{c}	49.09 ± 0.22^{abc}
F-values for two-way ANOVA (juvenile vs adult current-year needles)						
Tree age (*F*1,32)			164.7***	26.4***	22.2***	0.013 ns
Species (*F*2,32)			7.35**	64.6***	14.9***	0.40 ns
Tree age × Species (*F*2,32)			3.67*	29.9***	3.37*	29.8***
F-values for two-way ANOVA (adult needles of different age)						
Needle age (*F*2,51)			12.5***	78.6***	2.45 ns	13.1***
Species (*F*2,51)			6.65**	37.8***	7.20*	32.5***
Needle age × Species (*F*3,51)			3.38*	2.25 ns	2.14 ns	4.9**

Table 3. Average (±SE) volume fractions of different needle tissues in three Mediterranean *Pinus* species in dependence on needle and tree ages. Table reproduced from Kuusk *et al*. (2018a)

Species	Tree age class	Needle age	Tissue volume fraction							
			Total mecha-nical	Epidermal tissues	Central cylinder	Resin ducts	Total meso-phyll	Mesophyll air spaces	Mesophyll without air spaces	Chloroplasts
P. halepensis	Seedling	juv	0.317 ± 0.015^{a}	0.122 ± 0.006^{ab}	0.195 ± 0.012^{a}	0.0262 ± 0.0023^{a}	0.657 ± 0.015^{d}	0.162 ± 0.014^{cd}	0.495 ± 0.015^{de}	0.088 ± 0.021^{b}
P. halepensis	Mature	m0	0.4908 ± 0.0041^{d}	0.2160 ± 0.0022^{c}	0.2745 ± 0.005^{bc}	0.081 ± 0.011^{d}	0.428 ± 0.006^{a}	0.106 ± 0.0056^{abc}	0.322 ± 0.007^{a}	0.0223 ± 0.0030^{a}
P. halepensis	Mature	m1	0.474 ± 0.009^{d}	0.202 ± 0.009^{c}	0.272 ± 0.010^{b}	0.0729 ± 0.0033 ^{cd}	0.453 ± 0.007^{ab}	0.102 ± 0.010^{abc}	0.351 ± 0.007^{ab}	0.053 ± 0.006^{ab}
P. nigra	Seedling	juv	0.267 ± 0.008^{a}	0.1006 ± 0.0034^{a}	0.1664 ± 0.0051^{a}	0.0193 ± 0.0010^{a}	0.714 ± 0.007^{e}	0.1963 ± 0.0034^{d}	0.517 ± 0.005^{e}	0.058 ± 0.010^{ab}
P. nigra	Mature	m0	0.410 ± 0.006^{bc}	0.1494 ± 0.0047^{b}	0.260 ± 0.007^{b}	0.0341 ± 0.0039^{a}	0.556 ± 0.006^{c}	0.117 ± 0.015^{bc}	0.439 ± 0.019^{cd}	0.0418 ± 0.0030^{ab}
P. nigra	Mature	m1	0.3959 ± 0.0049^{b}	0.1310 ± 0.0026^{ab}	0.265 ± 0.006^{b}	0.0360 ± 0.0018^{ab}	0.568 ± 0.006^{c}	0.133 ± 0.007^{bc}	0.435 ± 0.011^{cd}	0.0301 ± 0.0043^{a}
P. nigra	Mature	m2	0.394 ± 0.008^{b}	0.113 ± 0.011^{ab}	0.281 ± 0.007^{bc}	0.0406 ± 0.0019^{ab}	0.565 ± 0.009^{c}	0.1251 ± 0.0029^{bc}	0.440 ± 0.009^{cd}	0.028 ± 0.007^{a}

P. pinea	Seedling	juv	0.3061 ± 0.0029^{a}	0.113 ± 0.014^{ab}	0.193 ± 0.011^{a}	0.0246 ± 0.0020^{a}	0.6693 ± 0.0032^{de}	0.191 ± 0.009^{d}	0.478 ± 0.009^{de}	0.083 ± 0.018^{b}
P. pinea	Mature	m0	0.468 ± 0.016^{d}	0.132 ± 0.008^{ab}	0.335 ± 0.009^{d}	0.0340 ± 0.006^{ab}	0.493 ± 0.017^{b}	0.127 ± 0.016^{bc}	0.365 ± 0.012^{ab}	0.0211 ± 0.0023^{a}
P. pinea	Mature	m1	0.4711 ± 0.009^{d}	0.1315 ± 0.0047^{ab}	0.340 ± 0.012^{d}	0.0755 ± 0.0021^{cd}	0.453 ± 0.008^{ab}	0.049 ± 0.012^{a}	0.404 ± 0.010^{bc}	0.044 ± 0.016^{ab}
P. pinea	Mature	m2	0.4545 ± 0.0033^{cd}	0.128 ± 0.006^{ab}	0.3262 ± 0.0047^{cd}	0.0559 ± 0.0015^{bc}	0.4896 ± 0.0045^{b}	0.0779 ± 0.0032^{ab}	0.412 ± 0.006^{bc}	0.0285 ± 0.0030^{a}
F-values for two-way ANOVA (juvenile vs adult current-year needles)										
Tree age (*F*1,19)			284.7***	35.3***	176.0***	27.6***	339.6***	33.2***	90.0***	25.1***
Species (*F*2,19)			17.4***	11.6***	14.8***	10.5***	27.5**	1.54 ns	12.9***	0.11 ns
Tree age × Species (*F*2,19)			0.84 ns	6.48**	5.29*	6.61**	3.80*	0.32 ns	4.34*	3.05 ns
F-values for two-way ANOVA (adult needles of different age)										
Needle age (*F*2,26)			1.42 ns	4.09*	0.18 ns	3.67*	0.44 ns	2.56 ns	2.60 ns	2.70 ns
Species (*F*2,26)			45.6***	51.9***	44.9***	33.3***	79.2***	7.22**	27.8***	0.50 ns
Needle age × Species (*F*3,26)			0.43	1.53 ns	1.23 ns	6.81**	3.35*	5.60**	1.40 ns	4.11*

F-values for two-way ANOVA (juvenile vs adult current-year needles)										
Tree age (*F*1,19)			284.7***	35.3***	176.0***	27.6***	339.6***	33.2***	90.0***	25.1***
Species (*F*2,19)			17.4***	11.6***	14.8***	10.5***	27.5**	1.54 ns	12.9***	0.11 ns
Tree age × Species (*F*2,19)			0.84 ns	6.48**	5.29*	6.61**	3.80*	0.32 ns	4.34*	3.05 ns
F-values for two-way ANOVA (adult needles of different age)										
Needle age (*F*2,26)			1.42 ns	4.09*	0.18 ns	3.67*	0.44 ns	2.56 ns	2.60 ns	2.70 ns
Species (*F*2,26)			45.6***	51.9***	44.9***	33.3***	79.2***	7.22**	27.8***	0.50 ns
Needle age × Species (*F*3,26)			0.43	1.53 ns	1.23 ns	6.81**	3.35*	5.60**	1.40 ns	4.11*

n = 3–6 for each average. Data presentation and statistical analyses as in Table 1. [1] The fraction of total mechanical tissues is the sum of epidermal tissues and central cylinder, the fraction of epidermal tissues includes epidermis and hypodermis and the total mesophyll fraction corresponds to mesophyll with intercellular air spaces

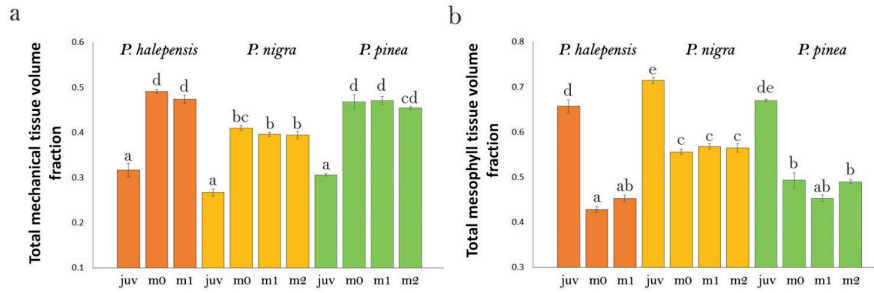

Figure 4
Total mechanical tissue volume fraction and total mesophyll tissue volume fraction according to needle age, showing that the total fraction of mechanical tissue is in all cases lower in juvenile than in adult needles and vice versa is true for mesophyll tissue.

Among the adult needles, leaf tissue distribution was weakly affected by needle age (Table 2), but significantly by species: *P. halepensis* and *P. pinea* had greater fractions of mechanical tissues and a lower fraction of mesophyll than *P. nigra*. The correlation between mechanical and mesophyll tissue fractions were negative. The fraction of chloroplasts and the fraction of mesophyll with and without air space were positively correlated. The volume fraction of epidermal tissues scaled positively with needle density and with needle dry to fresh mass ratio. The fraction of central cylinder and the total fraction of mechanical tissues scaled positively with density, with dry to fresh mass ratio, with $M_{A,T}$ and with V/S_T.

Ultrastructural analysis showed that juvenile needles had thinner cell walls than current-year mature needles in *P. nigra* and in *P. pinea*, but not in *P. halepensis* (Table 3). Chloroplasts in juvenile needles had greater width in *P. halepensis* and *P. nigra* and greater thickness and circumference in *P. halepensis* than the chloroplasts in mature needles (Table 3). Mesophyll surface (S_m/S_p) and chloroplast surface area (S_c/S_p) exposed to intercellular air space per projected leaf area did not differ significantly among juvenile and mature needles (Table 4), but the ratio of chloroplast surface area exposed to intercellular air space to mesophyll surface area exposed to intercellular air space (S_c/S_m) (Figure 3., a) was

greater in juvenile than in adult needles in *P. nigra* and *P. pinea*. Among different needle age classes in mature needles, current year needles in *P. nigra* and *P. pinea* had greater cell wall thickness than older needles (Figure 3., b). Needle age did not affect chloroplast dimensions, but older needles occasionally had greater S_m/S_p or S_c/S_p, and there seemed to be no consistent age-dependent patterns between needle age and these traits.

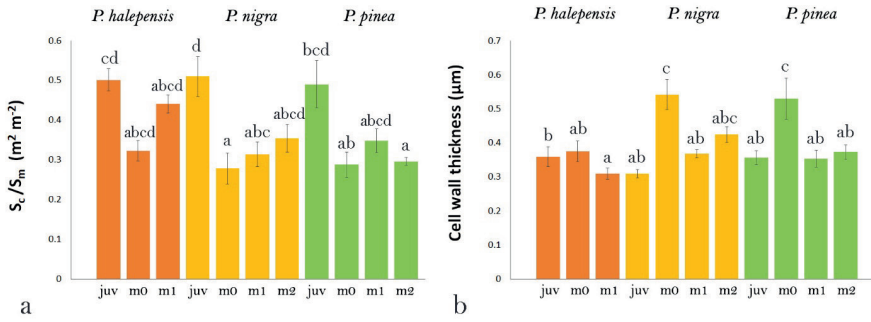

Figure 5
Differences in ratio of chloroplast surface area exposed to intercellular air space to mesophyll surface area exposed to intercellular air space (S_c/S_m) in dependence of needle and plant age in *Pinus halepensis*, *P. nigra* and *P. pinea* (a). Differences in needle cell wall thickness in dependence of needle and plant age in *Pinus halepensis*, *P. nigra* and *P. pinea* (b). Needle ages are: juv = juvenile current year, m = mature current year, m1 = mature 1-year-old, m2 = mature 2-year-old. Data correspond to average ±SE values of 5-8 replicates. Different letters show statistical significance among needle age classes and species at $P < 0.05$ (ANOVA followed by a Tukey post-hoc test).

Table 4. Ultrastructural data. Modified from Kuusk *et al*. (2018a)

Species	Tree age class	Needle age	Chloroplast width (μm)	Chloroplast thickness (μm)	Chloroplast circumference (μm)	Exposed surface area per projected area (m^2 m^{-2})	
						Mesophyll (S_m/S_p)	Chloroplasts (S_c/S_p)
P. halepensis	Seedling	(juv)	2.40 ± 0.13^{d}	4.69 ± 0.18^{d}	11.43 ± 0.45^{d}	35 ± 5^{abcd}	17.7 ± 3.2^{ab}
P. halepensis	Mature	(m0)	1.46 ± 0.12^{ab}	2.62 ± 0.15^{ab}	6.49 ± 0.38^{ab}	24.1 ± 2.9^{abc}	7.6 ± 0.8^{a}
P. halepensis	Mature	(m1)	1.44 ± 0.08^{a}	2.59 ± 0.14^{a}	6.50 ± 0.28^{a}	48.8 ± 3.8^{cd}	21.1 ± 0.7^{b}
P. nigra	Seedling	(juv)	1.90 ± 0.12^{bc}	3.58 ± 0.13^{c}	8.67 ± 0.31^{c}	22.2 ± 2.3^{ab}	11.6 ± 2.0^{ab}
P. nigra	Mature	(m0)	2.02 ± 0.09^{d}	3.17 ± 0.13^{abc}	8.0 ± 0.28^{abc}	37.7 ± 4.5^{abcd}	10.5 ± 2.0^{ab}
P. nigra	Mature	(m1)	1.81 ± 0.08^{abc}	3.61 ± 0.13^{c}	8.56 ± 0.27^{c}	44.1 ± 1.7^{bcd}	13.7 ± 1.2^{ab}
P. nigra	Mature	(m2)	1.63 ± 0.08^{abc}	3.42 ± 0.17^{bc}	8.05 ± 0.34^{abc}	51 ± 7^{d}	18.0 ± 3.1^{ab}
P. pinea	Seedling	(juv)	1.64 ± 0.06^{abc}	3.41 ± 0.17^{c}	7.88 ± 0.35^{abc}	18.1 ± 1.2^{a}	9.0 ± 1.3^{a}
P. pinea	Mature	(m0)	1.88 ± 0.09^{abc}	3.52 ± 0.17^{c}	8.63 ± 0.31^{c}	29.3 ± 3.8^{abcd}	9.6 ± 1.5^{a}
P. pinea	Mature	(m1)	1.93 ± 0.17^{d}	3.31 ± 0.25^{bc}	8.3 ± 0.6^{bc}	52.1 ± 2.4^{d}	18.0 ± 1.5^{ab}
P. pinea	Mature	(m2)	1.61 ± 0.09^{abc}	3.08 ± 0.014^{abc}	7.56 ± 0.32^{abc}	43 ± 6^{bcd}	12.6 ± 1.7^{ab}
Tree age (*F*1,29)			1.62 ns	14.6***	11.0**	1.41ns	1.98ns
Species (*F*2,29)			2.8ns	3.21ns	4.57*	1.56ns	1.54ns
Tree age × Species (*F*2,29)			6.78*	10.3***	12.3***	3.74*	1.94ns
Needle age (*F*2,28)			2.53ns	0.37ns	0.83ns	8.49**	11.48***
Species (*F*2,28)			3.76*	5.91**	6.05**	1.41ns	0.71ns
Needle age × Species (*F*3,28)			0.30 ns	0.96ns	0.41ns	2.78 ns	5.26**

5.2 Photosynthesis and needle age (Article II)

Foliage net assimilation rate per unit dry mass (A_m) was greater for juvenile than for adult current-year needles. Net assimilation per unit projected area (A_p) was greater in juvenile needles when all species were analyzed together. Analogously to A_m, nitrogen use efficiency (the ratio of A_m to N_m, E_N) was significantly greater in juvenile than in adult current-year needles (Table 5).

Table 5. Influences of tree age and needle age on net assimilation rate (A) and mesophyll diffusion conductance (g_m) expressed per unit dry mass (A_m and $g_{m,m}$) and needle projected area (A_p and $g_{m,p}$), photosynthetic nitrogen use efficiency (E_N, the ratio of A_p and nitrogen content per projected area) and CO_2 drawdown from substomatal cavities to chloroplasts (C_i-C_c) in three Mediterranean *Pinus* species. Table reproduced from Kuusk *et al.* (2018b).

Species	Tree age class	Needle age	$A_{m,Ci}$ = 250 (µmol g^{-1} s^{-1})	$A_{p,Ci}$ = 250 (µmol m^{-2} s^{-1})	E_N (µmol g^{-1} s^{-1})	$g_{m,m}$ (mmol g^{-1} s^{-1})	$g_{m,p}$ (mmol m^{-2} s^{-1})	CO_2 drawdown, C_i-C_c (µmol mol^{-1})
P. halepensis	seedling	juv	0.052 ± 0.009^{b}	6.6 ± 0.9 ^{cd}	4.7 ± 0.6^{cd}	1.19 ± 0.09^{b}	153 ± 11^{c}	44 ± 8^{a}
P. halepensis	mature	m0	0.0222 ± 0.0029^{b}	5.0 ± 0.7^{abcd}	2.51 ± 0.41^{abc}	0.300±0.030^{a}	67 ± 6^{ab}	74 ± 7^{bc}
P. halepensis	mature	m1	0.0126 ± 0.0025^{a}	2.89 ± 0.40^{a}	1.40 ± 0.23^{ab}	0.168±0.025^{a}	38.9 ± 3.7^{a}	73.5 ± 4.5^{bc}
P. nigra	seedling	juv	0.065 ± 0.010^{b}	6.5 ± 0.7^{cd}	7.0 ± 1.2^{d}	1.30 ± 0.11^{b}	133 ± 10^{c}	50 ± 6^{a}
P. nigra	mature	m0	0.0262 ± 0.0009^{a}	6.33±0.28^{cd}	2.51 ± 0.16^{abc}	0.352±0.043^{a}	84 ± 7^{b}	78 ± 9^{bc}
P. nigra	mature	m1	0.0170 ± 0.0014^{a}	4.59±0.37^{abcd}	1.52 ± 0.09^{a}	0.196±0.020^{a}	53 ± 5^{ab}	87.2 ± 2.5^{c}
P. nigra	mature	m2	0.0128 ± 0.0011^{a}	3.60 ± 0.30ab	1.35 ± 0.15^{a}	0.152±0.015^{a}	42.8 ± 4.3^{a}	85 ± 5^{c}
P. pinea	seedling	juv	0.052 ± 0.010^{b}	7.0 ± 0.6^{d}	3.6 ± 0.6^{bc}	1.15 ± 0.24b	155 ± 17^{c}	45.6 ± 2.2^{ab}
P. pinea	mature	m0	0.0195 ± 0.0016^{a}	5.16 ± 0.43^{bcd}	1.62 ± 0.22^{ab}	0.268±0.011^{a}	70.9 ± 3.3^{ab}	72.7 ± 4.8^{bc}
P. pinea	mature	m1	0.0177 ± 0.0030^{a}	4.21 ± 0.36^{abc}	1.33 ± 0.20^{a}	0.185±0.029^{a}	44.3 ± 4.0^{a}	95.7 ± 2.1^{c}
P. pinea	mature	m2	0.0098 ± 0.0012^{a}	3.33 ± 0.37^{ab}	0.95 ± 0.09^{a}	0.120±0.010^{a}	40.5 ± 2.6^{a}	81 ± 6^{c}
F-values for two-way ANOVA (juvenile vs. adult current-year needles)								
Tree age ($F1$, 23)			51.4***	5.41*	37.1***	92.2***	88.8***	30.6***
Species ($F2$, 23)			0.93ns	0.56ns	5.31*	0.50ns	0.12ns	0.34ns
Tree age × Species ($F2$, 23)			0.32ns	0.77ns	2.33ns	0.04ns	2.04ns	0.02ns
F-values for two-way ANOVA (adult needles of different age)								
Needle age ($F2$, 37)			19.4***	19.6***	18.7***	33.3***	39.9***	3.33*
Species ($F2$, 37)			2.15ns	5.64**	5.79**	2.33ns	4.79*	2.48ns
Needle age × Species ($F3$, 37)			1.12ns	0.52ns	1.59ns	0.82ns	0.41ns	2.02ns

The young trees were two years old and 0.2–0.3 m tall, and the mature cone-bearing trees were 15–21 m tall at the time of sampling. Needle age codes as: juv — juvenile current year; m0 — mature current year; m1 — mature one year old; m2 — mature two year old. Due to leaf-to-leaf differences in stomatal openness, net assimilation rates were standardized to a common intercellular CO_2 concentration (C_i) of 250 μmol mol^{-1} with the Farquhar *et al.* (1980) photosynthesis model. n = 4–6 for each average value, except for E_N (n = 3–6 for each average estimate, and n = 19 for the residuals of the F-values for the ANOVA with juvenile vs. adult needles, and n = 26 for the ANOVA with adult needle ages). Different letters show statistical significance among averages for different species and needle age class combinations at $P < .05$ (one-way ANOVA followed by a Tukey post hoc test). For two-way ANOVA, the statistical significance is denoted as: $^{*}P < .05$, $^{**}P < .01$, $^{***}P < .001$, ns—not significant.

Analysis of needle biochemical potentials, maximum carboxylase activity of Rubisco (V_{cmax}) and photosynthetic electron transport (J_{max}) derived from the net assimilation vs. chloroplastic CO_2 (C_c) response curves, indicated that juvenile needles had greater V_{cmax} and J_{max} per unit dry mass than adult current-year needles. Photosynthetic electron transport rate estimated from chlorophyll fluorescence (J_{ETR}) per dry mass was also greater for juvenile that for adult current-year needles. V_{cmax} and J_{max} per unit projected area varied less, but J_{max} per unit projected area was greater in juvenile than in adult current-year needles. Mesophyll diffusion conductance (g_m) was greater in juvenile than in adult current-year needles when expressed both per unit dry mass and projected area (Table 1). The CO_2 drawdown, from sub-stomatal cavities to chloroplasts, C_i-C_c, was lower for juvenile than for adult current-year needles (Table 1). Analysis of the needle age effects on adult needles across all species indicated that foliage net assimilation rates, foliage biochemical potentials, V_{cmax} and J_{max}, and g_m both per unit dry mass and area, and nitrogen use efficiency generally decreased with increasing needle age. Needle age effects on CO_2 drawdown were less, but still significant. Leaf photosynthetic characteristics (foliage net assimilation rate, E_N, V_{cmax}, J_{max} and g_m) correlated positively with needle mesophyll volume fraction (measured as the fraction of needle mesophyll in needle cross-section) and negatively with volume fractions of mechanical tissues. The correlations were stronger for mass-based photosynthetic characteristics. Photosynthetic nitrogen use efficiency was a stronger determinant of net

assimilation rate than nitrogen content. Higher nitrogen use efficiency was associated with enhanced mesophyll diffusion conductance. (Kuusk *et al* 2018b)

5.3 Changes in leaf structure, photosynthesis and isoprene emission due to growth at elevated temperature (Article III)

Increases in growth temperature were associated with about 1.2-fold larger and about 1.4-fold thinner leaves (Fig. 2, Table 5) with 1.6-fold lower leaf dry mass per unit area (M_A, Table 5).

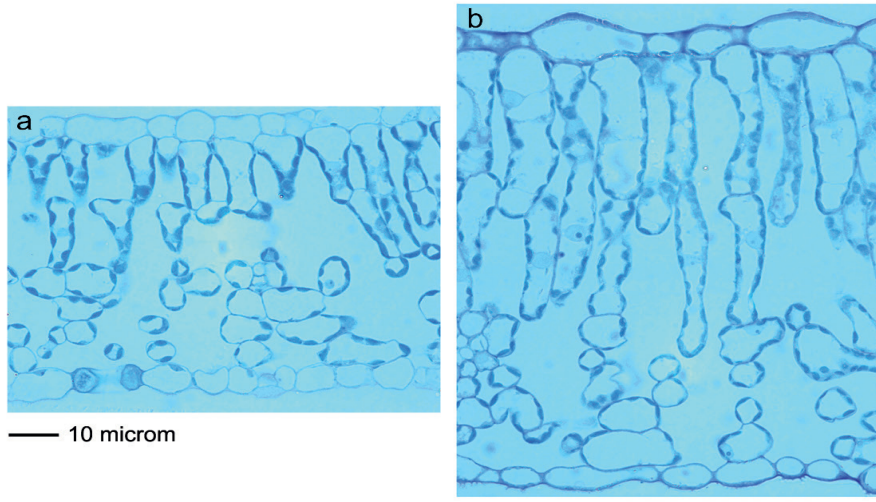

Figure 6
Representative cross-sections of hybrid aspen (*Populus tremula x P. tremuloides*, clone H200) leaves. Image **a** - leaves developed under high temperature (day/night temperatures 35/27°C) and image **b** - control (25/20°C) conditions. Photos by Vivian Kuusk.

Decreases in leaf thickness primarily resulted from decreases in the thickness of palisade (1.6-fold) and to a smaller degree in spongy mesophyll thickness (1.3-fold). The ratio of palisade to spongy mesophyll thickness also decreased from an average (±SE) of 1.60±0.08 to 1.22±0.06 with increasing growth temperature. Leaf density, the ratio of M_A to leaf thickness was similar among the treatments. Thinner leaves had reduced number of chloroplasts per unit leaf area and smaller chloroplast size (Table 5). Main observed changes were in leaf thickness, M_A, and the number of chloroplasts per leaf dry mass (1.2-fold greater in the high temperature-grown plants, Table 5).

At higher growth temperature leaves had higher stomatal conductance and therefore greater intercellular CO_2 concentrations. Increased growth temperature shifted the optimum temperature of net assimilation and CO_2-limited photosynthetic electron transport rate to higher temperatures. Leaves grown at higher temperature had higher mass-based net assimilation rate and electron transport rate. Dark respiration rate, J_{max} and net assimilation rate per dry mass were not significantly different among the treatments.

On a leaf area basis, both the isoprene emission rate (I) and the pool size of the substrate for the isoprene synthase enzyme, DMADP (C_{DMADP}), were greater in the control than in the high temperature treatment but on a leaf dry mass basis, I and C_{DMADP} values were similar among the growth temperature treatments. (Rasulov *et al.* 2015)

Mass-based photosynthetic characteristics differed little among the treatments, but higher growth temperature resulted in significantly increased leaf area and therefore higher photosynthesis and isoprene emission per unit leaf area. These structural changes might explain the study-to-study differences in growth temperature effects on foliage area-based physiological characteristics.

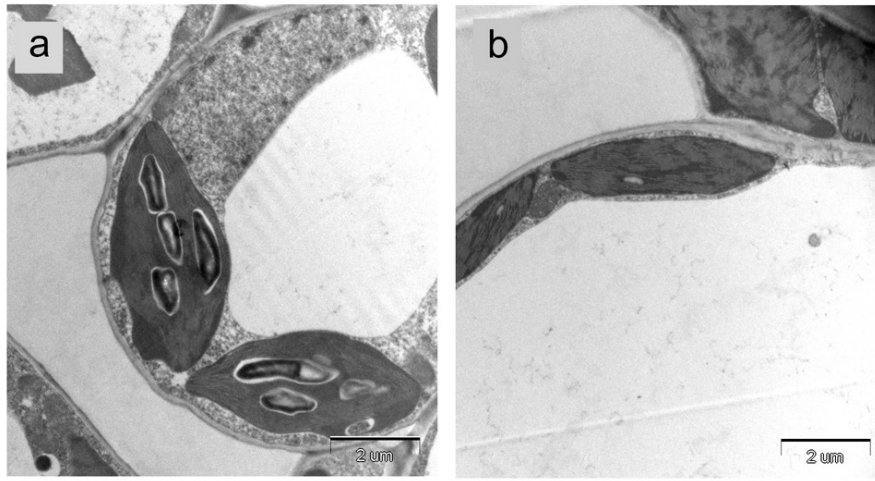

Figure 7
Cells on image **a** developed under control (day/night temperatures of 25/20 °C) and on image **b** at high temperature (35/27 °C) conditions. Magnification 7000x. TEM photoghraps taken by Vivian Kuusk.

Table 6. Leaf structural characteristics (average ± SE) in hybrid aspen (*Populus tremula* x *P. tremuloides*) clone H200, grown at different temperatures.

Characteristic	Growth temperature (day/night)	
	25/20 °C	35/27 °C
Leaf area (cm^2)	67.5±2.4 [a]	82.3±2.7 [b]
Leaf dry mass per unit area ($g\ m^{-2}$)	47.6±1.7 [a]	30.5±1.1 [b]
Leaf thickness (μm)	133.9±3.3 [a]	93.5±2.8 [b]
Palisade mesophyll thickness (μm)	71.5±3.1 [a]	40.9±2.6 [b]
Spongy mesophyll thickness (μm)	44.3±1.0 [a]	34.4±0.8 [b]
Total chloroplast number per cm^2 leaf area (palisade + spongy)	$(46.3±3.7)*10^6$ [a]	$(36.4±2.3)*10^6$ [a]
Chloroplast length (μm)	4.41±0.17 [a]	4.14±0.18 [a]
Chloroplast width (μm)	1.99±0.09 [a]	1.52±0.11 [b]
Chloroplast area (μm^2)	7.23±0.49 [a]	4.99±0.51 [b]

Averages with the same letter are not statistically different ($P > 0.05$ according to ANOVA, $n = 6$, for leaf structural measurements and $n = 30$-42 for leaf anatomical measurements). Modified table reproduced from Rasulov *et al*. (2015).

6. DISCUSSION

6.1 Age-dependent modifications in needle morphology and needle photosynthetic properties in Mediterranean pines (Articles I and II)

The aim of these studies was to quantify the changes in morphological, anatomical and chemical characteristics of the needle during the transition from juvenile to adult, and to find responses to the decrease in photosynthetic potential during heteroblastic changes and needle ageing.

During heteroblastic change, a significant reorganization of foliage characteristics occurs. In our study with Mediterranean *Pinus* species, juvenile and adult needles showed differences in the main anatomical, morphological and photosynthetic traits of all three studied species which very well explain their variations in photosynthetic potentials.

The first and most easily noticeable differences were the changes in needle shape and size. Juvenile needles were shorter and their cross-section was rhomboidal, sectorial and intermediate between those two variants. Adult needles were semi-elliptical to semi-circular in cross-section. All adult needles, except current-year needles, were thicker than juveniles and first-year adult needles. The latter had a similar thickness.

Cross-sectional shape – juvenile needles had rhomboidal to sectorial shape, but adult needles had hemi-elliptical cross-sections (Figure 1). There is also a major variation in biomass investments in structural and assimilative tissues across plant ages, ~1.5-fold lower investment in support, and concomitantly higher investment in mesophyll in juvenile than in adult needles (Figure 1, Table 2). Needle ultrastructural analyses revealed that increased mesophyll volume fraction was associated with a greater volume fraction of chloroplasts in juvenile needles. The surface area of mesophyll cells (S_m/S_p) and chloroplasts (S_c/S_p) exposed to intercellular air space per projected leaf area scaled with V/A_T and did not differ among juvenile and adult needles. However, juvenile needles had larger chloroplasts and filled a greater area of mesophyll cell walls that were exposed to intercellular air space (greater Sc/Sm ratio). This evidence suggests that the structure and ultrastructure of juvenile needles might result in greater photosynthetic activity per mass of juvenile needles. If so, this would imply a shorter payback time of juvenile foliage, and

greater carbon availability for growth, and thus, be an important factor enhancing early growth and recruitment of the juveniles (Climent et al. 2011a, b, Mediavilla et al. 2014).

Lower assimilation rate in older conifer has been historically explained by decrease in stomatal conductance (Yoder et al. 1994, Greenwood et al. 2008). Older needles have more robust needles and lower mesophyll diffusion conductance from substomatal cavities to chloroplasts can also constrain their photosynthesis as explained in Niinemets (1997b) and Niinemets (2002). Current finding that juvenile needles have lower cell wall thickness and greater S_c/S_m is consistent with this hypothesis. On the other hand, differences in the volume fractions of mesophyll and chloroplasts suggest that differences in needle biomass distribution between support and photosynthetic tissues can constitute another key factor accounting for enhanced photosynthesis rates in juvenile needles. (Kuusk *et al* 2018a)

6.2 Age-dependent modifications in needle photosynthetic properties in Mediterranean pines (Article II)

The results show important differences in foliage photosynthetic potentials and mesophyll conductance among juvenile and different-aged adult needles. The reason of these differences lies mainly in needle structural modifications and the different proportion of support and assimilative tissues. Enhanced assimilation rate per unit foliage biomass (Table 4) implies that the juvenile foliage has a shorter time to pay back the carbon cost used for foliage construction. Thus, juveniles have a greater carbon availability for growth of new biomass, thereby importantly contributing to their early growth and recruitment (Climent *et al* 2011a, Climent *et al* 2011b, Mediavilla *et al* 2014). Our study confirms that heteroblastic modifications in foliage photosynthesis rate are quantitatively much greater than changes in mass- and area-based photosynthesis rates due to the gradual ontogenetic drift in mature plants (compare with Niinemets, 2002, Räim *et al*, 2012, Steppe *et al*, 2011, Woodruff *et al*, 2009). As our study demonstrated, higher net assimilation rate at a given intercellular CO_2 concentration in juvenile needles was associated both with enhanced biochemical photosynthesis capacities, *V*cmax and *J*max (Figures 1 and S1), and enhanced mesophyll diffusion conductance (g_m) that affects net assimilation rate by altering the chloroplastic CO_2 concentration (C_c). At the ultrastructural level, greater g_m-limitation of photosynthesis in

adult trees was associated with thicker cell walls in *P. nigra* and *P. pinea* and with lower chloroplast to exposed mesophyll surface area ratio in *P. halepensis*. We suggest that the main advantage of juvenile needles is more effective photosynthesis, which provides the young seedling with necessary carbon building blocks for establishing extensive root systems and later on for development of more durable adult needles which are more resistant to mechanical stress and more tolerant to drought. (Kuusk et al., 2018b)

Both the heteroblastic change and needle ageing were associated with lower fractions of nitrogen invested in photosynthetic functions and reduced mesophyll conductance in structurally more robust needles (Table 5).

6.3 Temperature-dependent modifications in leaf anatomy and physiological performance (Article III)

In our study, acclimation to high growth temperature led to major changes in anatomy, morphology and chemistry of hybrid aspen leaves (Fig. 6,7, Table 6). Most importantly high temperature-grown leaves were thinner with lower leaf dry mass per unit area (M_A). In addition, high growth temperature led to less densely packed mesophyll, with fewer mesophyll cells and fewer chloroplasts per unit leaf area (Fig. 6, Table 6). Thus, leaf photosynthetic capacity per unit area was reduced. Despite lower number of chloroplasts per unit leaf area, the chloroplasts were smaller and chloroplast number per unit leaf dry mass was greater. Thus, foliage photosynthetic capacity per unit dry mass was enhanced upon acclimation to high temperature. Furthermore, expression of leaf photosynthetic capacity per unit dry mass also illustrated much better the improvement of leaf heat resistance of leaf photosynthetic apparatus. Indeed, on an area basis, leaf photosynthetic capacity per unit leaf area measured at 45 °C was similar in moderate and high temperature grown plants, but on a leaf dry mass basis, the photosynthetic capacity was significantly higher in high-temperature grown plants. This was further reflected in greater activation energies and optimum temperatures (T_{opt}) of net assimilation rates and CO_2 limited electron transport rates in high-temperature grown plants.

Like foliage photosynthetic capacity, leaf isoprene emission rate per unit area was also suppressed by high growth temperature. However, when

expressed on the basis of leaf dry mass, isoprene emission rate was actually enhanced, especially at temperatures 40-45 °C. These results have major implications for the hypothesis of leaf heat protection by isoprene. In particular, the temperature range 40-45 °C is most relevant for isoprene-dependent protection of leaf photosynthetic machinery. Apart from the rise of emissions, the mass-based enhancement of isoprene emissions was also associated with greater isoprene concentrations in leaf intercellular airspace, and thus, further suggest that acclimation to increased growth temperature led to greater leaf heat protection by isoprene. Again, this evidence indicates that looking only at isoprene emissions on an area basis, can lead to a flawed interpretation of how growth temperature alters leaf functioning. Overall, these results underscore the importance of consideration of leaf ultrastructural changes in interpreting the temperature-dependent modifications in leaf physiological activity.

In addition to modification in leaf anatomy and physiological activity, leaf expansion growth was enhanced, resulting in larger leaves, which influences positively the whole canopy leaf area and mass. Such increases in whole canopy leaf area in high temperature grown plants have been also observed in several other studies. However, it is important that an increase in whole canopy leaf area is only possible when there is enough water to support higher whole canopy leaf area. In our study conducted under optimum water availability, stomatal conductance to water vapor was also enhanced in plants grown under high temperature. In natural conditions, heat stress often interacts with drought, and this might strongly limit leaf area growth. Furthermore, drought strongly affects leaf ultrastructural traits as well, and drought-dependent changes that are typically opposite to the temperature-driven modifications We argue that future studies should look at leaf ultrastructural alterations in leaves grown under combined heat and drought stresses.

7. CONCLUSIONS

Natural selection tends to lead to optimal form and function in plant leaves, even if it does not do so for all features of all organisms (Parkhurst *et al*. 1972). As photosynthetic carbon assimilation is the most important role for plant leaves and their form is optimal when it maximizes net photosynthesis rate (Givnish, 1983) one may postulate that both juvenile and adult needle forms serve the plant in the best possible way. However, what is "the best" depends on plant ontogenetic stage and environmental conditions, and some of the phenotypic modifications in a real environmental setting might actually reflect a compromise between maximization of leaf carbon gain and leaf survival for sufficiently long period of time to pay back the costs of leaf construction (ontogenetic changes during needle lifespan, acclimation of foliage to environmental stress). Our studies show that structural modifications driven either by age or stress caused by higher temperature during leaf growth cause major anatomical differences inside leaves and influence its photosynthetic performance, heat tolerance and isoprene emission. There is a coordinated change in the combinations of foliage structural and photosynthetic traits upon heteroblastic change and differences among primary and secondary needles are quantitatively much larger than needle age-dependent modifications (Article I). Juvenile plants have "cheaper" leaves with lower volume fractions of mechanical and higher volume fractions of photosynthetic tissues than adult needles. These differences are compatible with lower leaf payback time, and all these traits can contribute to rapid increases in size, contributing to seedling and sapling establishment in the community. The only risk of investment in juvenile type leaves is their reduced tolerance of stresses like drought and frost. This explains the need to grow adult type, more robust needles once the plant has escaped competition and established in the community (Article I).

This thesis demonstrates that differences in foliage photosynthetic characteristics among primary needles in young plants and secondary needles in mature plants primarily resulted from differences in foliage structure. Less robust foliage of juvenile needles is associated with greater photosynthetic activity per unit biomass investment. This contributes to enhanced growth and seedling establishment, whereas the advantage of greater mechanical robustness of secondary needles in adult trees

is tolerance of harsh environmental conditions in the upper canopy. Increases in leaf robustness can alter foliage photosynthetic activity not only due to changes in tissue chemical composition, but also due to changes in mesophyll conductance and changes in the share of nitrogen between photosynthetic and non-photosynthetic functions (Article II).

This thesis highlighted major temperature-dependent alterations in leaf anatomy and morphology and demonstrated that these structural modifications mainly drove the treatment effects on foliage photosynthetic and isoprene emission characteristics expressed per unit leaf area. Thus, structural effects clearly influenced the mechanisms of temperature-driven photosynthetic acclimation. So far, variable responses of leaf photosynthetic capacity per unit area to growth temperature have been observed among studies and these differences have been difficult to explain. In fact, structural changes might explain the study-to-study differences in how growth temperature affects foliage area-based physiological characteristics (Article III). Although studies of foliage photosynthetic differentiation have often neglected leaf anatomical characteristics, this thesis demonstrates that leaf anatomical traits are of paramount importance in determining the magnitude of changes in photosynthetic capacity and furthermore change the extent to which photosynthetic capacity is controlled by diffusional limitations (mesophyll conductance) and biochemical potentials (nitrogen investment in rate-limiting proteins). I conclude that further studies of photosynthetic differentiation should consider the whole suite of structural, physiological and biochemical traits.

REFERENCES

Aasamaa, K., Niinemets, Ü., Sõber, A. (2005). Leaf hydraulic conductance in relation to anatomical and functional traits during *Populus tremula* leaf ontogeny. Tree Physiology 25, pp. 1409–1418.

Adler P.B., Salguero-Gómez, R., Compagnoni A., Hsu, J. S., Ray-Mukherjee, J., Mbeau-Ache, C., Franco M. (2014) Functional traits explain variation in plant life history strategies. Proceedings of the National Academy of Sciences of the United States of America: January 14, 111 (2), pp. 740 -745.

Alonso-Forn, D., Peguero-Pina, J.J., Ferrio, J.P., García-Plazaola, J.I., Martín-Sánchez, R., Niinemets, Ü., Sancho-Knapik, D., Gil-Pelegrín, E. (2022) Cell-level anatomy explains leaf age-dependent declines in mesophyll conductance and photosynthetic capacity in the evergreen Mediterranean oak *Quercus ilex* subsp. *rotundifolia*, *Tree Physiology*, 42, issue 10, pp. 1988–2002.

Apple, M., Tiekotter, K., Snow, M., Young, J., Soeldner, A., Phillips, D., Tingey, D., Bond, B.J. (2002) Needle anatomy changes with increasing tree age in Douglas-fir. Tree Physiology, 22(2-3), pp.129-136.

Arneth, A., Monson, R.K., Schurgers, G., Niinemets Ü., Palmer, P.I. (2008) Why are estimates of global isoprene emissions so similar (and why is this not so for monoterpenes)? Atmospheric Chemistry and Physics, 8(2), pp. 7017-7050.

Atzmon, N., Moshe, Y., Schiller, G. (2004) Ecophysiological response to severe drought in *Pinus halepensis* Mill. trees of two provenances. Plant Ecology, 171, pp. 15–22.

Bannister, P., Neuner, G. (2001) Frost resistance and the distribution of conifers. In: Conifer cold hardiness. Eds Bigras, F.J. and Colombo, S.J. Dordrecht, Kluwer Academic Publishers, pp. 3-22.

Baquedano, F.J., Castillo, F.J. (2007) Drought tolerance in the Mediterranean species *Quercus coccifera, Quercus ilex, Pinus halepensis*, and *Juniperus phoenicea*. Photosynthetica, 45(2), pp. 229-238.

Baquedano, F.J., Valladares, F., Castillo, F. J. (2008) Phenotypic plasticity blurs ecotypic divergence in the response of Querqus coccifera and

Pinus halepensis to water stress. Europea Journal of Forest Research, 127, pp. 495-506.

Barbéro M., Loisel R., Quézel P., Richardson D.M. and Romane F. (1998) Pines of the Mediterranean Basin. In: Richardson D.M. (ed.), Ecology and Biogeography of Pinus. Cambridge UniversityPress, Cambridge, pp. 153–170.

Barriopedro, D., García-Herrera, R., Ordóñez, C., Miralles, D. G., Salcedo-Sanz, S. (2023) Heat waves: physical understanding and scientific challenges. Reviews of Geophysics, 61, e2022RG000780.

Barton, K. E. (2024). The ontogenetic dimension of plant functional ecology. *Functional Ecology*, 38, pp. 98–113.

Benomar, L., Moutaoufik, M.T., Elferjani, R., Isabel, N., DesRochers, A., El Guellab, A., Khlifa, R., Idrissi Hassania, L.A. (2019) Thermal acclimation of photosynthetic activity and RuBisCO content in two hybrid poplar clones. PLoS One, 11, pp. 14(2).

Bernacchi, C. J., Singsaas, E. L., Pimentel, C., Portis, A. R. Jr, Long, S. P. (2001) Improved temperature response functions for models of Rubisco-limited photosynthesis. *Plant, Cell and Environment*, 24, pp. 253– 259.

Boddi, S., Morassi Bonzi, L., Calamassi, R. (2002) Structure and ultrastructure of *Pinus halepensis* primary needles. Flora - Morphology, Distribution, Functional Ecology of Plants, vol. 197(1), pp. 10-23

Bozzola, J. J., Russell, L. D. 1992. Electron Microscopy. Principles and Techniques for Biologists: Jones and Bartlett Eds.

Burns, W.A. (1978) Thick sections: technique and applications. In: Trump, B.F., Jones, R.J. (eds) Diagnostic electron microscopy. Wiley, New York, NY, pp. 146–178.

Cabanettes, A., Rapp, M. (1978) Biomasse, minéralomasse et productivité d'un écosystème à Pins pignons (*Pinus pinea* L.) du littoral méditerranéen. I. Biomasse. Oecologia Plantarum 13, pp. 271–286.

Cao, Y., Pan, Y., Yang, Y., Liu, T., Wang, M., Li, Y., Guo, S. (2024) Variation of mesophyll conductance mediated by nitrogen form is related to changes in cell wall property and chloroplast number, *Horticulture Research*, 11(6), pp. 112.

Carriquí, M., Nadal, M., Flexas, J. (2021) Acclimation of mesophyll conductance and anatomy to light during leaf aging in Arabidopsis thaliana. Physiologia Plantarum, 172, pp. 1894–1907.

Cescatti, A., Niinemets, Ü. (2004) Sunlight capture. Leaf to landscape. In: Smith, W.K., Vogelmann, T.C., Chritchley, C. (eds) Photosynthetic adaptation. Chloroplast to landscape. Springer, Berlin, pp. 42–85.

Chameides, W.L., Lindsay, R.W., Richardson, J., Kiang, C.S. (1988) The role of biogenic hydrocarbons in urban photochemical smog: Atlanta as a case study. Science 241, pp. 1473–1475.

Climent, J., Aranda, I., Alonso, J., Pardos, J. A., Gil, L. (2006a). Developmental constraints limit the response of Canary Island pine seedlings to combined shade and drought. Forest Ecology and Management, 231, pp. 164–168.

Climent, J., Chambel, M.R., López, R., Mutke, S., Alía, R., Gil, L. (2006b) Population divergence for heteroblasty in the Canary Island pine (*Pinus canariensis*, *Pinaceae*) Botany, 93(6), pp. 840-848.

Climent, J., Silva, F., Chambel, M., Pardos, M., Almeida, M. (2009) Freezing injury in primary and secondary needles of Mediterranean pine species of contrasting ecological niches. Annals of Forest Science 66(407), pp 1-8.

Climent, J., Chambel, M.R., Pardos, M., Lario, F., Villar-Salvador, P. (2011a) Biomass allocation and foliage heteroblasty in hard pine species respond differentially to reduction in rooting volume. European Journal of Forest Research 130, pp. 841–850.

Climent, J., San-Martín, R., Chambel, M.R., Mutke, S. (2011b) Ontogenetic differentiation between Mediterranean and Eurasian pines (sect. *Pinus*) at the seedling stage. Trees 25, pp. 175–186.

Cohu, C.M., Muller, O., Adams III, W.W., Demmig-Adams, B. (2014). Leaf anatomical and photosynthetic acclimation to cool temperature and high light in two winter versus two summer annuals. Physiologia Plantarum, 152(1) pp. 164-173.

Copolovici, L., Kännaste, A., Remmel, T., Vislap, V., Niinemets, Ü. (2011) Volatile emissions from *Alnus glutinosa* induced by herbivory are quantitatively related to the extent of damage. Journal of Chemical Ecology, January, 37(1), pp. 18-28.

Crous, K.Y., Campany, C., Lopez, R., Cano, F., Ellsworth, D.S., (2021) Canopy position affects photosynthesis and anatomy in mature *Eucalyptus* trees in elevated CO_2. Tree Physiology, 41(2), pp. 206-222.

Dallimore, W., Jackson, A.B., Harrison. S.G. (1967) A handbook of *Coniferae* and *Ginkgoaceae*, 4th ed. New York: St. Martin's Press. xix, pp. 729.

Doak, C. C. 1935. Evolution of foliar types, dwarf shoots, and cone scales of Pinus. Illinois Biological Monographs 13: 1–106.

Escudero, A., Valladares, F. (2016) Trait-based plant ecology: moving towards a unifying species coexistence theory. Oecologia, 180(4), pp. 919–922.

Euler, H., Bergman, B., Hellstrom, H. (1934) Über das Verhältnis von Chloroplastenzahl und Chlorophyllkonzentration bei *Elodea densa*. Berichte der Deutschen Botanischen Gesellschaft, 52, pp. 458-462.

Evans J.R., von Caemmerer S., Setchell B.A., Hudson G.S. (1994) The relationship between CO2 transfer conductance and leaf anatomy in transgenic tobacco with a reduced content of rubisco. Functional Plant Biology 21, 475– 495.

Evans, J. R., Kaldenhoff, R., Genty, B., Terashima, I., (2009) Resistances along the CO_2 diffusion pathway inside leaves, *Journal of Experimental Botany*, 60(8), pp. 2235–2248.

Fahlvik, N., Rytter, L., Stener, L.G. (2021) Production of hybrid aspen on agricultural land during one rotation in southern Sweden. Journal of Forest Research 32**,** pp. 181–189.

Fares, S., Mahmood, T., Liu, S., Loreto, F., Centritto, M. (2011) Influence of growth temperature and measuring temperature on isoprene emission, diffusive limitations of photosynthesis and respiration in hybrid poplars. Atmospheric Environment, 45(1), pp. 155-161.

Farjon, A. (1984) Pines: drawings and descriptions of the genus *Pinus*. Leiden: Brill & Backhuys.

Farjon, A. (2010) A Handbook of the world's conifers. Leiden, Netherlands: Brill Academic Publishers.

Farjon, A., Filer, D. (2013). An atlas of the world's conifers. Leiden, The Netherlands: Brill.

Farquhar, G.D., von Caemmerer, S., Berry, J.A. (1980) A biochemical model of photosynthetic CO_2 assimilation in leaves of C_3 species. Planta, 149, 78–90.

Fehsenfeld., F., Calvert, J., Fall, R., Goldan, P., Guenther. A.B., Hewitt, C.N., Lamb, B., Liu, S., Trainer, M., Westberg, H. (1992) Emissions of volatile organic compounds from vegetation and the implications for atmospheric chemistry: natural sources of acid precursors, neutralizing compounds, and oxidants. Global Biogeochemical Cycles 6, pp. 389–430.

Flexas, J., Clemente-Moreno, M.J., Bota, J., Brodribb, T.J., Gago, J., Mizokami, Y., Nadal, M., Perera-Castro, A.V., Roig-Oliver, M., Sugiura, D., Xiong, D., Carriquí, M. (2021) Cell wall thickness and composition are involved in photosynthetic limitation, *Journal of Experimental Botany*, 72(11), pp. 3971–3986.

Flexas, J., Ribas-Carbó, M., Diaz-Espejo, A., Galmés, J., Medrano, H. (2008) Mesophyll conductance to CO2: current knowledge and future prospects. Plant, Cell and Environment, 31, pp. 602– 621.

Flexas, J., Diaz-Espejo, A., Galmés, J., Kaldenhoff, R., Medrano, H., Ribas-Carbo, M. (2007) Rapid variations of mesophyll conductance in response to changes in CO2 concentration around leaves. Plant, Cell and Environment, 30, pp. 1284– 1298.

Gebauer, R., Volařík, D., Urban, J., Børja, I., Nagy, N.E., Eldhuset, T.D., Krokene, P. (2011) Effect of thinning on anatomical adaptations of Norway spruce needles. Tree Physiology, 31, pp. 1103–1113.

Genty, B., Briantais, J.-M., Baker, N.R. (1989) The relationship between the quantum yield of photosynthetic electron transport and quenching of chlorophyll fluorescence. Biochimica et Biophysica Acta, 990, pp. 87-92.

Givnish, T.J., Sytsma K.J., Smith, J.F., Hahn, W.J. (1994) Thorn-like prickles and heterophylly in Cyanea – adaptations to extinct avian browsers on Hawaii. Proceedings of the National Academy of Sciences of the United States of America 91: 2819-2814.

Goebel, K. (1889) Ueber die Jugendzustände der Pflanzen. Flora 72: 1-44.

Goebel, K. (1900) Organography of plants. I. General organography. (English translation by I. B. Balfour). Reprinted by Hafner, NewYork. pp. 707.

Gorishina, T. K. (1983) Photosynthetic apparattus of the plants and environmental conditions. (Горышина, Т.К. Фотосинтетический аппарат растений и условия среды. Ленинградский университет) ISBN: 5-288-00145-6

Greenwood, R.M., Atkinson, I.A.E. (1977) Evolution of divaricating plants in New Zealand in relation to moa browsing. Proceedings of the New Zealand 24: 21-33

Greenwood, M.S., Ward, M.H., Day, M.E., Adams, S.L., Bond, B.J. (2008) Age-related trends in red spruce foliar plasticity in relation to declining productivity. Tree Physiology, 28, pp. 225–232.

Guenther, A., Karl, T., Harley, P., Wiedinmyer, C., Palmer, P.I., Geron, C. (2006) Estimates of global terrestrial isoprene emissions using MEGAN (model of emissions of gases and aerosols from nature). Atmospheric Chemistry and Physics Discussions, 6, pp. 107–173.

Haberlandt, G. (1882) Vergleichende Anatomie des assimilatorischen Gewebesystems der Pflanzen. Jahrbücher für Wissenschaftliche Botanik 1882. Bd 13 Berlin

Hanba, Y.T., Miyazawa, S.-I., Kogami, H., Terashima, I. (2001) Effects of leaf age on internal CO2 transfer conductance and photosynthesis in tree species having different types of shoot phenology. Functional Plant Biology, 28, pp. 1075– 1084.

Hanba, Y.T., Miyazawa, S.I., Terashima I. (1999) The influence of leaf thickness on the CO2 transfer conductance and leaf stable carbon isotope ratio for some evergreen tree species in Japanese warm-temperate forests. Functional Ecology, 13, pp. 632– 639.

Harley, P.C., Loreto, F., di Marco, G., Sharkey, T. D. (1992). Theoretical considerations when estimating the mesophyll conductance to CO_2 flux by analysis of the response of photosynthesis to CO_2. Plant Physiology, 98, pp. 1429–1436.

Hartikainen, K., Nerg, A.M., Kivimäenpää, M., Kontunen-Soppela, S., Mäenpää, M., Oksanen, E., Rousi, M., Holopainen, T. (2009) Emissions of volatile organic compounds and leaf structural characteristics of European aspen (*Populus tremula*) grown under elevated ozone and temperature. Tree Physiology, 29(9), pp. 1163-73.

Higuchia, H., Sakuratania, T., Utsunomiyab, N. (1999) Photosynthesis, leaf morphology, and shoot growth as affected by temperatures in

cherimoya (*Annona cherimola* Mill.) trees. Scientia Horticulturae, 80(1–2), pp. 91-104.

Hussain, S., Ulhassan, Z., Brestic, M. Zivcak, M., Zhou, W., Suleyman, I.A., Yang, X., Safdar, M.E., Yang, W., Liu, W. (2021) Photosynthesis research under climate change. Photosynthesis Research 150, pp. 5–19.

Jahan, E., Sharwood, R.E., Tissue, D.T. (2023) Effects of leaf age during drought and recovery on photosynthesis, mesophyll conductance and leaf anatomy in wheat leaves. Frontiers In Plant Science, 14, 1091418.

Jellings A. J., Usher, M.B., Leech, P.M. (1983) Chloroplast size in tall and short phenotypes of *Poa flabellata* on South Georgia. British Antarctic Survey Bulletin, 59, pp. 41-46.

Jellings A. J., Usher, M.B., Leech, P.M. (1983) Variation in the chloroplast to cell area index in *Deschampsia antarctica* along a 16^0 latitudinal gradient. British Antarctic Survey Bulletin, No. 61, pp. 13-20.

Joffe, R., Tosens, T., Berthe, A., Jolivet, Y., Niinemets, Ü. & Gandin, A. (2024) Reduced mesophyll conductance under chronic O3 exposure in poplar reflects thicker cell walls and increased subcellular diffusion pathway lengths according to the anatomical model. Plant, Cell & Environment, pp. 1–18.

Jones, C.S. (1999) An essay on juvenility, phase change, and heteroblasty in seed plants. International Journal of Plant Science 160 (6 Suppl.): S105–S111.

Kariya, K., Tsunoda, S. (1972) Relationship of chlorophyll content, chloroplast area index and leaf photosynthesis rate in *Brassica*. Tohoku Journal of Agricultural Research, vol. 23.

Keenan, T.F, Niinemets, Ü. (2016) Global leaf trait estimates biased due to plasticity in the shade. Nature Plants, 3, 16201.

Kienast, F., Schweingruber, F.H., Bräker, O.U., Schär, E. (1987) Tree-ring studies on conifers along ecological gradients and the potential of single-year analyses. Canadian Journal of Forest Research, 17(7), pp.683-696.

Kiendler-Scharr, A., Wildt, J., Dal Maso, M., Hohaus, T., Kleist, E., Mentel, T.F., Tillmann, R., Uerlings, R., Schurr, U., Wahner, A. (2009) New particle formation in forests inhibited by isoprene emissions. Nature, 461, pp. 381–384.

Klaus W., 1989. Mediterranean pines and their history. Plant Syst. Evol. 162, pp. 133–163.

Knauer, J., Cuntz, M., Evans, J.R., Niinemets, Ü., Tosens, T., Veromann-Jürgenson, L.-L., Werner, C. and Zaehle, S. (2022), Contrasting anatomical and biochemical controls on mesophyll conductance across plant functional types. New Phytologist, 236, pp. 357-368.

Kogami, H., Hanba, Y.T., Kibe, T., Terashima, I. Masuzawa, T. (2001) CO2 transfer conductance, leaf structure and carbon isotope composition of Polygonum cuspidatum leaves from low and high altitudes. Plant, Cell and Environment, 24, pp. 529– 538.

Kuusk V., Niinemets, Ü., Valladares, F. (2018a) A major trade-off between structural and photosynthetic investments operative across plant and needle ages in three Mediterranean pines. Tree Physiology 38, pp. 543–557.

Kuusk V., Niinemets, Ü., Valladares, F. (2018b) Structural controls on photosynthetic capacity through juvenile-to-adult transition and needle aging in Mediterranean pines. Functional Ecology 32, pp. 1479–1491.

Laisk, A., Oja, V., Rasulov, B., Rämma, H., Eichelmann, H., Kasparova, I., Vapaavuori, E. (2002) A computer-operated routine of gas exchange and optical measuremnets to diagnose photosynthetic apparatus in leaves. Plant, Cell and Environment, 25, pp. 923-943.

Lange, B.M. (2015) The Evolution of Plant Secretory Structures and Emergence of Terpenoid Chemical Diversity. Annual Review of Plant Biology, 66, pp. 139-159.

Le Maitre, D.C. (1998) Pines in cultivation: a global view. In: Ecology and Biogeography of *Pinus* (1998) Ed. David M. Richardson, Cambridge University Press.

Lester, D. 1968. Developmental patterns of axillary meristematic activity in seedlings of Pinus. Botanical Gazette, 129, pp. 206–210.

Li, Z., Ratliff, E.A, Sharkey, T.D. (2011) Effect of temperature on postillumination isoprene emission in oak and poplar. Plant Physiology, 155(2), pp. 1037-1046.

Lichtenthaler, H.K., Buschmann, C. (2001) Chlorophylls and carotenoids: measurement and characterisation by UV-VIS. In: Current Protocols in Food Analytical Chemistry (eds Wrolstad, R.E.,

Acree, T.E., Decker, E.A., Penner M.H., Reid, D.S., Schwartz, S.J., Sporns, P.), pp. F4.3.1–F4.3.8. John Wiley & Sons, Madison, WI, USA.

Loreto, F., Mannozzi, M., Maris, C., Nascetti, P., Ferranti, F., Pasqualini, S. (2001a) Ozone quenching properties of isoprene and its antioxidant role in leaves. Plant Physiology, 126, pp. 993–1000.

Loreto, F., Velikova, V. (2001b) Isoprene produced by leaves protects the photosynthetic apparatus against ozone damage, quenches ozone products and reduces lipid peroxidation of cellular membranes. Plant Physiology, 127, pp. 1781-1787.

Loreto, F., Fineschi, S. (2015) Reconciling functions and evolution of isoprene emission in higher plants. New Phytologist, 206, pp. 578–582.

Mauri, A., Di Leo, M., de Rigo, D., Caudullo, G. (2016) *Pinus halepensis* and *Pinus brutia* in Europe: distribution, habitat, usage and threats. In: San-Miguel-Ayanz, J., de Rigo, D., Caudullo, G., Houston Durrant, T., Mauri, A. (Eds.), European Atlas of Forest Tree Species. Publ. Off. EU, Luxembourg, pp. 122-123.

Mediavilla, S., Herranz, M., Gonzales-Zurdo, P., Escudero, A. (2013) Ontogenetic transition in leaf traits: a new cost associated with the increase in leaf longevity. Journal of Plant Ecology, 7(6), pp. 567-575.

Mediavilla, S., Herranz, M., González-Zurdo, P., Escudero, A. (2014) Ontogenetic transition in leaf traits: a new cost associated with the increase in leaf longevity. Journal of Plant Ecology, 7, pp. 567–575.

Mercer, E. H. (1963) A scheme for section staining in electron microscopy. Journal of the Royal Microscopical Society, 81, pp. 179-186.

Miller, P.M., Eddleman, L.E., Miller, J.M. (1995) *Juniperus occidentalis* juvenile foliage: advantages and disadvantages for a stress-tolerant, invasive conifer. Canadian Journal of Forest Research, 25(3), pp. 470-479.

Mousseau M. (1967) Les phénomènes de regulation structurale et fonctionelle de l`appareil photosynthétique de Teucrium scorodonia: un mécanisme dàdaptation aux conditions d`éclairement. Oecologia Plantarum, 1.

Moussouris, Y., Regato, P. (1999) Forest Harvest: An Overview of Non Timber Forest Products in the Mediterranean region.

Muller, O., Stewart, J.J., Cohu, C.M., Polutchko, S.K., Demmig-Adams, B., Adams III, W.W. (2014). Leaf architectural, vascular and photosynthetic acclimation to temperature in two biennials. Physiologia Plantarum, 152(4), pp. 763-772.

Niinemets, Ü. (1997b) Distribution patterns of foliar carbon and nitrogen as affected by tree dimensions and relative light conditions in the canopy of *Picea abies*. Trees, 11, pp. 144–154.

Niinemets, Ü. (2001) Global-scale climatic controls of leaf dry mass per area, density, and thickness in trees and shrubs. Ecology, 82(2), pp. 453-469.

Niinemets, Ü. (2002) Stomatal conductance alone does not explain the decline in foliar photosynthetic rates with increasing tree age and size in *Picea abies* and *Pinus sylvestris*. Tree Physiology, 22, pp. 515–535.

Niinemets, Ü. (2010) A review of light interception in plant stands from leaf to canopy in different plant functional types and in species with varying shade tolerance. Ecological Research, 25, pp. 693–714.

Niinemets, Ü. (2014). Improving modeling of the "dark part" of canopy carbon gain. Tree Physiology, 34, pp. 557–563.

Niinemets, Ü., Arneth, A., Kuhn, U., Monson, R. K., Peñuelas, J., and Staudt, M. (2010) The emission factor of volatile isoprenoids: stress, acclimation, and developmental responses. Biogeosciences, 7, pp. 2203–2223.

Niinemets, Ü., Cescatti, A., Rodeghiero, M., Tosens, T. (2005) Leaf internal diffusion conductance limits photosynthesis more strongly in older leaves of Mediterranean evergreen broad-leaved species. Plant, Cell and Environment, 28, pp. 1552–1566.

Niinemets, Ü., Copolovici, L., Hüve, K. (2010) High within-canopy variation in isoprene emission potentials in temperate trees: Implications for predicting canopy-scale isoprene fluxes, Journal of Geophysical Research, 115, pp. 1-19.

Niinemets, Ü., Diaz-Espejo, A., Flexas, J., Galmes, J., Warren C.R. (2009a) Role of mesophyll diffusion conductance in constraining potential photosynthetic productivity in the field. Journal of Experimental Botany, 60, pp. 2249– 2270.

Niinemets, Ü., Ellsworth, D.S., Lukjanova A., Tobias. M. (2001) Site fertility and the morphological and photosynthetic acclimation of *Pinus sylvestris* needles to light. Tree Physiology, 21, pp. 1231–1244.

Niinemets, Ü., Hauff, K., Bertin, N., Tenhunen, J. D., Steinbrecher, R., Seufert, G. (2002). Monoterpene emissions in relation to foliar photosynthetic and structural variables in Mediterranean evergreen *Quercus* species. The New Phytologist, 153, pp. 243–256.

Niinemets, Ü., Keenan T.F., Hallik, L. (2015c) A worldwide analysis of within-canopy variations in leaf structural, chemical and physiological traits across plant functional types. New Phytologist, 205, pp. 973-993.

Niinemets Ü, Kull, O. (1995) Effects of light availability and tree size on the architecture of assimilative surface in the canopy of Picea abies: variation in needle morphology. Tree Physiology, 15, pp. 307–315.

Niinemets, Ü., Lukjanova, A., Sparrow, A.D., Turnbull, M.H. (2005) Light acclimation of cladode photosynthetic potentials in *Casuarina glauca*: trade-offs between physiological and structural investments. Functional Plant Biology, 32, pp. 571–582.

Niinemets, Ü., Lukjanova, A., Turnbull, M.H., Sparrow, A.D. (2007) Plasticity in mesophyll volume fraction governs the light-acclimation in needle photosynthesis in two pines. Tree Physiology, 27, pp. 1137–1151.

Niinemets, Ü., Oja, V., Kull, O. (1999b) Shape of leaf photosynthetic electron transport versus temperature response curve is not constant along canopy light gradients in temperate deciduous trees. Plant, Cell and Environment, 22**,** pp. 1497–1514.

Niinemets, Ü., Sun, Z. (2015) How light, temperature, and measurement and growth [CO_2] interactively control isoprene emission in hybrid aspen, *Journal of Experimental Botany*, 66, 3, pp. 841–851.

Niinemets, Ü., Tenhunen, J.D. (1997a). A model separating leaf structural and physiological effects on carbon gain along light gradients for the shade-tolerant species *Acer saccharum*. Plant, Cell and Environment, 20, pp. 845–866.

Niinemets, Ü., Tenhunen, J.D., Canta, N.R., Chaves, M.M., Faria, T., Pereira, J.S., Reynolds, J.F. (2008) Interactive effects of nitrogen and phosphorus on the acclimation potential of foliage photosynthetic

properties of cork oak, *Quercus suber*, to elevated atmospheric CO_2 concentrations. Global Change Biology, 5**,** pp. 455–470.

Niinemets, Ü., Tenhunen, J.D., Harley, P.C., Steinbrecher, R. (1999a) A model of isoprene emission based on energetic requirements for isoprene synthesis and leaf photosynthetic properties for *Liquidambar* and *Quercus*. Plant, Cell and Environment, 22, pp. 1319–1336.

Niinemets, Ü., Rasulov, B., Talts, E. (2021) CO_2 -responsiveness of leaf isoprene emission: Why do species differ? Plant Cell and Environment, 44(9), pp. 3049-3063.

Niinemets, Ü., Sun, Z. (2015a) How light, temperature, and measurement and growth [CO_2] interactively control isoprene emission in hybrid aspen, Journal of Experimental Botany, 66(3), pp. 841–851.

Niinemets, Ü., Sun, Z., Talts, E. (2015b) Controls of the quantum yield and saturation light of isoprene emission in different-aged aspen leaves. Plant, Cell and Environment, 38(12), pp. 2707-20.

Niinemets, Ü., Wright, I. J., Evans, J. R. (2009b). Leaf mesophyll diffusion conductance in 35 Australian sclerophylls covering a broad range of foliage structural and physiological variation. Journal of Experimental Botany, 60, pp. 2433–2449.

Niklas, K.J. (1989) Mechanical behaviour of plant tissues as inferred from the theory of pressurized cellular solids. American Journal of Botany, 76, pp. 929–937.

Niklas, K.J. (1991) Effects of tissue volume and location on the mechanical consequences of dehydration of petioles. American Journal of Botany, 78, pp. 361–369.

Oleksyn, J., Tjoelker, M., Lorenc-Plucińska, G., Konwińska, A., Żytkowiak, R., Karolewski, P., Reich, P.B. (1997) Needle CO_2 exchange, structure and defense traits in relation to needle age in *Pinus heldreichii* Christ – a relict of Tertiary flora. Trees 12, 82–89.

Palacio-López, K., Beckage, B., Scheiner. S., Molofsky, J. (2015) The ubiquity of phenotypic plasticity in plants: a synthesis. Ecology and Evolution, 5(16), pp. 3389-400.

Parkhurst, D.F. (1994) Diffusion of CO_2 and other gases inside leaves. Tansley Review No. 65. New Phytologist, 126, pp. 449–479.

Peñuelas, J., Llusià, J. (2002) Linking photorespiration, monoterpenes and thermotolerance in *Quercus*. New Phytologist, 155, pp. 227–237.

Peñuelas, J., Llusià, J. (2003) BVOCs: plant defense against climate warming? Trends in Plant Science, 8(3), pp. 105-9.

Percival, S., Onyenedum, J.G., Chitwood D.C., Husbands A.Y. (2024) Topological data analysis reveals core heteroblastic and ontogenetic programs embedded in leaves of grapevine (*Vitaceae*) and maracuyá (*Passifloraceae*). PLOS Computational Biology.

Poorter, L. (1999) Growth responses of fifteen rain forest trees pecies to a light gradient; the relative importance of morphological and physiological traits. Functional Ecology13, pp. 396–410.

Poorter, L. Bongers, F. (2006a) Leaf traits are good predictors of plant performance across 53 rain forest species. Ecology, 87, pp. 1733-1743.

Poorter, L., Bongers, F., Sterck, F. J., Wöll H. (2005) Beyond the regeneration phase: differentiation of height–light trajectories among tropical tree species. Journal of Ecology, 93, pp. 256–267.

Poorter, H., Niinemets, Ü., Poorter, L., Wright, I.J., Villar, R., (2009) Tansley review. Causes and consequences of variation in leaf mass per area (LMA): a meta-analysis. New Phytologist, 182, pp. 565-588.

Poorter, H., Pepin, S., Rijkers, T., Jong, Y. de, Evans, J. R., Körner C. (2006b) Construction costs, chemical composition and payback time of high- and low-irradiance leaves. Journal of Experimental Botany, 57:355–371.

Potosnak, M.J. (2014) Including the interactive effect of elevated CO_2 concentration and leaf temperature in global models of isoprene emission. Plant, Cell and Environment, 37(8), Special Issue: Plant Volatiles, pp. 1723-1726.

Prioul J.-L. (1973) Éclairement de croissance de infrastructure des chloroplasts de *Lolium multiflorum* Lam. Relations annales de résistance en transfer de CO_2. Photosynthetica, 7, N 4.

Pyke, K.A., Leech, R.M. (1992). Chloroplast division and expansion is radically altered by nuclear mutations in *Arabidopsis thaliana*. Plant Physiology, 99, pp. 1005-1008.

Rasulov, B., Copolovici, L., Laisk, A., Niinemets, Ü. (2009a) Postillumination isoprene emission: in vivo measurements of dimethylallyldiphosphate pool size and isoprene synthase kinetics in aspen leaves. Plant Physiology, 149, pp. 1609–1618.

Rasulov, B., Hüve, K., Välb,e M., Laisk, A., Niinemets Ü. (2009b) Evidence that light, carbon dioxide and oxygen dependencies of leaf isoprene emission are driven by energy status in hybrid aspen. Plant Physiology, 151, pp. 448–460.

Rasulov, B., Hüve, K., Laisk, A., Niinemets, Ü. (2011) Induction of a longerterm component of isoprene release in darkened aspen leaves: origin and regulation under different environmental conditions. Plant Physiology, 156**,** pp. 816–831.

Rasulov B., Hüve K., Bichele I., Laisk A., Niinemets Ü. (2010) Temperature response of isoprene emission in vivo reflects a combined effect of substrate limitations and isoprene synthase activity: a kinetic analysis. Plant Physiology 154, pp. 1558-1570.

Rasulov, B., Bichele, I., Hüve, K., Vislap, V., Niinemets, Ü. (2015). Acclimation of isoprene emission and photosynthesis to growth temperature in hybrid aspen: resolving structural and physiological controls. Plant, Cell and Environment, 38, pp. 751–766.

Rodeghiero, M., Niinemets, Ü., & Cescatti, A. (2007). Major diffusion leaks of clamp-on leaf cuvettes still unaccounted: How erroneous are the estimates of Farquhar *et al*. model parameters? Plant, Cell and Environment, 30, pp. 1006–1022.

Rundel, P.W., Yoder, B.J. (1998) Ecophysiology of *Pinus*. In: Ecology and Biogeography of *Pinus*. Ed. Richardson, D.M. Cambridge University Press, Cambridge, pp. 296-323.

Räim, O., Kaurilind, E., Hallik, L., Merilo, E. (2012). Why does needle photosynthesis decline with tree height in Norway spruce? Plant Biology, 14, pp. 306–314.

Sack, L., Scoffoni, C. (2013) Leaf venation: structure, function, development, evolution, ecology and applications in the past, present and future. New Phytologist, 198(4), pp. 983-1000.

Sáez, P.L., Vallejos, V., Sancho-Knapik, D., Cavieres, L.A., Ramírez, C.F., Bravo, L.A., Peguero-Pina, J.J., Gil-Pelegrín, E., Galmés, J. (2024) Leaf hydraulic properties of Antarctic plants: effects of growth temperature and its coordination with photosynthesis, *Journal of Experimental Botany*, 75(7), pp. 2013 2026.

Santos-Del-Blanco, L., Bonser, S.P., Valladares, F., Chambel, M.R., Climent, J. (2013) Plasticity in reproduction and growth among 52 range-wide populations of a Mediterranean conifer: adaptive

responses to environmental stress. Journal of Evolutionary Biology, 26(9), pp. 1912-24.

Scarpella, E. and Meijer, A.H. (2004), Pattern formation in the vascular system of monocot and dicot plant species. New Phytologist, 164, pp. 209-242.

Sokoloff, D.D., Jura-Morawiec, J., Zoric, L., Fay, M.F. (2021) Plant anatomy: at the heart of modern botany. *Botanical Journal of the Linnean Society*, 195(3), pp. 249–253.

Sharkey, T., Singsaas, E. (1995) Why plants emit isoprene. Nature 374, 769.

Sharkey, T.D, Singsaas, E.L., Vanderveer, P.J., Geron, C. (1996) Field measurements of isoprene emission from trees in response to temperature and light. *Tree Physiology*, 16, 7, pp. 649–654.

Sharkey, T.D. (2005) Effects of moderate heat stress on photosynthesis: importance of thylakoid reactions, rubisco deactivation, reactive oxygen species, and thermotolerance provided by isoprene. Plant Cell and Environment, 28 (3), pp. 269-277.

Sharkey, T.D., Yeh, S. (2001) Isoprene emission from plants. Annual Review of Plant Biology, 52, pp. 407–436.

Sharkey, T.D., Wiberley, A.E., Donohue, A.R. (2008) Isoprene emission from plants: why and how. Annals of Botany, January, 101(1), pp. 5-18.

Sharkey, T.D., Monson, R.K. (2014) The future of isoprene emission from leaves, canopies and landscapes. Plant, Cell and Environment, 37, 8, Special Issue: Plant Volatiles, pp. 1727-1740.

Sharkey, T.D., Monson, R.K. (2017) Isoprene research - 60 years later, the biology is still enigmatic. Plant, Cell and Environment, 40(9), pp.1671-1678.

Singsaas, E.L., Lerdau, M., Winter, K., Sharkey, T.D. (1997) Isoprene increases thermotolerance of isoprene-emitting species. Plant Physiology, 115(4), pp. 1413-1420.

Steppe, K., Niinemets, Ü., Teskey, R. O. (2011). Tree size- and age-related changes in leaf physiology and their influence on carbon gain. In: Meinzer, F.C., Dawson, T., Lachenbruch, B. (Eds.) Size- and age-related changes in tree structure and function, pp. 235–253.

Sun Z., Hüve K., Vislap V., Niinemets Ü. (2013) Elevated [CO_2] magnifies isoprene emissions under heat and improves thermal resistance in hybrid aspen. Journal of Experimental Botany, 64(18), pp. 5509-23.

Syvertsen, J.P., Lloyd, J., McConchie, C., Kriedemann P.E., Farquhar, G.D. (1995) On the relationship between leaf anatomy and CO_2 diffusion through the mesophyll of hypostomatous leaves. Plant Cell and Environment, 18, pp. 149–157.

Taipale, D., Kerminen, V.-M., Ehn, M., Kulmala, M., Niinemets, Ü. (2021) Modelling the influence of biotic plant stress on atmospheric aerosol particle processes throughout a growing season. Atmospheric Chemistry and Physics, 21, pp. 17389–17431.

Terashima, I., Hanba, Y.T., Tazoe, Y., Vyas, P., Yano, S. (2006) Irradiance and phenotype: comparative eco-development of sun and shade leaves in relation to photosynthetic CO2 diffusion. Journal of Experimental Botany, 57, pp. 343– 354.

Terashima, I., Hanba, Y., Tholen, T.D., Niinemets, Ü. (2011). Leaf functional anatomy in relation to photosynthesis. Plant Physiology, 155, pp. 108–116.

Thain, J.F. (1983) Curvature correction factors in the measurement of cell surface areas in plant tissues. Journal of Experimental Botany, 34, pp. 87– 94.

Tosens, T., Niinemets, Ü., Vislap, V., Eichelmann, H., Castro Dies, P. (2012). Developmental changes in mesophyll diffusion conductance and photosynthetic capacity under different light and water availabilities in Populus tremula: How structure constrains function. Plant, Cell and Environment, 35, pp. 839–856.

Trainer, M., Williams, E.J., Parrish, D.D., Buhr, M.P., Allwine, E.J., Westberg, H.H., Fehsenfeld, F.C., Liu, S.C. (1987) Models and observations of the impact of natural hydrocarbons on rural ozone. Nature, 329, pp. 705–707.

Tullus, H., Tullus. A., Soo, T., Vares, A. (2008) Hybrid aspen (*Populus tremula* L.× *P. tremuloides* Michx.) complex study programme in hemiboreal Estonia. Conference presentation on the 23rd Session of IPC (Food and Agriculture Organisation of the United Nations) October 26 – 30, 2008 Beijing. (https://www.fao.org/forestry/ipc2008/51759/en/).

Tullus, H., Tullus, A., Rytter, L. (2013) Short-rotation forestry for supplying biomass for energy production. In: Kellomäki S., Kilpeläinen A., Alam A. (eds) Forest BioEnergy Production. Springer, New York, NY.

Vares, A., Tullus, A., Raudoja, A. (2003) Hübriidhaab: ökoloogia ja majandamine. Triip, Tartu.

Veromann-Jürgenson, L.-L., Brodribb, T., Laanisto, L., Bruun-Lund, S., Niinemets, Ü., Nuño, S. L. Rinnan, R., Puglielli, G., Tosens, T. (2020) Predictability of leaf morphological traits for paleoecological reconstruction: the case of leaf cuticle and leaf dry mass per area. International Journal of Plant Sciences, 181(1), pp. 129–141.

Vickers, C.E., Possell, M., Cojocariu, C.I., Velikova, V.B., Laothawornkitkul, J., Ryan, A., Mullineaux, P.M., Hewitt, C.N. (2009) Isoprene synthesis protects transgenic tobacco plants from oxidative stress. Plant, Cell & Environment, 32, pp. 520–531.

Viñas, R.A., Caudullo, G., Oliveira, S., de Rigo D. (2016) *Pinus pinea* in Europe: distribution, habitat, usage and threats. In: San-Miguel-Ayanz, J., de Rigo, D., Caudullo, G., Houston Durrant, T., Mauri, A. (Eds.) European Atlas of Forest Tree Species, Publication Office of the European Union, Luxembourg, pp. 130-131.

Viveros, R., Sáez, P.L., Ramírez, C., Fuentes, F., Labra, N., Vinka Anic, Cavieres, L.A., Mesophyll conductance limits photosynthesis and relates to anatomical traits in high-elevation plants in the Andes, Environmental and Experimental Botany, 226, pp. 2-10.

von Caemmerer, S., Farquhar, G.D. (1981) Some relationships between the biochemistry of photosynthesis and the gas exchange of leaves. Planta, 153, pp. 376–387.

Way, D.A., Yamori, W. (2014) Thermal acclimation of photosynthesis: On the importance of adjusting our definitions and accounting for thermal acclimation of respiration. Photosynthesis Research, 119, pp. 89–100.

Went, F.W. (1960) Blue hazes in the atmosphere. Nature, 187, pp. 641–643.

Winn, A.A. (1999) The Functional Significance and Fitness Consequences of Heterophylly. International Journal of Plant Sciences 160: S6, pp. 113-121.

Wise, R.R., Hoober, J.K. (ed-s) (2007) The structure and function of plastids. Springer.

Wood, B., Turner, A. (1995) Palaeoanthropology. Out of Africa and into Asia. Nature, 16, 378(6554), pp. 239-40.

Woodruff, D.R., Meinzer, F.C., Lachenbruch, B., Johnson, D.M. (2009). Coordination of leaf structure and gas exchange along a height gradient in a tall conifer. Tree Physiology, 29, pp. 261–272.

Wright, I.J., Cannon, K. (2001) Relationships between leaf lifespan and structural defences in a low-nutrient, sclerophyll flora. Functional Ecology, 15, pp. 351-359.

Wright, I.J., Reich, P.B., Westoby, M., Ackerly, D.D., Baruch, Z., Bongers, F., Cavender-Bares, J., Chapin, T., Cornelissen, J.H.C., Diemer, M., Flexas, J., Garnier, E., Groom, P.K., Gulias, J., Hikosaka, K., Lamont, B.B., Lee, T., Lee, W., Niinemets, Ü., Veneklaas, E.J. ... et, al. (2004). The worldwide leaf economics spectrum. Nature, 428 (6985), 821–827.

Way, D. A., & Yamori, W. (2014). Thermal acclimation of photosynthesis: On the importance of adjusting our definitions and accounting for thermal acclimation of respiration. Photosynthesis Research, 119, 89–100.

Withington, J.M., Reich, P.B., Oleksyn, J., Eissenstat, D.M. (2006) Comparisons of structure and life span in roots and leaves among temperate trees. Ecological Monographies, 76, pp. 381–397.

Yoder BJ, Ryan MG, Waring RH, Schoettle AW, Kaufmann MR (1994) Evidence of reduced photosynthetic rates in old trees. Forest Science, 40, pp. 513–527.

Zotz G, Wilhelm K, Becker A (2011) Heteroblasty – a review. Botanical Reviews, 77, pp. 109–151.

Electronic references in order as they appear in the text:

https://www.conifers.org/pi/Pinus_halepensis.php

https://www.conifers.org/pi/Pinus_nigra.php

Farjon, Aljos. 2010. *A Handbook of the World's Conifers*. Leiden, Netherlands: Brill Academic Publishers.

https://en.wikipedia.org/wiki/Pinus_nigra

https://plants.sc.egov.usda.gov/java/

https://en.wikipedia.org/wiki/Stone_pine

https://et.wikipedia.org/wiki/H%C3%BCbriidhaab#Kasvatamine_Eestis)

SUMMARY IN ESTONIAN

Taimelehtede sisestruktuuri vanusest ja kasvamisaegsest temperatuurist tingitud muutused.

Täpne arusaamine sellest, kuidas taimed keskkonnatingimustega kohanevad ning ontogeneesi käigus muutuvad, võimaldab meil kasvatamiseks valida parimate võimalike tunnustega liigid ja sordid. Kohanemisel mängib olulist rolli taimede siseehitus ehk anatoomia ja antud töö keskendubki anatoomiliste ja füsioloogiliste muutuste uurimisele, mis leiavad aset taime vananemise käigus ning vastusena kõrgele kasvutemperatuurile.

Taimed on Maa ökosüsteemi kõige olulisem komponent, sest neist sõltub kõigi teiste elusolendite eksistents. Kuna taimed ei saa asukohta vahetada, siis on neil evolutsiooni käigus tekkinud võime oludega kohaneda ja ennast vastavalt vajadusele muuta. Kui taim on alles väike, on tema jaoks kõige olulisem ellu jäämine ja piisavalt kiire kasvamine, tugeva juurestiku ja lehestiku kasvatamine. Kolme Vahemeremaades kasvava männi (*Pinus halepensis*, *P. pinea*, *P. nigra*) näitel demonstreerime, kuidas okaste anatoomiast sõltuvalt nende fotosünteesivõime ajas muutub ning mis seda põhjustab. Selgitame fotosünteetiliselt aktiivse mesofülli ja tugikoe osakaalu mõju okkas mesofülli juhtivusele ning lämmastiku kasutamise efektiivsusele. Töö teeb unikaalseks okastes vanuse suurenedes aset leidvate muutuste täpne kaardistamine ning nende seostamine fotosünteesivõimega. (Artiklid I ja II)

Isopreeni eritavad peaaegu kõikide taimede lehed. See on kõige levinum lenduvühend maailmas, mille emissiooni mõjutab tugevalt taime kasvukeskkond. Isopreen on keemiliselt väga reaktiivne ning mõjutab seetõttu tugevalt atmosfäärikeemiat. Kuna tegemist on laialt levinud ja üliolulise ainega, siis on vaja täpselt teada selle eritumise kõiki nüansse, et isopreeniga seotud mudelid ning tulevikuennustused oleksid täpsemad. Antud uurimistöö näitab, et kasvuaegne kõrgem temperatuur muudab olulisel määral lehe anatoomiat ning sellest tulenevalt ka fotosünteesi ning isopreeni eritumist lehe pindala kohta. Lehe sisestruktuuri muutusi kõrgel ja madalal valgustugevusel on palju uuritud, kuid temperatuurist tingitud muutuste uurimine on alles algusjärgus. Selles töös tegime kindlaks, et anatoomilised muutused mõjutavad fotosünteesiaparaadi

kohanemist kõrgematele temperatuuridele. Need muutused võivad ka olla põhjuseks, miks on erinevates kasvuaegse kõrgema temperatuuri mõju uurimustes pindalapõhiselt välja toodud füsioloogilistes näitajates nii suured erinevused. (Artikkel III)

Tööde eesmärk oli paremini mõista taimede anatoomias toimuvaid muutusi, mis leiavad aset nende jaoks keerulistes tingimustes: kui noor taim ennast oma kasvukohal sisse seab ning kui taim peab kasvama tema jaoks normaalsest kõrgemal temperatuuril.

ACKNOWLEDGEMENTS

I thank my supervisor professor Ülo Niinemets for exceptional patience and all his ideas, which really made me think and find solutions to seemingly impossible problems.

I thank my parents for always supporting me.

I thank my family for being patient, kind and inspirational.

I thank all my former and present day colleagues for interesting and supportive conversations.

I give my special thanks to Bahtijor Rasulov who has invented, designed and made the unique equipment for gas-exchange measurements and gave us plov, which united our lab staff in an unprecedented way.

I

ORIGINAL PUBLICATIONS

Vivian Kuusk, Ülo Niinemets, Fernando Valladares (2018a) A major trade-off between structural and photosynthetic investments operative across plant and needle ages in three Mediterranean pines. *Tree Physiology* 38: 543–557.

Tree Physiology 38, 543–557
doi:10.1093/treephys/tpx139

Research paper

A major trade-off between structural and photosynthetic investments operative across plant and needle ages in three Mediterranean pines

Vivian Kuusk[1], Ülo Niinemets[1,2,5] and Fernando Valladares[3,4]

[1]Institute of Agricultural and Environmental Sciences, Estonian University of Life Sciences, Kreutzwaldi 1 Tartu 51014, Estonia; [2]Estonian Academy of Sciences, Kohtu 6, 10130 Tallinn, Estonia; [3]LINCGlobal, Departamento de Biogeografía y Cambio Global, Museo Nacional de Ciencias Naturales, MNCN-CSIC, Serrano 115 dpdo, 28006 Madrid, Spain; [4]Departamento de Biología y Geología, ESCET, Universidad Rey Juan Carlos, Tulipán s/n, 28933 Móstoles, Spain; [5]Corresponding author (ylo.niinemets@emu.ee)

Received May 5, 2017; accepted October 3, 2017; published online December 21, 2017; handling Editor Sean Thomas

Pine (*Pinus*) species exhibit extensive variation in needle shape and size between juvenile (primary) and adult (secondary) needles (heteroblasty), but few studies have quantified the changes in needle morphological, anatomical and chemical traits upon juvenile-to-adult transition. Mediterranean pines keep juvenile needles longer than most other pines, implying that juvenile needles play a particularly significant role in seedling and sapling establishment in this environment. We studied needle anatomical, morphological and chemical characteristics in juvenile and different-aged adult needles in Mediterranean pines *Pinus halepensis* Mill., *Pinus pinea* L. and *Pinus nigra* J. F. Arnold subsp. *salzmannii* (Dunal) Franco hypothesizing that needle anatomical modifications upon juvenile-to-adult transition lead to a trade-off between investments in support and photosynthetic tissues, and that analogous changes occur with needle aging albeit to a lower degree. Compared with adult needles, juvenile needles of all species were narrower with 1.6- to 2.4-fold lower leaf dry mass per unit area, and had ~1.4-fold thinner cell walls, but needle nitrogen content per dry mass was similar among plant ages. Juvenile needles also had ~1.5-fold greater mesophyll volume fraction, ~3-fold greater chloroplast volume fraction and ~1.7-fold greater chloroplast exposed to mesophyll exposed surface area ratio, suggesting overall greater photosynthetic activity. Changes in needle traits were similar in aging adult needles, but the magnitude was generally less than the changes upon juvenile to adult transition. In adult needles, the fraction in support tissues scaled positively with known ranking of species tolerance of drought (*P. halepensis* > *P. pinea* > *P. nigra*). Across all species, and needle and plant ages, a negative correlation between volume fractions of mesophyll and structural tissues was observed, manifesting a trade-off between biomass investments in different needle functions. These results demonstrate that within the broad trade-off, juvenile and adult needle morphophysiotypes are separated by varying investments in support and photosynthetic functions. We suggest that the ecological advantage of the juvenile morphophysiotype is maximization of carbon gain of establishing saplings, while adult needle physiognomy enhances environmental stress tolerance of established plants.

Keywords: cell wall thickness, heteroblasty, needle age, needle morphology, nitrogen content, *Pinus halepensis*, *Pinus nigra*, *Pinus pinea*, primary needles, secondary needles.

Introduction

Increases in tree age and height are associated with profound changes in foliage anatomy, morphology and chemistry with major impacts on foliage photosynthetic capacity (Niinemets and Kull 1995, Day et al. 2001, Niinemets 2002, Thomas and Winner 2002, Woodruff et al. 2009, Thomas 2010, Steppe et al. 2011, Mediavilla et al. 2014) that alter whole-tree carbon gain and competitive ability. Particularly in conifers, increases in tree age and size are associated with reductions in foliage photosynthetic capacity per dry mass (Steppe et al. 2011). There is a continuous age- and size-dependent change in leaf traits through plant life called ontogenetic drift, which has been

© The Author(s) 2017. Published by Oxford University Press. All rights reserved. For Permissions, please email: journals.permissions@oup.com

Downloaded from https://academic.oup.com/treephys/article/38/4/543/4769388 by Estonian University of Life Sciences user on 23 September 2020

studied in the majority of investigations looking at tree age and size effects on foliage structure and function. However, changes in leaf traits are characteristically the largest during development from juvenile to adult leaves and many species exhibit an almost abrupt developmental change called heteroblasty (Zotz et al. 2011). Heteroblasty is particularly pronounced in some plant genera, but the variation in the extent of heteroblastic changes in different species is poorly known, and although heteroblasty is widely considered as adaptive, there are few studies examining its role in altering plant survivorship and competitive relations (Day and Greenwood 2011, Climent et al. 2011*b*).

Pine (*Pinus*) species exhibit remarkably large differences in needle morphology and function between juvenile and adult phases (Climent et al. 2011*b*), with juveniles characterized by less sclerophytic needles that have smaller cross-sectional area (Boddi et al. 2002) and lower leaf dry mass per unit area (Pardos et al. 2009, Mediavilla et al. 2014), but greater photosynthetic capacity (Niinemets 2002), ultimately leading to a shorter needle payback time (Day and Greenwood 2011). The factors responsible for greater assimilation potentials of juvenile needles are poorly known. They could involve any of the three key limitations of photosynthesis: stomatal, biochemical (total amount of photosynthetic enzymes) and mesophyll diffusion (Flexas et al. 2012). Past studies have demonstrated that both stomatal and biochemical limitations increase with increasing plant age and size (Day et al. 2001, Niinemets 2002, Woodruff et al. 2009, Steppe et al. 2011, Räim et al. 2012).

In fact, anatomical differences among juvenile and adult needles can directly impact photosynthesis by altering the fraction of photosynthetically competent mesophyll tissue. With increasing needle structural robustness upon juvenile-to-adult transition, the fractional investment in support tissues, including strongly lignified epidermal and hypodermal tissues and central cylinder, is expected to increase, inevitably resulting in lower fractions of mesophyll tissues. Such a possible trade-off could importantly further contribute to reductions of the carbon gain of adult needles. So far, it has been demonstrated that there is a significant variation in the mesophyll volume fraction among pine species, and this variation explains species differences in photosynthetic activity (Niinemets et al. 2007). However, for adult needles, tree size and age-dependent anatomical and structural modifications only moderately or not at all altered the share among mesophyll and support tissues (Richardson et al. 2000, Apple et al. 2002, Greenwood et al. 2008), but so far, there is no information on juvenile-to-adult transition effects on fractional distribution of photosynthetic and support tissues.

Compared with European boreal and temperate pine species, the juvenile period lasts longer in Mediterranean pines (Climent et al. 2011*b*), implying that this period of plant life plays a particularly significant role in seedling and sapling establishment in highly stressful Mediterranean environments. Here we studied anatomical and photosynthetic differences between juvenile and mature needles of three Mediterranean pine species—*Pinus halepensis* Mill., *Pinus pinea* L. and *Pinus nigra* J. F. Arnold subsp. *salzmannii* (Dunal) Franco. All three pine species bear single juvenile (primary) and paired adult (secondary) needles in fascicles. The seedlings and young juvenile saplings (as described in Hanley et al. 2004) can carry juvenile needles for several years until they are gradually replaced by adult needles (Boddi et al. 2002). Juvenile needles are bluish, short and elliptical or rhomboidal in shape, while adult secondary needles are dark green and significantly longer and thicker (Climent et al. 2006*a*). We hypothesized that there is a trade-off between support and photosynthetic investments upon juvenile to adult transition.

As needle age also influences foliage structure and chemistry (Teskey et al. 1984, Niinemets 2002, Weiskittel et al. 2008, Niinemets et al. 2012, Mediavilla et al. 2014), but the anatomical and structural modifications in ageing needles are poorly understood, we studied non-senescent adult needles of three different age classes (current-year, 1-year-old and 2-year-old needles). We hypothesized that ageing also leads to accumulation of structural biomass similar to juvenile-to-adult transition, thereby resulting in reduction in foliage nitrogen content. However, because ageing cannot change the basic leaf morphological framework, e.g., position, number and size of cells in the leaf cross-section, we expected that the needle age-dependent changes in older needles are quantitatively less significant than modifications occurring upon juvenile-to-adult transition.

The results of this study highlight a major trade-off between investments in support and physiologically active tissues, and also show that plant age-dependent modifications are more profound than needle age-dependent alterations.

Materials and methods

Study species

Pinus halepensis is found growing in marls, limestone, dolomites, acid sands and sandstone, mostly in subhumid and semiarid climates from lowlands (up to 700 m) to submontane (from 700 to 1300 m) areas, and is the most drought tolerant of the three investigated species (Barbéro et al. 1998, Atzmon et al. 2004). *Pinus nigra* subsp. *salzmannii* prefers limestone, dolomites, acid sands and volcanic (ultrabasic) rocks and mostly humid areas in mid-montane to mountainous (from 900–1000 m up to 1600–1800 m) areas (Kienast et al. 1987, Barbéro et al. 1998). *Pinus pinea* grows on dolomites and sandstone in subhumid climates, mostly at lowland to submontane areas, and its environmental requirements are in between *P. halepensis* and *P. nigra* (Cabanettes and Rapp 1978, Barbéro et al. 1998). Needle life span in mature plants is 2.7 years for *P. halepensis* (Niinemets 2010), 3.8 years for *P. nigra* (Withington et al. 2006) and 4.1 years for *P. pinea* (Mediavilla et al. 2014). The life span of juvenile needles in saplings is less, ~1–1.5 years (Mediavilla et al. 2014, and personal observations).

Downloaded from https://academic.oup.com/treephys/article/38/4/543/4769388 by Estonian University of Life Sciences user on 23 September 2020

Measurement sites and plants

The mature cone-bearing plants were studied at Alto Tajo Natural Park, Los Cerrillos sampling site, in the vicinity of Villar de Cobeta, central Spain (Guadalajara, Castilla-La Mancha, 40.8480°N, 2.1812°W). The climate in the study area is continental Mediterranean with hot and dry summers and cold and dry winters. According to Molina de Aragón climatic station (40.8444°N, 1.8853°W, elevation 1063 m), the mean annual rainfall is 490 mm and mean annual temperature is 10.2 °C. The site has a mean elevation of 950 m, with steep slopes and cliffs covered with Mediterranean-type shrublands, and 5–20 m high open forests dominated by *Quercus ilex*, L. subsp. *ballota* (Desf.) Samp. on south-facing slopes and *P. nigra* subsp. *salzmannii* on north-facing slopes. The upper parts of the plateaus are dominated by *Juniperus thurifera* L., *Pinus sylvestris* L. and *Buxus sempervirens* L. Soils are basic, rocky and poorly developed over the limestone bedrock. Five trees were randomly chosen for each species for sampling of needles of different age classes. Mean tree diameter at breast height, mean tree height and estimated tree age were 40 cm, 15 m and 95 years for *P. halepensis*, 44 cm, 17 m and 90 years for *P. pinea* and 60 cm, 21 m and 100 years for *P. nigra*. Representative terminal branchlets carrying only needles (without cones) were sampled from mid-height and from the southern aspect of upper canopy and were exposed to a daily integrated quantum flux density of ~40 mol m^{-2} day^{-1}.

To study juvenile foliage, 2-year-old juvenile plants were bought from a local nursery at El Seranillo Forestry Center, Guadalajara and transplanted to 5 L pots filled with a mixture (4:4:1:1, v/v) of compost, vermiculite, perlite and sand, with slow release N:P:K (14:13:13) fertilizer with micronutrients (Osmocote, Scotts Miracle-Gro Company, Marysville, OH, USA, Baquedano and Castillo 2007, Baquedano et al. 2008 for details). The juvenile saplings were grown at the greenhouses of Museo Nacional de Ciencias Naturales (CSIC) in Madrid, Spain (40.440°N, 3.690°W, elevation 682 m). The pots had big holes in the bottom and were buried into soil. There were nine pots per m^2 and the soil temperature was ambient. The plants were grown under full sunlight with the mean daily integrated photosynthetic quantum flux density during spring of 41 mol m^{-2} day^{-1}. Current-year juvenile needles that had formed under the new growth conditions were used for the measurements.

An apparent limitation of this experiment is that juvenile and adult foliage could not be studied at the same environmental setting. However, this limitation was inevitable as the juvenile plants were very rare in the field and were only found in shaded habitats and we intended to avoid shade effects interfering with our analysis (Poorter et al. 2009, Niinemets et al. 2015, Keenan and Niinemets 2016). Shading effects on leaf structure are typically much greater than the effects of nutrients or water availability (Poorter et al. 2009 for a review), although in particularly tall tree canopies, shading and water availability can collectively affect foliage structure (Koch et al. 2004, Woodruff et al. 2007). To avoid the confounding shading effects, we used potted saplings grown under full sunlight and similar environmental conditions as those prevailing in the field. In fact, often the studies on plant size and age versus leaf structure and function are carried out along the chronosequence of different stands to avoid the shading effects that would be inevitable when different-aged individuals are sampled within the same stand. Although such experimental designs introduce a certain level of confounding variability due to possible differences in site conditions, we argue that avoiding the shading effects inevitable in studies with different-sized plants in the same stands (Poorter et al. 2009 for major sources of shading effects) is superior to controlling for other sources of variability (e.g., Chandler and Dale 1993, Helmisaari 1990, Niinemets et al. 2001 for illustration of moderate effects of site fertility on foliage structural traits in conifers). In addition, we argue that the general trade-offs among needle fractional investments in different tissues through needle ages, plant ages and species are not dependent on site effects.

Foliage sampling

At the field site, branches of randomly chosen mature plants growing at full sunlight (one branch from each individual tree) were collected from the mid-height of the canopy to reduce the influence of light on needle characteristics (Gebauer et al. 2011, Niinemets et al. 2015) in October 2005 and in August 2006. To maintain the needle hydration state, the branches were cut under water, the cut ends were maintained in water and the branches were transported to the laboratory for foliage structural measurements.

In adult trees bearing secondary needles, needles of age classes with at least 50% needles present were studied. Three different age classes (current-year, 1-year-old and 2-year-old needles) were investigated in *P. nigra* and *P. pinea*. In *P. halepensis*, which has a shorter leaf life span than the other two species, current-year and 1-year-old needles were studied. In the case of juvenile plants where the canopy mainly (>90%) consisted of juvenile (primary) current-year needles, only this needle age class was studied. In 2005 we measured five juvenile plants from each studied species and five branches from adult trees per species. In 2006, two branches from *P. halepensis*, three branches from *P. pinea* and four branches from *P. nigra* mature trees were measured. In total, 24 branches (from seven trees of *P. halepensis*, eight trees of *P. pinea* and nine trees of *P. nigra*) and 15 juvenile plants (five of each species) were used, and altogether 5–8 samples for each tree age × leaf age × species combination, on average 6.7, were available.

Measurements of needle morphological and anatomical characteristics

At least 10 needles from each age class were randomly sampled from each branch. Needle length (*L*), width (*W*) and thickness

Downloaded from https://academic.oup.com/treephys/article/38/4/543/4769388 by Estonian University of Life Sciences user on 23 September 2020

(T) from the central needle part were measured with Starrett Digital calipers (model 727, L. S. Starrett Company, Athol, MA, USA), and average needle projected area, S_P, was calculated as WL. Altogether 190 (juvenile current year, and mature different age classes) needles were measured for *P. halepensis*, 290 for *P. pinea* and 310 for *P. nigra*.

Needles for preparation of free-hand cross-sections for anatomy were randomly selected from the set of harvested needles (a subsample of three needles) for each species, branch and age class. The sections taken from the central parts of the needles were stained with phloroglucinol and HCl to specifically visualize the lignified tissues in red (Weisner test) as in Niinemets et al. (2005*a*, 2007). The images were viewed at 20–100× magnification and digital pictures were taken with a Nikon Eclipse E600 microscope and Nikon digital DS-Fi1 camera (Nikon Corporation, Tokyo, Japan). Needle cross-section width, thickness, circumference (U), needle cross-sectional area (S_S) and the area of the lignified tissues were measured from the images using UTHSCSA Image Tool for Windows Version 3.00 software (UTHSCSA, TX, San Antonio, USA, 1995–2002). From these measurements, the ratio of needle total (S_T) to projected surface area, S_T/S_P, was calculated as U/W and needle volume to total area ratio, V/S_T, as S_S/U, needle volume to projected area ratio as S_S/W and needle total area as UL (Niinemets and Kull 1995, Niinemets et al. 2007). Comparison of thickness and width measurements from free-hand sections by microscopy and from intact needles by calipers indicated a strong correspondence between two types of measurements (within 5%).

In addition to the free-hand sections, needle samples were taken for electron microscopy next to the site of taking the free-hand sections from the middle part of the needle and fixed by infiltrating with 2% glutaric aldehyde in 0.2 M phosphate buffer (pH 7.2) under negative pressure in a syringe. After fixation, the samples were dehydrated in ethanol series and embedded in Epoxy Embedding Medium (Sigma-Aldrich Chemie, Steinheim, Germany) as described by Bozzola and Russell (1992). An OM U2 Ultra Microtome (American Optical Corporation, Reichert Products, Buffalo, NY, USA) with a 45° diamond knife (Diatome, Hatfield, PA, USA) was used for cutting semithin sections for light microscopy (1.5–2 µm) and ultrathin sections (70–90 nm) for transmission electron microscopy (TEM). The semithin sections were stained with Toluidine Blue as described in Burns (1978) and viewed and photographed with a Zeiss Axioplan 2 (Carl Zeiss Microscopy, Jena, Germany) microscope using a 40× magnifying objective with 0.63× lens and a digital camera AxioCam HRc (Carl Zeiss Microscopy). From these images, epidermis, endodermis, hypodermis, mesophyll, mesophyll air spaces, central cylinder and resin ducts areas were measured using the UTHSCSA Image Tool as described in Niinemets et al. (2007). For each sample, 5–10 sections were measured and averages were calculated.

Uranyl acetate and lead citrate were used to contrast the ultrathin (90–100 nm) sections as in Copolovici et al. (2011) and the samples were viewed under a Philips Tecnai 10 TEM (FEI, Eindhoven, The Netherlands) that was operated with an accelerating voltage of 80 kV. Digital pictures were taken with an Olympus Veleta 2 K × 2 K sidemounted TEM CCD camera (Olympus Soft Imaging Solutions GmbH, Germany, Münster, Germany). Magnifications of 7000–10,000× were used to measure cell wall thickness, chloroplast length, thickness and circumference with the UTHSCSA Image Tool (6–12 chloroplasts were measured from each section and 5–15 sections, on average 7.5 sections per sample were measured). Mesophyll (S_m/S_P) and chloroplast (S_c/S_P) surface area exposed to intercellular air space per unit of projected leaf area were also measured from the TEM micrographs at 1250–3700× magnification and calculated according to Evans et al. (1994) using a curvature correction factor of 1.27 (Thain 1983). The volume of mesophyll per needle projected area (V_m/S_P) and the volume of chloroplasts per projected area (V_c/S_P) were also calculated, and ultimately the fraction of chloroplasts in needle cross-section, f_{chl}, was calculated as $V_c/V_m f_{ma}$, where f_{ma} is the fraction of mesophyll in needle cross-section without intercellular air space.

Estimation of needle dry mass per unit area, density, dry to fresh mass ratio, carbon and nitrogen contents

Fresh mass of sample needles was immediately estimated after measurements of needle dimensions. Then needles were oven-dried for 48 h at 70 °C and nitrogen (N_m) and carbon (C_m) contents per dry mass were measured with a Perkin Elmer series II CHNS/O Analyzer 2400 (Perkin Elmer Life and Analytical Sciences, Inc., Boston, MA, USA).

From these measurements, needle dry to fresh mass ratio, needle dry mass ($M_{A,P}$) and needle nitrogen content ($N_{A,P}$) per projected area were calculated. Considering that the trait values per total area are given as the values per projected area divided by S_T/S_P, needle dry mass ($M_{A,T}$) and nitrogen content ($N_{A,T}$) per total needle area were also calculated. Leaf dry mass per unit area can be expressed as a product of leaf density (D) and thickness (Witkowski and Lamont 1991, Niinemets 1999, Poorter et al. 2009), and for needle-leaved species with complex cross-sectional geometry as the product of needle density and volume to area ratio (Niinemets and Kull 1995). Thus needle density was calculated as $D = \frac{M_{A,T}}{V/S_T}$.

Statistical analyses

Average values for all needles taken from the given branch and needle age class were calculated prior to the statistical analyses. One-way ANOVAs followed by Tukey's post-hoc test were used

Downloaded from https://academic.oup.com/treephys/article/38/4/543/4769388 by Estonian University of Life Sciences user on 23 September 2020

to analyze the differences in trait means among study years, needle age classes and among trees of different age using Statistica 6 (StatSoft Inc., Tulsa, OK, USA) and R 3.1.1 (R Development Core Team 2012). Because the study year was not significant in any of the analyses, the data for both years were pooled in all analyses. For simplicity, two-way ANOVAs were carried out to test for the global effects of species and effects of heteroblasty on the traits of current-year needles in saplings and mature trees (species and plant age as main factors), and effects of species and needle age on traits of adult needles in mature trees (species and needle age as main factors with needle ages as juv—current year juvenile needles, m0—current year needles in mature trees, m1—1-year old needles in mature trees and m2—2-year-old needles in mature trees). One-way ANOVAs were also conducted to separate the differences among the trait means for different combinations of tree age (juvenile vs adult), needle age and species. The relationships among traits were studied by linear and non-linear (log or power) regression analyses. All r^2 values reported in the text refer to linear regressions unless noted. All statistical tests were considered significant at $P < 0.05$.

Results

Age and species effects on needle shape and morphology

The cross-section of adult (secondary) needles was hemi-elliptical to hemi-circular in all three *Pinus* species, but the cross-section of juvenile (primary) needles was rhomboidal in *P. halepensis*, sectorial in *P. pinea* and intermediate between sectorial and rhomboidal shapes in *P. nigra* (Figure 1). Thickness of juvenile and adult current-year needles was similar, but juvenile needles were narrower with smaller circumference and cross-sectional area than adult needles (Table 1). Due to differences in needle shape, needle total to projected area ratio (S_T/S_P) was smaller in juvenile than in adult needles, except for *P. nigra* where this trait did not differ among juvenile and current-year adult needles (Table 1).

Needle dry mass per unit total ($M_{A,T}$, Figure 2A) and projected ($M_{A,P}$, Table 2) area was lower in juvenile than in adult needles in all species. Analysis of the variation in the components of $M_{A,T}$, needle volume to total area ratio (V/S_T) and needle density (D) indicated that differences in $M_{A,T}$ among juvenile and adult current-year needles were driven by lower V/S_T in all species

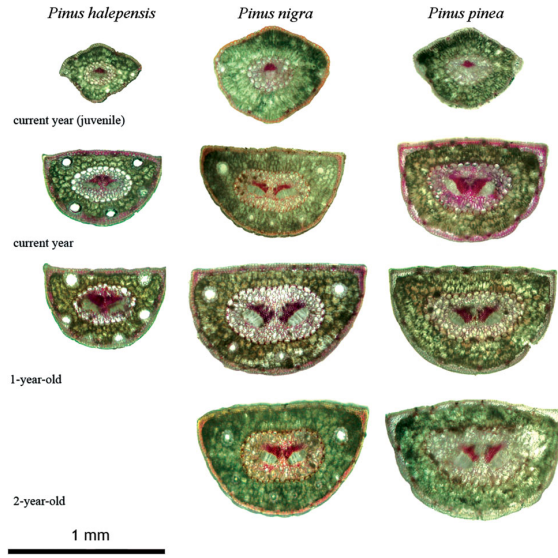

Figure 1. Representative free-hand needle cross-sections of juvenile (primary) current-year and different-aged adult (secondary) needles in three Mediterranean *Pinus* species. Juvenile needles were sampled from 2-year-old 0.2–0.3 m tall young plants, while the adult needles were sampled from 15 to 21 m tall cone-bearing mature trees. Needle cross-sections were stained with phloroglucinol that specifically stains lignified tissues.

Downloaded from https://academic.oup.com/treephys/article/38/4/543/4769388 by Estonian University of Life Sciences user on 23 September 2020

Table 1. Effects of tree and needle age on average (±SE) needle linear dimensions (thickness (T), width (W), circumference (U)), needle total area (S_T) and total to projected area ratio (S_T/S_P) in the three Mediterranean *Pinus* species.

Species	Tree age class	Needle age	T (mm)	W (mm)	U (mm)	S_T (mm^2)	S_T/S_P
P. halepensis	Seedling	(juv)	0.431 ± 0.014^{a}	0.541 ± 0.015^{a}	1.412 ± 0.042^{a}	19.1 ± 0.8^{a}	2.608 ± 0.015^{a}
P. halepensis	Mature	(m0)	0.478 ± 0.016^{a}	0.738 ± 0.017^{a}	2.065 ± 0.043^{ab}	26.1 ± 1.0^{a}	2.798 ± 0.017^{bc}
P. halepensis	Mature	(m1)	0.479 ± 0.014^{a}	0.773 ± 0.018^{a}	2.21 ± 0.06^{bc}	28.7 ± 0.5^{ab}	2.862 ± 0.043^{c}
P. nigra	Seedling	(juv)	0.615 ± 0.012^{b}	0.727 ± 0.036^{a}	1.95 ± 0.10^{ab}	24.4 ± 1.7^{a}	2.69 ± 0.07^{ab}
P. nigra	Mature	(m0)	0.579 ± 0.010^{b}	1.008 ± 0.020^{b}	2.85 ± 0.08^{cd}	37.7 ± 1.2^{bc}	2.826 ± 0.026^{bc}
P. nigra	Mature	(m1)	0.637 ± 0.024^{b}	1.126 ± 0.036^{ab}	3.14 ± 0.09^{de}	44.3 ± 1.4^{c}	2.789 ± 0.034^{bc}
P. nigra	Mature	(m2)	0.660 ± 0.028^{b}	1.179 ± 0.042^{ab}	3.29 ± 0.10^{de}	43.0 ± 1.6^{c}	2.792 ± 0.032^{bc}
P. pinea	Seedling	(juv)	0.644 ± 0.019^{b}	0.74 ± 0.09^{a}	2.02 ± 0.26^{ab}	28.3 ± 1.5^{ab}	2.722 ± 0.036^{abc}
P. pinea	Mature	(m0)	0.612 ± 0.027^{b}	1.134 ± 0.032^{ab}	3.15 ± 0.08^{de}	42.4 ± 1.7^{c}	2.778 ± 0.021^{abc}
P. pinea	Mature	(m1)	0.674 ± 0.025^{b}	1.33 ± 0.12^{b}	3.68 ± 0.36^{e}	46.8 ± 5.6^{c}	2.760 ± 0.023^{abc}
P. pinea	Mature	(m2)	0.651 ± 0.019^{b}	1.250 ± 0.017^{b}	3.41 ± 0.06^{de}	44.1 ± 1.5^{c}	2.726 ± 0.017^{abc}
F-values for two-way ANOVA (juvenile vs adult current-year needles)							
Tree age ($F_{1,32}$)			0.22 ns	134.9***	155.0***	83.2***	18.7***
Species ($F_{2,32}$)			38.3***	59.0***	57.0***	39.8***	1.02 ns
Tree age × Species ($F_{2,32}$)			2.64 ns	4.91*	3.55*	3.04 ns	1.79 ns
F-values for two-way ANOVA (adult needles of different age)							
Needle age ($F_{2,51}$)			3.72*	4.85*	4.09*	2.77 ns	0.63 ns
Species ($F_{2,51}$)			29.7***	42.7***	36.6***	28.7***	3.17 ns
Needle age × Species ($F_{3,51}$)			1.16 ns	1.13 ns	0.96 ns	0.36	1.11 ns

$n = 5$–8 (on average 6.7) for all average values. Seedlings were 2 years old and 0.2–0.3 m tall at the time of sampling, while the mean height of mature trees was 15 m for *P. halepensis*, 17 m for *P. pinea* and 21 m for *P. nigra* at the time of sampling. Needle ages as: juv, juvenile current year; m0, mature current year; m1, mature 1-year-old; m2, mature 2-year-old needles. Different letters denote statistical significance of average values for different species and needle age class combinations at $P < 0.05$ (one-way ANOVA followed by a Tukey post-hoc test based on $F_{10,63}$). In the case of two-way ANOVA, significance levels as: *$P < 0.05$, **$P < 0.01$, ***$P < 0.001$, ns, not significant.

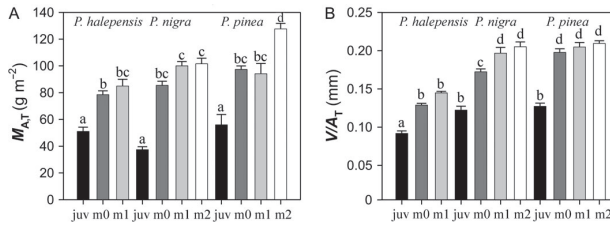

Figure 2. Differences in leaf dry mass per unit total needle area ($M_{A,T}$) and needle volume to total area ratio (V/A_T) in dependence of needle and plant age in three Mediterranean *Pinus* species. $M_{A,T}$ is the product of needle density (Table 2) and V/A_T. Needle ages as: juv, juvenile current year; m0, mature current year; m1, mature 1-year-old; m2, mature 2-year-old needles (Figure 1 for representative needle cross-sections). Data correspond to average ±SE values of 5–8 (on average 6.7) replicates, and different letters show statistical significance among needle age classes and species at $P < 0.05$ (ANOVA followed by a Tukey post-hoc test).

(Figure 2B), and by lower density in juvenile needles of *P. nigra* (Table 2). Needle dry to fresh mass ratio was lower for juvenile than for adult current-year needles in *P. halepensis* (Table 2).

Among adult needles in mature trees, needle linear dimensions, i.e., needle thickness, width and circumference, increased somewhat with needle age (Table 1). $M_{A,T}$ and $M_{A,P}$ were greater in 2-year-old needles than in current-year and 1-year-old needles of *P. pinea* (Figure 2A, Table 2), while V/S_T was greater in 1- and 2-year-old needles than in current year needles in *P. nigra* (Figure 2B). Needle dry to fresh mass ratio was greater in 1- and 2-year-old needles than in current-year needles in all species (Table 2).

Although the heteroblastic and needle age-dependent changes were broadly similar in different species, most needle dimensions ($M_{A,T}$, $M_{A,P}$ and V/S_T) were smaller for needles of given age in *P. halepensis* than in *P. nigra* and *P. pinea* (Figures 1 and 2, Tables 1 and 2). In addition, $M_{A,T}$ (Figure 2A) and $M_{A,P}$ (Table 2) of 2-year-old needles of *P. pinea* were greater than those in *P. nigra*, reflecting greater needle density of *P. pinea* 2-year-old-needles (Table 2).

Downloaded from https://academic.oup.com/treephys/article/38/4/543/4769388 by Estonian University of Life Sciences user on 23 September 2020

Table 2. Variations in needle dry mass per unit area ($M_{A,F}$), dry to fresh mass ratio ($R_{D/F}$), density (D) and carbon content (C_m) in relation to tree and needle age in three Mediterranean *Pinus* species.

Species	Tree age class	Needle age	$M_{A,F}$ (g m^{-2})	$R_{D/F}$ (g g^{-1})	D (g cm^{-3})	C_m (%)
P. halepensis	Seedling	(juv)	133 ± 9^{a}	0.393 ± 0.007^{a}	0.555 ± 0.026^{bc}	48.12 ± 0.15^{a}
P. halepensis	Mature	(m0)	219 ± 8^{b}	0.4687 ± 0.0035^{cd}	0.611 ± 0.027^{c}	50.62 ± 0.21^{cde}
P. halepensis	Mature	(m1)	244 ± 16^{bc}	0.514 ± 0.010^{e}	0.586 ± 0.034^{c}	51.3 ± 0.6^{de}
P. nigra	Seedling	(juv)	99.9 ± 4.8^{a}	0.357 ± 0.007^{a}	0.308 ± 0.021^{a}	49.71 ± 0.31^{abc}
P. nigra	Mature	(m0)	241 ± 7^{bc}	0.3798 ± 0.0021^{a}	0.498 ± 0.023^{bc}	49.50 ± 0.11^{abc}
P. nigra	Mature	(m1)	279 ± 8^{bc}	0.472 ± 0.019^{cde}	0.518 ± 0.038^{bc}	51.54 ± 0.20^{de}
P. nigra	Mature	(m2)	284 ± 12^{c}	0.511 ± 0.010^{de}	0.501 ± 0.032^{bc}	52.24 ± 0.33^{e}
P. pinea	Seedling	(juv)	153 ± 23^{a}	0.4009 ± 0.005^{ab}	0.44 ± 0.06^{ab}	50.15 ± 0.11^{bcd}
P. pinea	Mature	(m0)	270 ± 8^{bc}	0.382 ± 0.007^{a}	0.495 ± 0.019^{bc}	48.78 ± 0.26^{ab}
P. pinea	Mature	(m1)	260 ± 21^{bc}	0.4442 ± 0.0006^{bc}	0.464 ± 0.041^{bc}	49.28 ± 0.08^{abc}
P. pinea	Mature	(m2)	347 ± 9^{d}	0.484 ± 0.008^{cde}	0.611 ± 0.023^{c}	49.09 ± 0.22^{abc}
F-values for two-way ANOVA (juvenile vs adult current-year needles)						
Tree age ($F_{1,32}$)			164.7***	26.4***	22.2***	0.013 ns
Species ($F_{2,32}$)			7.35**	64.6***	14.9***	0.40 ns
Tree age × Species ($F_{2,32}$)			3.67*	29.9***	3.37*	29.8***
F-values for two-way ANOVA (adult needles of different age)						
Needle age ($F_{2,51}$)			12.5***	78.6***	2.45 ns	13.1***
Species ($F_{2,51}$)			6.65**	37.8***	7.20*	32.5***
Needle age × Species ($F_{3,51}$)			3.38*	2.25 ns	2.14 ns	4.9**

Sample number, data presentation and statistical analyses as in Table 1, except for C_m ($n = 3$–6 for each average estimate, and $n = 19$ for the residuals of the *F*-values for juvenile vs adult comparison and $n = 26$ for comparisons of adult needle ages).

Age and species differences in distribution of needle volume among photosynthetic and structural tissues

Visual assessment of needle cross-sections indicates that epidermis, hypodermis, endodermis, xylem and partly the cells of the transfusion tissue that surrounds the vascular bundles in the central cylinder had lignified cell walls that stained red upon phloroglucinol treatment (Figure 1). Although a non-quantitative measure, the staining intensity of different mechanical tissue fractions was visibly greater in adult than in juvenile needles (Figure 1).

The volume fraction of epidermal tissues (f_e, sum of epidermis and hypodermis, Figure 1) was lower in juvenile than in adult current-year needles of *P. halepensis* and current-year needles of *P. nigra*, and the fraction of central cylinder (f_c) was lower in juvenile than in adult needles in all species (Table 3). Thus, the total fraction of mechanical tissues (f_{tm}), the sum of epidermal tissues and the central cylinder, was in all cases lower in juvenile than in adult current-year needles (Table 3). The volume fraction of resin ducts was smaller, and the fractions of total mesophyll, mesophyll without air spaces, mesophyll air spaces and chloroplasts were greater in juvenile than in adult current-year needles (Table 3).

Among the adult needles, leaf tissue distribution was weakly affected by needle age (Table 3). However, the species effect was significant in all cases, reflecting mainly greater fractions of mechanical tissues and a lower fraction of mesophyll in *P. halepensis* and *P. pinea* than in *P. nigra* (Table 3). Across all data, mechanical tissue fractions were positively correlated with each other ($r^2 = 0.39$ for f_e vs f_{tm} and $r^2 = 0.77$ for f_c vs f_{tm}, $P < 0.001$ for both), except for the correlation among f_e and f_c ($r^2 = 0.04$, $P > 0.1$). The mechanical and mesophyll tissue fractions were negatively correlated (e.g., for f_{tm}, $r^2 = 0.98$ for total mesophyll and $r^2 = 0.77$ for the mesophyll fraction without intercellular air space, $P < 0.001$ for both). The fraction of chloroplasts and the fraction of mesophyll with ($r^2 = 0.20$) and without air space ($r^2 = 0.21$) were positively correlated ($P < 0.001$ for both).

The f_e scaled positively with needle density ($r^2 = 0.18$, $P < 0.01$) and with needle dry to fresh mass ratio ($r^2 = 0.10$, $P < 0.05$), while f_c and f_{tm} scaled positively with density ($r^2 = 0.26$ for f_c and $r^2 = 0.34$ for f_{tm}, $P < 0.001$ for both), with dry to fresh mass ratio ($r^2 = 0.17$ for f_c and $r^2 = 0.23$ for f_{tm}, $P < 0.01$), with $M_{A,T}$ ($r^2 = 0.66$ and $r^2 = 0.52$ for f_{tm}, $P < 0.001$) and with V/S_T ($r^2 = 0.55$ for f_c and $r^2 = 0.33$ for f_{tm}, $P < 0.001$). The relationships of the fractions of total mesophyll and mesophyll without air spaces with these four structural traits were analogous to f_{tm}, but negative (see Figure 4A for the correlation with $M_{A,T}$).

Differences in needle ultrastructure among plant and needle ages and species

Juvenile needles had thinner cell walls than current-year mature needles in *P. nigra* and in *P. pinea*, but not in *P. halepensis* (Table 4). Chloroplasts in juvenile needles had greater width in *P. halepensis* and *P. nigra* and greater thickness and circumference in *P. halepensis* than the chloroplasts in mature needles (Table 4). Mesophyll surface (S_m/S_P) and chloroplast surface area (S_c/S_P) exposed to intercellular air space per projected leaf area did not differ among juvenile and mature needles, but the

Downloaded from https://academic.oup.com/treephys/article/38/4/543/4769388 by Estonian University of Life Sciences user on 23 September 2020

Downloaded from https://academic.oup.com/treephys/article/38/4/543/4769388 by Estonian University of Life Sciences user on 23 September 2020

Table 3. Average (±SE) volume fractions of different needle tissues in three Mediterranean *Pinus* species in dependence on needle and tree ages.

Species	Tree age class	Needle age	Tissue volume fraction[1]							
			Total mechanical	Epidermal tissues	Central cylinder	Resin ducts	Total mesophyll	Mesophyll air spaces	Mesophyll without air spaces	Chloroplasts
P. halepensis	Seedling	(juv)	0.317 ± 0.015^{a}	0.122 ± 0.006^{ab}	0.195 ± 0.012^{a}	0.0262 ± 0.0023^{a}	0.657 ± 0.015^{d}	0.162 ± 0.014^{cd}	0.495 ± 0.015^{de}	0.088 ± 0.021^{b}
P. halepensis	Mature	(m0)	0.4908 ± 0.0041^{d}	0.2160 ± 0.0022^{c}	0.2745 ± 0.005^{bc}	0.081 ± 0.011^{d}	0.428 ± 0.006^{a}	0.106 ± 0.0056^{abc}	0.322 ± 0.007^{a}	0.0223 ± 0.0030^{a}
P. halepensis	Mature	(m1)	0.474 ± 0.009^{d}	0.202 ± 0.009^{c}	0.272 ± 0.010^{b}	0.0729 ± 0.0033^{cd}	0.453 ± 0.007^{ab}	0.102 ± 0.010^{abc}	0.351 ± 0.007^{ab}	0.053 ± 0.006^{ab}
P. nigra	Seedling	(juv)	0.267 ± 0.008^{a}	0.1006 ± 0.0034^{a}	0.1664 ± 0.0051^{a}	0.0193 ± 0.0010^{a}	0.714 ± 0.007^{e}	0.1963 ± 0.0034^{d}	0.517 ± 0.005^{e}	0.058 ± 0.010^{ab}
P. nigra	Mature	(m0)	0.410 ± 0.006^{bc}	0.1494 ± 0.0047^{b}	0.260 ± 0.007^{b}	0.0341 ± 0.0039^{a}	0.556 ± 0.006^{c}	0.117 ± 0.015^{abc}	0.439 ± 0.019^{cd}	0.0418 ± 0.0030^{ab}
P. nigra	Mature	(m1)	0.3959 ± 0.0049^{b}	0.1310 ± 0.0026^{ab}	0.265 ± 0.006^{b}	0.0360 ± 0.0018^{ab}	0.568 ± 0.006^{c}	0.133 ± 0.007^{abc}	0.435 ± 0.011^{cd}	0.0301 ± 0.0043^{a}
P. nigra	Mature	(m2)	0.394 ± 0.008^{b}	0.113 ± 0.011^{ab}	0.281 ± 0.007^{bc}	0.0406 ± 0.0019^{ab}	0.565 ± 0.009^{c}	0.1251 ± 0.0029^{bc}	0.440 ± 0.009^{cd}	0.028 ± 0.007^{a}
P. pinea	Seedling	(juv)	0.3061 ± 0.0029^{a}	0.113 ± 0.014^{ab}	0.193 ± 0.011^{a}	0.0246 ± 0.0020^{a}	0.6693 ± 0.0032^{de}	0.191 ± 0.009^{d}	0.478 ± 0.009^{de}	0.083 ± 0.018^{b}
P. pinea	Mature	(m0)	0.468 ± 0.016^{d}	0.132 ± 0.008^{ab}	0.335 ± 0.009^{d}	0.0340 ± 0.006^{ab}	0.493 ± 0.017^{b}	0.127 ± 0.016^{bc}	0.365 ± 0.012^{ab}	0.0211 ± 0.0023^{a}
P. pinea	Mature	(m1)	0.4711 ± 0.009^{d}	0.1315 ± 0.0047^{ab}	0.340 ± 0.012^{d}	0.0755 ± 0.0021^{cd}	0.453 ± 0.008^{ab}	0.049 ± 0.012^{a}	0.404 ± 0.010^{bc}	0.044 ± 0.016^{ab}
P. pinea	Mature	(m2)	0.4545 ± 0.0033^{cd}	0.128 ± 0.006^{ab}	0.3262 ± 0.0047^{cd}	0.0559 ± 0.0015^{bc}	0.4896 ± 0.0045^{b}	0.0779 ± 0.0032^{ab}	0.412 ± 0.006^{bc}	0.0285 ± 0.0030^{a}
F-values for two-way ANOVA (juvenile vs adult current-year needles)										
Tree age ($F_{1,19}$)			284.7***	35.3***	176.0***	27.6***	339.6***	33.2***	90.0***	25.1***
Species ($F_{2,19}$)			17.4***	11.6***	14.8***	10.5***	27.5**	1.54 ns	12.9***	0.11 ns
Tree age x Species ($F_{2,19}$)			0.84 ns	6.48**	5.29*	6.61**	3.80*	0.32 ns	4.34*	3.05 ns
F-values for two-way ANOVA (adult needles of different age)										
Needle age ($F_{2,26}$)			1.42 ns	4.09*	0.18 ns	3.67*	0.44 ns	2.56 ns	2.60 ns	2.70 ns
Species ($F_{2,26}$)			45.6***	51.9***	44.9***	33.3***	79.2***	7.22**	27.8***	0.50 ns
Needle age x Species ($F_{3,26}$)			0.43	1.53 ns	1.23 ns	6.81**	3.35*	5.60**	1.40 ns	4.11*

n = 3–6 for each average estimate. Data presentation and statistical analyses as in Table 1. [1]The fraction of total mechanical tissues is the sum of epidermal tissues and central cylinder, the fraction of epidermal tissues includes epidermis and hypodermis and the total mesophyll fraction corresponds to mesophyll with intercellular air spaces

Downloaded from https://academic.oup.com/treephys/article/38/4/543/4769388 by Estonian University of Life Sciences user on 23 September 2020

Table 4. Average (±SE) needle ultrastructural characteristics in three Mediterranean *Pinus* species as dependent on needle and tree ages.

Species	Tree age class	Needle age	Cell wall thickness (μm)	Chloroplast width (μm)	Chloroplast thickness (μm)	Chloroplast circumference (μm)	Exposed surface area per projected area ($m^2 \cdot m^{-2}$)		S_c/S_m
							Mesophyll (S_m/S_p)	Chloroplasts (S_c/S_p)	
P. halepensis	Seedling	(juv)	0.359 ± 0.029^{b}	2.40 ± 0.13^{d}	4.69 ± 0.18^{d}	11.43 ± 0.45^{cd}	35 ± 5^{abcd}	17.7 ± 3.2^{ab}	0.501 ± 0.028^{cd}
P. halepensis	Mature	(m0)	0.375 ± 0.031^{ab}	1.46 ± 0.12^{ab}	2.62 ± 0.15^{ab}	6.49 ± 0.38^{ab}	24.1 ± 2.9^{abc}	7.6 ± 0.8^{a}	0.323 ± 0.026^{abcd}
P. halepensis	Mature	(m1)	0.301 ± 0.016^{a}	1.44 ± 0.08^{a}	2.59 ± 0.14^{a}	6.50 ± 0.28^{a}	48.8 ± 3.8^{cd}	21.1 ± 0.7^{b}	0.441 ± 0.023^{abcd}
P. nigra	Seedling	(juv)	0.309 ± 0.012^{ab}	1.90 ± 0.12^{bc}	3.58 ± 0.13^{c}	8.67 ± 0.31^{c}	22.2 ± 2.3^{ab}	11.6 ± 2.0^{ab}	0.51 ± 0.05^{d}
P. nigra	Mature	(m0)	0.542 ± 0.044^{c}	2.02 ± 0.09^{d}	3.17 ± 0.13^{abc}	8.00 ± 0.28^{abc}	37.7 ± 4.5^{abcd}	10.5 ± 2.0^{ab}	0.278 ± 0.039^{a}
P. nigra	Mature	(m1)	0.368 ± 0.012^{ab}	1.81 ± 0.08^{abc}	3.61 ± 0.13^{c}	8.56 ± 0.27^{c}	44.1 ± 1.7^{bcd}	13.7 ± 1.2^{ab}	0.314 ± 0.031^{abc}
P. nigra	Mature	(m2)	0.424 ± 0.023^{abc}	1.63 ± 0.08^{abc}	3.42 ± 0.17^{bc}	8.05 ± 0.34^{abc}	51 ± 7^{d}	18.0 ± 3.1^{ab}	0.354 ± 0.035^{abcd}
P. pinea	Seedling	(juv)	0.356 ± 0.021^{ab}	1.64 ± 0.06^{abc}	3.41 ± 0.17^{c}	7.88 ± 0.35^{abc}	18.1 ± 1.2^{a}	9.0 ± 1.3^{a}	0.49 ± 0.06^{bcd}
P. pinea	Mature	(m0)	0.53 ± 0.06^{c}	1.88 ± 0.09^{abc}	3.52 ± 0.17^{c}	8.63 ± 0.31^{c}	29.3 ± 3.8^{abcd}	9.6 ± 1.5^{a}	0.288 ± 0.032^{ab}
P. pinea	Mature	(m1)	0.354 ± 0.025^{ab}	1.93 ± 0.17^{d}	3.31 ± 0.25^{bc}	8.3 ± 0.6^{bc}	52.1 ± 2.4^{d}	18.0 ± 1.5^{ab}	0.348 ± 0.030^{abcd}
P. pinea	Mature	(m2)	0.373 ± 0.021^{ab}	1.61 ± 0.09^{abc}	3.08 ± 0.14^{abc}	7.56 ± 0.32^{abc}	43 ± 6^{bcd}	12.6 ± 1.7^{ab}	0.296 ± 0.017^{a}
F-values for two-way ANOVA (juvenile vs adult current-year needles)									
Tree age ($F_{1,29}$)			12.2**	1.62 ns	14.6***	11.0**	1.41 ns	1.98 ns	23.5***
Species ($F_{2,29}$)			1.10 ns	2.80 ns	3.21 ns	4.57*	1.56 ns	1.54 ns	0.012 ns
Tree age × Species ($F_{2,29}$)			21.75 ns	6.78*	10.3***	12.3***	3.74*	1.94 ns	0.12 ns
F-values for two-way ANOVA (adult needles of different age)									
Needle age ($F_{2,28}$)			5.47**	2.53 ns	0.37 ns	0.83 ns	8.49**	11.48***	1.96 ns
Species ($F_{2,28}$)			2.72 ns	3.76*	5.91**	6.05**	1.41 ns	0.71 ns	2.24 ns
Needle age × Species ($F_{3,28}$)			0.31 ns	0.30 ns	0.96 ns	0.41 ns	2.78 ns	5.26**	1.35 ns

$n = 3–8$ for each average estimate (on average 5.3). Data presentation and statistical analyses as in Table 1.

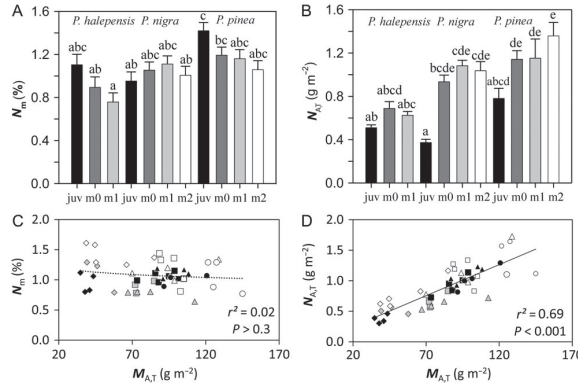

Figure 3. Effects of needle and plant age on needle nitrogen content per dry mass (N_m, A) and on nitrogen content per total needle area ($N_{A,T}$, B) and correlations of N_m (C) and $N_{A,T}$ (D) with needle dry mass per unit total area in three Mediterranean *Pinus* species. Data presentation, sample number and statistical analysis in (A) and (B) as in Figure 2. Data in (C) and (D) were fitted by linear regressions (n = 74) and different symbols correspond to: gray = *Pinus halepensis*, black = *Pinus nigra*, white = *Pinus pinea*; diamonds = juv, squares = m0, triangles = m1, circles = m2.

ratio S_c/S_m was greater in juvenile than in adult needles in *P. nigra* and *P. pinea* (Table 4).

Among different needle age classes in mature needles, current-year needles in *P. nigra* and *P. pinea* tended to have a greater cell wall thickness than older needles (Table 4). Needle age did not affect chloroplast dimensions, but older needles occasionally had greater S_m/S_P or S_c/S_P, and no consistent age-dependent patterns between needle age and these traits were observed (Table 4).

Across all data, the fraction of needle cross-section in chloroplasts (f_{chl}) was positively correlated with S_c/S_P (r^2 = 0.13, P < 0.05) and with S_c/S_m (r^2 = 0.32, P < 0.001), but not with S_m/S_P (r^2 = 0.01, P > 0.6). S_m/S_P was positively correlated with $M_{A,P}$ (r^2 = 0.30, P < 0.001), but S_c/S_P was not related to $M_{A,P}$ (r^2 = 0.01, P > 0.5), and thus, S_c/S_m was negatively correlated with $M_{A,P}$ (r^2 = 0.30, P < 0.001).

Needle nitrogen and carbon contents as affected by needle and plant age

Nitrogen content per dry mass (N_m) was not different among juvenile and adult current-year needles, and also did not differ among different ages of adult needles, but N_m varied among species (Figure 3A). In contrast, nitrogen content per unit total area ($N_{A,T}$), the product of N_m and $M_{A,T}$, was lower in juvenile than in adult current-year needles. $N_{A,T}$ also varied among species, but it did not differ among different ages of adult needles (Figure 3B). The differences in nitrogen content per projected area ($N_{A,P}$), the product of N_m and $M_{A,P}$ were analogous to those in $N_{A,T}$ (data not shown).

Across all data, N_m was not correlated with $M_{A,T}$ (Figure 3C) and $M_{A,P}$ (r^2 = 0.02, P > 0.2), but weak negative correlations were observed between N_m and needle density (r^2 = 0.10, P < 0.05), and the fraction of epidermal tissues (r^2 = 0.23, P < 0.005), and weak positive correlations were observed between N_m and the fractions of mesophyll without air spaces (r^2 = 0.09, P < 0.05) and with air spaces (Figure 4B). Positive correlations were observed among $N_{A,T}$ and $M_{A,T}$ (Figure 3D), and $N_{A,P}$ and $M_{A,P}$ (r^2 = 0.72, P < 0.001).

Needle carbon content per dry mass (C_m) was lower in juvenile than in adult current-year needles of *P. halepensis*, but not for other species × tree age combinations (Table 2). For adult needles, C_m increased with increasing needle age in *P. halepensis* and *P. nigra* (Table 2). Across all data, C_m was positively correlated with needle dry to fresh mass ratio (r^2 = 0.30, P < 0.001). This correlation was even stronger (r^2 = 0.42, P < 0.001) without the data for *P. pinea*, which had a lower C_m than the other species (Table 2). For the pooled data of *P. halepensis* and *P. nigra*, C_m also scaled positively with $M_{A,T}$ (r^2 = 0.30, P < 0.01), V/S_T (r^2 = 0.44, P < 0.001), volume fractions of central cylinder (r^2 = 0.36, P < 0.001) and total mechanical tissues (r^2 = 0.15, P < 0.05).

Discussion

Heteroblasty in Mediterranean pines: modifications in needle morphology

Heteroblastic change constitutes a major rearrangement of foliar characteristics. In our study with Mediterranean *Pinus* species,

Downloaded from https://academic.oup.com/treephys/article/38/4/543/4769388 by Estonian University of Life Sciences user on 23 September 2020

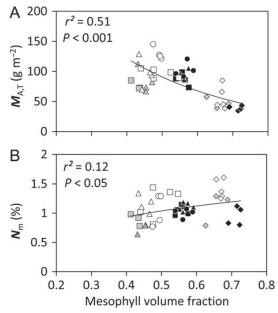

Figure 4. Correlations of leaf dry mass per unit total needle area (A) and needle nitrogen content per dry mass (B) with total mesophyll volume fraction across different needle ages in three Mediterranean *Pinus* species (Table 3 for data on volume fractions of mesophyll without intercellular air space and air space volume). Symbols as in Figure 3C and D. The data were fitted by non-linear equations in the form $y = ax^b$.

juvenile (primary) needles differed from adult (secondary) needles in key anatomical, morphological and photosynthetic traits in all three studied species. In particular, heteroblastic leaf development was associated with major changes in needle cross-sectional shape with juvenile needles having rhomboidal to sectorial shape, in strong contrast to the characteristic hemi-elliptical cross-section of adult needles (Figure 1). From the perspective of light harvesting, different cross-sectional shapes might have a similar efficiency of light interception as was the case for *P. pinea* where needle total to projected area ratio, S_T/S_P, was similar among juvenile and adult needles (Cescatti and Niinemets 2004 for a discussion). However, differences in needle shape among plant ages resulted in a greater exposed surface area at a given total needle area (lower S_T/S_P; Table 1) in *P. halepensis* and *P. nigra*, implying a greater efficiency of light interception in juvenile than in adult needles (Cescatti and Niinemets 2004 for a discussion). Of course, ultimate testing of differences in needle light harvesting efficiency would also require shoot-scale analyses, but so far, there is evidence that foliage spatial aggregation is less in young than in old conifer plants (Niinemets et al. 2005*b*).

Juvenile needles were also narrower, with smaller circumference and with lower volume to total area ratio (V/A_T; Table 1, Figure 2). They also had lower dry to fresh mass ratio, and density (D, Table 2). As a result, needle dry mass per unit area ($M_{A,T}$), the product of V/A_T and D, was smaller in juvenile than in adult needles (Figure 2). This evidence is in agreement with previous studies demonstrating increases in needle linear dimensions, dry mass per unit area and density with increasing tree age and size in several conifers (Steele et al. 1989, Niinemets and Kull 1995, Greenwood et al. 2008, Pardos et al. 2009, Räim et al. 2012).

Although foliage nitrogen content per dry mass was weakly affected by heteroblasty in our study, this low variability is in agreement with other studies demonstrating that nitrogen content per dry mass is not always associated with tree age and size (Day et al. 2001, Niinemets 2002) or it can be even lower in juvenile than in adult plants (Juárez-López et al. 2008, Mediavilla et al. 2014). In fact, with increasing leaf structural robustness, a greater fraction of leaf nitrogen can be associated with cell walls, and this is expected to lead to lower photosynthetic nitrogen-use efficiency (Takashima et al. 2004, Onoda et al. 2017).

Past studies on tree age effects on foliage structural characteristics in conifers have mainly focused on the ontogenetic drift that occurs continuously through plant lifetimes in adult foliage (Introduction, Zotz et al. 2011, see Greenwood et al. 2008 for specification of terminology). However, differently from the ontogenetic drift, heteroblastic changes in needle morphology observed in the current study are much greater, e.g., 1.6- to 2.4-fold for leaf dry mass per unit area (Table 2), than the changes typically observed for adult needles in aging trees (Introduction). We admit that differences in sampling locations (common garden for juveniles vs field environment for adult trees) might partly affect the observed differences. Due to strong shading effects that could interfere with plant age effects, we considered that sampling under comparable light conditions, which was only possible using common garden trials for juveniles, was most important to discern patterns arising from heteroblasty (see also Materials and methods). In fact, leaf shape—sectorial and rhomboidal in juveniles versus hemi-elliptical in adults—is not altered by growth conditions (field vs common garden). Furthermore, as shading reduces needle width and thickness and has a minor effect on needle density (Niinemets et al. 2001, 2007), we suppose that if needles of juveniles were sampled in the shade of adult trees, the differences among juveniles and adults would have been even bigger. So we conclude that the differences among adult and juvenile needles reported in our paper are robust and do not qualitatively depend on the study design.

Heteroblastic changes in needle anatomical and chemical traits

Our study demonstrates a major variation in biomass investments in structural and assimilative tissues across plant ages, ~1.5-fold lower investment in support, and concomitantly higher investment in mesophyll in juvenile than in adult needles (Figure 1, Table 3). The heteroblastic change in the share of different needle tissues (Table 3) observed in our study differs from the ontogenetic drift in conifers that only moderately alters the tissue volume fractions (Apple et al. 2002) or does not alter at all (Richardson et al. 2000, Greenwood et al. 2008), although a substantial decrease in air space volume fraction with increasing tree size has been reported (Apple et al. 2002, Greenwood et al. 2008).

Downloaded from https://academic.oup.com/treephys/article/38/4/543/4769388 by Estonian University of Life Sciences user on 23 September 2020

Ultrastructural analysis of needle mesophyll characteristics demonstrated that increased mesophyll volume fraction was associated with a greater volume fraction of chloroplasts in juvenile needles (Table 4). The surface area of mesophyll cells (S_m/S_P) and chloroplasts (S_c/S_P) exposed to intercellular air space per projected leaf area scaled with V/A_T and did not differ among juvenile and adult needles (Table 4). However, juvenile needles had larger chloroplasts and filled a greater area of mesophyll cell walls that were exposed to intercellular air space (greater S_c/S_m ratio). This evidence suggests that the structure and ultrastructure of juvenile needles might result in greater photosynthetic activity per mass of juvenile needles. If so, this would imply a shorter payback time of juvenile foliage, and greater carbon availability for growth, and thus, be an important factor enhancing early growth and recruitment of the juveniles (Climent et al. 2011*a*, *b*, Mediavilla et al. 2014).

Lower assimilation rate in older conifer trees is a well-known phenomenon (Yoder et al. 1994, Niinemets 2002, Greenwood et al. 2008, Räim et al. 2012), but the underlying mechanisms of this decline are not entirely understood. Initially, it was suggested that the reduction in foliage photosynthesis rate in older trees mainly reflects decreases in stomatal conductance (Yoder et al. 1994, Greenwood et al. 2008). However, now there is increasing evidence that lower stomatal conductance is not the only factor responsible for the decline in photosynthesis rate with tree age (Niinemets 2002, Räim et al. 2012). In addition to stomata, lower mesophyll diffusion conductance from substomatal cavities to chloroplasts in more robust needles in older trees has been proposed as the factor constraining their photosynthesis (Niinemets 1997*b*, 2002), and the finding of lower cell wall thickness and greater S_c/S_m in juvenile needles is consistent with this hypothesis. On the other hand, differences in the volume fractions of mesophyll and chloroplasts suggest that differences in needle biomass distribution between support and photosynthetic tissues can constitute another key factor accounting for enhanced photosynthesis rates in juvenile needles. Detailed gas-exchange measurements are needed to test these hypotheses in the future.

Needle age-dependent changes in foliage structure and function

We observed that increases in the age of adult needles were associated with moderate increases in needle linear dimensions (width and thickness, Table 1) and volume to total area ratio, and greater needle dry mass per unit area (Table 2, Figure 2). However, the fractional tissue distribution (Table 3) and needle ultrastructural characteristics (Table 4) were weakly dependent on needle age. Increases in needle linear dimensions have been attributed to needle secondary growth (Gilmore et al. 1995, Niinemets 1997*a*). Secondary growth leads to enhanced needle volume to area ratio, explaining the increase of $M_{A,P}$ and $M_{A,T}$ with increasing needle age in our study. Increases in dry mass per unit area have also been associated with increases in accumulation of cell wall material and stronger lignification of cell walls (Niinemets 1997*a*, Niinemets and Lukjanova 2003). Increased dry to fresh mass ratio in older needles in our study is compatible with greater investment in cell walls (Table 2), but surprisingly, cell wall thickness was occasionally even greater in current-year needles than in older needles (Table 4). However, at a given thickness of cell walls, there might be major differences in the porosity of cell walls (Tosens et al. 2012), e.g., the porosity might decrease due to lignification and stronger cross-linkage of different cell wall matrix polymers in older needles. Among the chemicals having carbon concentration higher than the average (~65% for lignin, 53.5% for proteins and 88% for non-oxygenated terpenoids), lignin comprises a major fraction (e.g., cellulose contains 44% carbon). Thus, increases in leaf carbon content with increasing needle age (Table 2) might suggest a greater lignification of cell walls in older needles, although we cannot rule out increases in terpenoid accumulation. On the other hand, relaxation and expansion of cell walls with moderate addition of new cell wall material during secondary growth could also be involved in changed cell wall thickness, but so far, understanding of the process of needle secondary growth is very limited.

Despite the fact that important age-dependent changes were observed in needle functional traits, needle age-dependent changes were in most cases less pronounced than heteroblastic modifications, with the exception of leaf thickness (Table 1). Nevertheless, heteroblasty and needle aging brought about similar modifications in foliage structural and physiological traits, overall resulting in increasingly sclerophyllous needles with increasing plant and needle age, likely increasing the leaf payback time in mature plants (Day and Greenwood 2011).

Trade-offs between structural and functional investments across plant and needle ages and species

Greater structural robustness in adult needles and especially in older adult needles was associated with lower mesophyll volume fraction, suggesting that being structurally more robust is inevitably associated with a reduced amount of photosynthesizing biomass. This fundamental trade-off operating across species, plant ages and needle ages may be related to the changes in life history characteristics of juvenile versus adult plants during ontogeny. While greater investment in photosynthesizing tissue can enhance growth rates in seedlings and saplings, concomitantly lower foliage mechanical robustness can limit foliage longevity and compromise the tolerance of periods of environmental stress. Indeed, juvenile pine needles have a shorter life span (Mediavilla et al. 2014), and lower drought tolerance (Fernandez et al. 1999, Climent et al. 2006*a*, 2006*b*, Pardos et al. 2009) compared with the adults. There is also evidence

Downloaded from https://academic.oup.com/treephys/article/38/4/543/4769388 by Estonian University of Life Sciences user on 23 September 2020

that juvenile needles of some conifer species are less frost resistant (Climent et al. 2009, Pardos et al. 2014), and this can be directly related to less robust foliage with greater elasticity of cell walls (Niinemets 2016). Furthermore, juvenile leaves with lower fiber fractions can be more sensitive to herbivore attacks (Karban and Thaler 1999, Loney et al. 2006). However, this might not always be the case as herbivory sensitivity also depends on differences in investments in secondary protective chemicals as well as leaf surface characteristics (Brennan et al. 2001, Lawrence et al. 2003).

Heteroblasty was the largest source of variation in tissue volume fractions, whereas the tissue distribution between photosynthetic and support components was remarkably similar among juvenile needles of the different species. This is in contrast with the important species differences observed among adult needles (Table 3) as has been observed in other studies (Richardson et al. 2000, Apple et al. 2002, Niinemets et al. 2007). The species ranked as *P. halepensis* > *P. pinea* > *P. nigra* according to the fraction of mechanical tissues in adult needles, while the reverse was the case for mesophyll volume fraction (Table 3). This ranking is in agreement with known distribution of species across climatic gradients, with *P. halepensis* inhabiting the harshest, severely water-limited environments, *P. pinea* intermediate sites and *P. nigra* more mesic habitats, again suggesting that the trade-off between structural and photosynthetic investments can affect species' ecological potentials.

Conclusions

Our study highlights a coordinated change in the combinations of foliage structural and photosynthetic traits upon heteroblastic change and demonstrates that differences among primary and secondary needles are quantitatively much larger than needle age-dependent modifications. Juvenile plants carrying primary needles have less robust foliage with lower volume fractions of mechanical and higher volume fractions of photosynthetic tissues than adult needles. These differences are compatible with lower leaf payback time, and all these traits can contribute to rapid increases in size, contributing to seedling and sapling establishment in the community. Furthermore, the juvenile needles of *P. halepensis* have greater efficiency of light interception due to greater exposed surface area at a given total needle surface area, likely also contributing to plant recruitment under the canopy of adult trees. Greater photosynthetic investments in juvenile needles allow for enhanced carbon gain and establishment within the community, but this might have a cost in terms of reduced leaf life span and in terms of reduced tolerance of environmental stresses such as drought and frost.

Conflict of interest

None declared.

Funding

The study was supported by grants from the Consejo Superior de Investigaciones Cientificas (CSIC, Spain) and the Estonian Academy of Sciences (joint grant for collaboration between scientific institutions of Estonia and CSIC), the Estonian Ministry of Science and Education (institutional grant IUT-8-3) and the European Commission through the European Regional Fund (the Center of Excellence EcolChange).

References

Apple M, Tiekotter K, Snow M, Young J, Soeldner A, Phillips D, Tingey D, Bond BJ (2002) Needle anatomy changes with increasing tree age in Douglas-fir. Tree Physiol 22:129–136.

Atzmon N, Moshe Y, Schiller G (2004) Ecophysiological response to severe drought in *Pinus halepensis* Mill. trees of two provenances. Plant Ecol 171:15–22.

Baquedano FJ, Castillo FJ (2007) Drought tolerance in the Mediterranean species *Quercus coccifera*, *Quercus ilex*, *Pinus halepensis*, and *Juniperus phoenicea*. Photosynthetica 45:229–238.

Baquedano FJ, Valladares F, Castillo FJ (2008) Phenotypic plasticity blurs ecotypic divergence in the response of *Quercus coccifera* and *Pinus halepensis* to water stress. Eur J For Res 127:495–506.

Barbéro M, Loisel R, Quézel P, Richardson DM, Romane F (1998) Pines of the Mediterranean basin. In: Richardson DM (ed) Ecology and biogeography of *Pinus*. Cambridge: University Press, Cambridge, pp 153–170.

Boddi S, Bonzi LM, Calamassi R (2002) Structure and ultrastructure of *Pinus halepensis* primary needles. Flora 197:10–23.

Bozzola JJ, Russell LD (1992) Electron microscopy. Principles and techniques for biologists. Jones & Bartlett Publishers, New York, NY.

Brennan EB, Weinbaum SA, Rosenheim JA, Karban R (2001) Heteroblasty in *Eucalyptus globulus* (Myricales: Myricaceae) affects ovipositonal and settling preferences of *Ctenarytaina eucalypti* and *C. spatulata* (Homoptera: Psyllidae). Environ Entomol 30:1144–1149.

Burns WA (1978) Thick sections: technique and applications. In: Trump BF, Jones RJ (eds) Diagnostic electron microscopy. Wiley, New York, NY, pp 146–178.

Cabanettes A, Rapp M (1978) Biomasse, minéralomasse et productivité d'un écosystéme à pins pignons (*Pinus pinea* L.) du littoral Méditerranéen. Acta Oecol/Oecol Plantarum 13:271–286.

Cescatti A, Niinemets Ü (2004) Sunlight capture. Leaf to landscape. In: Smith WK, Vogelmann TC, Chritchley C (eds) Photosynthetic adaptation. Chloroplast to landscape. Springer, Berlin, pp 42–85.

Chandler JW, Dale JE (1993) Photosynthesis and nutrient supply in needles of Sitka spruce [*Picea sitchensis* (Bong.) Carr.]. New Phytol 125:101–111.

Climent J, Aranda I, Alonso J, Pardos JA, Gil L (2006*a*) Developmental constraints limit the response of Canary Island pine seedlings to combined shade and drought. For Ecol Manage 231:164–168.

Climent J, Chambel MR, López R, Mutke S, Alía R, Gil L (2006*b*) Population divergence for heteroblasty in the Canary Island pine (*Pinus canariensis*, Pinaceae). Am J Bot 93:840–848.

Climent J, Costa e Silva F, Chambel MR, Pardos M, Almeida MH (2009) Freezing injury in primary and secondary needles of Mediterranean pine species of contrasting ecological niches. Ann For Sci 66:407.

Climent J, Chambel MR, Pardos M, Lario F, Villar-Salvador P (2011*a*) Biomass allocation and foliage heteroblasty in hard pine species respond differentially to reduction in rooting volume. Eur J For Res 130:841–850.

Climent J, San-Martín R, Chambel MR, Mutke S (2011*b*) Ontogenetic differentiation between Mediterranean and Eurasian pines (sect. *Pinus*) at the seedling stage. Trees 25:175–186.

Downloaded from https://academic.oup.com/treephys/article/38/4/543/4769388 by Estonian University of Life Sciences user on 23 September 2020

Copolovici L, Kännaste A, Remmel T, Vislap V, Niinemets Ü (2011) Volatile emissions from *Alnus glutinosa* induced by herbivory are quantitatively related to the extent of damage. J Chem Ecol 37:18–28.

Day ME, Greenwood MS (2011) Regulation of ontogeny in temperate conifers. In: Meinzer FC, Dawson T, Lachenbruch B (eds) Size- and age-related changes in tree structure and function. Springer, Berlin, pp 91–119.

Day ME, Greenwood MS, White AS (2001) Age-related changes in foliar morphology and physiology in red spruce and their influence on declining photosynthetic rates and productivity with tree age. Tree Physiol 21:1195–1204.

Evans JR, von Caemmerer S, Setchell BA, Hudson GS (1994) The relationship between CO_2 transfer conductance and leaf anatomy in transgenic tobacco with a reduced content of Rubisco. Aust J Plant Physiol 21:475–495.

Fernandez M, Gil L, Pardos JA (1999) Response of *Pinus pinaster* Ait. provenances at early age to water supply. I. Water relation parameters. Ann For Sci 56:179–187.

Flexas J, Barbour MM, Brendel O et al. (2012) Mesophyll diffusion conductance to CO_2: an unappreciated central player in photosynthesis. Plant Sci 193–194:70–84.

Gebauer R, Volařík D, Urban J, Børja I, Nagy NE, Eldhuset TD, Krokene P (2011) Effect of thinning on anatomical adaptations of Norway spruce needles. Tree Physiol 31:1103–1113.

Gilmore DW, Seymour RS, Halteman WA, Greenwood MS (1995) Canopy dynamics and the morphological development of *Abies balsamea*: effects of foliage age on specific leaf area and secondary vascular development. Tree Physiol 15:47–55.

Greenwood MS, Ward MH, Day ME, Adams SL, Bond BJ (2008) Age-related trends in red spruce foliar plasticity in relation to declining productivity. Tree Physiol 28:225–232.

Hanley ME, Fenner M, Whibley H, Darvill B (2004) Early plant growth: identifying the end point of the seeding phase. New Phyol 163: 61–66.

Helmisaari H-S (1990) Temporal variation in nutrient concentrations of *Pinus sylvestris* needles. Scand J For Res 5:177–193.

Juárez-López FJ, Escudero A, Mediavilla S (2008) Ontogenetic changes in stomatal and biochemical limitations to photosynthesis of two co-occurring Mediterranean oaks differing in leaf life span. Tree Physiol 28:367–374.

Karban R, Thaler JS (1999) Plant phase change and resistance to herbivory. Ecology 80:510–517.

Keenan TF, Niinemets Ü (2016) Global leaf trait estimates biased due to plasticity in the shade. Nat Plants 3:16201.

Kienast F, Schweingruber FH, Bräker OU, Schär E (1987) Tree-ring studies on conifers along ecological gradients and the potential of single-year analyses. Can J For Res 17:683–696.

Koch GW, Sillett SC, Jennings GM, Davis SD (2004) The limits to tree height. Nature 428:851–854.

Lawrence R, Potts BM, Whitham TG (2003) Importance of plant ontogeny, host genetic variation, and leaf age for a common herbivore. Ecology 84:1171–1178.

Loney PE, McArthur C, Potts BM, Jordan GJ (2006) How does ontogeny in a *Eucalyptus* species affect patterns of herbivory by brushtail possums? Funct Ecol 20:982–988.

Mediavilla S, Herranz M, González-Zurdo P, Escudero A (2014) Ontogenetic transition in leaf traits: a new cost associated with the increase in leaf longevity. J Plant Ecol 7:567–575.

Niinemets Ü (1997*a*) Acclimation to low irradiance in *Picea abies*: influences of past and present light climate on foliage structure and function. Tree Physiol 17:723–732.

Niinemets Ü (1997*b*) Distribution patterns of foliar carbon and nitrogen as affected by tree dimensions and relative light conditions in the canopy of *Picea abies*. Trees 11:144–154.

Niinemets Ü (1999) Research review. Components of leaf dry mass per area – thickness and density – alter leaf photosynthetic capacity in reverse directions in woody plants. New Phytol 144:35–47.

Niinemets Ü (2002) Stomatal conductance alone does not explain the decline in foliar photosynthetic rates with increasing tree age and size in *Picea abies* and *Pinus sylvestris*. Tree Physiol 22:515–535.

Niinemets Ü (2010) A review of light interception in plant stands from leaf to canopy in different plant functional types and in species with varying shade tolerance. Ecol Res 25:693–714.

Niinemets Ü (2016) Does the touch of cold make evergreen leaves tougher? Tree Physiol 36:267–272.

Niinemets Ü, Kull O (1995) Effects of light availability and tree size on the architecture of assimilative surface in the canopy of *Picea abies*: variation in needle morphology. Tree Physiol 15:307–315.

Niinemets Ü, Lukjanova A (2003) Needle longevity, shoot growth and branching frequency in relation to site fertility and within-canopy light conditions in *Pinus sylvestris*. Ann For Sci 60:195–208.

Niinemets Ü, Ellsworth DS, Lukjanova A, Tobias M (2001) Site fertility and the morphological and photosynthetic acclimation of *Pinus sylvestris* needles to light. Tree Physiol 21:1231–1244.

Niinemets Ü, Lukjanova A, Sparrrow AD, Turnbull MH (2005*a*) Light-acclimation of cladode photosynthetic potentials in *Casuarina glauca*: trade-offs between physiological and structural investments. Funct Plant Biol 32:571–582.

Niinemets Ü, Sparrow A, Cescatti A (2005*b*) Light capture efficiency decreases with increasing tree age and size in the southern hemisphere gymnosperm *Agathis australis*. Trees 19:177–190.

Niinemets Ü, Lukjanova A, Turnbull MH, Sparrow AD (2007) Plasticity in mesophyll volume fraction governs the light-acclimation in needle photosynthesis in two pines. Tree Physiol 27:1137–1151.

Niinemets Ü, García-Plazaola JI, Tosens T (2012) Photosynthesis during leaf development and ageing. In: Flexas J, Loreto F, Medrano H (eds) Terrestrial photosynthesis in a changing environment. A molecular, physiological and ecological approach. Cambridge University Press, Cambridge, pp 353–372.

Niinemets Ü, Keenan TF, Hallik L (2015) Tansley review. A worldwide analysis of within-canopy variations in leaf structural, chemical and physiological traits across plant functional types. New Phytol 205: 973–993.

Onoda Y, Wright IJ, Evans JR, Hikosaka K, Kitajima K, Niinemets Ü, Poorter H, Tosens T, Westoby M (2017) Physiological and structural tradeoffs underlying the leaf economics spectrum. New Phytol 214:1447–1463.

Pardos M, Calama R, Climent J (2009) Difference in cuticular transpiration and sclerophylly in juvenile and adult pine needles relates to the species-specific rates of development. Trees 23:501–508.

Pardos M, Climent J, Almeida H, Calama R (2014) The role of developmental stage in frost tolerance of *Pinus pinea* L. seedlings and saplings. Ann For Sci 71:551–562.

Poorter H, Niinemets Ü, Poorter L, Wright IJ, Villar R (2009) Tansley review. Causes and consequences of variation in leaf mass per area (LMA): a meta-analysis. New Phytol 182:565–588.

R Development Core Team (2012) R: a language and environment for statistical computing. The R Foundation for Statistical Computing, Vienna. http://www.R-project.org/.

Räim O, Kaurilind E, Hallik L, Merilo E (2012) Why does needle photosynthesis decline with tree height in Norway spruce? Plant Biol 14: 306–314.

Richardson AD, Berlyn GP, Ashton PMS, Thadani R, Cameron IR (2000) Foliar plasticity of hybrid spruce in relation to crown position and stand age. Can J Bot 78:305–317.

Steele MJ, Coutts MP, Yeoman MM (1989) Developmental changes in Sitka spruce as indices of physiological age. I. Changes in needle morphology. New Phytol 113:367–375.

Downloaded from https://academic.oup.com/treephys/article/38/4/543/4769388 by Estonian University of Life Sciences user on 23 September 2020

Steppe K, Niinemets Ü, Teskey RO (2011) Tree size- and age-related changes in leaf physiology and their influence on carbon gain. In: Meinzer FC, Dawson T, Lachenbruch B (eds) Size- and age-related changes in tree structure and function. Springer, Berlin, pp 235–253.

Takashima T, Hikosaka K, Hirose T (2004) Photosynthesis or persistence: nitrogen allocation in leaves of evergreen and deciduous *Quercus* species. Plant Cell Environ 27:1047–1054.

Teskey RO, Grier CC, Hinckley TM (1984) Change in photosynthesis and water relations with age and season in *Abies amabilis*. Can J For Res 14:77–84.

Thain JF (1983) Curvature correction factors in the measurement of cell surface areas in plant tissues. J Exp Bot 34:87–94.

Thomas SC (2010) Photosynthetic capacity peaks at intermediate size in temperate deciduous trees. Tree Physiol 30:555–573.

Thomas SC, Winner WE (2002) Photosynthetic differences between saplings and adult trees: an integration of field results by meta-analysis. Tree Physiol 22:117–127.

Tosens T, Niinemets Ü, Westoby M, Wright IJ (2012) Anatomical basis of variation in mesophyll resistance in eastern Australian sclerophylls: news of a long and winding path. J Exp Bot 63:5105–5119.

Weiskittel AR, Temesgen H, Wilson DS, Maguire DA (2008) Sources of within- and between-stand variability in specific leaf area of three ecologically distinct conifer species. Ann For Sci 65:103.

Withington JM, Reich PB, Oleksyn J, Eissenstat DM (2006) Comparisons of structure and life span in roots and leaves among temperate trees. Ecol Monogr 76:381–397.

Witkowski ETF, Lamont BB (1991) Leaf specific mass confounds leaf density and thickness. Oecologia 88:486–493.

Woodruff DR, McCulloh KA, Warren JM, Meinzer FC, Lachenbruch B (2007) Impacts of tree height on leaf hydraulic architecture and stomatal control in Douglas-fir. Plant Cell Environ 30:559–569.

Woodruff DR, Meinzer FC, Lachenbruch B, Johnson DM (2009) Coordination of leaf structure and gas exchange along a height gradient in a tall conifer. Tree Physiol 29:261–272.

Yoder BJ, Ryan MG, Waring RH, Schoettle AW, Kaufmann MR (1994) Evidence of reduced photosynthetic rates in old trees. For Sci 40: 513–527.

Zotz G, Wilhelm K, Becker A (2011) Heteroblasty – a review. Bot Rev 77:109–151.

Downloaded from https://academic.oup.com/treephys/article/38/4/543/4769388 by Estonian University of Life Sciences user on 23 September 2020

II

Vivian Kuusk, Ülo Niinemets, and Fernando Valladares (2018b) Structural controls on photosynthetic capacity through juvenile-to-adult transition and needle aging in Mediterranean pines. *Functional Ecology* 32:1479–1491.

Received: 18 September 2017 | Accepted: 18 February 2018
DOI: 10.1111/1365-2435.13087

RESEARCH ARTICLE

Functional Ecology | BRITISH ECOLOGICAL SOCIETY

Structural controls on photosynthetic capacity through juvenile-to-adult transition and needle ageing in Mediterranean pines

Vivian Kuusk[1] | Ülo Niinemets[1,2] | Fernando Valladares[3,4]

[1]Institute of Agricultural and Environmental Sciences, Estonian University of Life Sciences, Tartu, Estonia

[2]Estonian Academy of Sciences, Tallinn, Estonia

[3]LINCGlobal, Departamento de Biogeografía y Cambio Global, Museo Nacional de Ciencias Naturales, MNCN-CSIC, Madrid, Spain

[4]Departamento de Biología y Geología, ESCET, Universidad Rey Juan Carlos, Móstoles, Spain

Correspondence
Ülo Niinemets
Email: ylo.niinemets@emu.ee

Funding information
European Regional Development Fund; Eesti Teadusagentuur, Grant/Award Number: IUT 8-3; Consejo Superior de Investigaciones Cientificas; European Regional Fund, Grant/Award Number: Center of Excellence EcolChange

Handling Editor: Mark Tjoelker

Abstract

1. Needle photosynthetic potentials strongly vary among primary (juvenile) and secondary (adult) needles (heteroblasty) in *Pinus* species, but there is limited understanding of the underlying structural, diffusional and chemical controls.
2. We studied differences in needle photosynthetic characteristics among current-year juvenile and adult needles and among different-aged adult needles in Mediterranean pines *Pinus halepensis* Mill., *P. pinea* L. and *P. nigra* J. F. Arnold subsp. *salzmannii* (Dunal) Franco, hypothesizing that needle anatomical modifications upon juvenile-to-adult transition lead to reduced photosynthetic capacity due to greater limitation of photosynthesis by mesophyll conductance and due to an increase in the share of support tissues at the expense of photosynthetic tissues. We also hypothesized that such alterations occur with needle ageing, but to a lower degree.
3. Photosynthetic capacity per dry mass was 2.4- to 2.7-fold higher in juvenile needles, and this was associated with 3.4- to 3.7-fold greater mesophyll diffusion conductance, 2- to 2.5-fold greater maximum carboxylase activity of Rubisco (V_{cmax}) and 2.2- to 3-fold greater capacity for photosynthetic electron transport (J_{max}). The latter differences were driven by modifications in mesophyll volume fraction and changes in the share of nitrogen between structural and photosynthetic functions. Analogous changes in photosynthetic characteristics occurred with needle ageing, but their extent was less.
4. These results indicate that conifer foliage photosynthetic machinery undergoes a profound change from a fast return strategy in juveniles to slow return stress-resistant strategy in adults and that this strategy shift is driven by modifications in foliage biomass investments in support and photosynthetic functions as well as by varying mesophyll diffusional controls on photosynthesis. Changes in needle morphophysiotype during tree and needle ageing need consideration in predicting changes in tree photosynthetic potentials through tree ontogeny and during and among growing seasons.

KEYWORDS
mesophyll conductance, nitrogen content, photosynthetic capacity, *Pinus halepensis*, *Pinus nigra*, *Pinus pinea*, primary needles, secondary needles

© 2018 The Authors. Functional Ecology
© 2018 British Ecological Society

TABLE 1 Influences of tree age and needle age on net assimilation rate (A) and mesophyll diffusion conductance (g_m) expressed per unit dry mass (A_m and $g_{m,m}$) and needle projected area (A_P and $g_{m,P}$), photosynthetic nitrogen use efficiency (E_N, the ratio of A_P and nitrogen content per projected area) and CO_2 drawdown from substomatal cavities to chloroplasts (C_i-C_c) in three Mediterranean *Pinus* species

Species	Tree age class	Needle age	$A_{m,Ci=250}$ (μmol g^{-1} s^{-1})	$A_{P,Ci=250}$ (μmol m^{-2} s^{-1})	E_N (μmol g^{-1} s^{-1})	$g_{m,m}$ (mmol g^{-1} s^{-1})	$g_{m,P}$ (mmol m^{-2} s^{-1})	CO_2 drawdown, C_i-C_c (μmol/mol)
Pinus halepensis	Seedling	(juv)	0.052 ± 0.009^{b}	6.6 ± 0.9^{cd}	4.7 ± 0.6^{cd}	1.19 ± 0.09^{b}	153 ± 11^{c}	44 ± 8^{a}
P. halepensis	Mature	(m0)	0.0222 ± 0.0029^{a}	5.0 ± 0.7^{abcd}	2.51 ± 0.41^{abc}	0.300 ± 0.030^{a}	67 ± 6^{ab}	74 ± 7^{bc}
P. halepensis	Mature	(m1)	0.0126 ± 0.0025^{a}	2.89 ± 0.40^{a}	1.40 ± 0.23^{ab}	0.168 ± 0.025^{a}	38.9 ± 3.7^{a}	73.5 ± 4.5^{bc}
P. nigra	Seedling	(juv)	0.065 ± 0.010^{b}	6.5 ± 0.7^{cd}	7.0 ± 1.2^{d}	1.30 ± 0.11^{b}	133 ± 10^{c}	50 ± 6^{a}
P. nigra	Mature	(m0)	0.0262 ± 0.0009^{a}	6.33 ± 0.28^{cd}	2.51 ± 0.16^{abc}	0.352 ± 0.043^{a}	84 ± 7^{b}	78 ± 9^{bc}
P. nigra	Mature	(m1)	0.0170 ± 0.0014^{a}	4.59 ± 0.37^{abcd}	1.52 ± 0.09^{a}	0.196 ± 0.020^{a}	53 ± 5^{ab}	87.2 ± 2.5^{c}
P. nigra	Mature	(m2)	0.0128 ± 0.0011^{a}	3.60 ± 0.30^{ab}	1.35 ± 0.15^{a}	0.152 ± 0.015^{a}	42.8 ± 4.3^{a}	85 ± 5^{c}
P. pinea	Seedling	(juv)	0.052 ± 0.010^{b}	7.0 ± 0.6^{d}	3.6 ± 0.6^{bc}	1.15 ± 0.24^{b}	155 ± 17^{c}	45.6 ± 2.2^{ab}
P. pinea	Mature	(m0)	0.0195 ± 0.0016^{a}	5.16 ± 0.43^{bcd}	1.62 ± 0.22^{ab}	0.268 ± 0.011^{a}	70.9 ± 3.3^{ab}	72.7 ± 4.8^{bc}
P. pinea	Mature	(m1)	0.0177 ± 0.0030^{a}	4.21 ± 0.36^{abc}	1.33 ± 0.20^{a}	0.185 ± 0.029^{a}	44.3 ± 4.0^{a}	95.7 ± 2.1^{c}
P. pinea	Mature	(m2)	0.0098 ± 0.0012^{a}	3.33 ± 0.37^{ab}	0.95 ± 0.09^{a}	0.120 ± 0.010^{a}	40.5 ± 2.6^{a}	81 ± 6^{c}
F-values for two-way ANOVA (juvenile vs. adult current-year needles)								
Tree age ($F_{1, 23}$)			51.4***	5.41*	37.1***	92.2***	88.8***	30.6***
Species ($F_{2, 23}$)			0.93ns	0.56ns	5.31*	0.50ns	0.12ns	0.34ns
Tree age × Species ($F_{2, 23}$)			0.32ns	0.77ns	2.33ns	0.04ns	2.04ns	0.02ns
F-values for two-way ANOVA (adult needles of different age)								
Needle age ($F_{2, 37}$)			19.4***	19.6***	18.7***	33.3***	39.9***	3.33*
Species ($F_{2, 37}$)			2.15ns	5.64**	5.79**	2.33ns	4.79*	2.48ns
Needle age × Species ($F_{3, 37}$)			1.12ns	0.52ns	1.59ns	0.82ns	0.41ns	2.02ns

The young trees were 2 years old and 0.2–0.3 m tall, and the mature cone-bearing trees were 15–21 m tall at the time of sampling. Needle age codes as: juv—juvenile current year; m0—mature current year; m1—mature 1-year-old; m2—mature 2-year-old. Due to leaf-to-leaf differences in stomatal openness, net assimilation rates were standardized to a common intercellular CO_2 concentration (C_i) of 250 μmol mol^{-1} with the Farquhar et al. (1980) photosynthesis model. $n = 4–6$ for each average value, except for E_N ($n = 3–6$ for each average estimate, and $n = 19$ for the residuals of the *F*-values for the ANOVA with juvenile vs. adult needles, and $n = 26$ for the ANOVA with adult needle ages). Different letters show statistical significance among averages for different species and needle age class combinations at $p < .05$ (one-way ANOVA followed by a Tukey post hoc test). For two-way ANOVA, the statistical significance is denoted as: $*p < .05$, $**p < .01$, $***p < .001$, ns—not significant.

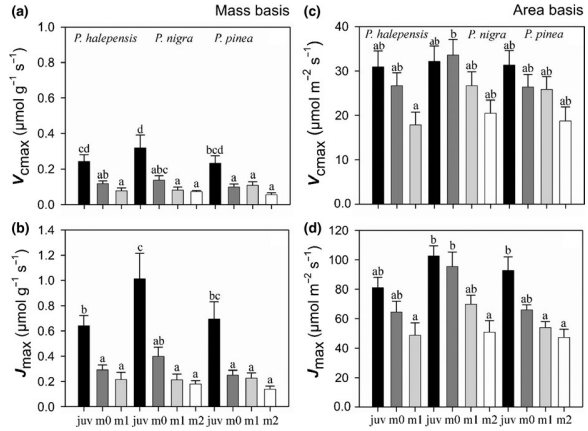

FIGURE 1 Variation in the maximum carboxylase activity of Rubisco (V_{cmax}; a, c) and the capacity for photosynthetic electron transport (J_{max}; b, d) expressed per unit needle dry mass (a, b) and projected needle area (c, d) as driven by needle and tree age in three Mediterranean *Pinus* species. V_{cmax} and J_{max} were derived from net assimilation (A) vs. chloroplastic CO_2 (C_c)–response curves. n = 4–6 for each leaf age × species combination. Table 1 shows corresponding values of net assimilation rate (A) and mesophyll diffusion conductance (g_m). Needle age codes as: juv—juvenile (primary) current year; m0—mature (secondary) current year; m1—mature 1-year-old; m2—mature 2-year-old needles. The juvenile needles were studied in 2-year-old 0.2- to 0.3-m-tall young plants, and the secondary needles in 15- to 21-m-tall cone-bearing mature trees. Different letters denote statistical significance of average values for different species and needle age class combinations at $p < .05$ (one-way ANOVA followed by a Tukey post hoc test). According to two-way ANOVA comparing juvenile and adult current-year needles in different species, tree age effect was significant for a, b and c, species effect for b and d, and tree age × species interaction was not significant in any of the relationships. According to two-way ANOVA comparing adult needle ages in different species, needle age was significant in all cases, species effect for c and d, and needle age × species interaction was not significant in any of the cases (Table 1 for details of the two-way ANOVA models)

1 | INTRODUCTION

Profound modifications in foliage structural and photosynthetic traits occur with increases in tree age and size (Day, Greenwood, & White, 2001; Mediavilla, Herranz, González-Zurdo, & Escudero, 2014; Niinemets, 2002; Niinemets & Kull, 1995; Steppe, Niinemets, & Teskey, 2011; Woodruff, Meinzer, Lachenbruch, & Johnson, 2009). Particularly large trait alterations occur upon juvenile-to-adult transition, a change called heteroblasty (Zotz, Wilhelm, & Becker, 2011). Heteroblastic modifications in foliage morphology are especially large in pine species (Boddi, Bonzi, & Calamassi, 2002; Climent, San-Martín, Chambel, & Mutke, 2011; Kuusk, Niinemets, & Valladares, 2018b; Mediavilla et al., 2014; Pardos, Calama, & Climent, 2009). Juvenile (primary) pine needles are solitary and have different cross-sectional shape, ellipsoidal or rhomboidal, compared to adult (secondary) needles that have semi-elliptical (two-needled species) or sectorial (species with three or more needles in fascicles) shape (Climent, Aranda, Alonso, Pardos, & Gil, 2006; Kuusk et al., 2018b). In addition, needle linear dimensions, thickness and width, and needle dry mass per unit area are typically lower in juvenile needles (Boddi et al., 2002; Kuusk et al., 2018b; Mediavilla et al., 2014; Pardos et al., 2009).

Despite lower needle cross-sectional area, juvenile needles have greater net assimilation rates on both needle area and dry mass basis (Niinemets, 2002), but the mechanisms responsible for greater juvenile needle photosynthesis have not yet been fully resolved. Previous research has indicated that photosynthesis in older and larger conifer trees is more severely limited by stomatal conductance, albeit larger trees also have lower foliage biochemical photosynthesis potentials, maximum carboxylase activity of Rubisco (V_{cmax}) and the capacity for photosynthetic electron transport (J_{max}) (Day et al., 2001; Niinemets, 2002; Räim, Kaurilind, Hallik, & Merilo, 2012; Steppe et al., 2011; Woodruff et al., 2009). It has further been suggested that photosynthesis in structurally more robust needles in older and larger trees is more strongly limited by mesophyll diffusion conductance from substomatal cavities to chloroplasts due to longer effective diffusion path lengths (Niinemets, 2002), but the experimental support to this hypothesis is lacking (Niinemets, Díaz-Espejo, Flexas, Galmés, & Warren, 2009 for a review).

The concept of leaf economics spectrum describes coordinated variations in leaf structure and physiological activity through high return lavish strategy to conservative low return stress-tolerant strategy focusing on three main traits ("core traits"), leaf dry mass per unit area, nitrogen content and photosynthetic capacity (Wright,

Structural/chemical traits	Physiological traits				
	$A_{m,Ci=250}$	$A_{P,Ci=250}$	E_N	$g_{m,m}$	$g_{m,P}$
Fraction in epidermal tissues	−0.367*	−0.378**	−0.313*	−0.367**	−0.365*
Fraction in central cylinder	−0.783***	−0.541***	−0.770***	−0.796***	−0.650***
Total mechanical fraction	−0.786***	−0.605***	−0.754***	−0.780***	−0.683***
Total mesophyll faction	0.774***	0.639***	0.738***	0.789***	0.713***
Mesophyll fraction without air space	0.646***	0.544***	0.605***	0.660***	0.587***
Dry mass per unit projected area ($M_{A,P}$)	−0.743***	−0.523***	−0.762***	−0.743***	−0.650***
Volume to projected area ratio (V/S_P)	−0.639***	−0.397**	−0.717***	−0.659***	−0.567***
Density (D)	−0.422***	−0.316*	−0.762***	−0.401**	−0.335**
Dry to fresh mass ratio ($R_{D/F}$)	−0.591***	−0.648***	−0.561***	−0.581***	−0.655***
Nitrogen content per dry mass (N_m)	0.330*	0.493***	0.061^{ns}	0.337*	0.437**
Nitrogen content per projected area ($N_{A,P}$)	−0.558***	−0.213^{ns}	−0.663***	−0.569***	−0.397**

TABLE 2 Correlations of needle photosynthetic traits, net assimilation rate (A) and mesophyll diffusion conductance (g_m) expressed per unit needle dry mass (A_m and $g_{m,m}$) and needle projected area (A_P and $g_{m,P}$), and photosynthetic nitrogen use efficiency (E_N, the ratio of A_P and nitrogen content per projected area) with needle structural and chemical traits across all needle and tree ages in three Mediterranean species (Pearson correlation coefficients)

n = 46 for the combinations of photosynthesis vs. tissue volume fractions and chemical traits and for all correlations with E_N, and n = 57 for the other traits. Statistical significance as in Table 1.
Tissue mechanical fraction is the sum of the needle volume fractions in epidermal tissues (epidermis and hypodermis) and central cylinder. Net assimilation rates were standardized for all leaves to a common intercellular CO_2 concentration (C_i) of 250 µmol/mol as in Table 1. Additional methods for structural trait estimation are provided in Kuusk et al. (2018b), and all data accompanying this article are available from the Dryad Digital Repository (Kuusk et al., 2018a). Statistical significance as in Table 1.

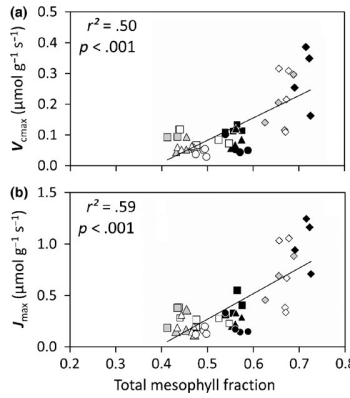

FIGURE 2 Relationships of maximum carboxylase activity of Rubisco (V_{cmax}; a) and capacity for photosynthetic electron transport (J_{max}; b) per unit dry mass with mesophyll volume fraction in three Mediterranean *Pinus* species. Data for all species and needle and plant ages pooled were fitted by linear regressions. Mesophyll volume fraction is given without intercellular air space (Kuusk et al., 2018b for details about its estimation). Different symbols as: grey = *Pinus halepensis*, black = *Pinus nigra*, white = *Pinus pinea*; diamonds = juv, squares = m0, triangles = m1, circles = m2. Figure 1 for the definition of age codes

Reich, et al., 2004). The economics spectrum relationships have been developed by pooling plants with varying age (Kattge et al., 2011;). So far, possible implications of juvenile-to-adult transition on leaf trait relationships have not been explored and the traits in seedlings and adult plants are considered as parts of the same general economics spectrum. However, there is a strategy shift from juvenile physiologically active and less stress-tolerant strategy to adult more sclerophyllous higher stress tolerance strategy (Climent, San-Martín, et al., 2011; Harper, 1989; Karban & Thaler, 1999; Kuusk et al., 2018b; Mediavilla et al., 2014; Pardos et al., 2009), suggesting that heteroblastic changes could alter the trait relationships. Mesophyll diffusion conductance and fractional tissue distribution do not belong to the "core" traits of the leaf economics spectrum as initially defined (Wright, Reich, et al., 2004), but they both can alter foliage photosynthetic capacity at given leaf dry mass per unit area and nitrogen content. Existence of a trade-off between structural and photosynthetic functions could mean that leaf photosynthetic capacity changes more at a given dry mass per unit area and nitrogen content than predicted by the broadleaf economics spectrum relationships.

We studied modifications in foliage photosynthetic characteristics upon juvenile-to-adult transition in three Mediterranean pine species—*Pinus halepensis* Mill., *P. pinea* L. and *P. nigra* J. F. Arnold subsp. *salzmannii* (Dunal) Franco. Differently from European pines in wetter climates where juvenile needles are present in up to 1-year-old seedlings, young Mediterranean pines typically carry juvenile needles longer, for 2–3 years (Climent, San-Martín, et al.,

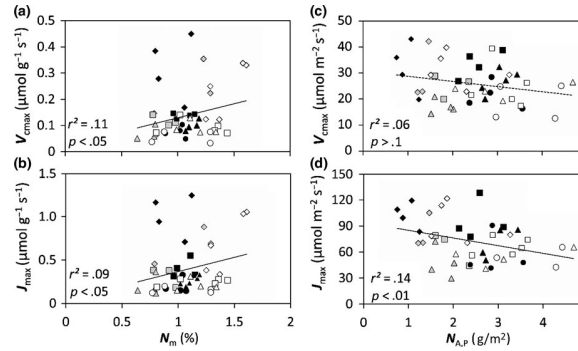

FIGURE 3 Correlations of maximum carboxylase activity of Rubisco (V_{cmax}; a, c) and capacity for photosynthetic electron transport (J_{max}; b, d) per unit dry mass (a, b) and projected area (c, d) with nitrogen content per unit dry mass (a, b) and per unit projected area (c, d) in three Mediterranean *Pinus* species. Linear regressions were used to fit data (all species and needle and plant ages pooled). Symbols as in Figure 2

2011), suggesting that heteroblastic differences constitute an important seedling adaptation in Mediterranean highly stressful environments. We have previously reported that juvenile needles have lower needle density, greater fraction of mesophyll tissue in needles, thinner mesophyll cell walls and greater chloroplast to exposed mesophyll cell wall surface area, while secondary needles in adult trees are characterized by the opposite suite of these traits (Kuusk et al., 2018b). Here, we hypothesized that these trait differences result in concomitant variations in needle photosynthetic capacity and that the alteration in needle photosynthetic potentials is driven by the trade-off between support and photosynthetic investments demonstrated in Kuusk et al. (2018b), and furthermore, that the greater structural robustness in adult needles is associated with a stronger limitation of photosynthesis by mesophyll diffusion conductance.

Needle age also influences foliage structural traits and nutrient content (Mediavilla et al., 2014; Niinemets, 2002; Niinemets, García-Plazaola, & Tosens, 2012; Teskey, Grier, & Hinckley, 1984; Weiskittel, Temesgen, Wilson, & Maguire, 2008), but the effects of these modifications on age-dependent changes in needle photosynthetic potentials are still not fully resolved. Thus, in mature trees we studied variation in foliage photosynthetic potentials in non-senescent adult current-year, 1-year-old and 2-year-old needles. We hypothesized that the age-dependent changes in photosynthetic activity with needle age are also driven by changes in mesophyll conductance and accumulation of support tissues, but that trait changes with needle age are comparatively less extensive than modifications upon juvenile-to-adult transition.

2 | MATERIAL AND METHODS

2.1 | Measurement sites and plant sampling

Full details of study sites, plants and plant sampling are provided in Kuusk et al. (2018b). In short, the study was conducted in sites with continental Mediterranean climate characterized by hot dry summers and relatively cold dry winters. Adult cone-bearing trees were investigated at Alto Tajo Natural Park, Central Spain (Guadalajara, Castilla-La Mancha, 40.8480°N, 2.1812°W, mean elevation 950 m). The mean annual rainfall at the site is 490 mm and mean annual temperature 10.2°C (Molina de Aragón whether station, 40.8444°N, 1.8853°W, elevation 1,063 m). In each species, five mature plants at full sunlight were randomly selected for sampling. The trees were 90–100 years old and 15–21 m tall (Kuusk et al., 2018b for species averages). Terminal branchlets without cones (one branch from each individual tree) were taken from the southern part of the upper canopy (average seasonal integrated quantum flux density of ca. 40 mol m^{-2} day^{-1}) to minimize shading effects on foliage characteristics (Gebauer et al., 2011; Niinemets, Keenan, & Hallik, 2015) in October 2005 and in August 2006. The branches were cut under water, and the cut ends were kept in water and transported to the laboratory for gas-exchange and anatomical measurements. Previous studies have indicated that use of cut branches allows for obtaining representative estimates of foliage gas-exchange characteristics, except stomatal conductance that can differ from the values in the field (e.g., Niinemets, Cescatti, Rodeghiero, & Tosens, 2005; Peñuelas et al., 2010).

There were very few seedlings at the field site, as is common in Mediterranean forests, and the seedlings in the understorey of mature trees were shaded and no recent clear-cut or disturbed areas were available. Therefore, to study juvenile foliage, 2-year-old juvenile trees were obtained from a local nursery at El Seranillo Forestry Center, Guadalajara. They were grown in 5-L pots filled with a mixture (4:4:1:1, v/v) of compost, vermiculite, perlite and sand at the Museo Nacional de Ciencias Naturales (CSIC) in Madrid, Spain (40.440°N, 3.690°W, elevation 682 m). The pots were buried in the soil such that pot soil temperature was ambient, and were exposed to full sunlight (average daily integrated photosynthetic quantum flux density of 41 mol m^{-2} day^{-1}). For the measurements, current-year juvenile foliage formed in the new growth conditions was used. Obviously, the current experimental design introduces unknown sources of variation due to somewhat different growth

environments for mature and juvenile trees, but such problems are inherent to comparisons of different sized and aged plants. Kuusk et al. (2018b) provide a thorough discussion of potential disadvantages and advantages of our design. Because foliage shading is quantitatively the most important environmental factor affecting leaf structure and function (Niinemets et al., 2015; Keenan & Niinemets, 2016; Poorter, Niinemets, Poorter, Niinemets, Poorter, Wright, & Villar, 2009), we considered our design more appropriate than the alternative of comparing high light exposed adult and shaded understorey juvenile plants. We note that the experimental design used here is analogous to studies carried out along the chronosequence of different stands and is also appropriate from an ecological perspective as shade-intolerant Mediterranean pine seedlings cannot persist in the understorey, and can reach the canopy only once a major gap forms in the canopy (Climent, San-Martín, et al., 2011; Kuusk et al., 2018b).

In adult trees carrying secondary needles, current-year, 1-year-old and 2-year-old needles were measured, except for *P. halepensis* that supported only two needle age classes due to shorter needle life span. In the juveniles, where the canopy was chiefly made up of primary current-year needles, only primary needles formed at the growth conditions were studied. In 2005, five juvenile plants, and four to five branches from adult trees from each studied species were measured for foliage photosynthesis characteristics. In 2006, additional branches from adult trees were measured: two branches from *P. halepensis*, three branches from *P. pinea* and three branches from *P. nigra*. In total, 24 branches from adult trees (from eight trees of each species) and 15 juvenile plants (five of each species) were used. Thus, for each tree age × leaf age × species combination, altogether four to six samples (on average 5.2) were measured.

2.2 | Needle gas-exchange measurements

Gas-exchange measurements were carried out with a Li-Cor 6400 portable gas-exchange system (Version 5; Li-Cor, Inc., Lincoln, NE, USA) using the 2-cm^2 leaf chamber fluorimeter measurement head. Needles were enclosed side by side to avoid overlap between the needles and standard environmental conditions of chamber block temperature of 25°C, ambient CO_2 concentration of 400 μmol/mol, quantum flux density of 2,200 μmol m^{-2} s^{-1} (10% blue light) were established, and the leaves were conditioned in the chamber until stomata opened and steady-state gas-exchange rates were established, typically in 30 min after needle enclosure. After reaching the steady state, the CO_2–response curve was measured first, followed by the light–response curve. In the case of the CO_2–response curve, ambient CO_2 concentrations were prepared in sequence of 400, 600, 900, 1,200, 1,600, 200, 300, 200 and 50 μmol/mol and steady-state rates of net assimilation were recorded at each CO_2 concentration. In the case of the light–response curve, light intensity was changed in the sequence of 1,200, 1,800, 800, 500, 250, 125, 80, 30 and 0 μmol m^{-2} s^{-1} and again steady-state rates at each light level were recorded. At the end of the measurements, light was switched off and the rate of dark respiration was measured when the cuvette temperature stabilized and leaf gas-exchange reached a steady state, typically in 4–5 min after switching off the light. At each CO_2 and light level, a saturating light flash of 6,800 μmol m^{-2} s^{-1} was given to estimate the effective quantum yield of photosystem II:

$$\Phi_{PSII} = (F'_m - F_s)/F'_m, \quad (1)$$

where F'_m is the maximum and F_s the steady-state fluorescence yield of light-adapted leaves (Genty, Briantais, & Baker, 1989). From these measurements, the rate of photosynthetic electron transport from chlorophyll fluorescence, J_{ETR}, was calculated as:

$$J_{ETR} = 0.5\zeta\Phi_{PSII}Q, \quad (2)$$

where Q is the quantum flux density and ζ is the leaf absorptance (an average value of 0.9 was used in this study in accordance with estimates of quantum yields obtained from light–response curves).

2.3 | Estimations of Farquhar, von Caemmerer, and Berry (1980) photosynthesis model characteristics and mesophyll conductance

Before calculation of foliage gas-exchange rates, the data were corrected for CO_2 and water vapour diffusion leaks according to Rodeghiero, Niinemets, and Cescatti (2007) using diffusion leak coefficients of 0.445 μmol/s for CO_2 and 5.11 μmol/s for water vapour. After diffusion corrections, all gas-exchange rates were calculated according to von Caemmerer and Farquhar (1981) using the leaf areas estimated from leaf anatomical measurements as detailed in the next section (between 1.5 and 2 cm^2 projected leaf area was included in the leaf chamber). Farquhar et al. (1980) model of photosynthesis was first fitted to net assimilation (A) vs. intercellular CO_2 (C_i)–response curves and the apparent values of the maximum carboxylase activity of ribulose-1,5-bisophosphate carboxylase/oxygenase (Rubisco, $V_{cmax,Ci}$) and the capacity for photosynthetic electron transport ($J_{max,Ci}$) were estimated as in Niinemets et al. (2005) using the Rubisco kinetic characteristics from Bernacchi, Singsaas, Pimentel, Portis, and Long (2001).

Based on gas-exchange and chlorophyll fluorescence measurements (Harley, Loreto, di Marco, & Sharkey, 1992), mesophyll diffusion conductance to CO_2 was estimated as:

$$g_m = \frac{A}{C_i - \frac{\Gamma^*[J_{ETR}+8(A+R_d)]}{J_{ETR}-4(A+R_d)}}, \quad (3)$$

where Γ^* is the hypothetical CO_2 compensation point in the absence of dark respiration and R_d is the non-mitochondrial respiration rate in light (taken as half of the dark respiration rate, e.g., Way & Yamori, 2014; Niinemets, 2014). Using the values of g_m, chloroplastic CO_2 concentrations corresponding to each C_i value were calculated as $C_c = C_i - A/g_m$ and A vs. C_c–response curves were obtained. Farquhar et al. (1980) photosynthesis model was re-fitted to these data, and C_c-based estimates of foliage photosynthetic potentials ($V_{cmax,Cc}$) and $J_{max,Cc}$) were determined.

As at the given chamber block temperature, leaf temperatures varied somewhat (between 24 and 30°C), both C_i- and C_c-based

estimates of foliage biochemical potentials were standardized to a common temperature of 25°C using the shape of the specific activity of Rubisco of Niinemets and Tenhunen (1997) for V_{cmax}, and the shape of J_{max} temperature–response curve characteristic to Mediterranean species (temperature optimum of 39.7°C, Niinemets et al., 2002). As V_{cmax} and J_{max} calculated from C_i and C_c curves were strongly correlated (r^2 = .82 for V_{cmax} and r^2 = .92 for J_{max}, p < .001 for both), we only demonstrate data for C_c-based estimates.

Branch-to-branch differences in leaf temperature were also associated with a certain variation in vapour pressure deficit (1.41–2.82 kPa, average ± SE = 2.050 ± 0.013 kPa) and degree of stomatal limitation of photosynthesis (as evident in a certain variation in C_i values at the reference ambient CO_2 concentrations common in experiments using cut twigs). Thus, the parameterized Farquhar et al. (1980) photosynthesis model was used to obtain standardized estimates of leaf net assimilation rates independent of stomatal conductance at a C_i value of 250 μmol/mol as in Niinemets, Wright, and Evans (2009).

2.4 | Calculation of leaf area enclosed in the gas-exchange cuvette and foliage chemical and structural data

After photosynthesis measurements, needles enclosed in the gas-exchange cuvette were harvested and total needle length (L), the length of enclosed needle section (L_E), width (W) and thickness (T) were measured with Starrett Digital callipers (model 727, L. S. Starrett Company, Athol, MA, USA). From these measurements, average needle projected area, S_P, was calculated as WL, and needle projected area enclosed in the chamber as the sum of the products $L_E W$ of individual needles enclosed in the chamber ($\sum_{i=1}^{i=n} L_{E,i} W_i$, where n is the number of needles enclosed in the chamber).

Measurements of needle volume (V), total to projected area ratio (S_T/S_P), dry mass per unit projected ($M_{A,P}$) and total ($M_{A,T}$) needle area, density (D, needle volume per dry mass), volume to projected area ratio, V/S_P, dry to fresh mass ratio, $R_{D/F}$, nitrogen content per unit projected ($N_{A,P}$) and total ($N_{A,T}$) needle area, tissue volume fractions in support (volume fractions in epidermis, hypodermis and central cylinder) and photosynthetic mesophyll, and needle ultrastructural characteristics are described in Kuusk et al. (2018b). Foliage photosynthetic characteristics per total area were calculated as the values per projected area divided by S_T/S_P. Needle photosynthetic characteristics per dry mass were calculated as the values expressed per projected area divided by $M_{A,P}$. Area- and mass-based physiological traits characterize different facets of leaf functioning. Dry mass-based foliage photosynthetic potentials characterize the photosynthetic return on biomass investment in leaves, and area-based capacities indicate the integrated outcome of differences in leaf structure and photosynthetic capacity of single mesophyll cells (Niinemets & Sack, 2006; Onoda et al., 2017; Wright, Reich, et al., 2004). Expressions of g_m per area and dry mass both characterize the extent to which CO_2 diffusion from intercellular air space to chloroplasts limits photosynthesis, but given that both intercellular and chloroplastic CO_2 concentrations are leaf volume-weighted estimates, diffusion limitations generally scale more strongly with g_m per dry mass (Niinemets, Díaz-Espejo, et al., 2009).

2.5 | Statistical analyses

Differences in average trait values among study years, needle ages and among adult and juvenile trees were tested by ANOVA followed by Tukey's post hoc tests with STATISTICA 6 (StatSoft, Inc., Tulsa, USA) and R 3.1.1 with default packages (R Development Core Team, 2012) as in Kuusk et al. (2018b). As the year of study was not significant in any of the analyses, it was removed from the final analyses. Two-way ANOVAs were used to test for effects of species and heteroblasty among current-year needles, and effects of species and needle age among adult needles. Relationships among leaf traits were explored by linear (Pearson) correlation and nonlinear regression analyses. All statistical effects were considered significant at p < .05. The data accompanying this article are available from the Dryad Digital Repository (Kuusk, Niinemets, & Valladares, 2018a).

3 | RESULTS

3.1 | Tree and needle age, and species-dependent changes in needle photosynthetic characteristics

Foliage net assimilation rate per unit dry mass (A_m) was greater for juvenile than for adult current-year needles (Table 1). Net assimilation rate per unit projected area (A_P), the product of needle dry mass per projected area ($M_{A,P}$) and A_m was less variable, but juvenile needles nevertheless had a greater A_P when all species were analysed together (Table 1). Analogously to A_m, nitrogen use efficiency (the ratio of A_m to N_m, E_N) was significantly greater in juvenile than in adult current-year needles (Table 1).

Analysis of needle biochemical potentials, maximum carboxylase activity of Rubisco (V_{cmax}) and photosynthetic electron transport (J_{max}) derived from the net assimilation vs. chloroplastic CO_2 (C_c)–response curves indicated that juvenile needles had greater V_{cmax} and J_{max} per unit dry mass than adult current-year needles (Figure 1a,b for species-specific differences and Figure S1A,B in Supporting Information for all species pooled). The estimate of photosynthetic electron transport rate from chlorophyll fluorescence (J_{ETR}, Equation 2) per dry mass was also greater for juvenile that for adult current-year needles (p < .001). Again, V_{cmax} and J_{max} per unit projected area varied less (Figures 1c,d, and S1D,E), but J_{max} per unit projected area was greater in juvenile than in adult current-year needles (Figures 1d and S1E).

Mesophyll diffusion conductance (g_m) was greater in juvenile than in adult current-year needles when expressed both per unit dry mass and projected area (Table 1, Figure S1C,F). The CO_2 drawdown from substomatal cavities to chloroplasts, C_i-C_c, was lower for juvenile than for adult current-year needles (Table 1, Figure S1C).

Analysis of the needle age effects on adult needles across all species indicated that foliage net assimilation rates, foliage biochemical potentials, V_{cmax} and J_{max}, and g_m both per unit dry mass and area, and nitrogen use efficiency generally decreased with increasing

needle age (Figures 1 and S1, Table 1). Needle age effects on CO_2 drawdown were less, but still significant (Table 1, Figure S1C).

Both tree age and needle age-dependent modifications occurred similarly in all species (no significant species × tree age and species × needle age interactions, Figure 1 and Table 1), but species differed in average values of some photosynthetic traits (E_N, J_{max} per unit area and dry mass for current-year juvenile and adult needles, and A_m, A_P, and area-based g_m, V_{cmax} and J_{max} for different-aged adult needles; Figure 1 and Table 1). This mainly reflected superior photosynthetic characteristics in *P. nigra* (Figure 1 and Table 1).

3.2 | Correlations of leaf photosynthetic characteristics with leaf structural and chemical traits

Foliage net assimilation rate and underlying partial determinants, E_N, V_{cmax}, J_{max} and g_m, scaled positively with needle mesophyll volume fraction (measured as the fraction of needle mesophyll in needle cross-section) and negatively with volume fractions of mechanical tissues (Figure 2a,b; Table 2), whereas the correlations were stronger for mass-based photosynthetic characteristics (Table 2; r^2 = .26 for V_{cmax} and r^2 = .36 for J_{max} expressed per unit area vs. total mesophyll fraction, p < .001 for both). Needle traits characterizing leaf structural robustness, $M_{A,P}$, density (D) and volume to projected surface area ratio (V/S_P; $M_{A,P} = DV/S_P$, and needle dry to fresh mass ratio ($R_{D/F}$) were generally also negatively associated with both area- and mass-based V_{cmax} and J_{max} (p < .01 for all, except for V_{cmax} per area vs. D, p > .07). Again, these negative relationships were stronger for mass-based (Table 2; for the four structural traits, average r^2 = .35 for relationships with V_{cmax} and r^2 = .40 for relationships with J_{max}) than for area-based (Table 2; average r^2 = .15 for relationships with V_{cmax} and r^2 = .25 for relationships with J_{max}) V_{cmax} and J_{max}.

There were weak positive correlations of mass-based foliage photosynthetic characteristics, A, g_m (Table 2) and V_{cmax} (Figure 3a) and J_{max} (Figure 3b), with foliage nitrogen content per dry mass. However, the correlations of area-based characteristics with nitrogen content per area were even non-significant or negative (Table 2; Figure 3c,d). In fact, photosynthetic nitrogen use efficiency was a stronger determinant of net assimilation rate than nitrogen content ($A_m = E_N N_m$ and $A_P = E_N N_{A,P}$; r = .92 for A_m vs. E_N and r = .71 for A_P vs. E_N, p < .001 for both). Higher nitrogen use efficiency was associated with enhanced mesophyll diffusion conductance (r = .83 for mass-based g_m vs. E_N and r = .68, for area-based g_m vs. E_N, p < .001 for both).

4 | DISCUSSION

4.1 | Heteroblastic changes in needle photosynthesis

The results of this study collectively demonstrate important differences in foliage photosynthetic potentials and mesophyll conductance among juvenile and different-aged adult needles and that these differences primarily result from modifications in needle structure and the share of support and assimilative tissues. Although for the current dataset, heteroblasty only weakly affected needle nitrogen content per dry mass (Kuusk et al., 2018b), foliage net assimilation rate per dry mass standardized to a common intercellular CO_2 concentration (A_m) was strongly enhanced, 2.4- to 2.7-fold in the juvenile needles of the three pine species studied (Table 1). Net assimilation rate per projected area (A_p), the product of A_m and needle dry mass per unit projected area ($M_{A,P}$), was also moderately greater in juvenile needles (Table 1), indicating that the heteroblastic changes in mass-based photosynthetic capacity, both due to changes in tissue distribution between assimilative and structural tissues and in photosynthetic capacity of individual mesophyll cells, were quantitatively greater than needle biomass accumulation per area. An enhanced assimilation rate per unit foliage biomass implies that the juvenile foliage has a shorter time to pay back the carbon cost used for foliage construction. Thus, juveniles have a greater carbon availability for growth of new biomass, thereby importantly contributing to their early growth and recruitment (Climent, Chambel, Pardos, Lario, & Villar-Salvador, 2011; Climent, San-Martín, et al., 2011; Mediavilla et al., 2014).

Similarly to the current study, a decrease of A_m with increasing tree age and size has been consistently observed in conifers (Day et al., 2001; Mediavilla et al., 2014; Miller, Eddleman, & Miller, 1995; Niinemets, 2002; Räim et al., 2012; Steppe et al., 2011; Woodruff et al., 2009). As observed in our study (Figure 3), this decrease is often associated with much lower variation in foliage nitrogen content per dry mass among different-aged and sized trees (Day et al., 2001; Juárez-López, Escudero, & Mediavilla, 2008; Mediavilla et al., 2014; Niinemets, 2002). Area-based net assimilation rate also typically decreases with increasing tree age and size in conifers (Day et al., 2001; Greenwood, Ward, Day, Adams, & Bond, 2008; Niinemets, 2002; Räim et al., 2012; Steppe et al., 2011), but as also observed in our study (Table 1), the decrease is typically less than in the mass-based rate. Furthermore, quantitatively, heteroblastic modifications in foliage photosynthesis rate are much greater than changes in mass- and area-based photosynthesis rates due to the gradual ontogenetic drift in mature plants (our study vs., e.g., Niinemets, 2002; Räim et al., 2012; Steppe et al., 2011; Woodruff et al., 2009).

It has been suggested that the reduction in the assimilation rate in older trees reflects mainly changes in stomatal conductance (Greenwood et al., 2008; Yoder, Ryan, Waring, Schoettle, & Kaufmann, 1994), but there is evidence that the reduction in stomatal conductance is not the only factor responsible for the decline in photosynthesis rate with tree age (Niinemets, 2002; Räim et al., 2012). In fact, older plants might have an even greater stomatal conductance, but still reduced photosynthesis rate (Day et al., 2001). As our study demonstrated, higher net assimilation rate at a given intercellular CO_2 concentration in juvenile needles was associated both with enhanced biochemical photosynthesis capacities, V_{cmax} and J_{max} (Figures 1 and S1), and enhanced mesophyll diffusion conductance (g_m, Table 1, Figure S1) that affects net assimilation rate by altering the chloroplastic CO_2 concentration (C_c). Mesophyll conductance and foliage photosynthetic capacity can vary in a

coordinated manner such that the CO_2 drawdown from substomatal cavities to chloroplasts, C_i–C_c = A/g_m, is invariable (Evans & Loreto, 2000). However, this is typically not the case across species with varying structure, and C_i–C_c is often greater, and accordingly, g_m-limitation of photosynthesis is more severe in species with more robust foliage structure (Onoda et al., 2017; Tomás et al., 2013; Tosens, Niinemets, Westoby, & Wright, 2012; Veromann, Tosens, Laanisto, & Niinemets, 2017). Our study demonstrated that C_i–C_c was lower in juvenile needles (Table 1, Figure S1), indicating that the mesophyll diffusion limited the rate of photosynthesis to a lower extent in juvenile needles. Such a lower control of photosynthesis by g_m and accordingly, a greater efficiency of use of resources invested in photosynthetic machinery in younger plants has been hypothesized (Niinemets, 2002), but to our knowledge, this had not yet been experimentally confirmed. At the ultrastructural level, greater g_m-limitation of photosynthesis in adult trees was associated with thicker cell walls in *P. nigra* and *P. pinea* and with lower chloroplast to exposed mesophyll surface area ratio in *P. halepensis* (Kuusk et al., 2018b), indicating that the effective diffusion pathway lengths were indeed greater in secondary needles in adult trees than in primary needles in young trees.

Given the frequent and severe drought and temperature stress conditions in Mediterranean environments and sustained biotic stress pressure, the lack of foliage robustness can be a significant limitation to survival of juvenile plants and can explain why successful seedling establishment in Mediterranean conditions can occur only in favourable years with moderate stress conditions (Braza & García, 2011; Prévosto, Gavinet, Ripert, & Fernandez, 2015). Therefore, we suggest that the main advantage of juvenile needles is more effective photosynthesis, which provides the young seedling with necessary carbon building blocks for establishing extensive root systems and later on for development of more durable adult needles which are more resistant to mechanical stress and more tolerant to drought.

4.2 | Modifications in foliage photosynthetic characteristics with needle age

Older needles of the three studied pine species had significantly lower photosynthesis rate per unit needle dry mass and area (Table 1). The reduction in mass-based photosynthesis rate is a characteristic age-dependent change (Oleksyn et al., 1997; Teskey et al., 1984), but there is a variability in the age-dependent changes in area-based photosynthesis (Jensen, Warren, Hanson, Childs, & Wullschleger, 2015; Niinemets, 2002; Tissue, Griffin, Turnbull, & Whitehead, 2001). This variability is driven by differences in how the components of A_P vary with leaf age. For the current dataset, the relative magnitude of the age effects on A_m (1.7-2-fold reduction in our study, Table 1) was greater than on dry mass per unit area (1.1- to 1.3-fold increase for $M_{A,P}$) (Kuusk et al., 2018b), resulting in a significant reduction in A_P with leaf age (Table 1).

The age-dependent reduction in A_m has been associated with a decrease in foliage nitrogen content per dry mass (Oleksyn et al., 1997) that is expected to lead to concomitant reductions in the foliage photosynthetic potentials V_{cmax} and J_{max} (Ethier, Livingston, Harrison, Black, & Moran, 2006; Warren, 2006). Although changes in needle age were primarily associated with reductions in foliage biochemical potentials in our study (Figures 1 and S1A–D), the age effects on foliage nitrogen content were not significant (Kuusk et al., 2018b) in agreement with several other studies demonstrating moderate or minor differences in N_m in needles of different age (Ethier et al., 2006; Warren, 2006). A reduction in V_{cmax} and J_{max} at given N_m might reflect a change in the share of foliage nitrogen distribution between photosynthetic and structural functions (e.g., Warren & Adams, 2000). Especially in sclerophyllous species, a large fraction of foliage nitrogen is associated with cell walls (Dong et al., 2015; Hikosaka & Shigeno, 2009; Onoda et al., 2017; Takashima, Hikosaka, & Hirose, 2004), and given the age-dependent reduction in V_{cmax} and J_{max} observed in our study, it is likely that this fraction increased with increasing leaf structural robustness in ageing needles. It has also been suggested that Rubisco becomes progressively inactivated with increasing needle age, explaining partly the age-dependent reduction in V_{cmax} (Ethier et al., 2006; Warren, 2006).

Increases in leaf age also resulted in a reduction in mesophyll diffusion conductance (Table 1, Figure S1C,F) as observed in several evergreen species (Ethier et al., 2006; Niinemets et al., 2005; Warren, 2006). Given that the decrease in g_m was associated with concomitant increases in the CO_2 drawdown C_i-C_c (Table 1, Figure S1C), reduced g_m indeed limited photosynthesis more in older leaves. Such a greater limitation of photosynthesis by within-leaf diffusion in older leaves has been observed previously in several Mediterranean broadleaved evergreen species (Niinemets et al., 2005). Lower g_m in older needles in our study was associated with longer diffusion pathways due to increases in needle cross-sectional dimensions and lower chloroplast to exposed mesophyll surface area (Kuusk et al., 2018b), and possibly also with lower cell wall porosity of more strongly lignified cell walls in older needles.

4.3 | The implications of the trade-offs between structural and functional investments for foliage photosynthesis

In addition to greater g_m-limitation, more robust secondary needles in mature trees had a lower needle volume fraction in photosynthetic mesophyll (Kuusk et al., 2018b). Such a difference was directly associated with foliage photosynthetic capacity across all data, as the fractional investment in mesophyll was strongly correlated with foliage net assimilation rate (Table 2). Furthermore, the positive correlations with mesophyll volume fraction and foliage photosynthetic potentials (Figure 2) suggest that needles with greater mesophyll volume fraction indeed had greater concentrations of photosynthesizing enzymes.

The mass-based photosynthesis rate varied more among juvenile and adult needles (2.3–2.7-fold, Table 1) than the mesophyll volume fraction (1.3–1.5-fold, Kuusk et al., 2018b), partly reflecting concomitant changes in mesophyll diffusion conductance with tree

age (Table 1). Nevertheless, the photosynthetic potentials (V_{cmax} and J_{max}; Figures 1a,b and S1A,B) that are not directly affected by g_m also varied somewhat more than mesophyll volume fraction. Given the moderate increase of N_m with increasing mesophyll volume faction (Kuusk et al., 2018b), a greater variation in V_{cmax} and J_{max} suggests a positive scaling of nitrogen investments in photosynthetic machinery with mesophyll volume fraction. Indeed, a strong positive correlation was observed between mesophyll volume fraction and nitrogen use efficiency (Table 2).

Species differences in adult needle photosynthesis were small in our study (Table 1), indicating that the moderate species variation in mesophyll volume fraction did not affect needle photosynthetic activity to a large extent. This suggests a certain compensation resulting from species differences in nitrogen content, *P. halepensis* < *P. nigra* ≤ *P. halepensis* (Kuusk et al., 2018b) and in nitrogen use efficiency (Table 1).

4.4 | Weak relationships of foliage photosynthetic characteristics with nitrogen content

Leaf economics spectrum (Wright, Reich, et al., 2004) is a concept describing the covariation of suites of leaf traits across the whole range of strategies from a low return stress-tolerant (low A_m and N_m, high M_A) to a high return, luxurious (high A_m and N_m, low M_A) strategy. The three most prominent relationships in the leaf economics spectrum are the positive correlation between A_m and N_m and negative correlations between A_m and M_A, and N_m and M_A (Wright, Reich, et al., 2004). Across all the data in our study, the negative correlation between A_m and $M_{A,P}$ was highly significant (Table 2), but A_m and N_m were weakly correlated and the correlations of N_m vs. $M_{A,P}$ and $M_{A,T}$ were not significant. It has been suggested that due to inherent inter- and intraspecific variability, broad relationships might not simply be evident within datasets covering only part of the economics spectrum, for example, within the data coming from the low or fast return ends of the economics spectrum (Reich, 1993; Wright, Groom, et al., 2004). On the other hand, it has been argued that different combinations of traits can drive vegetation performance in different parts of the economics spectrum, and thus, although contrasting, "local" relationships can have important functional implications (Diemer, Körner, & Prock, 1992; Niinemets, 2015).

The Mediterranean pines studied here are located at the low return end of the economics spectrum, but nevertheless, variation in foliage photosynthetic capacity, leaf structure and nitrogen content was extensive (Kuusk et al., 2018b; Table 1). However, needle age- and plant age-dependent variations within this dataset primarily affected A_m and $M_{A,P}$ and $M_{A,T}$ and much less N_m, and the key trait explaining the variation of A_m at given N_m was the nitrogen use efficiency which reflects nitrogen distribution among photosynthetically active and non-active leaf functions and the efficiency with which photosynthetic proteins are engaged, that is, mesophyll conductance and the degree of activation of rate-limiting proteins (Onoda et al., 2017). Both the heteroblastic change and needle ageing were associated with lower fractions of nitrogen invested in photosynthetic functions and reduced mesophyll conductance in structurally more robust needles (Table 1). In fact, from global databases, there is evidence that the fraction of nitrogen invested in the photosynthetic machinery and the slope of N_m vs. A_m relationships decreases with increasing leaf mechanical robustness (Niinemets, 1999; Onoda et al., 2017; Reich, Kloeppel, Ellsworth, & Walters, 1995). These studies together with our observations suggest that leaf trait variation at the low return end of the economics spectrum can result in suites of trait combinations that might deviate from the universal relationships. This deviation uncovered here emphasizes the importance of tree and needle age and species effects in altering mesophyll diffusion conductance and distribution of nitrogen among photosynthetic and non-photosynthetic functions, and ultimately foliage nitrogen use efficiency.

5 | CONCLUSIONS

This study highlights major differences in foliage photosynthetic characteristics among primary needles in young plants and secondary needles in mature plants and demonstrates that these differences primarily result from differences in foliage structure. Less robust foliage of juvenile needles is associated with greater photosynthetic activity per unit biomass investment. This that contributes to enhanced growth and seedling establishment, whereas the advantage of greater mechanical robustness of secondary needles in adult trees is tolerance of harsh environmental conditions in the upper canopy. However, as this study demonstrates, the inherent trade-off of greater mechanical resistance is a reduced fraction of needle biomass in photosynthetic tissues and lower mesophyll diffusion conductance. As the result of greater diffusion limitations, any given nitrogen investment in photosynthetic machinery results in lower photosynthetic returns in more robust needles.

Tree age- and needle age-dependent modifications in needle photosynthetic traits were qualitatively similar, indicating that increasingly sclerophyllous needle structure in older trees and in ageing needles has the same basic effects on foliage photosynthesis. However, as hypothesized, age-dependent changes in needle photosynthesis were less than differences due to tree age (Table 1), indicating that juvenile-to-adult transition is a much more profound change in needle functioning.

It has been suggested that due to large evolutionary and plastic modifications in foliar structure, structural limitations of foliar photosynthesis play at least as significant role as physiological and biochemical constraints (Niinemets & Sack, 2006). In the case of pine species studied here, heteroblasty and needle age, two characteristic sources of trait variation in conifers, produced an extensive continuum of variation in photosynthetic and structural traits, but limited variation in foliage nitrogen content. This resulted in several trait relationships deviating from the global leaf economics spectrum, suggesting that increases in leaf robustness can alter foliage photosynthetic activity not only due to changes in tissue chemical

composition, but also due to changes in mesophyll conductance and changes in the share of nitrogen between photosynthetic and non-photosynthetic functions.

ACKNOWLEDGEMENTS

Financial support for this research was provided by grants from the Consejo Superior de Investigaciones Cientificas (CSIC, Spain) and the Estonian Academy of Sciences (a grant for collaboration between scientific institutions of Estonia and CSIC), the Estonian Ministry of Science and Education (institutional grant IUT-8-3) and the European Commission through the European Regional Fund (the Center of Excellence EcolChange).

AUTHORS' CONTRIBUTIONS

Ü.N. and F.V. proposed the initial hypothesis, F.V. and V.K. made the experimental plan, V.K. carried out the experimental work, V.K. and Ü.N. analysed the data, V.K. and Ü.N. wrote the first draft of the MS, and all authors contributed to the subsequent versions of the MS and approved the final version of the study.

DATA ACCESSIBILITY

The data accompanying this article have been archived in the Dryad Digital Repository under https://doi.org/10.5061/dryad.hs20gv7 (Kuusk et al., 2018a).

ORCID

Ülo Niinemets http://orcid.org/0000-0002-3078-2192

REFERENCES

Bernacchi, C. J., Singsaas, E. L., Pimentel, C., Portis, A. R. Jr, & Long, S. P. (2001). Improved temperature response functions for models of Rubisco-limited photosynthesis. *Plant, Cell and Environment*, *24*, 253–259. https://doi.org/10.1111/j.1365-3040.2001.00668.x

Boddi, S., Bonzi, L. M., & Calamassi, R. (2002). Structure and ultrastructure of *Pinus halepensis* primary needles. *Flora*, *197*, 10–23. https://doi.org/10.1078/0367-2530-00008

Braza, R., & García, M. B. (2011). Spreading recruitment over time to cope with environmental variability. *Plant Ecology*, *212*, 283–292. https://doi.org/10.1007/s11258-010-9821-y

Climent, J., Aranda, I., Alonso, J., Pardos, J. A., & Gil, L. (2006). Developmental constraints limit the response of Canary Island pine seedlings to combined shade and drought. *Forest Ecology and Management*, *231*, 164–168. https://doi.org/10.1016/j.foreco.2006.05.042

Climent, J., Chambel, M. R., Pardos, M., Lario, F., & Villar-Salvador, P. (2011). Biomass allocation and foliage heteroblasty in hard pine species respond differentially to reduction in rooting volume. *European Journal of Forest Research*, *130*, 841–850. https://doi.org/10.1007/s10342-010-0476-y

Climent, J., San-Martín, R., Chambel, M. R., & Mutke, S. (2011). Ontogenetic differentiation between Mediterranean and Eurasian pines (sect. *Pinus*) at the seedling stage. *Trees: Structure and Function*, *25*, 175–186. https://doi.org/10.1007/s00468-010-0496-8

Day, M. E., Greenwood, M. S., & White, A. S. (2001). Age-related changes in foliar morphology and physiology in red spruce and their influence on declining photosynthetic rates and productivity with tree age. *Tree Physiology*, *21*, 1195–1204. https://doi.org/10.1093/treephys/21.16.1195

Diemer, M., Körner, C., & Prock, S. (1992). Leaf life spans in wild perennial herbaceous plants: A survey and attempts at a functional interpretation. *Oecologia*, *89*, 10–16. https://doi.org/10.1007/BF00319009

Dong, T., Li, J., Zhang, Y., Korpelainen, H., Niinemets, Ü., & Li, C. (2015). Partial shading of lateral branches affects growth, and foliage nitrogen- and water-use efficiencies in the conifer *Cunninghamia lanceolata* growing in a warm monsoon climate. *Tree Physiology*, *35*, 632–643. https://doi.org/10.1093/treephys/tpv036

Ethier, G. J., Livingston, N. J., Harrison, D. L., Black, T. A., & Moran, J. A. (2006). Low stomatal and internal conductance to CO_2 versus Rubisco deactivation as determinants of the photosynthetic decline of ageing evergreen leaves. *Plant, Cell and Environment*, *29*, 2168–2184. https://doi.org/10.1111/j.1365-3040.2006.01590.x

Evans, J. R., & Loreto, F. (2000). Acquisition and diffusion of CO_2 in higher plant leaves. In R. C. Leegood, T. D. Sharkey, & S. von Caemmerer (Eds.), *Photosynthesis: Physiology and metabolism* (pp. 321–351). Dordrecht, The Netherlands: Kluwer Academic. https://doi.org/10.1007/0-306-48137-5

Farquhar, G. D., von Caemmerer, S., & Berry, J. A. (1980). A biochemical model of photosynthetic CO_2 assimilation in leaves of C_3 species. *Planta*, *149*, 78–90. https://doi.org/10.1007/BF00386231

Gebauer, R., Volařík, D., Urban, J., Børja, I., Nagy, N. E., Eldhuset, T. D., & Krokene, P. (2011). Effect of thinning on anatomical adaptations of Norway spruce needles. *Tree Physiology*, *31*, 1103–1113. https://doi.org/10.1093/treephys/tpr081

Genty, B., Briantais, J.-M., & Baker, N. R. (1989). The relationship between the quantum yield of photosynthetic electron transport and quenching of chlorophyll fluorescence. *Biochimica et Biophysica Acta*, *990*, 87–92. https://doi.org/10.1016/S0304-4165(89)80016-9

Greenwood, M. S., Ward, M. H., Day, M. E., Adams, S. L., & Bond, B. J. (2008). Age-related trends in red spruce foliar plasticity in relation to declining productivity. *Tree Physiology*, *28*, 225–232. https://doi.org/10.1093/treephys/28.2.225

Harley, P. C., Loreto, F., di Marco, G., & Sharkey, T. D. (1992). Theoretical considerations when estimating the mesophyll conductance to CO_2 flux by analysis of the response of photosynthesis to CO_2. *Plant Physiology*, *98*, 1429–1436. https://doi.org/10.1104/pp.98.4.1429

Harper, J. L. (1989). The value of a leaf. *Oecologia*, *80*, 53–58. https://doi.org/10.1007/BF00789931

Hikosaka, K., & Shigeno, A. (2009). The role of Rubisco and cell walls in the interspecific variation in photosynthetic capacity. *Oecologia*, *160*, 443–451. https://doi.org/10.1007/s00442-009-1315-z

Jensen, A. M., Warren, J. M., Hanson, P. J., Childs, J., & Wullschleger, S. D. (2015). Needle age and season influence photosynthetic temperature response and total annual carbon uptake in mature *Picea mariana* trees. *Annals of Botany*, *116*, 821–832. https://doi.org/10.1093/aob/mcv115

Juárez-López, F. J., Escudero, A., & Mediavilla, S. (2008). Ontogenetic changes in stomatal and biochemical limitations to photosynthesis of two co-occurring Mediterranean oaks differing in leaf life span. *Tree Physiology*, *28*, 367–374. https://doi.org/10.1093/treephys/28.3.367

Karban, R., & Thaler, J. S. (1999). Plant phase change and resistance to herbivory. *Ecology*, *80*, 510–517. https://doi.org/10.1890/0012-9658(1999)080[0510:PPCART]2.0.CO;2

Kattge, J., Díaz, S., Lavorel, S., Prentice, C., Leadley, P., Bönisch, G., … Wirth, C. (2011). TRY – A global database of plant traits. *Global Change Biology*, *17*, 2905–2935. https://doi.org/10.1111/j.1365-2486.2011.02451.x

Keenan, T. F., & Niinemets, Ü. (2016). Global leaf trait estimates biased due to plasticity in the shade. *Nature Plants*, *3*, 16201. https://doi.org/10.1038/nplants.2016.201

Kuusk, V., Niinemets, Ü., & Valladares, F. (2018a). Data from: Structural controls on photosynthetic capacity through juvenile-to-adult transition and needle ageing in Mediterranean pines. *Dryad Digital Repository*, https://doi.org/10.5061/dryad.hs20gv7

Kuusk, V., Niinemets, Ü., & Valladares, F. (2018b). A major trade-off between structural and photosynthetic investments operative across plant and needle ages in three Mediterranean pines. *Tree Physiology* (in press). https://doi.org/10.1093/treephys/tpx1139

Mediavilla, S., Herranz, M., González-Zurdo, P., & Escudero, A. (2014). Ontogenetic transition in leaf traits: A new cost associated with the increase in leaf longevity. *Journal of Plant Ecology*, *7*, 567–575. https://doi.org/10.1093/jpe/rtt059

Miller, P. M., Eddleman, L. E., & Miller, J. M. (1995). *Juniperus occidentalis* juvenile foliage: Advantages and disadvantages for a stress-tolerant, invasive conifer. *Canadian Journal of Forest Research*, *25*, 470–479. https://doi.org/10.1139/x95-052

Niinemets, Ü. (1999). Research review. Components of leaf dry mass per area –thickness and density – alter leaf photosynthetic capacity in reverse directions in woody plants. *The New Phytologist*, *144*, 35–47. https://doi.org/10.1046/j.1469-8137.1999.00466.x

Niinemets, Ü. (2002). Stomatal conductance alone does not explain the decline in foliar photosynthetic rates with increasing tree age and size in *Picea abies* and *Pinus sylvestris*. *Tree Physiology*, *22*, 515–535. https://doi.org/10.1093/treephys/22.8.515

Niinemets, Ü. (2014). Improving modeling of the "dark part" of canopy carbon gain. *Tree Physiology*, *34*, 557–563. https://doi.org/10.1093/treephys/tpu030

Niinemets, Ü. (2015). Is there a species spectrum within the world-wide leaf economics spectrum? Major variations in leaf functional traits in the Mediterranean sclerophyll *Quercus ilex*. *The New Phytologist*, *205*, 79–96. https://doi.org/10.1111/nph.13001

Niinemets, Ü., Cescatti, A., Rodeghiero, M., & Tosens, T. (2005). Leaf internal diffusion conductance limits photosynthesis more strongly in older leaves of Mediterranean evergreen broad-leaved species. *Plant, Cell and Environment*, *28*, 1552–1566. https://doi.org/10.1111/j.1365-3040.2005.01392.x

Niinemets, Ü., Díaz-Espejo, A., Flexas, J., Galmés, J., & Warren, C. R. (2009). Role of mesophyll diffusion conductance in constraining potential photosynthetic productivity in the field. *Journal of Experimental Botany*, *60*, 2249–2270. https://doi.org/10.1093/jxb/erp036

Niinemets, Ü., García-Plazaola, J. I., & Tosens, T. (2012). Photosynthesis during leaf development and ageing. In J. Flexas, F. Loreto & H. Medrano (Eds.), *Terrestrial photosynthesis in a changing environment. A molecular, physiological and ecological approach* (pp. 353–372). Cambridge, UK: Cambridge University Press. https://doi.org/10.1017/CBO9781139051477

Niinemets, Ü., Hauff, K., Bertin, N., Tenhunen, J. D., Steinbrecher, R., & Seufert, G. (2002). Monoterpene emissions in relation to foliar photosynthetic and structural variables in Mediterranean evergreen *Quercus* species. *The New Phytologist*, *153*, 243–256. https://doi.org/10.1046/j.0028-646X.2001.00323.x

Niinemets, Ü., Keenan, T. F., & Hallik, L. (2015). Tansley review. A worldwide analysis of within-canopy variations in leaf structural, chemical and physiological traits across plant functional types. *The New Phytologist*, *205*, 973–993. https://doi.org/10.1111/nph.13096

Niinemets, Ü., & Kull, O. (1995). Effects of light availability and tree size on the architecture of assimilative surface in the canopy of *Picea abies*: Variation in needle morphology. *Tree Physiology*, *15*, 307–315. https://doi.org/10.1093/treephys/15.5.307

Niinemets, Ü., & Sack, L. (2006). Structural determinants of leaf light-harvesting capacity and photosynthetic potentials. In K. Esser, U. E. Lüttge, W. Beyschlag, & J. Murata (Eds.), *Progress in botany* (pp. 385–419). Berlin, Germany: Springer. https://doi.org/10.1007/3-540-27998-9

Niinemets, Ü., & Tenhunen, J. D. (1997). A model separating leaf structural and physiological effects on carbon gain along light gradients for the shade-tolerant species *Acer saccharum*. *Plant, Cell and Environment*, *20*, 845–866. https://doi.org/10.1046/j.1365-3040.1997.d01-133.x

Niinemets, Ü., Wright, I. J., & Evans, J. R. (2009). Leaf mesophyll diffusion conductance in 35 Australian sclerophylls covering a broad range of foliage structural and physiological variation. *Journal of Experimental Botany*, *60*, 2433–2449. https://doi.org/10.1093/jxb/erp045

Oleksyn, J., Tjoelker, M. G., Lorenc-Plucińska, G., Konwińska, A., Żytkowiak, R., Karolewski, P., & Reich, P. B. (1997). Needle CO_2 exchange, structure and defence traits in relation to needle age in *Pinus heldreichii* Christ – a relict of Tertiary flora. *Trees: Structure and Function*, *12*, 82–89.

Onoda, Y., Wright, I. J., Evans, J. R., Hikosaka, K., Kitajima, K., Niinemets, Ü., … Westoby, M. (2017). Physiological and structural tradeoffs underlying the leaf economics spectrum. *The New Phytologist*, *214*, 1447–1463. https://doi.org/10.1111/nph.14496

Pardos, M., Calama, R., & Climent, J. (2009). Difference in cuticular transpiration and sclerophylly in juvenile and adult pine needles relates to the species-specific rates of development. *Trees: Structure and Function*, *23*, 501–508. https://doi.org/10.1007/s00468-008-0296-6

Peñuelas, J., Sardans, J., Llusià, J., Owen, S. M., Carnicer, J., Giambelluca, T. W., … Niinemets, Ü. (2010). Faster returns on 'leaf economics' and different biogeochemical niche in invasive compared with native plant species. *Global Change Biology*, *16*, 2171–2185.

Poorter, H., Niinemets, Ü., Poorter, L., Wright, I. J., & Villar, R. (2009). Tansley review. Causes and consequences of variation in leaf mass per area (LMA): A meta-analysis. *The New Phytologist*, *182*, 565–588. https://doi.org/10.1111/j.1469-8137.2009.02830.x

Prévosto, B., Gavinet, J., Ripert, C., & Fernandez, C. (2015). Identification of windows of emergence and seedling establishment in a pine Mediterranean forest under controlled disturbances. *Basic and Applied Ecology*, *16*, 36–45. https://doi.org/10.1016/j.baae.2014.10.008

R Development Core Team. (2012). *R: A language and environment for statistical computing*. Vienna, Austia: The R Foundation for Statistical Computing.

Räim, O., Kaurilind, E., Hallik, L., & Merilo, E. (2012). Why does needle photosynthesis decline with tree height in Norway spruce? *Plant Biology*, *14*, 306–314. https://doi.org/10.1111/j.1438-8677.2011.00503.x

Reich, P. B. (1993). Reconciling apparent discrepancies among studies relating life span, structure and function of leaves in contrasting plant life forms and climates: 'The blind men and the elephant retold'. *Functional Ecology*, *7*, 721–725. https://doi.org/10.2307/2390194

Reich, P. B., Kloeppel, B. D., Ellsworth, D. S., & Walters, M. B. (1995). Different photosynthesis-nitrogen relations in deciduous hardwood and evergreen coniferous tree species. *Oecologia*, *104*, 24–30. https://doi.org/10.1007/BF00365558

Rodeghiero, M., Niinemets, Ü., & Cescatti, A. (2007). Major diffusion leaks of clamp-on leaf cuvettes still unaccounted: How erroneous are the estimates of Farquhar *et al.* model parameters? *Plant, Cell and Environment*, *30*, 1006–1022. https://doi.org/10.1111/j.1365-3040.2007.001689.x

Steppe, K., Niinemets, Ü., & Teskey, R. O. (2011). Tree size- and age-related changes in leaf physiology and their influence on carbon gain. In F. C. Meinzer, T. Dawson, & B. Lachenbruch (Eds.), *Size- and age-related changes in tree structure and function* (pp. 235–253). Berlin, Germany: Springer. https://doi.org/10.1007/978-94-007-1242-3

Takashima, T., Hikosaka, K., & Hirose, T. (2004). Photosynthesis or persistence: Nitrogen allocation in leaves of evergreen and deciduous *Quercus* species. *Plant, Cell and Environment*, *27*, 1047–1054. https://doi.org/10.1111/j.1365-3040.2004.01209.x

Teskey, R. O., Grier, C. C., & Hinckley, T. M. (1984). Change in photosynthesis and water relations with age and season in *Abies*

amabilis. *Canadian Journal of Forest Research*, *14*, 77–84. https://doi.org/10.1139/x84-015

Tissue, D. T., Griffin, K. L., Turnbull, M. H., & Whitehead, D. (2001). Canopy position and needle age affect photosynthetic response in field-grown *Pinus radiata* after five years of exposure to elevated carbon dioxide partial pressure. *Tree Physiology*, *21*, 915–923. https://doi.org/10.1093/treephys/21.12-13.915

Tomás, M., Flexas, J., Copolovici, L., Galmés, J., Hallik, L., Medrano, H., … Niinemets, Ü. (2013). Importance of leaf anatomy in determining mesophyll diffusion conductance to CO_2 across species: Quantitative limitations and scaling up by models. *Journal of Experimental Botany*, *64*, 2269–2281. https://doi.org/10.1093/jxb/ert086

Tosens, T., Niinemets, Ü., Westoby, M., & Wright, I. J. (2012). Anatomical basis of variation in mesophyll resistance in eastern Australian sclerophylls: News of a long and winding path. *Journal of Experimental Botany*, *63*, 5105–5119. https://doi.org/10.1093/jxb/ers171

Veromann, L.-L., Tosens, T., Laanisto, L., & Niinemets, Ü. (2017). Extremely thick cell walls and low mesophyll conductance: Welcome to the world of ancient living! *Journal of Experimental Botany*, *68*, 1639–1653. https://doi.org/10.1093/jxb/erx045

von Caemmerer, S., & Farquhar, G. D. (1981). Some relationships between the biochemistry of photosynthesis and the gas exchange of leaves. *Planta*, *153*, 376–387. https://doi.org/10.1007/BF00384257

Warren, C. R. (2006). Why does photosynthesis decrease with needle age in *Pinus pinaster*? *Trees: Structure and Function*, *20*, 157–164. https://doi.org/10.1007/s00468-005-0021-7

Warren, C. R., & Adams, M. A. (2000). Trade-offs between the persistence of foliage and productivity in two Pinus species. *Oecologia*, *124*, 487–494. https://doi.org/10.1007/PL00008874

Way, D. A., & Yamori, W. (2014). Thermal acclimation of photosynthesis: On the importance of adjusting our definitions and accounting for thermal acclimation of respiration. *Photosynthesis Research*, *119*, 89–100. https://doi.org/10.1007/s11120-013-9873-7

Weiskittel, A. R., Temesgen, H., Wilson, D. S., & Maguire, D. A. (2008). Sources of within- and between-stand variability in specific leaf area of three ecologically distinct conifer species. *Annals of Forest Science*, *65*, 103. https://doi.org/10.1051/forest:2007075

Woodruff, D. R., Meinzer, F. C., Lachenbruch, B., & Johnson, D. M. (2009). Coordination of leaf structure and gas exchange along a height gradient in a tall conifer. *Tree Physiology*, *29*, 261–272.

Wright, I. J., Groom, P. K., Lamont, B. B., Poot, P., Prior, L. D., Reich, P. B., … Westoby, M. (2004). Leaf trait relationships in Australian plant species. *Functional Plant Biology*, *31*, 551–558. https://doi.org/10.1071/FP03212

Wright, I. J., Reich, P. B., Westoby, M., Ackerly, D. D., Baruch, Z., Bongers, F., … Villar, R. (2004). The world-wide leaf economics spectrum. *Nature*, *428*, 821–827. https://doi.org/10.1038/nature02403

Yoder, B. J., Ryan, M. G., Waring, R. H., Schoettle, A. W., & Kaufmann, M. R. (1994). Evidence of reduced photosynthetic rates in old trees. *Forest Science*, *40*, 513–527.

Zotz, G., Wilhelm, K., & Becker, A. (2011). Heteroblasty – A review. *Botanical Review*, *77*, 109–151. https://doi.org/10.1007/s12229-010-9062-8

SUPPORTING INFORMATION

Additional Supporting Information may be found online in the supporting information tab for this article.

How to cite this article: Kuusk V, Niinemets Ü, Valladares F. Structural controls on photosynthetic capacity through juvenile-to-adult transition and needle ageing in Mediterranean pines. *Funct Ecol*. 2018;32:1479–1491. https://doi.org/10.1111/1365-2435.13087

III

Bahtijor Rasulov, Irina Bichele, Katja Hüve, **Vivian Vislap,** Ülo Niinemets (2015) Acclimation of isoprene emission and photosynthesis to growth temperature in hybrid aspen: resolving structural and physiological controls. *Plant, Cell and Environment* 38: 751–766.

Plant, Cell & Environment

Plant, Cell and Environment (2015) **38**, 751–766 doi: 10.1111/pce.12435

Original Article

Acclimation of isoprene emission and photosynthesis to growth temperature in hybrid aspen: resolving structural and physiological controls

Bahtijor Rasulov[1,2], Irina Bichele[3], Katja Hüve[2], Vivian Vislap[2] & Ülo Niinemets[2,4]

[1]Institute of Technology, University of Tartu, Nooruse 1, Tartu 51010, Estonia, [2]Institute of Agricultural and Environmental Sciences, Estonian University of Life Sciences, Kreutzwaldi 1, Tartu 51014, Estonia, [3]Institute of Molecular and Cell Biology, University of Tartu, Riia 23, Tartu 51010, Estonia and [4]Estonian Academy of Sciences, Kohtu 6, Tallinn 10130, Estonia

ABSTRACT

Acclimation of foliage to growth temperature involves both structural and physiological modifications, but the relative importance of these two mechanisms of acclimation is poorly known, especially for isoprene emission responses. We grew hybrid aspen (*Populus tremula* x *P. tremuloides*) under control (day/night temperature of 25/20 °C) and high temperature conditions (35/27 °C) to gain insight into the structural and physiological acclimation controls. Growth at high temperature resulted in larger and thinner leaves with smaller and more densely packed chloroplasts and with lower leaf dry mass per area (M_A). High growth temperature also led to lower photosynthetic and respiration rates, isoprene emission rate and leaf pigment content and isoprene substrate dimethylallyl diphosphate pool size per unit area, but to greater stomatal conductance. However, all physiological characteristics were similar when expressed per unit dry mass, indicating that the area-based differences were primarily driven by M_A. Acclimation to high temperature further increased heat stability of photosynthesis and increased activation energies for isoprene emission and isoprene synthase rate constant. This study demonstrates that temperature acclimation of photosynthetic and isoprene emission characteristics per unit leaf area were primarily driven by structural modifications, and we argue that future studies investigating acclimation to growth temperature must consider structural modifications.

Key-words: dimethylallyl diphosphate; heat resistance; isoprene synthase; leaf anatomy; optimum temperature; photosynthetic electron transport rate; photosynthesis rate; temperature acclimation.

INTRODUCTION

Photosynthesis and respiration are considered the primary biological components regulating the biosphere-atmosphere carbon exchange (Ciais *et al*. 2001; Mahecha *et al*. 2010). However, there is a large and commonly ignored flux of biogenic volatile organic compounds (BVOC) generated by pathways of secondary metabolism that can significantly contribute to the carbon balance of the biosphere (Arneth *et al*. 2008; Guenther *et al*. 2012; Ashworth *et al*. 2013). Among BVOC, a central role is played by isoprene that has the greatest worldwide flux attributable to a single volatile compound (Guenther *et al*. 1993; Li & Sharkey 2013).

Both the primary and the secondary plant metabolism are strongly dependent on temperature, but the temperature sensitivities of different processes differ among plant species, and they often vary with growth conditions (Way & Oren 2010; Centritto *et al*. 2011; Smith & Dukes 2013; Way & Yamori 2014). In particular, acclimation to growth temperature can importantly alter the shape of the temperature responses of respiration and photosynthesis (Berry & Björkman 1980; Hopkins 1998) and isoprene emission (Wiberley *et al*. 2008). Although acclimation of physiological processes to long-term temperature is a well-known phenomenon, the degree of acclimation strongly varies among plant species and for different processes for reasons not yet fully understood (Berry & Björkman 1980; Tjoelker *et al*. 1999; Bunce 2000; Yamasaki *et al*. 2002; Loveys *et al*. 2003; Fares *et al*. 2011). Understanding such acclimation responses and mechanisms of acclimation are important in predicting plant responses to seasonal and year-to-year differences in temperature environments as well as the responses to future climate (Smith & Dukes 2013).

Acclimation of photosynthesis to high temperature is characteristically associated with shifts of the optimum temperature of photosynthesis to higher temperatures (Berry & Björkman 1980; Turnbull *et al*. 2002; Sage & Kubien 2007). Improved heat stability of photosynthesis is typically associated with changes in the stability of thylakoid membranes as the result of increases in the degree of membrane lipid saturation (Berry & Björkman 1980; Björkman *et al*. 1980; Devos *et al*. 1998; Sharkey *et al*. 2001). Given that the temperature responses of Rubisco and photosynthetic electron transport have different temperature sensitivities, temperature acclimation can also result from changes in the partitioning of

Correspondence: Ü. Niinemets. Fax: +3727313738; e-mail: ylo.niinemets@emu.ee

© 2014 John Wiley & Sons Ltd

rate-limiting photosynthetic proteins among the partial determinants of photosynthesis (Hikosaka 1997; Hikosaka *et al*. 1999). In addition, growth temperature-driven changes in the overall content of rate-limiting components of photosynthesis machinery can result in changes in maximum photosynthetic rates (Björkman *et al*. 1980; Stitt & Hurry 2002; Yamori *et al*. 2005; Sage & Kubien 2007).

In isoprene-emitting species, heat stability can be rapidly altered by isoprene emission. Isoprene is thought to dissolve in photosynthetic membranes and stabilize membrane lipids (Singsaas & Sharkey 2000; Sharkey & Yeh 2001; Velikova *et al*. 2011, 2012) as well as serve as a lipid-soluble antioxidant detoxifying heat stress generated reactive oxygen species and peroxidized membrane lipids (Vickers *et al*. 2009; Velikova *et al*. 2012; Possell & Loreto 2013). Thus, isoprene emission is considered particularly advantageous in responding to rapid increases in leaf temperature such as those occurring during light flecks (Behnke *et al*. 2007, 2013; Way *et al*. 2011).

Isoprene emission capacity can adapt to temperature environment, typically increasing after an increase in leaf temperature environment (Sharkey *et al*. 1999; Funk *et al*. 2003; Wiberley *et al*. 2008) as the result of enhanced expression of isoprene synthase gene and genes of the chloroplastic 2-C-methyl-D-erythritol 4-phosphate pathway responsible for isoprenoid synthesis in chloroplasts (Wiberley *et al*. 2008, 2009; Vickers *et al*. 2010). However, most work on isoprene emission responses to temperature environment stems from transfer experiments where plants developed at a certain temperature have been transferred to the new temperature environment. The effect of plant growth at different temperature environments per se has been investigated only in a few studies (Wiberley *et al*. 2008; Hartikainen *et al*. 2009; Fares *et al*. 2011) with contrasting results showing either enhanced (Wiberley *et al*. 2008), similar (Monson *et al*. 1992; Hartikainen *et al*. 2009; Centritto *et al*. 2011; Fares *et al*. 2011) or reduced emissions (Hartikainen *et al*. 2009) in plants grown under the higher temperature.

Although most work on temperature acclimation has focused on physiological responses, growth at different temperatures can also importantly modify leaf structure, whole plant leaf area and whole plant sink-source relationships (Starck *et al*. 1993; Morcuende *et al*. 1996; Hartikainen *et al*. 2009; Muhl *et al*. 2011; Xu *et al*. 2012). Structural modifications such as changes in chloroplast number, cell size and cell number per unit leaf area are relevant as they can change the amount of rate-limiting enzymes per unit leaf area and result in changes in the process rate per unit leaf area at any given temperature without concomitant changes in physiological potentials of single cells (Niinemets & Sack 2006; Niinemets *et al*. 2009; Poorter *et al*. 2009). It has been demonstrated that growth temperature-dependent changes in respiratory (Ow *et al*. 2008) and photosynthetic activities (Yamasaki *et al*. 2002; Yamori *et al*. 2005; Hartikainen *et al*. 2009; Ibrahim *et al*. 2010) were importantly affected by modifications in leaf dry mass per unit area, which connects area and mass-based process rates (Poorter *et al*. 2009). However, the role of growth temperature-driven structural modifications in acclimation of photosynthesis and isoprene emission has not been routinely studied.

The effects of growth temperature on isoprene emission versus temperature response relationships also vary among the studies with responses ranging from improved thermal sensitivity (Monson *et al*. 1992) to minor changes or even to reduced thermal sensitivity (Fares *et al*. 2011). Given that the temperature response of isoprene emission is driven by both the temperature effects on isoprene synthase activity and its immediate substrate dimethylallyl diphosphate (DMADP) pool size (Rasulov *et al*. 2010), gaining insight into such contrasting responses requires information of growth temperature effects on both of the partial controls of isoprene emission. As isoprene emission and photosynthetic carbon metabolism are strongly linked (Li & Sharkey 2013), improved heat resistance of leaves grown at higher temperature can result in maintenance of greater DMADP pools at higher temperature, thereby improving the isoprene emission at higher temperatures.

Here, we studied the effects of growth temperature on foliage photosynthetic and structural characteristics and isoprene emission in hybrid aspen (*Populus tremula* x *P. tremuloides*) with the specific aim to separate the structural and physiological controls in growth temperature acclimation. A recently developed *in vivo* method for estimation of DMADP pool size and determination of isoprene synthase rate constant and *in vivo* isoprene synthase kinetic characteristics (Rasulov *et al*. 2009a, 2011) was used to separate the substrate and enzyme level controls on isoprene emission under different conditions. Our results indicate that growth temperature did modify the heat resistance of photosynthesis and altered the temperature sensitivity of photosynthesis and isoprene emission rate, but the differences in foliage photosynthesis and isoprene emission rates per unit area were primarily driven by structural changes.

MATERIAL AND METHODS

Seedlings of hybrid aspen (*P. tremula* L. x *P. tremuloides* Michx.) clone H200 (Rasulov *et al*. 2009a,b, 2011) were used in the experiments. Dormant seedlings kept in a cold storage were planted in 4 L plastic pots filled with a mixture of peat and sand (1:1) and maintained at room temperature of 22 °C until dormancy was broken in 2–3 d. Thereafter, the seedlings were moved to Percival AR-95 HIL growth chambers (CLF PlantClimatics, GmbH, Wertingen, Germany) with contrasting temperature regimes (day/night) of 25/20 °C (lower temperature, control) and 35/27 °C (higher temperature). The ambient CO_2 concentration was between 380 and 420 μmol mol^{-1}, the relative humidity was maintained between 60 and 65% (corresponding to moderate differences in daytime water vapour pressure deficit of ca. 1.1 kPa for the control and 1.9 kPa for the high temperature treatment) and the quantum flux density of 500 μmol m^{-2} s^{-1} was provided for 14 h light period. The plants were watered daily to field capacity with the Hoagland nutrient solution for optimum water and nutrient supply. All measurements were conducted with fully expanded 20–24 days old leaves exhibiting peak physiological activity.

Measurements of gas-exchange rates and isoprene emission

An ultra-fast gas-exchange system (system half-time of approximately 0.15 s) was used for the measurements (Laisk *et al*. 2002; Rasulov *et al*. 2010). Briefly, the leaf is enclosed in a clip-on type leaf chamber with a volume of 2.4 cm^3 and a cross-sectional area of 8.04 cm^2. The leaf chamber is thermostated and the upper leaf surface is glued to the chamber glass window by a starch paste. Direct measurements by thin thermocouples and energy balance calculations indicated that leaf temperature was maintained within 0.5 °C of the leaf chamber water jacket. The system has two identical gas lines where different gas concentrations can be prepared and almost instantaneously, in less than 1 s, switched between the sample and the reference line. Such a setup is particularly appropriate for fast measurement of transient physiological responses, avoiding delays in the detection of leaf gas-exchange response signals because of stabilization of gas concentrations. The enclosed leaf area was illuminated with a Schott KL 1500 light source equipped with a heat-reflecting filter (Optical Coating Laboratory, CA, Santa Rosa, USA). The air was mixed from pure nitrogen, oxygen and CO_2 using calibrated dynamic mixers, and the air flow rate through the system was kept at 0.5 mmol s^{-1} (Laisk *et al*. 2002). A LI-6251 infrared gas analyser (LI-Cor, Inc., Lincoln, NE, USA) was used to measure the CO_2 concentration, a custom-made micropsychrometer was used for the water vapour concentration and a proton transfer reaction mass spectrometer (PTR-MS, high-sensitivity version; Ionicon Analytik GmbH, Innsbruck, Austria) for the isoprene concentration. The response time of the PTR-MS was approximately 0.1 s and the isoprene detection limit about 10 pmol mol^{-1}. The instrument was calibrated with an isoprene standard mixture of 5.74 μmol mol^{-1} isoprene in N_2 (Hills Scientific, Boulder, CO, USA).

The standard conditions used in these experiments were the leaf chamber CO_2 concentration of 360 μmol mol^{-1}, O_2 concentration of 21%, leaf temperature of 30 °C, light intensity (photosynthetic quantum flux density) of 650 μmol m^{-2} s^{-1} and water vapour pressure deficit between the leaf and the atmosphere (V_D) of 1.7 kPa. The measurements were conducted with attached leaves, and the protocol for all measurements included leaf enclosure, leaf stabilization under the standard conditions until the steady-state rates of CO_2 and H_2O vapour exchange, and isoprene emission were established, and then changing either CO_2 (360 versus 1200 μmol mol^{-1}), O_2 (21 versus 2%), light (quantum yield measurements) or temperature (temperature response curves) to measure different environmental responses. For the temperature response curves, leaf temperature was changed in steps of 5 °C, and each temperature change was followed by returning to the standard temperature and leaf stabilization as in Rasulov *et al*. (2010). Chamber air water vapour concentration was adjusted at each temperature to maintain the constant V_D and avoid changes in stomatal conductance because of altered V_D.

The quantum yields for CO_2 exchange (α_{CO2}) and isoprene emission (α_I) were measured over the incident light range of 20–75 μmol m^{-2} s^{-1} where the influence of the Kok effect is negligible. In addition, the initial slopes of the net assimilation versus CO_2 response curves over an ambient CO_2 range of 0–100 μmol mol^{-1} at both O_2 concentrations of 21 and 2% were also measured at the standard light intensity of 650 μmol m^{-2} s^{-1}.

All leaf gas-exchange characteristics were calculated according to von Caemmerer & Farquhar (1981). The maximum carboxylase activity or Rubisco (V_{cmax}) was estimated from the initial slopes of the CO_2 response curve at both O_2 concentrations and the capacity for photosynthetic electron transport (J_{max}) from the high-CO_2 concentration (1200 μmol mol^{-1}) measurements according to Niinemets *et al*. (1999b).

Measurements of chlorophyll fluorescence

A PAM 101 fluorimeter (Walz GmbH, Effeltrich, Germany) was used to measure chlorophyll fluorescence characteristics simultaneously with CO_2 and water vapour exchange. A Schott KL 1500 light source provided saturated pulses of white light of 14 000 μmol m^{-2} s^{-1} for 2 s to measure either the dark-adapted (F_m) or light-adapted (F_m') maximum fluorescence yields, while another Schott KL 1500 with a 720-nm narrow-pass interference filter (Andover Corp., Salem, NH, USA) was used for far-red light to estimate the dark-adapted minimum fluorescence yield (F_0). The fluorimeter operation frequency was 1.6 kHz for the darkened leaves and 100 kHz for the illuminated leaves and during saturated pulses. F_m and F_0 were typically measured 20 min after darkening. The dark-adapted PSII quantum yield was computed as $(F_m - F_0)/F_m$ and the quantum yield of illuminated leaves, Φ_{PSII}, as $(F_m' - F)/F_m'$, where F is the steady-state fluorescence yield. The rate of photosynthetic electron transport from chlorophyll fluorescence (J_{ETR}) was further calculated as (Schreiber *et al*. 1994):

$$J_{ETR} = \Phi_{PSII}\xi\beta Q, \quad (1)$$

where Q is the incident quantum flux density, ξ is the leaf absorptance (0.86 for the control and 0.81 for the high temperature-grown plants) and β is the fraction of absorbed light used to drive PSII electron transport (taken as 0.5 in this study).

Foliar structural measurements and determination of chlorophylls and carotenoids

Immediately after the gas-exchange measurements, leaf discs of 4 cm^2 were taken between the major leaf veins for estimation of leaf fresh and dry mass. For anatomical measurements, leaf samples were taken with a razor blade between the major veins from the central part of the leaves and cut into ca. 1 × 1 mm pieces for fixation.

The fresh mass of the leaf discs was estimated immediately and the dry mass after oven-drying at 70 °C for at least 48 h.

© 2014 John Wiley & Sons Ltd,

Additional leaf discs for foliar pigment analyses were frozen at −80 °C until the analysis. The frozen discs were pulverized in liquid N_2 and the pigments were extracted with 80% ice-cold acetone with some $CaCO_3$. The absorptances of the pigment solutions were measured with a dual-beam UV2550PC spectrophotometer (Shimadzu, Kyoto, Japan) at the wavelengths of 663.2, 646.8 and 470 nm, and the pigment contents were calculated according to the equations of Lichtenthaler *et al*. (2001).

Anatomical measurements

Preparation of foliar samples for light and transmission electron microscopy (TEM) follows the protocol of Copolovici *et al*. (2011). Briefly, the samples were fixed by infiltrating with buffered (0.2 M phosphate buffer, pH = 7.2) 2% glutaric aldehyde, dehydrated in ethanol series and embedded in Epoxy Embedding Medium (Sigma-Aldrich Chemie, Steinheim, Germany). Semi-thin (1.5–2 μm) cross- and paradermal sections and ultrathin (70–90 nm) cross-sections were cut with a Leica EM UC7 ultramicrotome (Leica Mikrosysteme GmbH, Vienna, Austria) equipped with a 45° diamond knife (Diatome, Hatfield, PA, USA).

The semi-thin sections were stained for 30 s with Toluidine Blue as described in Burns (1978) and Mercer (1963), viewed at 400–1000× magnification with a Zeiss Axioplan 2 microscope and the digital images were taken with an AxioCam HRc (Carl Zeiss Microscopy, Jena, Germany). Five cross-sections per leaf sample were measured in three locations for total leaf thickness, palisade mesophyll and spongy mesophyll thickness, and chloroplasts and cells were counted in these sections. On the same sections, leaf thickness, palisade mesophyll and spongy mesophyll thickness were measured. In addition, chloroplast and cell numbers were also estimated from 10 paradermal sections per sample, five cut through the palisade and five through the spongy mesophyll. From these measurements, the chloroplast number per leaf area (n_{chl}) was calculated as:

$$n_{chl} = n_{c,p} n_{chl,p,p} n_{chl,p,c} + n_{c,s} n_{chl,s,p} n_{chl,s,c}, \quad (2)$$

where $n_{c,p}$ is the number of cells in the palisade and $n_{c,s}$ that in the spongy parenchyma per unit leaf area, $n_{chl,p,p}$ is the chloroplast number per cell in the palisade parenchyma estimated from the paradermal section and $n_{chl,p,c}$ that estimated from the cross-section, and $n_{chl,s,p}$ is the chloroplast number in the spongy parenchyma estimated from the paradermal section and $n_{chl,s,c}$ that estimated from the cross-section.

Ultrathin sections for TEM were contrasted with uranyl acetate and lead citrate (Copolovici *et al*. 2011 for details) and samples were viewed with a Philips Tecnai 10 TEM (FEI, Eindhoven, the Netherlands) with an accelerating voltage of 80 kV. Digital images were taken with Olympus Veleta 2K × 2K sidemounted TEM CCD camera (Olympus Soft Imaging Solutions GmbH, Germany, Münster, Germany). Magnifications of 7000–10000× were used to measure chloroplast length, thickness and area (ca. 40 chloroplasts were measured in each case). All anatomical characteristics were separately measured for palisade and spongy mesophyll. Digital image analysis was carried out with UTHSCSA Image Tool for Windows 3.00 (UTHSCSA, San Antonio, TX, USA).

Determination of the DMADP pool size (C_{DMADP})

The post-illumination method of Rasulov *et al*. (2009a, 2010) was used to measure the pool size of the immediate precursor pool responsible for the isoprene emission in the steady state. The method is based on the assumption that post-illumination isoprene release continues at the expense of the available precursor pool synthesized prior to leaf darkening (Rasulov *et al*. 2009a, 2010; Li *et al*. 2011). Thus, the size of this pool (C_{DMADP}) was determined by integrating the fast, 200–400 s after darkening, dark decay of isoprene release (Rasulov *et al*. 2009a, 2010).

In addition to DMADP, the isoprene precursor, isopentenyl diphosphate (IDP), can be converted in the dark to DMADP by IDP isomerase and thus, contribute to the dark release of isoprene (Li *et al*. 2011). Although there is a variation in chloroplastic IDP/DMADP ratios among studies (Ramos-Valdivia *et al*. 1997; Zhou *et al*. 2013) likely indicating differences in the activity of chloroplastic IDP isomerase (Brüggemann & Schnitzler 2002), studies are in agreement that IDP/DMADP ratios are small. Nevertheless, even for relatively high IDP/DMADP ratios of ca. 0.5 (Weise *et al*. 2013), the method of Rasulov *et al*. (2009a, 2010) has provided DMADP pool size estimates in excellent agreement with destructive chemical estimations (Weise *et al*. 2013).

Estimation of the rate constant, the maximum rate (V_{max}) and Michaelis-Menten constant (K_m) for isoprene synthase

The DMADP pool size (C_{DMADP}) decreases after darkening because of DMADP conversion into isoprene according to a first-order reaction kinetics under strongly substrate-limited conditions (Loreto *et al*. 2004; Rasulov *et al*. 2009a,b). Given further that the isoprene synthase activation state does not vary during the light-dark transient (as confirmed by the rapid rise of isoprene emission upon illumination of the darkened leaves), isoprene emission rate at any given time t after darkening, $I(t)$, is driven by the C_{DMADP} pool size that has remained at this time, $C_{DMADP}(t)$ (the integral of isoprene emission rate from a given time t until cessation of isoprene emission). Thus, paired values of $I(t)$ versus $C_{DMADP}(t)$ were derived for the entire dark decay and the linear parts of this relationships were used to estimate the rate constant of isoprene synthase (k, s^{-1}) as in our previous studies (Rasulov *et al*. 2010, 2014; Sun *et al*. 2012b).

In vivo V_{max} and K_m for isoprene synthase were estimated from the Hanes-Wolff plots ($C_{DMADP}(t)/I(t)$ versus $C_{DMADP}(t)$) using the full dark decay of isoprene emission. The values of both characteristics were expressed per unit leaf area and dry mass.

Data analyses

Considering that fixation of six molecules of CO_2 is needed for the formation of one molecule of isoprene (e.g., Niinemets *et al.* 1999c), the fraction of carbon lost because of isoprene emission was estimated as $6I/A$, where I is the isoprene emission rate and A the net assimilation rate.

The temperature responses of net assimilation rate, photosynthetic electron transport rate and isoprene emission characteristics (trait p_i) were fitted by an Arrhenius-type temperature response function with an optimum:

$$p_i = \frac{e^{c_i - \Delta H_{a,i}/RT}}{1 + e^{(\Delta S_i T - \Delta H_{d,i})/RT}}, \quad (3)$$

where c_i is the scaling constant for the trait i, $\Delta H_{a,i}$ (J mol^{-1}) is the activation energy, $\Delta H_{d,i}$ (J mol^{-1}) is the deactivation energy, ΔS_i (J mol^{-1} K^{-1}) is the entropy term, T (K) is the leaf temperature and R (8.314 J mol^{-1} K^{-1}) is the gas constant. The temperature optimum for the trait i, $T_{opt,i}$, (Niinemets *et al.* 1999a) was further calculated as:

$$T_{opt,i} = \frac{\Delta H_{d,i}}{\Delta S_i + R \ln\left(\frac{\Delta H_{d,i}}{\Delta H_{a,i}} - 1\right)}. \quad (4)$$

Dark respiration and stomatal conductance versus temperature response curves that did not exhibit an optimum were fitted by exponential relationships in the form:

$$p_i = e^{c_i - \Delta H_{a,i}/RT}. \quad (5)$$

Note that the traditional estimate of temperature responses of chemical and biological processes, Q_{10}, the reaction rate at temperature T+10 relative to the rate at temperature T is given as:

$$Q_{10,i} = e^{\frac{\Delta H_{a,i}[1/T - 1/(T+10)]}{R}}. \quad (6)$$

The Q_{10} concept assumes that the rate of the exponential increase (slope) of the process rate with increasing temperature is independent of temperature. Equation 5 does not include such an assumption and is thus more flexible than the traditional Q_{10} analysis. Nevertheless, for rapid comparisons with other reported data, we also calculated the Q_{10} values. Treatment means for all traits (n = 4–32) were compared by analyses of variance (ANOVA) using Statistica 6.0 (StatSoft, Inc., Tulsa, OK, USA) and the growth temperature effects were considered significant at $P < 0.05$.

RESULTS

Growth temperature effects on foliage structural characteristics

Increases in growth temperature were associated with about 1.2-fold larger and about 1.4-fold thinner leaves (Fig. 1, Table 1) with 1.6-fold lower leaf dry mass per unit area (M_A, Table 1). Decreases in leaf thickness primarily resulted from decreases in the thickness of palisade (1.6-fold) and to a smaller degree in spongy mesophyll thickness (1.3-fold, Fig 1a,b, Table 1). The ratio of palisade to spongy mesophyll thickness also decreased from an average (±SE) of 1.60 ± 0.08 to 1.22 ± 0.06 with increasing growth temperature ($P < 0.001$ for the treatment effect). However, leaf density, the ratio of M_A to leaf thickness was similar among the treatments (0.34 g cm^{-3} for the control and 0.30 g cm^{-3} for plants grown at the higher temperature).

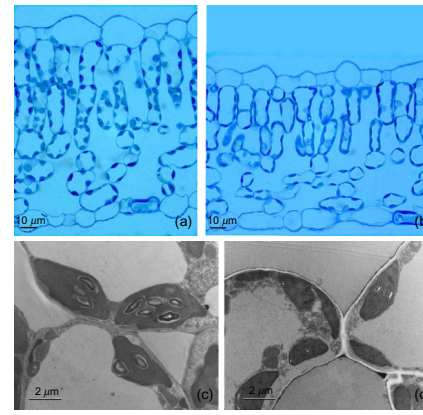

Figure 1. Representative cross-sections of hybrid aspen (*Populus tremula* x *P. tremuloides*, clone H200) leaves (a, b) and chloroplasts (c, d) developed under control (day/night temperatures of 25/20 °C) and high temperature (35/27 °C) conditions.

Decreased leaf thickness was also associated with reduced number of chloroplasts per unit leaf area and with reduced chloroplast size (Table 1). In addition, leaf pigment contents per unit leaf area also decreased. Changes in these traits were relatively smaller than in leaf thickness and M_A, and the number of chloroplasts per leaf dry mass was 1.2-fold greater in the high temperature-grown plants (Table 1). Ultrastructural measurements also indicated that leaf chloroplasts of the high temperature-grown plants had barely visible starch grains, while large starch grains were visible in the chloroplasts in the control treatment (Table 1, Fig. 1c,d).

Effects of growth temperature on foliage photosynthetic and respiratory activities

In analysing the effects of growth temperature on foliage photosynthetic characteristics, we first focus on the effects at the standard measurement temperature of 30 °C, and then consider modifications in the temperature responses. At the standard temperature, acclimation to the higher growth temperature resulted in reductions in net assimilation rate per unit leaf area at the ambient CO_2 concentration (Fig. 2a) and this reduction was associated with decreased maximum

© 2014 John Wiley & Sons Ltd,

Table 1. Leaf structural characteristics and pigment contents (mean ± SE) in hybrid aspen (*Populus tremula* x *P. tremuloides*, clone H200) grown at contrasting temperatures

Characteristic	Growth temperature (day/night)	
	25/20 °C	35/27 °C
Leaf area (cm^2)	67.5 ± 2.4a	82.3 ± 2.7b
Leaf dry mass per unit area ($g\ m^{-2}$)	47.6 ± 1.7a	30.5 ± 1.1b
Leaf thickness (μm)	133.9 ± 3.3a	93.5 ± 2.8b
Palisade mesophyll thickness (μm)	71.5 ± 3.1a	40.9 ± 2.6b
Spongy mesophyll thickness (μm)	44.3 ± 1.0a	34.4 ± 0.8b
Chloroplast number per cm^2 leaf area (palisade)	(38.8 ± 2.2)·10^6a	(29.3 ± 1.9)·10^6a
Chloroplast number per cm^2 leaf area (spongy)	(7.5 ± 0.5)·10^6a	(7.1 ± 0.3)·10^6a
Total chloroplast number per cm^2 leaf area (palisade + spongy)	(46.3 ± 3.7)·10^6a	(36.4 ± 2.3)·10^6a
Chloroplast length (μm)	4.41 ± 0.17a	4.14 ± 0.18a
Chloroplast width (μm)	1.99 ± 0.09a	1.52 ± 0.11b
Chloroplast area (μm^2)	7.23 ± 0.49a	4.99 ± 0.51b
Starch grain area per chloroplast (μm^2)	1.05 ± 0.11a	0.047 ± 0.11b
Chlorophyll content per area ($mg\ m^{-2}$)	413 ± 16a	302 ± 12b
Chlorophyll content per dry mass ($mg\ g^{-1}$)	9.11 ± 0.27a	9.20 ± 0.29a
Chl *a*/*b* ratio	2.68 ± 0.11b	2.38 ± 0.08b
Carotenoid content per area ($mg\ m^{-2}$)	88.4 ± 2.9a	58.9 ± 2.2b
Carotenoid content per dry mass ($mg\ g^{-1}$)	1.80 ± 0.05a	1.90 ± 0.05a

Means with the same letter are not statistically different ($P > 0.05$ according to ANOVA, $n = 6$, for leaf structural measurements and pigment contents and $n = 30$–42 for leaf anatomical measurements).

carboxylase activity of Rubisco (V_{cmax}, Table 2), decreased photosynthetic electron transport rate estimated from chlorophyll fluorescence at ambient CO_2 concentration (J_{ETR}, Fig. 2c) and from the CO_2-saturated net assimilation rate (J_{max}, Table 2) per unit area. Analogously to the net assimilation rate, dark respiration rate per unit area (Fig. 2e, Table 2) and the quantum yield of photosynthesis for the incident light (Table 2) were lower in the warmer treatment. The latter difference reflected lower chlorophyll content per leaf area (Table 1) and leaf absorptance (data not shown) in plants grown at the higher temperature. Conversely, stomatal conductance and intercellular CO_2 concentration were greater in plants grown at the higher temperature (Fig. 3, Table 2).

The growth temperature-dependent changes in assimilation rates and foliage biochemical capacities were strongly driven by temperature effects on leaf structure. In fact, dark respiration rate, J_{max} and net assimilation rate per dry mass were not significantly different among the treatments (Table 2, Fig. 2), while the CO_2-limited photosynthetic electron transport rate per dry mass (electron transport rate when photosynthesis is Rubisco-limited, Fig. 2d) was greater at higher growth temperature. However, V_{cmax} per dry mass was still greater for the control treatment (Table 2), indicating that the similarity of net assimilation rate per dry mass among the treatments reflected a greater intercellular CO_2 concentrations because of higher stomatal conductance at the higher growth temperature (Fig. 3).

Increased growth temperature shifted the optimum temperature of net assimilation to higher temperatures (Fig. 2a,b) and an analogous response was observed for the CO_2-limited photosynthetic electron transport rate (Fig. 2c,d). In addition, the activation energies, ΔH_A (Eqn 3) were smaller in plants grown at the lower temperature ($P < 0.05$ for both comparisons). This, together with greater optimum temperatures, resulted in greater mass-based net assimilation and electron transport rates at higher temperature (Fig. 2b,d). On the other hand, growth temperature did not affect the shapes of the dark respiration (Fig. 2e,f) and stomatal conductance (Fig. 3) versus temperature responses ($P > 0.3$ for the treatment effects on ΔH_A for both traits).

Influence of growth temperature on isoprene emission characteristics at the standard measurement temperature of 30 °C

As with the photosynthesis data, in this section, we first analyse the differences in growth treatments at the standard measurement temperature of 30 °C, and then focus on differences in the shape on temperature responses. On a leaf area basis, both the isoprene emission rate (I) and the pool size of the substrate for the isoprene synthase enzyme, DMADP (C_{DMADP}), were greater in the control than in the high temperature treatment (Fig. 4a,c, Table 2). However, on a leaf dry mass basis, I and C_{DMADP} values were similar among the growth temperature treatments (Fig. 4b,d, Table 2). Furthermore, the rate constant for isoprene synthase (k) was not significantly different between the growth temperature treatments (Fig. 5, Table 2). The percentage of photosynthetic carbon used for isoprene emission was also not significantly different among the treatments at this measurement temperature (Fig. 6). Similarly to the quantum yield for photosynthesis, the quantum yield for isoprene emission for the incident light was greater in the control treatment (Table 2).

The apparent kinetic characteristics of isoprene synthase, the maximum activity at substrate-saturated conditions, V_{max} per unit area (Fig. 7a) and the Michaelis-Menten constant for the area-based C_{DMADP} (Fig. 7c) were greater in the control treatment. However, similarly to I and C_{DMADP} (Fig. 4b,d), V_{max} per unit dry mass (Fig. 7b) and K_m for dry mass-based C_{DMADP} (Fig. 7d) were not different among the growth temperatures.

Modification of the temperature responses of isoprene emission characteristics by growth temperature

Growth temperature had minor effects on the optimum temperatures (T_{opt}) of isoprene emission characteristics (Figs 4,5

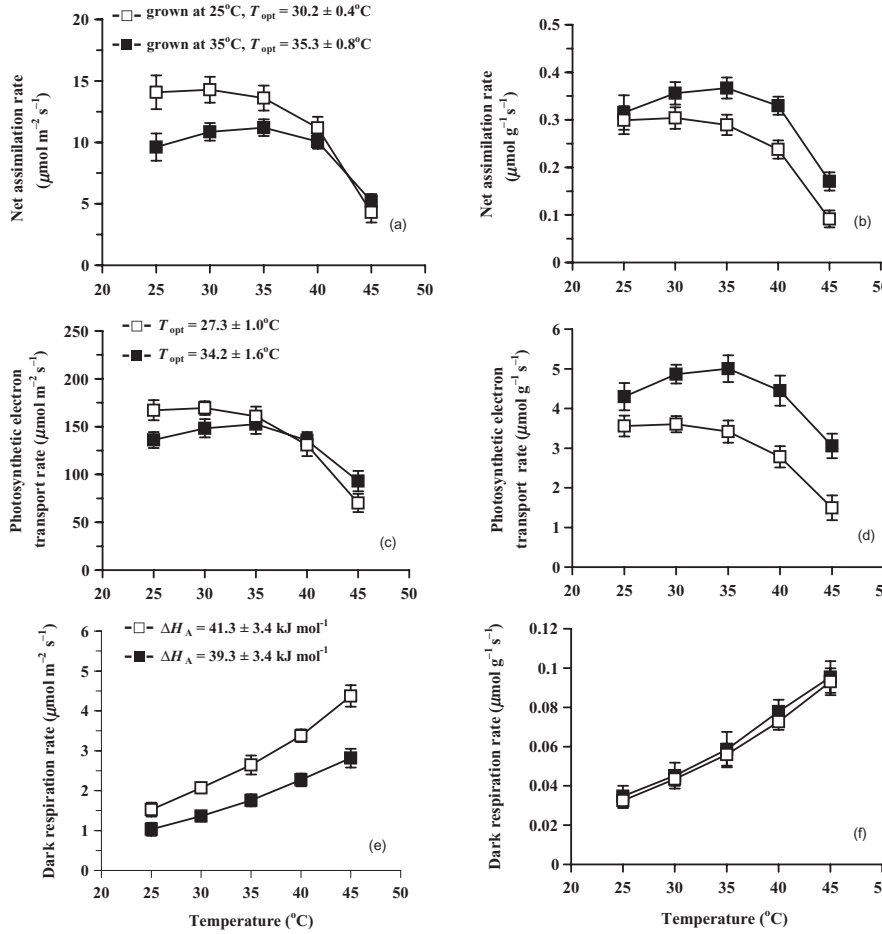

Figure 2. Temperature dependencies of light-saturated net assimilation rate (a, b), photosynthetic electron transport rate estimated from chlorophyll fluorescence (Eqn 1, c, d) and dark respiration rate (e, f) per unit leaf area (a, c, e) and per unit dry mass (b, d, f) in hybrid aspen grown at day/night temperatures of 25/20 °C (control) and 35/27 °C (high temperature treatment). Data were fitted by Eqn 3 (a–d) and Eqn 5 (e, f), and the values of the estimated optimum temperature (T_{opt}, Eqn 4) are indicated for (a) and (c) and the values of the activation energy ΔH_A (Eqn 5) for (e). The optimum temperatures in (a) and (c) are significantly different among the treatments [$P < 0.005$ for (a) and $P < 0.02$ for (c)]. The measurements in a–d were conducted at an ambient CO_2 concentration of 360 μmol mol^{-1} and at an incident quantum flux density of 650 μmol m^{-2} s^{-1} (a-d). Data are means ± SE ($n = 4$).

& 7) with only a slightly greater T_{opt} for apparent maximum isoprene synthase activity (V_{max}) in the control leaves (Fig. 7a). On the other hand, for the measurement temperature range of 25–35 °C, the average activation energy (ΔH_A) for I was 77.9 ± 1.7 kJ mol^{-1} for the control treatment and 108 ± 5 kJ mol^{-1} for the high temperature-grown plants ($P < 0.01$ for the differences among the treatments). These activation energies correspond to a Q_{10} of 2.77 ± 0.05 for the

© 2014 John Wiley & Sons Ltd,

Table 2. Effects of growth temperature on average (±SE) foliage photosynthetic and isoprene emission characteristics in hybrid aspen (*Populus tremula* x *P. tremuloides*, clone H200)

	Growth temperature (day/night)	
Trait	25/20 °C	35/27 °C
Photosynthetic characteristics		
A_n per area (μmol m^{-2} s^{-1})	14.73 ± 0.40a	11.18 ± 0.35b
A_n per dry mass (μmol g^{-1} s^{-1})	0.310 ± 0.009a	0.346 ± 0.018a
g_s (mmol m^{-2} s^{-1})	122 ± 7a	164 ± 8b
C_i (μmol mol^{-1})	182.3 ± 4.6a	247 ± 11b
R_d per area (μmol m^{-2} s^{-1})	2.07 ± 0.06b	1.36 ± 0.07b
R_d per dry mass (μmol g^{-1} s^{-1})	0.0436 ± 0.0016a	0.0421 ± 0.0023a
α_{CO2} (mol mol^{-1})	0.0441 ± 0.0026a	0.0338 ± 0.0025b
V_{cmax} per area (μmol m^{-2} s^{-1})	62.1 ± 1.6a	32.7 ± 1.4b
V_{cmax} per dry mass (μmol g^{-1} s^{-1})	1.309 ± 0.038a	1.010 ± 0.043b
J_{max} per area (μmol m^{-2} s^{-1})	120 ± 6a	80 ± 6b
J_{max} per dry mass (μmol g^{-1} s^{-1})	2.04 ± 0.06a	2.19 ± 0.15a
Isoprene emission characteristics		
I per area (nmol m^{-2} s^{-1})	28.8 ± 2.8a	17.8 ± 1.0b
I per dry mass (nmol g^{-1} s^{-1})	0.60 ± 0.05a	0.547 ± 0.027a
C_{DMADP} per area (nmol m^{-2} s^{-1})	1110 ± 90a	650 ± 60b
C_{DMADP} per dry mass (nmol g^{-1} s^{-1})	23.5 ± 2.3a	20.0 ± 1.8a
k (s^{-1})	0.0286 ± 0.0021a	0.0306 ± 0.0023a
V_{max} per area (nmol m^{-2} s^{-1})	79.5 ± 2.9a	48.8 ± 3.0b
V_{max} per dry mass (nmol g^{-1} s^{-1})	1.673 ± 0.037a	1.51 ± 0.11a
K_m per area (nmol m^{-2})	2640 ± 180a	1542 ± 30b
K_m per dry mass (nmol g^{-1})	55.6 ± 4.9a	47.7 ± 1.7a
α_I (mmol mol^{-1})	0.0743 ± 0.0010a	0.0700 ± 0.0010b

The photosynthetic characteristics are: A_n, net assimilation rate; g_s, stomatal conductance to water vapour; C_i, intercellular CO_2 concentration; R_d, dark respiration rate; α_{CO2}, quantum yield of photosynthesis for the incident light; V_{cmax}, apparent (C_i-based) maximum carboxylase activity of Rubisco; J_{max}, apparent (C_i-based) capacity for photosynthetic electron transport. The isoprene emission characteristics are: I, isoprene emission rate; C_{DMADP}, dimethylallyl diphosphate (DMADP) pool size; k, rate constant of isoprene synthase; V_{max}, apparent maximum activity of isoprene synthase; K_m, apparent Michaelis-Menten constant for isoprene synthase; α_I, quantum yield of isoprene emission for the incident light.

All measurements were conducted at 30 °C and saturating light intensity (Q) of 650 μmol m^{-2} s^{-1} was used for all measurements except for the quantum yields. The quantum yields were calculated as the linear slopes of the process rate versus incident Q over the Q range of 20–75 μmol m^{-2} s^{-1} and at the ambient [CO_2] of 360 μmol mol^{-1} and oxygen concentration of 21%. The value of V_{cmax} is reported as an average of V_{cmax} estimates determined from measurements at 21 and 2% O_2. Use of measurements at different O_2 concentrations renders the apparent V_{cmax} estimates less sensitive to Rubisco kinetic characteristics employed in the calculations.

Each value represents the mean ± SE of four measurements in different plants and means with different lowercase letters are statistically different at $P < 0.05$ according to ANOVA.

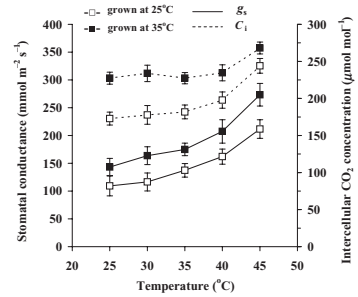

Figure 3. Temperature responses of stomatal conductance to water vapour and intercellular CO_2 concentration in hybrid aspen grown at the contrasting temperature regimes, control (day/night temperature 25/20 °C) and high temperature (35/27 °C). Measurement conditions, data presentation and replicates as in Fig. 2.

control and 4.14 ± 0.29 for the high-temperature treatment. The values of ΔH_A for C_{DMAPD} for the same temperature range were 63 ± 7 kJ mol^{-1} (Q_{10} = 2.31 ± 0.22) for the control and 76 ± 14 kJ mol^{-1} (Q_{10} = 2.9 ± 0.6) for the high temperature treatment ($P > 0.4$ for the difference among the treatments). Thus, the effects of measurement temperature on and growth temperature sensitivity of I and k were larger than those for C_{DMADP}.

The differences among treatments in activation energies for k and I were ultimately associated with greater k and mass-based I values at higher temperatures (Figs 4 & 5). As the result of much lower temperature sensitivity of photosynthesis than isoprene emission, the percentage of photosynthetic carbon lost because of isoprene emission increased with increasing temperature, and this increase was greater for plants grown under the lower temperature (Fig. 6).

Analogously, the temperature sensitivity was greater for the isoprene synthase apparent V_{max} than for the apparent K_m (Fig. 7). The Q_{10} values for V_{max} were 2.65 ± 0.08 for the control and 3.51 ± 0.15 for the high temperature treatment ($P < 0.005$ for difference among treatments), while the corresponding Q_{10} values for K_m were 2.16 ± 0.26 for the control and 2.18 ± 0.46 for the high temperature treatment ($P > 0.9$ for the treatment effect).

DISCUSSION

Modification of leaf structural characteristics and pigment contents by growth temperature

Our study demonstrates that acclimation to high growth temperature led to profound changes in anatomy, morphology and chemistry of hybrid aspen leaves (Fig. 1, Table 1). As an integral change, high temperature-grown leaves were thinner with lower leaf dry mass per unit area (M_A). In addition, high growth temperature led to less densely

© 2014 John Wiley & Sons Ltd,

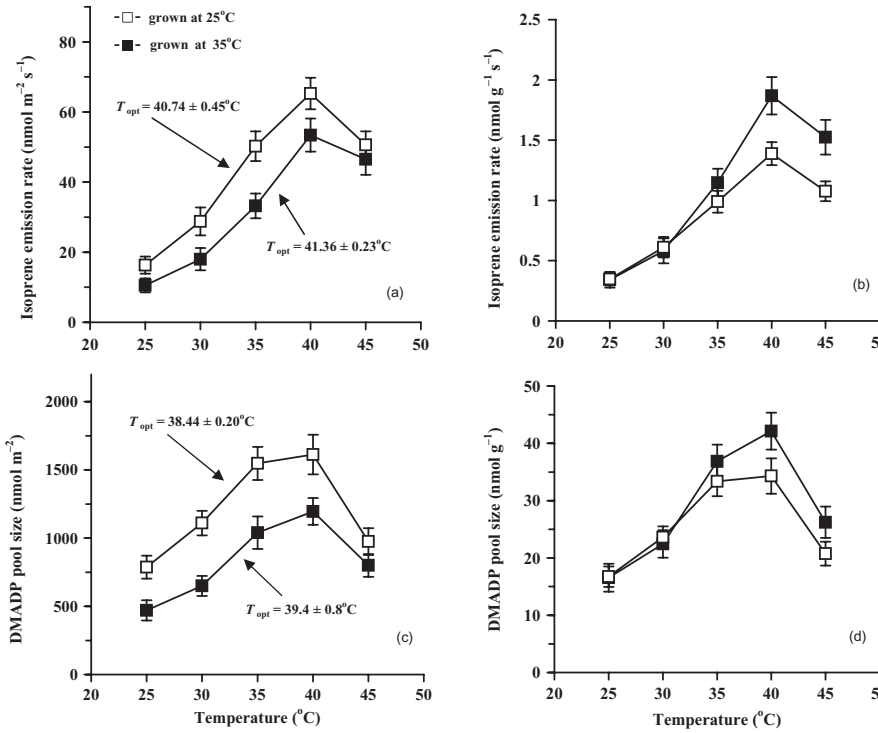

Figure 4. Temperature dependencies of isoprene emission rate (a, b) and the isoprene synthase substrate dimethylallyl diphosphate (DMADP) pool size (c, d) per unit leaf area (a, c) and per unit leaf dry mass (b, d) in hybrid aspen in dependence on growth temperature conditions, control (day/night temperature 25/20 °C) versus high temperature (35/27 °C). Measurement conditions and data presentation as in Fig. 2. The optimum temperatures for isoprene emission and DMADP pool size were not significantly different among the treatments ($P > 0.1$ for both).

packed mesophyll, with fewer mesophyll cells and fewer chloroplasts per unit leaf area (Fig. 1, Table 1). Despite lower number of chloroplasts per unit leaf area, the chloroplasts were smaller and chloroplast number per unit leaf dry mass was greater. These results are in a broad agreement with past studies demonstrating significant modifications in leaf anatomy and chloroplast characteristics (Jin *et al.* 2011), and decreased leaf thickness (Körner *et al.* 1989; Hartikainen *et al.* 2009; Muhl *et al.* 2011) in plants grown in warmer temperatures.

On the other hand, leaf expansion growth was enhanced, resulting in larger leaves (Table 1) and overall greater whole canopy leaf area and mass (data not shown). Such an enhancement of leaf expansion growth is a characteristic response to high growth temperatures in well-watered plants (Wardlaw & Bagnall 1981; Hewitt *et al.* 1985; Granier *et al.* 2000) and might reflect both enhanced light interception and enhanced sink activity, i.e., enhanced consumption of photoassimilates, at high temperatures. In fact, chloroplasts in high temperature-grown leaves were essentially depleted of starch (Table 1, Fig. 1c,d) in agreement with observations in other studies (Buttrose & Hale 1971; Gandin *et al.* 2011). In addition to a reduction of starch content because of enhanced sugar export from chloroplasts, there is also evidence that high temperatures might inhibit gluconeogenesis and increase sucrose synthesis (Ito *et al.* 2009; Yamakawa & Hakata 2010). Soluble sugars importantly enhance the thermotolerance of photosynthetic apparatus (Hüve *et al.* 2006, 2012; Sun *et al.* 2013), and thus, a possible elevation of soluble sugar content can be an important mechanism improving the heat resistance of photosynthesis.

© 2014 John Wiley & Sons Ltd,

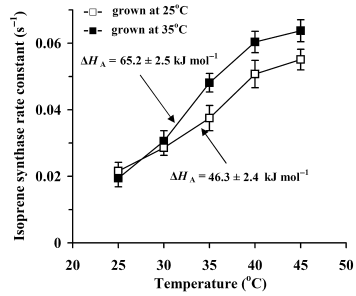

Figure 5. Temperature dependence of the rate constant of isoprene synthase (k) in hybrid aspen grown under control (day/night temperature 25/20 °C) and high temperature (35/27 °C) conditions. The first-order reaction rate constant was estimated as the slope of the linear part of dimethylallyl diphosphate pool size versus isoprene emission rate relationship through the dark decay of isoprene emission and corresponds to the environmental conditions (ambient CO_2 concentration of 360 μmol mol^{-1}, O_2 concentration of 21% and incident quantum flux density of 650 μmol m^{-2} s^{-1}) prior to leaf darkening. The number of replicates and data presentation as in Fig. 2. The activation energies for k (ΔH_a, kJ mol^{-1}, Eqn 3) are also demonstrated ($P < 0.001$ for the difference among the treatments).

Structural control of temperature acclimation of photosynthetic and respiratory characteristics

Our results demonstrate strong reductions in area-based foliage pigment content, biochemical potentials and net assimilation and dark respiration rates in high temperature-grown plants (Tables 1 & 2, Fig. 2). These results are analogous to previous studies demonstrating enhanced photosynthetic rates and greater photosynthetic electron transport and Rubisco carboxylase activity (Huner 1985; Mawson & Cummins 1989; Yamasaki *et al.* 2002; Yamori *et al.* 2005) and greater number and size of mitochondria and increased respiratory activity (Jin *et al.* 2011) per unit leaf area in plants grown at lower temperatures. However, as our study further demonstrates, the mass-based photosynthetic characteristics differed much less among the treatments, indicating that the photosynthetic potentials of single leaf cells were not strongly affected by changes in growth temperature (Table 2, Fig. 2). An increase of M_A with increasing growth light availability is well known (Niinemets & Sack 2006; Niinemets 2007; Niinemets & Anten 2009; Poorter *et al.* 2009), and this increase has been associated with increases in protein content and photosynthetic rate per area (Niinemets & Sack 2006; Niinemets 2007). Our results further underscore the important role of structural controls in temperature acclimation of photosynthesis.

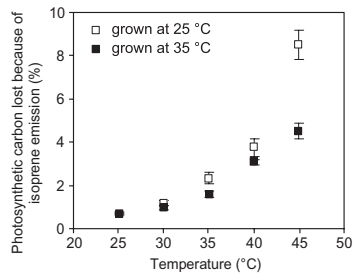

Figure 6. Temperature-dependent changes in the percentage of photosynthetic carbon lost because of isoprene emission in hybrid aspen leaves under control (day/night temperature 25/20 °C) and high temperature (35/27 °C) treatments.

In addition to the rates of photosynthesis, the quantum yield of photosynthesis for an incident light also decreased with increasing irradiance (Table 2) and this reduction was associated with reduced chlorophyll content per area (Table 1) and reduced leaf absorptance as has also been reported in several other studies (Hikosaka *et al.* 1999; Yamori *et al.* 2005). As chlorophyll content per dry mass did not vary with growth temperature (Table 1), modifications in leaf structure were also responsible for the reduction of quantum yields for the incident light in the high temperature-grown plants (Table 2). Despite the modifications in pigment content per unit leaf area were statistically significant, changes in chlorophyll content typically play a much smaller role in whole plant light interception than alterations in total leaf area (Niinemets 2007).

Differently from most of the photosynthetic characteristics, stomatal conductance was strongly enhanced upon growth at high temperatures, leading to enhanced intercellular CO_2 concentration (Fig. 3). In fact, as the maximum carboxylase activity of Rubisco per dry mass was somewhat decreased, enhanced intercellular CO_2 concentration was responsible for similar mass-based net assimilation rates in different temperature treatments. Enhanced stomatal conductance at higher growth temperature can be a structural response associated with greater stomatal size and/or density as reported in some studies (Ghosh *et al.* 1996; Pandey *et al.* 2007) although not always (Crawford *et al.* 2012). Maintenance of high stomatal conductance at higher temperatures clearly plays an important role in convective cooling of leaves (Crawford *et al.* 2012), and also importantly compensates for the reduced biochemical capacity of photosynthetic machinery by increasing the internal CO_2 concentration.

The maximum electron transport rate per dry mass estimated from the net assimilation rates at high CO_2 concentration did not differ among temperature treatments. However, in calculation of the capacity for photosynthetic electron transport rate at high CO_2 concentration, we did not consider the possible limitation of photosynthesis by triose phosphates that can lead to underestimation of the true electron transport capacity (Sharkey 1985). Given the overall strong coordination of Rubisco activity and electron transport

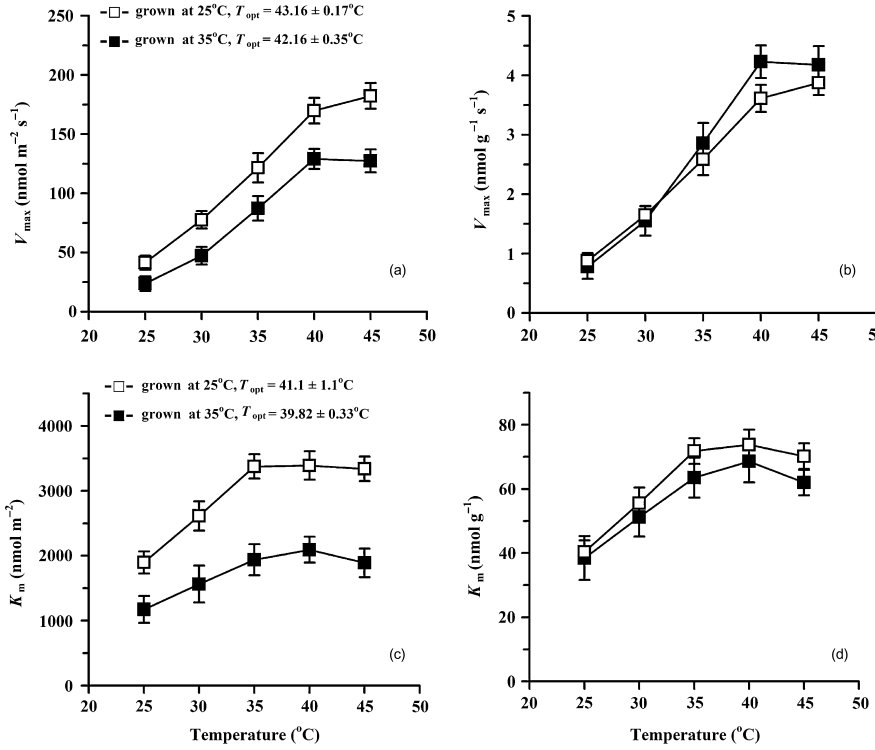

Figure 7. Temperature responses of the apparent maximum capacity, V_{max}, (a, b) and Michaelis-Menten constant K_m (c, d) of isoprene synthase in hybrid aspen grown under control (day/night temperature 25/20 °C) and high temperature (35/27 °C) treatments. Data fitting and presentation as in Fig. 2. The optimum temperatures for V_{max} were significantly different among the treatments ($P < 0.05$), while the optimum temperatures for K_m were not ($P > 0.3$).

capacity, the difference in growth temperature effects on Rubisco carboxylase and electron transport capacities might reflect a stronger feedback inhibition of photosynthesis at higher CO_2 in plants grown at lower temperature (e.g., Pammenter *et al*. 1993 for a discussion). Such a possible feedback limitation of maximum electron transport rate is also supported by reduced use of assimilates in plant growth as indicated by accumulation of starch in lower temperatures.

Effects of growth temperature on temperature responses of photosynthesis and respiration rates

In addition to structural modifications, growth at the higher temperature resulted in significantly improved heat resistance of net assimilation rates as evident in greater activation energies and optimum temperatures (T_{opt}) of net assimilation rates and CO_2-limited electron transport rates (Fig. 2a–d). Such an improved heat resistance is in line with past observations as discussed in the Introduction section and is typically associated with increased lipid saturation in thylakoid membranes (Pearcy 1978; Raison 1986; Kunst *et al*. 1989; Mawson & Cummins 1989; Shanklin & Cahoon 1998), and can also reflect increased leaf sugar contents as discussed above. In addition, increases in T_{opt} of photosynthesis can partly reflect increased stomatal conductance that reduces the rate of photorespiration at any given temperature and thereby shifts the optimum temperature to higher temperatures (Leegood 1995; Medlyn *et al*. 2002).

© 2014 John Wiley & Sons Ltd,

Past studies have indicated that the activation energy for the dark respiration often decreases upon growth at higher temperatures (Atkin & Tjoelker 2003; Atkin *et al*. 2005). However, there was no evidence of changes in the shape of dark respiration versus temperature response curve in our study (Fig. 2e,f) suggesting either that the mitochondrial capacity for respiration was unaffected by high growth temperature or that changes in the capacity were obscured by alterations in respiratory substrate availability. The latter possibility is plausible given the altered sink/source relations in plants grown at different temperatures.

Isoprene emission characteristics in relation to growth temperature

As with the area-based photosynthetic characteristics, isoprene emission rate, DMADP pool size (Table 2, Fig. 4) and apparent maximum rate and K_m for isoprene synthase at 30 °C (Table 2, Fig. 7) were greater in low temperature-grown plants. However, none of these characteristics was affected by growth temperature when expressed on a leaf dry mass basis (Figs 4 & 7 and Table 2), indicating that differences in area-based isoprene emission characteristics were primarily driven by leaf structural modifications. Furthermore, the rate constant of isoprene synthase (Fig. 5) and the fraction of carbon lost because of isoprene emission (Fig. 6) also did not depend on growth temperature at the measurement temperature of 30 °C, further indicating that isoprene emission scaled to DMADP pool size and net assimilation rate similarly in both temperature treatments. Contrasting growth temperature effects on the area-based isoprene emission rates have been observed across the studies (see Introduction section), and we argue that these contrasting effects primarily result from study-to-study differences in leaf morphological response to growth temperature. We also emphasize that the effects of longer-term temperature on isoprene emission characteristics can be different for transfer experiments where leaves developed at a given temperature are transferred to another temperature. In these experiments, any acclimation to changed conditions is primarily biochemical and physiological (Geron *et al*. 2000; Mayrhofer *et al*. 2005; Wiberley *et al*. 2008; Sun *et al*. 2012a).

Temperature response of isoprene emission characteristics

As demonstrated previously (Rasulov *et al*. 2010; Li *et al*. 2011), the optimum temperature for isoprene emission (Fig. 4a,b) is co-determined by the temperature effects on the DMADP pool size (Fig. 4c,d) and on the isoprene synthase rate constant (Fig. 5). Thus, the key issue is how the share of different controls is affected by acclimation to different growth temperatures. Our data do demonstrate that the DMADP pool size starts to decrease earlier with increasing temperature (Fig. 4c,d) than the isoprene synthase rate constant or V_{max} of isoprene synthase (Fig. 7a,b). Furthermore, our data demonstrate that K_m of isoprene synthase increases with increasing temperature, indicating that progressively higher DMADP pools are needed to reach a given value of isoprene emission rate (Fig. 7c,d). Such a temperature-dependent increase of K_m is characteristic for many enzymes and indicates weaker associations in the enzyme-substrate complex at higher temperature (Hajdu *et al*. 2009).

Despite the similarity of mass-based isoprene emission characteristics at 30 °C (Table 2), and similarly high optimum temperatures for isoprene emission between 40 and 41 °C (Fig. 4a,b), a number of important differences were observed among the growth temperature treatments in responses of isoprene emission characteristics to higher temperatures (Figs 4–7). In low temperature-grown plants, the activation energies were almost identical to those observed in hybrid aspen grown in similar conditions (Rasulov *et al*. 2010). However, in the current study, the activation energy for isoprene emission was greater in leaves grown at greater temperature, and this was associated with greater mass-based emission rates at higher temperatures (Fig. 4b). These effects resulted from a greater activation energy for isoprene synthase rate constant (Fig. 5), while the activation energy for DMADP pool size did not differ among the treatments, suggesting that the rate of substrate production was not affected by growth temperature. This seems surprising given the improved heat tolerance of photosynthetic apparatus in high temperature-grown plants (Fig. 2). In fact, plants grown at the lower temperature used a greater fraction of photosynthetic carbon for isoprene emission at higher temperatures (Fig. 6). It is plausible that in high temperature-grown plants with a greater growth rate and reduced sink limitation of photosynthesis, alternative pathways for DMADP consumption in synthesis of higher molecular mass isoprenoids (Rasulov *et al.* 2014 for a discussion) were also more strongly activated such that the availability for DMADP for isoprene synthesis was ultimately similar for both treatments.

As isoprene synthase activity is affected by pH and cellular ionic medium characteristics (Sasaki *et al*. 2005; Köksal *et al*. 2010), possible growth temperature effects on subcellular environment might also play a role in the observed patterns. Thus, differences in the isoprene synthase rate constant (Fig. 5) and V_{max} (Fig. 7a,b) might reflect changes in chloroplastic conditions in plants grown at different temperatures. Such changes are likely given that heat stress gradually leads to leakiness of chloroplast membranes and reduced proton gradient (Schrader *et al*. 2004; Zhang & Sharkey 2009) bringing pH in actively photosynthesizing chloroplasts (ca. 7.8–8) closer to the cytosolic values (6–6.5). Given that the pH optimum for isoprene is ca. 8, such a reduction of pH would importantly affect the rate of isoprene synthesis, especially in low temperature-grown plants with lower heat resistance of membranes.

Apart from subcellular effects, *Populus* has multiple isoprene synthase genes (Vickers *et al*. 2010) and expression of a more heat-resistant isoprene synthase might provide a complementary explanation for improved temperature kinetics. However, so far there is no evidence of differences in heat resistance of different isoprene synthase isoforms as well as on the regulation of expression of different isoforms

by growth temperature. Finally, smaller chloroplasts (Table 1) with almost missing starch grains might also mean reduced diffusive limitations between the sites of DMADP synthesis and isoprene synthase. Overall, these results are consistent with improved heat stability of isoprene synthesis in high temperature acclimated leaves, but do not support the suggestion of a greater requirement for isoprene synthesis to cope with sustained high temperatures.

CONCLUSIONS

Our study demonstrates that increases in growth temperature resulted in major changes in leaf anatomy and morphology and that these structural modifications mainly drove the treatment effects on foliage photosynthetic and isoprene emission characteristics expressed per unit leaf area. While structural acclimation to growth light regime is well recognized (Niinemets & Anten 2009; Poorter *et al*. 2009), temperature acclimation studies do not routinely address growth temperature effects on leaf structure. As our study demonstrates, consideration of structural effects clearly provides insight into the mechanisms of temperature-driven photosynthetic acclimation. In fact, structural changes might explain the study-to-study differences in growth temperature effects on foliage area-based physiological characteristics that have been difficult to explain so far.

Higher growth temperature also enhanced the heat stability of photosynthetic characteristics, but had surprisingly minor effects on the heat stability of isoprene emission traits. As noted in the Introduction section, there are important study-to-study differences in the effects of growth temperature on the shape of the temperature response of isoprene emission (Monson *et al*. 1992; Fares *et al*. 2011). We argue that such contrasting effects most likely result from differences in how growth temperature affects the isoprene precursor DMADP pool size. In our study, where a higher growth temperature was associated with enhanced sink activity, growth temperature effects on DMADP pool size were minor. However, much stronger pathway up-regulation may occur when primary metabolism is curbed by limited sink activity (Harding *et al*. 1990; Starck *et al*. 1993). Although our study demonstrated that growth temperature might also affect the isoprene synthase characteristics, we argue that the overall pathway flux can be potentially more strongly affected by DMADP pool size and isoprene synthase expression (Rasulov *et al*. 2009b, 2010; Li *et al*. 2011; Li & Sharkey 2013). We conclude that analyses of temperature acclimation of photosynthesis and isoprene emission should consider both structural and physiological adjustments and that more experimental studies are needed to gain insight into the effects of sink strength on expression of isoprenoid synthesis pathway.

ACKNOWLEDGMENTS

Funding for this research was provided by the Estonian Ministry of Science and Education (institutional grant IUT-8-3), the Estonian Science Foundation (grant 9253), the European Commission through the European Regional Fund (the Center of Excellence in Environmental Adaptation) and the European Research Council (advanced grant 322603, SIP-VOL+).

REFERENCES

Arneth A., Monson R.K., Schurgers G., Niinemets Ü. & Palmer P.I. (2008) Why are estimates of global isoprene emissions so similar (and why is this not so for monoterpenes)? *Atmospheric Chemistry and Physics* **8,** 4605–4620.

Ashworth K., Boissard C., Folberth G., Lathière J. & Schurgers G. (2013) Global modeling of volatile organic compound emissions. In *Biology, Controls and Models of Tree Volatile Organic Compound Emissions* (eds Ü. Niinemets & R.K. Monson), pp. 451–487. Springer, Berlin, Germany.

Atkin O.K. & Tjoelker M.G. (2003) Thermal acclimation and the dynamic response of plant respiration to temperature. *Trends in Plant Science* **8,** 343–351.

Atkin O.K., Bruhn D., Hurry V.M. & Tjoelker M. (2005) The hot and the cold: unravelling the variable response of plant respiration to temperature. Evans review no. 2. *Functional Plant Biology* **32,** 87–105.

Behnke K., Ehlting B., Teuber M., Bauerfeind M., Louis S., Hänsch R., . . . Schnitzler J.-P. (2007) Transgenic, non-isoprene emitting poplars don't like it hot. *The Plant Journal* **51,** 485–499.

Behnke K., Ghirardo A., Janz D., Kanawati B., Esperschütz J., Zimmer I., . . . Rosenkranz M. (2013) Isoprene function in two contrasting poplars under salt and sunflecks. *Tree Physiology* **33,** 562–578.

Berry J. & Björkman O. (1980) Photosynthetic response and adaptation to temperature in higher plants. *Annual Review of Plant Physiology* **31,** 491–543.

Björkman O., Badger M.R. & Armond P.A. (1980) Response and adaptation of photosynthesis to high temperatures. In *Adaptation of Plants to Water and High Temperature Stress* (eds N.C. Turner & P.J. Kramer), pp. 233–249. John Wiley & Sons, New York – Chichester – Brisbane – Toronto.

Brüggemann N. & Schnitzler J.-P. (2002) Relationship of isopentenyl diphosphate (IDP) isomerase activity to isoprene emission of oak leaves. *Tree Physiology* **22,** 1011–1018.

Bunce J.A. (2000) Acclimation of photosynthesis to temperature in eight cool and warm climate herbaceous C_3 species: temperature dependence of parameters of a biochemical photosynthesis model. *Photosynthesis Research* **63,** 59–67.

Burns W.A. (1978) Thick sections: technique and applications. In *Diagnostic Electron Microscopy* (eds B.F. Trump & R.J. Jones), pp. 146–161. Wiley, New York, NY, USA.

Buttrose M.S. & Hale C.R. (1971) Effects of temperature on accumulation of starch or lipid in chloroplasts of grapevine. *Planta* **101,** 166–170.

von Caemmerer S. & Farquhar G.D. (1981) Some relationships between the biochemistry of photosynthesis and the gas exchange of leaves. *Planta* **153,** 376–387.

Centritto M., Brilli F., Fodale R. & Loreto F. (2011) Different sensitivity of isoprene emission, respiration and photosynthesis to high growth temperature coupled with drought stress in black poplar (*Populus nigra*) saplings. *Tree Physiology* **31,** 275–286.

Ciais P., Friedlingstein P., Friend A. & Schimel D.S. (2001) Integrating global models of terrestrial primary productivity. In *Terrestrial Global Productivity* (eds H.A. Mooney, B. Saugier & J. Roy), pp. 449–478. Academic Press, Inc, San Diego, CA, USA.

Copolovici L., Kännaste A., Remmel T., Vislap V. & Niinemets Ü. (2011) Volatile emissions from *Alnus glutinosa* induced by herbivory are quantitatively related to the extent of damage. *Journal of Chemical Ecology* **37,** 18–28.

Crawford A.J., McLachlan D.H., Hetherington A.M. & Franklin K.A. (2012) High temperature exposure increases plant cooling capacity. *Current Biology* **22,** R396–R397.

Devos N., Ingouff M., Loppes R. & Matagne R.F. (1998) Rubisco adaptation to low temperatures: a comparative study in psychrophilic and mesophilic unicellular algae. *Journal of Phycology* **34,** 655–660.

Fares S., Mahmood T., Liu S., Loreto F. & Centritto M. (2011) Influence of growth temperature and measuring temperature on isoprene emission, diffusive limitations of photosynthesis and respiration in hybrid poplars. *Atmospheric Environment* **45,** 155–161.

© 2014 John Wiley & Sons Ltd,

Funk J.L., Jones C.G., Baker C.J., Fuller H.M., Giardina C.P. & Lerdau M.T. (2003) Diurnal variation in the basal emission rate of isoprene. *Ecological Applications* **13,** 269–278.

Gandin A., Gutjahr S., Dizengremel P. & Lapointe L. (2011) Source-sink imbalance increases with growth temperature in the spring geophyte *Erythronium americanum*. *Journal of Experimental Botany* **62,** 3467–3479.

Geron C., Guenther A., Sharkey T. & Arnts R.R. (2000) Temporal variability in basal isoprene emission factor. *Tree Physiology* **20,** 799–805.

Ghosh A.K., Ichii M., Asanuma K. & Kusutani A. (1996) Optimum and sub-optimal temperature effects on stomata and photosynthesis rate of determinate soybeans. *Acta Horticulturae* **440,** 81–86.

Granier C., Turc O. & Tardieu F. (2000) Co-ordination of cell division and tissue expansion in sunflower, tobacco, and pea leaves: dependence or independence of both processes? *Journal of Plant Growth Regulation* **19,** 45–54.

Guenther A.B., Zimmerman P.R., Harley P.C., Monson R.K. & Fall R. (1993) Isoprene and monoterpene emission rate variability: model evaluations and sensitivity analyses. *Journal of Geophysical Research* **98,** 12609–12617.

Guenther A.B., Jiang X., Heald C.L., Sakulyanontvittaya T., Duhl T., Emmons L.K. & Wang X. (2012) The Model of Emissions of Gases and Aerosols from Nature version 2.1 (MEGAN2.1): an extended and updated framework for modeling biogenic emissions. *Geoscientific Model Development* **5,** 1471–1492.

Hajdu I., Szilagyi A., Kardos J. & Zavodszky P. (2009) A link between hinge-bending domain motions and the temperature dependence of catalysis in 3-isopropylmalate dehydrogenase. *Biophysical Journal* **96,** 5003–5012.

Harding S.A., Guikema J.A. & Paulsen G.M. (1990) Photosynthetic decline from high temperature stress during maturation of wheat. II. Interaction with source and sink processes. *Plant Physiology* **92,** 654–658.

Hartikainen K., Nerg A.-M., Kivimäenpää M., Kontunen-Soppela S., Mäenpää M., Oksanen E., . . . Holopainen T. (2009) Emissions of volatile organic compounds and leaf structural characteristics of European aspen (*Populus tremula*) grown under elevated ozone and temperature. *Tree Physiology* **29,** 1163–1173.

Hewitt J.D., Casey L.L. & Zobel R.W. (1985) Effect of day length and night temperature on starch accumulation and degradation in soybean. *Annals of Botany* **56,** 513–522.

Hikosaka K. (1997) Modelling optimal temperature acclimation of the photosynthetic apparatus in C_3 plants with respect to nitrogen use. *Annals of Botany* **80,** 721–730.

Hikosaka K., Murakami A. & Hirose T. (1999) Balancing carboxylation and regeneration of ribulose-1,5-bisphosphate in leaf photosynthesis: temperature acclimation of an evergreen tree, *Quercus myrsinaefolia*. *Plant, Cell & Environment* **22,** 841–849.

Hopkins W.G. (1998) *Introduction to Plant Physiology*, 2nd edn, John Wiley, New York, NY, USA.

Huner N.P.A. (1985) Acclimation of winter rye to cold hardening temperatures results in an increased capacity for photosynthetic electron transport. *Canadian Journal of Botany* **63,** 506–511.

Hüve K., Bichele I., Tobias M. & Niinemets Ü. (2006) Heat sensitivity of photosynthetic electron transport varies during the day due to changes in sugars and osmotic potential. *Plant, Cell & Environment* **29,** 212–228.

Hüve K., Bichele I., Ivanova H., Keerberg O., Pärnik T., Rasulov B., . . . Niinemets Ü. (2012) Temperature responses of dark respiration in relation to leaf sugar concentration. *Physiologia Plantarum* **144,** 320–334.

Ibrahim M.A., Mäenpää M., Hassinen V., Kontunen-Soppela S., Malec L., Rousi M., . . . Oksanen E.J. (2010) Elevation of night-time temperature increases terpenoid emissions from *Betula pendula* and *Populus tremula*. *Journal of Experimental Botany* **61,** 1583–1595.

Ito S., Hara T., Kawanami Y., Watanabe T., Thiraporn K., Ohtake N., . . . Ohyama T. (2009) Carbon and nitrogen transport during grain filling in rice under high-temperature conditions. *Journal of Agronomy and Crop Science* **195,** 368–376.

Jin B., Wang L., Wang J., Jiang K.Z., Wang Y., Jiang X.X., . . . Teng N.J. (2011) The effect of experimental warming on leaf functional traits, leaf structure and leaf biochemistry in *Arabidopsis thaliana*. *BMC Plant Biology* **11,** 35.

Köksal M., Zimmer I., Schnitzler J.-P. & Christianson D.W. (2010) Structure of isoprene synthase illuminates the chemical mechanism of teragram atmospheric carbon emission. *Journal of Molecular Biology* **402,** 363–373.

Körner C., Neumayer M., Pelaez Menendez-Riedl S. & Smeets-Scheel A. (1989) Functional morphology of mountain plants. *Flora* **182,** 353–383.

Kunst L., Browse J. & Somerville C. (1989) A mutant of *Arabidopsis* deficient in desaturation of palmitic acid in leaf lipids. *Plant Physiology* **90,** 943–947.

Laisk A., Oja V., Rasulov B., Rämma H., Eichelmann H., Kasparova I., . . . Vapaavuori E. (2002) A computer-operated routine of gas exchange and optical measurements to diagnose photosynthetic apparatus in leaves. *Plant, Cell & Environment* **25,** 923–943.

Leegood R.C. (1995) Effects of temperature on photosynthesis and photorespiration. In *Environment and Plant Metabolism: Flexibility and Acclimation* (ed. N. Smirnoff), pp. 45–62. Bios Scientific Publishers Ltd., Oxford, UK.

Li Z. & Sharkey T.D. (2013) Molecular and pathway controls on biogenic volatile organic compound emissions. In *Biology, Controls and Models of Tree Volatile Organic Compound Emissions* (eds Ü. Niinemets & R.K. Monson), pp. 119–151. Springer, Berlin, Germany.

Li Z., Ratliff E.A. & Sharkey T.D. (2011) Effect of temperature on postillumination isoprene emission in oak and poplar. *Plant Physiology* **155,** 1037–1046.

Lichtenthaler H.K. & Buschmann C. (2001) Chlorophylls and carotenoids: measurement and characterisation by UV-VIS. In *Current Protocols in Food Analytical Chemistry* (eds R.E. Wrolstad, T.E. Acree, E.A. Decker, M.H. Penner, D.S. Reid, S.J. Schwartz, . . . P. Sporns), pp. F4.3.1–F4.3.8. John Wiley & Sons, Madison, WI, USA.

Loreto F., Pinelli P., Brancaleoni E. & Ciccioli P. (2004) ^{13}C labelling reveals chloroplastic and extra-chloroplastic pools of dimethylallyl pyrophosphate and their contribution to isoprene formation. *Plant Physiology* **135,** 1903–1907.

Loveys B.R., Atkinson L.J., Sherlock D.J., Roberts R.L., Fitter A.H. & Atkin O.K. (2003) Thermal acclimation of leaf and root respiration: an investigation comparing inherently fast- and slow-growing plant species. *Global Change Biology* **9,** 895–910.

Mahecha M.D., Reichstein M., Carvalhais N., Lasslop G., Lange H., Seneviratne S.I., . . . Richardson A.D. (2010) Global convergence in the temperature sensitivity of respiration at ecosystem level. *Science* **329,** 838–840.

Mawson B.T. & Cummins W.R. (1989) Thermal acclimation of photosynthetic electron transport activity by thylakoids of *Saxifraga cernua*. *Plant Physiology* **89,** 325–332.

Mayrhofer S., Teuber M., Zimmer I., Louis S., Fischbach R.J. & Schnitzler J.-P. (2005) Diurnal and seasonal variation of isoprene biosynthesis-related genes in grey poplar leaves. *Plant Physiology* **139,** 474–484.

Medlyn B.E., Dreyer E., Ellsworth D., Forstreuter M., Harley P.C., Kirschbaum M.U.F., . . . Loustau D. (2002) Temperature response of parameters of a biochemically based model of photosynthesis. II. A review of experimental data. *Plant, Cell & Environment* **25,** 1167–1179.

Mercer E.H. (1963) A scheme for section staining in electron microscopy. *Journal of the Royal Microscopical Society* **81,** 179–186.

Monson R.K., Jaeger C.H., Adams W.W. III, Driggers E.M., Silver G.M. & Fall R. (1992) Relationships among isoprene emission rate, photosynthesis, and isoprene synthase activity as influenced by temperature. *Plant Physiology* **98,** 1175–1180.

Morcuende R., Pérez P., Martínez-Carrasco R., Martín del Molino I. & Sanchez de la Puente L. (1996) Long- and short-term responses of leaf carbohydrate levels and photosynthesis to decreased sink demand in soybean. *Plant, Cell & Environment* **19,** 976–982.

Muhl Q.E., Du Toit E.S. & Robbertse P.J. (2011) Leaf adaptation to temperature regimes in *Moringa oleifera* (horseradish tree). *International Journal of Agriculture and Biology* **13,** 1021–1024.

Niinemets Ü. (2007) Photosynthesis and resource distribution through plant canopies. *Plant, Cell & Environment* **30,** 1052–1071.

Niinemets Ü. & Anten N.P.R. (2009) Packing the photosynthesis machinery: from leaf to canopy. In *Photosynthesis in Silico: Understanding Complexity from Molecules to Ecosystems* (eds A. Laisk, L. Nedbal & Govindjee), pp. 363–399. Springer Verlag, Berlin, Germany.

Niinemets Ü. & Sack L. (2006) Structural determinants of leaf light-harvesting capacity and photosynthetic potentials. In *Progress in Botany* (eds K. Esser, U.E. Lüttge, W. Beyschlag & J. Murata), pp. 385–419. Springer Verlag, Berlin, Germany.

Niinemets Ü., Oja V. & Kull O. (1999a) Shape of leaf photosynthetic electron transport versus temperature response curve is not constant along canopy light gradients in temperate deciduous trees. *Plant, Cell & Environment* **22,** 1497–1514.

Niinemets Ü., Tenhunen J.D., Canta N.R., Chaves M.M., Faria T., Pereira J.S. & Reynolds J.F. (1999b) Interactive effects of nitrogen and phosphorus on the

acclimation potential of foliage photosynthetic properties of cork oak, *Quercus suber*, to elevated atmospheric CO_2 concentrations. *Global Change Biology* **5,** 455–470.

Niinemets Ü., Tenhunen J.D., Harley P.C. & Steinbrecher R. (1999c) A model of isoprene emission based on energetic requirements for isoprene synthesis and leaf photosynthetic properties for *Liquidambar* and *Quercus*. *Plant, Cell & Environment* **22,** 1319–1336.

Niinemets Ü., Wright I.J. & Evans J.R. (2009) Leaf mesophyll diffusion conductance in 35 Australian sclerophylls covering a broad range of foliage structural and physiological variation. *Journal of Experimental Botany* **60,** 2433–2449.

Ow L.F., Griffin K.L., Whitehead D., Walcroft A.S. & Turnbull M.H. (2008) Thermal acclimation of leaf respiration but not photosynthesis in *Populus deltoides* x *nigra*. *The New Phytologist* **178,** 123–134.

Pammenter N.W., Loreto F. & Sharkey T.D. (1993) End product feedback effects on photosynthetic electron transport. *Photosynthesis Research* **35,** 5–14.

Pandey R., Chacko P.M., Choudhary M.L., Prasad K.V. & Pal M. (2007) Higher than optimum temperature under CO_2 enrichment influences stomata anatomical characters in rose (*Rosa hybrida*). *Scientia Horticulturae* **113,** 74–81.

Pearcy R.W. (1978) Effect of growth temperature on the fatty acid composition of the leaf lipids in *Atriplex lentiformis* (Torr.) Wats. *Plant Physiology* **61,** 484–486.

Poorter H., Niinemets Ü., Poorter L., Wright I.J. & Villar R. (2009) Causes and consequences of variation in leaf mass per area (LMA): a meta-analysis. *The New Phytologist* **182,** 565–588.

Possell M. & Loreto F. (2013) The role of volatile organic compounds in plant resistance to abiotic stresses: responses and mechanisms. In *Biology, Controls and Models of Tree Volatile Organic Compound Emissions* (eds Ü. Niinemets & R.K. Monson), pp. 209–235. Springer, Berlin, Germany.

Raison J.K. (1986) Alterations in the physical properties and thermal response of membrane lipids: correlations with acclimation to chilly and high temperature. In *Frontiers of Membrane Research in Agriculture* (eds J.B. St. John, E. Berlin & P.C. Jackson), pp. 383–401. Rowman and Allanheld, Totoma, NJ, USA.

Ramos-Valdivia A.C., Heijden R. & Verpoorte R. (1997) Isopentenyl diphosphate isomerase: a core enzyme in isoprenoid biosynthesis. A review of its biochemistry and function. *Natural Product Reports* **14,** 591–603.

Rasulov B., Copolovici L., Laisk A. & Niinemets Ü. (2009a) Postillumination isoprene emission: in vivo measurements of dimethylallyldiphosphate pool size and isoprene synthase kinetics in aspen leaves. *Plant Physiology* **149,** 1609–1618.

Rasulov B., Hüve K., Välbe M., Laisk A. & Niinemets Ü. (2009b) Evidence that light, carbon dioxide and oxygen dependencies of leaf isoprene emission are driven by energy status in hybrid aspen. *Plant Physiology* **151,** 448–460.

Rasulov B., Hüve K., Bichele I., Laisk A. & Niinemets Ü. (2010) Temperature response of isoprene emission in vivo reflects a combined effect of substrate limitations and isoprene synthase activity: a kinetic analysis. *Plant Physiology* **154,** 1558–1570.

Rasulov B., Hüve K., Laisk A. & Niinemets Ü. (2011) Induction of a longer-term component of isoprene release in darkened aspen leaves: origin and regulation under different environmental conditions. *Plant Physiology* **156,** 816–831.

Rasulov B., Bichele I., Laisk A. & Niinemets Ü. (2014) Competition between isoprene emission and pigment synthesis during leaf development in aspen. *Plant, Cell & Environment* **37,** 724–741.

Sage R.F. & Kubien D.S. (2007) The temperature response of C_3 and C_4 photosynthesis. *Plant, Cell & Environment* **30,** 1086–1106.

Sasaki K., Ohara K. & Yazaki K. (2005) Gene expression and characterization of isoprene synthase from *Populus alba*. *FEBS Letters* **579,** 2514–2518.

Schrader S.M., Wise R.R., Wacholtz W.F., Ort D.R. & Sharkey T.D. (2004) Thylakoid membrane responses to moderately high leaf temperature in Pima cotton. *Plant, Cell & Environment* **27,** 725–735.

Schreiber U., Bilger W. & Neubauer C. (1994) Chlorophyll fluorescence as a nonintrusive indicator for rapid assessment of in vivo photosynthesis. In *Ecophysiology of Photosynthesis* (eds E.-D. Schulze & M.M. Caldwell), pp. 49–70. Springer Verlag, Berlin – Heidelberg – New York – London – Paris – Tokyo – Hong Kong – Barcelona – Budapest.

Shanklin J. & Cahoon E.B. (1998) Desaturation and related modifications of fatty acids. *Annual Review of Plant Physiology and Plant Molecular Biology* **49,** 611–641.

Sharkey T.D. (1985) Photosynthesis in intact leaves of C_3 plants: physics, physiology and rate limitations. *The Botanical Review* **51,** 53–105.

Sharkey T.D. & Yeh S.S. (2001) Isoprene emission from plants. *Annual Review of Plant Physiology and Plant Molecular Biology* **52,** 407–436.

Sharkey T.D., Singsaas E.L., Lerdau M.T. & Geron C.D. (1999) Weather effects on isoprene emission capacity and applications in emissions algorithms. *Ecological Applications* **9,** 1132–1137.

Sharkey T.D., Badger M.R., von Caemmerer S. & Andrews T.J. (2001) Increased heat sensitivity of photosynthesis in tobacco plants with reduced Rubisco activase. *Photosynthesis Research* **67,** 147–156.

Singsaas E.L. & Sharkey T.D. (2000) The effects of high temperature on isoprene synthesis in oak leaves. *Plant, Cell & Environment* **23,** 751–757.

Smith N.G. & Dukes J.S. (2013) Plant respiration and photosynthesis in global-scale models: incorporating acclimation to temperature and CO_2. *Global Change Biology* **19,** 45–63.

Starck Z., Wazynska Z. & Kucewicz O. (1993) Comparative effects of heat stress on photosynthesis and chloroplast ultrastructure in tomato plants with source-sink modulated by growth regulators. *Acta Physiologiae Plantarum* **15,** 125–133.

Stitt M. & Hurry V.M. (2002) A plant for all seasons: alteration in photosynthetic carbon metabolism during cold acclimation in *Arabidopsis*. *Current Opinion in Plant Biology* **5,** 199–206.

Sun Z., Copolovici L. & Niinemets Ü. (2012a) Can the capacity for isoprene emissions acclimate to environmental modifications during autumn senescence in temperate deciduous tree species *Populus tremula*? *Journal of Plant Research* **125,** 263–274.

Sun Z., Niinemets Ü., Hüve K., Noe S.M., Rasulov B., Copolovici L. & Vislap V. (2012b) Enhanced isoprene emission capacity and altered light responsiveness in aspen grown under elevated atmospheric CO_2 concentration. *Global Change Biology* **18,** 3423–3440.

Sun Z., Hüve K., Vislap V. & Niinemets Ü. (2013) Elevated [CO_2] magnifies isoprene emissions under heat and improves thermal resistance in hybrid aspen. *Journal of Experimental Botany* **64,** 5509–5523.

Tjoelker M.G., Oleksyn J. & Reich P.B. (1999) Acclimation of respiration to temperature and CO_2 in seedlings of boreal tree species in relation to plant size and relative growth rate. *Global Change Biology* **5,** 679–691.

Turnbull M.H., Murthy R. & Griffin K.L. (2002) The relative impacts of daytime and night-time warming on photosynthetic capacity in *Populus deltoides*. *Plant, Cell & Environment* **25,** 1729–1737.

Velikova V., Várkonyi Z., Szabó M., Maslenkova L., Nogues I., Kovács L., . . . Loreto F. (2011) Increased thermostability of thylakoid membranes in isoprene-emitting leaves probed with three biophysical techniques. *Plant Physiology* **157,** 905–916.

Velikova V., Sharkey T.D. & Loreto F. (2012) Stabilization of thylakoid membranes in isoprene-emitting plants reduces formation of reactive oxygen species. *Plant Signaling & Behavior* **7,** 139–141.

Vickers C.E., Gershenzon J., Lerdau M.T. & Loreto F. (2009) A unified mechanism of action for volatile isoprenoids in plant abiotic stress. *Nature Chemical Biology* **5,** 283–291.

Vickers C.E., Possell M., Hewitt C.N. & Mullineaux P.M. (2010) Genetic structure and regulation of isoprene synthase in poplar (*Populus* spp.). *Plant Molecular Biology* **73,** 547–558.

Wardlaw I.F. & Bagnall D. (1981) Phloem transport and the regulation of growth of *Sorghum bicolor* (Moench) at low temperature. *Plant Physiology* **68,** 411–414.

Way D.A. & Oren R. (2010) Differential responses to changes in growth temperature between trees from different functional groups and biomes: a review and synthesis of data. *Tree Physiology* **30,** 669–688.

Way D.A. & Yamori W. (2014) Thermal acclimation of photosynthesis: on the importance of adjusting our definitions and accounting for thermal acclimation of respiration. *Photosynthesis Research* **119,** 89–100.

Way D.A., Schnitzler J.-P., Monson R.K. & Jackson R.B. (2011) Enhanced isoprene-related tolerance of heat- and light-stressed photosynthesis at low, but not high, CO_2 concentrations. *Oecologia* **166,** 273–282.

Weise S.E., Li Z., Sutter A.E., Corrion A., Banerjee A. & Sharkey T.D. (2013) Measuring dimethylallyl diphosphate available for isoprene synthesis. *Analytical Biochemistry* **435,** 27–34.

Wiberley A.E., Donohue A.R., Meier M.E., Westphal M.M. & Sharkey T.D. (2008) Regulation of isoprene emission in *Populus trichocarpa* leaves subjected to changing growth temperature. *Plant, Cell & Environment* **31,** 258–267.

Wiberley A.E., Donohue A.R., Westphal M.M. & Sharkey T.D. (2009) Regulation of isoprene emission from poplar leaves throughout a day. *Plant, Cell & Environment* **32,** 939–947.

Xu C.-Y., Salih A., Ghannoum O. & Tissue D.T. (2012) Leaf structural characteristics are less important than leaf chemical properties in determining the response of leaf mass per area and photosynthesis of *Eucalyptus saligna* to industrial-age changes in [CO_2] and temperature. *Journal of Experimental Botany* **63,** 5829–5841.

Yamakawa H. & Hakata M. (2010) Atlas of rice grain filling-related metabolism under high temperature: joint analysis of metabolome and transcriptome demonstrated inhibition of starch accumulation and induction of amino acid accumulation. *Plant and Cell Physiology* **51,** 795–809.

Yamasaki T., Yamakawa T., Yamane Y., Koike H., Satoh K. & Katoh S. (2002) Temperature acclimation of photosynthesis and related changes in photosystem II electron transport in winter wheat. *Plant Physiology* **128,** 1087–1097.

Yamori W., Noguchi K. & Terashima I. (2005) Temperature acclimation of photosynthesis in spinach leaves: analyses of photosynthetic components and temperature dependencies of photosynthetic partial reactions. *Plant, Cell & Environment* **28,** 536–547.

Zhang R. & Sharkey T.D. (2009) Photosynthetic electron transport and proton flux under moderate heat stress. *Photosynthesis Research* **100,** 29–43.

Zhou C., Li Z., Wiberley-Bradford A.E., Weise S.E. & Sharkey T.D. (2013) Isopentenyl diphosphate and dimethylallyl diphosphate ratio measured with recombinant isopentenyl diphosphate isomerase and isoprene synthase. *Analytical Biochemistry* **440,** 130–136.

Received 27 June 2014; received in revised form 13 August 2014; accepted for publication 14 August 2014

CURRICULUM VITAE

Name: Vivian
Surname: Kuusk (until 2015 Vislap)
Date of birth: 23.08.1976
Employment: Estonian University of Life Sciences
Position: specialist

Education:

2007-2024	PhD studies in Agronomy, Estonian University of Life Sciences
1999 - 2002	MsSci Estonian University of Life Sciences
1994 - 1998	BSc studies in Horticulture, Estonian University of Life Sciences

Professional employment:

2012–...	Estonian University of Life Sciences, Institute of Agricultural and Environmental Sciences, specialist
2004–2007	University of Tartu, Faculty of Biology and Geography, Institute of Molecular- and Cell Biology, Chair of Biophysics and Plant Physiology, researcher
1998–2004	University of Tartu, Faculty of Science and Technology, Institute of Molecular- and Cell Biology, Chair of Biophysics and Plant Physiology, senior laboratory assistant

Maternity leaves: 2002-2005, 2006-2009, 2017-2020

Scholarships:
DORA travel grants for visiting PhD students summer school in Orvieto, Italy 2008 and
12th EEF Congress (European Ecological Federation), Avila, Spain 2011.

CURRICULUM VITAE

Nimi:	Vivian Kuusk (kuni 2015 Vislap)
Töökoht:	Eesti Maaülikool, Põllumajandus- ja keskkonnainstituut
Ametikoht:	spetsialist

Hariduskäik:

2007 - ...	Doktoriõpe põllumajanduse erialal, Eesti Maaülikool
1999 - 2002	Magistriõpe botaanika erialal, Eesti Maaülikool
1994 - 1998	Bakalaureuseõpe aianduse erialal, Eesti Maaülikool

Teenistuskäik:

2012 -...	Eesti Maaülikool, Põllumajandus- ja keskkonnainstituut, spetsialist
2004 - 2007	Tartu Ülikool, Molekulaar- ja rakubioloogia instituut, Biofüüsika ja taimefüsioloogia õppetool, erakorraline teadur
1998–2004	Tartu Ülikool, Molekulaar- ja rakubioloogia instituut, Biofüüsika ja taimefüsioloogia õppetool, vanemlaborant

Lapsepuhkusel: 2002-2005, 2006-2009, 2017-2020

Grandid
DORA reisigrandid doktorantide suvekoolis osalemiseks Itaalias, Orvietos, 2008. aastal ja
12th EEF kongressil (European Ecological Federation), Avilas, Hispaanias, 2011. aastal postriettekande tegemiseks.

Work for the thesis was supported by grants from
the Consejo Superior de Investigaciones Cientificas (CSIC, Spain) and Estonian Academy of Sciences (a grant for collaboration between scientific institutions of Estonia and CSIC),
the Estonian Ministry of Science and Education (institutional grant IUT-8-3),
the European Commission through the European Regional Fund (the Center of Excellence in Environmental Adaptation),
European Commission through the European Regional Fund (the Center of Excellence EcolChange),

the Estonian Science Foundation (grant 9253),
and the European Research Council (advanced grant 322603, SIP-VOL+).

LIST OF 1.1 PUBLICATIONS

Wuyun, Tana; Zhang, Lu; Tosens, Tiina; Liu, Bin; Mark, Kristiina; Morales-Sánchez, José Ángel; Rikisahedew, Jesamine Jöneva; **Kuusk, Vivian**; Niinemets, Ülo (2024) Extremely thin but very robust: Surprising cryptogam trait combinations at the end of the leaf economics spectrum. Plant Diversity, Apr 26; 46(5): 621-629.
DOI: 10.1016/j.pld.2024.04.009

Kuusk, Vivian; Niinemets, Ülo; Valladares, Fernando (2018). A major trade-off between structural and photosynthetic investments operative across plant and needle ages in three Mediterranean pines. Tree Physiology, 38, 543–557.
DOI: 10.1093/treephys/tpx139

Kuusk, Vivian; Niinemets, Ülo; Valladares, Fernando (2018). Structural controls on photosynthetic capacity through juvenile-to-adult transition and needle ageing in Mediterranean pines. Functional Ecology, 32 (6), 1479–1491.
DOI: 10.1111/1365-2435.13087

Rasulov, Bahtijor; Bichele, Irina; Hüve, Katja; **Vislap, Vivian**; Niinemets, Ülo (2015). Acclimation of isoprene emission and photosynthesis to growth temperature in hybrid aspen: resolving structural and physiological controls. Plant Cell & Environment, 38 (4), 751–766.
DOI: 10.1111/pce.12435

Sun, Zhihong; Hüve, Katja; **Vislap, Vivian**; Niinemets, Ülo (2013). Elevated [CO_2] magnifies isoprene emissions under heat and improves thermal resistance in hybrid aspen. Journal of Experimental Botany, 64 (18), 5509–5523.
DOI: 10.1093/jxb/ert318

Tomás, Magdalena; Flexas, Jaume; Copolovici, Lucian; Galmés, Jeroni; Hallik, Lea; Medrano, Hipólito; Ribas-Carbó, Miquel; Tosens, Tiina; **Vislap, Vivian**; Niinemets, Ülo (2013). Importance of leaf anatomy in determining mesophyll diffusion conductance to CO_2 across

species: quantitative limitations and scaling up by models. Journal of Experimental Botany, 64 (8), 2269–2281.
DOI: 10.1093/jxb/ert086

Sun, Zhihong; Niinemets, Ülo; Hüve, Katja; Noe, Steffen; Rasulov, Bahtijor; Copolovici, Lucian; **Vislap, Vivian** (2012). Enhanced isoprene emission capacity and altered light responsiveness in aspen grown under elevated atmospheric CO_2 concentration. Global Change Biology, 18 (11), 3423–3440.
DOI: 10.1111/j.1365-2486.2012.02789.x

Tosens, Tiina; Niinemets, Ülo; **Vislap, Vivian**; Eichelmann, Hillar; Castro-Díez, Pilar (2012). Developmental changes in mesophyll diffusion conductance and photosynthetic capacity under different light and water availabilities in *Populus tremula*: how structure constrains function. Plant Cell & Environment, 35 (5), 839–856.
DOI: 10.1111/j.1365-3040.2011.02457.x

Copolovici, Lucian; Kännaste, Astrid; Remmel, Triinu; **Vislap, Vivian**; Niinemets, Ülo (2011). Volatile emissions from *Alnus glutinosa* induced by herbivory are quantitatively related to the extent of damage. Journal of Chemical Ecology, 37 (1), 18–28.
DOI: 10.1007/s10886-010-9897-9

Oja, Tatjana; Jaaska, Vello; Vislap, Vivian (2003). Breeding System, Evolution and Taxonomy of *Bromus arvensis, B. japonicus* and *B. squarrosus (Poaceae)*. Plant Systematics and Evolution, 242, 101–117.
DOI 10.1007/s00606-003-0024-z

VIIS VIIMAST KAITSMIST

KESHAV NAGPAL
TSINKOKSIIDI NANOSTRUKTUURIDE POLÜMEERKAPSELDAMINE FOTODIOODIRAKENDUSTE JAOKS
POLYMER ENCAPSULATION OF ZINC OXIDE NANOSTRUCTURES FOR PHOTODIODE APPLICATIONS
Professor Protima Rauwel, professor Erwan Yann Rauwel
26. august 2024

MARINA LOCH
NEONATAALPERIOODI MÕJU PIIMALEHMADE TERVISELE JA TOODANGULE
NEONATAL EFFECTS ON HEALTH AND PERFORMANCE OF DAIRY COWS
Professor Toomas Orro, vanemlektor Tarmo Niine
27. september 2024

HIMANSU SEKHAR MISHRA
DISAINISEKKUMISTE INTEGREERITUD HINDAMINE SINIALADEL TERVISE JA HEAOLU EDENDAMISEKS
AN INTEGRATED EVALUATION OF BLUE SPACE DESIGN INTERVENTIONS FOR HEALTH AND WELL-BEING
Tenuuriprofessor Simon Bell, professor Mart Külvik
14. november 2024

KRISTIINA PALM-HELLENURM
TORMI JA SANITAARRAIE PIKAAEGNE MÕJU METSATAIMESTIKU TAASTUMISELE JA ARENGULE
DELAYED STORM AND SALVAGE LOGGING EFFECTS ON FOREST VEGETATION RECOVERY AND DEVELOPMENT
Teadur Floortje Vodde, kaasprofessor Kalev Jõgiste, teadur Tea Tullus
3. detsember 2024

JOHANNA PIIBOR
LEHMA EMAKA EKSTRATSELLULAARSETE VESIIKULITE PROTEOOMIPROFIIL INNATSÜKLI VÄLTEL JA ENDOMETRIIDI PUHUL
PROTEOME PROFILE OF BOVINE UTERINE EXTRACELLULAR VESICLES DURING THE OESTROUS CYCLE AND IN ENDOMETRITIS
Professor Andres Valdmann
3. detsember 2024

ISSN 2382-7076
ISBN 978-9916-91-010-8 (trükis)
ISBN 978-9916-91-011-5 (pdf)